ADAPTATIONS OF *METHANOCOCCUS MARIPALUDIS* TO ITS UNIQUE LIFESTYLE

by

YUCHEN LIU

(Under the Direction of William B. Whitman)

ABSTRACT

Methanococcus maripaludis is an obligate anaerobic, methane-producing archaeon. In addition to the unique methanogenesis pathway, unconventional biochemistry is present in this organism in adaptation to its unique lifestyle.

The Sac10b homolog in *M. maripaludis*, Mma10b, is not abundant and constitutes only ~ 0.01% of the total cellular protein. It binds to DNA with sequence-specificity. Disruption of *mma10b* resulted in poor growth of the mutant in minimal medium. These results suggested that the physiological role of Mma10b in the mesophilic methanococci is greatly diverged from the homologs in thermophiles, which are highly abundant and associate with DNA without sequence-specificity.

M. maripaludis synthesizes lysine through the DapL pathway, which uses diaminopimelate aminotransferase (DapL) to catalyze the direct transfer of an amino group from L-glutamate to L-tetrahydrodipicolinate (THDPA), forming LL-diaminopimelate (LL-DAP). This is different from the conventional acylation pathway in many bacteria that convert THDPA to LL-DAP in three steps: succinylation or acetylation, transamination, and desuccinylation or deacetylation. The DapL pathway eliminates the expense of using succinyl-CoA or acetyl-CoA and may represent a thriftier mode for lysine biosynthesis.

Methanogens synthesize cysteine primarily on $tRNA^{Cys}$ via the two-step SepRS/SepCysS pathway. In the first step, $tRNA^{Cys}$ is aminoacylated with *O*-phosphoserine (Sep) by *O*-phosphoseryl-tRNA synthetase (SepRS). In the second step, the Sep moiety on Sep-$tRNA^{Cys}$ is converted to cysteine with a sulfur source to form Cys-$tRNA^{Cys}$ by Sep-tRNA:Cys-tRNA synthase (SepCysS). The nature of the physiological sulfur donor for the tRNA-dependent cysteine biosynthesis is unknown. Based upon activity assays in *M. maripaludis* cell extracts, a rhodanese-like, protein-mediated sulfur transfer is proposed to be involved in the sulfur assimilation for cysteine biosynthesis. This is different from cysteine biosynthesis in enteric bacteria and plants, which use direct sulfhydrylation with sulfide.

Finally, *M. maripaludis* does not use cysteine as the sulfur source for Fe-S cluster biosynthesis. Instead, the sulfur in Fe-S clusters is derived predominantly from exogenous sulfide. This challenges the concept that cysteine is always the sulfur source for Fe-S cluster biosynthesis. The unique sulfur metabolism in *M. maripaludis* may be an adaptation to sulfide-rich living environments.

INDEX WORDS: archaea, methanogens, *Methanococcus maripaludis*, DNA-binding protein, lysine biosynthesis, cysteine biosynthesis, iron-sulfur cluster, methionine biosynthesis, rhodanese

ADAPTATIONS OF *METHANOCOCCUS MARIPALUDIS* TO ITS UNIQUE LIFESTYLE

by

YUCHEN LIU

B.S., Shanghai Jiao Tong University, 2003

A Dissertation Submitted to the Graduate Faculty of The University of Georgia in Partial Fulfillment of the Requirements for the Degree

DOCTOR OF PHILOSOPHY

ATHENS, GEORGIA

2010

ADAPTATIONS OF *METHANOCOCCUS MARIPALUDIS* TO ITS UNIQUE LIFESTYLE

by

YUCHEN LIU

Major Professor:	William B. Whitman
Committee:	Michael W.W. Adams
	I. Jonathan Amster
	Lawrence J. Shimkets
	Juergen Wiegel

Electronic Version Approved:

Maureen Grasso
Dean of the Graduate School
The University of Georgia
August 2010

DEDICATION

To my grandparents, Fu Xifeng and Yang Jingzhen, my parents, Liu Hongliang and Fu Rongyue, and my husband, Fan Jianguo.

ACKNOWLEDGEMENTS

First and foremost, I must thank Barny Whitman, who brought me to this country and taught me how to be a scientist. He has spent tremendous time to guide me to think carefully and deeply on every experimental phenomenon we have encountered. Without his encouragements and great ideas, I would not be able to do any of this research. His devotion to science has set a good example for me and will continue to inspire me in my future work. Furthermore, I thank my labmates, Magdalena Sieprawska-Lupa, Boguslaw Lupa, Christopher Reisch, Kamlesh Jangid, Felipe Sarmiento, Nickolaus Galloway, Iris Porat, Tiffany Major, and James Henrikson, for their company and supports. I also thank my committee members for many helpful suggestions for the research and this dissertation.

TABLE OF CONTENTS

Page

CHAPTER 1

INTRODUCTION AND LITERATURE REVIEW[1]

---

[1]Liu, Y., and W. B. Whitman. 2008. Metabolic, phylogenetic, and ecological diversity of the methanogenic archaea. Ann. N.Y. Acad. Sci. 1125:171-189.

Abstract

Although of limited metabolic diversity, methanogenic archaea or methanogens possess great phylogenetic and ecological diversity. Only three types of methanogenic pathways are known: CO_2-reduction, methyl-group reduction, and the aceticlastic reaction. Cultured methanogens are grouped into five orders based upon their phylogeny and phenotypic properties. In addition, uncultured methanogens that may represent new orders are present in many environments. The ecology of methanogens highlights their complex interactions with other anaerobes and the physical and chemical factors controlling their function.

Introduction

Biological methane production or methanogenesis is an important process in the global carbon cycle, processing about 1.6 % of the carbon fixed every year by plants and algae (48). Biologically generated methane can either serve as a substrate for aerobic or anaerobic methane oxidation or be emitted to the atmosphere. Methane emitted to the atmosphere is a major greenhouse gas, whose atmospheric concentration has increased by 3-fold in the last 200 years (48). The current global methane emission is 500-600 Tg CH_4 yr^{-1} (71). About 74 % of the emitted methane is derived from biological methanogenesis (127). The major sources of methane emissions are listed in Table 1-1.

Methanogens are microorganisms that produce methane as the end product of anaerobic respiration. All methanogens are strictly anaerobic archaea belonging to the *Euryarchaeota*. They are a large and diverse group, all of which are obligate methane-producers that obtain all or most of their energy from methanogenesis. The methanogenesis pathway is complex, requiring a number of unique coenzymes and membrane-bound enzyme complexes, the details of which have been recently reviewed (48).

Methanogens have been cultivated from a wide variety of anaerobic environments. In addition to temperate habitats, they are also common in environments of extreme temperatures, salinity, and pH. The common methanogenic habitats include marine sediments, freshwater

sediments, flooded soils, human and animal gastrointestinal tracts, termites, anaerobic digestors, landfill, geothermal systems, and heartwood of trees.

1. Methanogenic substrates

Although the methanogens are very diverse, they can only utilize a restricted number of substrates. The substrates are limited to three major types: CO_2, methyl-group containing compounds, and acetate (Table 1-2). Most organic substances, for instance carbohydrates and long chain fatty acids and alcohols are not substrates for methanogenesis. Instead, these compounds must first be processed by anaerobic bacteria or eukaryotes to produce the substrates actually used by the methanogens. Thus, in most methanogenic environments, most of the energy available for growth is utilized by these nonmethanogenic organisms. It is an interesting physiological mystery as to why methanogens do not directly utilize complex organic matter, bypassing their dependency on other organisms.

The first type of substrate is CO_2. Most methanogens are hydrogenotrophs that can reduce CO_2 to methane with H_2 as the primary electron donor. Many hydrogenotrophic methanogens can also use formate as the major electron donor. In this case, four molecules of formate are oxidized to CO_2 by formate dehydrogenase (Fdh) before one molecule of CO_2 is reduced to methane. In hydrogenotrophic methanogenesis, CO_2 is reduced successively to methane through the formyl, methylene, and methyl levels (Fig. 1-1A). The C-1 moiety is carried by special coenzymes, methanofuran (MFR), tetrahydromethanopterin (H_4MPT), and coenzyme

M (CoM). Initially, CO_2 binds to MFR and is reduced to the formyl level. In this first reduction step, ferredoxin (Fd), which is reduced with H_2, is the direct electron donor. The formyl group is then transferred to H_4MPT, forming formyl-H_4MPT. The formyl group is then dehydrated to methenyl group, which is subsequently reduced to methylene-H_4MPT and then to methyl-H_4MPT. Reduced F_{420} ($F_{420}H_2$) is the direct electron donor in these two reduction steps. The methyl group is then transferred to CoM, forming methyl-CoM. The last reduction step reduces methyl-CoM to methane by methyl coenzyme M reductase (Mcr), which is the key enzyme in methanogenesis. Coenzyme B (CoB) is the direct electron donor in this reduction, and the oxidized CoB forms a heterodisulfide with CoM (CoM-S-S-CoB). Finally, the heterodisulfide is reduced to regenerate the thiols. Thermodynamically, two reactions, the methyl transfer from H_4MPT to CoM and the reduction of the heterodisulfide, are exergonic and involved in energy conservation. The methyl transfer reaction is catalyzed by methyl-H_4MPT:HS-CoM methyltransferase (Mtr), which is a membrane-bound complex. The reduction of the heterodisulfide is catalyzed by heterodisulfide reductase (Hdr), which is a membrane-bound complex in *Methanosarcina* and coupled to $F_{420}H_2$ dehydrogenase (Fpo) when H_2 is present. The reduction of CO_2 to formyl-MFR is endergonic and driven by ion gradient via the membrane-bound energy conserving hydrogenase (Ech).

Some hydrogenotrophic methanogens can also use secondary alcohols such as 2-propanol, 2-butanol, and cyclopentanol as electron donors. A small number can use ethanol (7,

41, 130, 131). The secondary alcohols are oxidized to ketones via coenzyme F_{420}-dependent secondary alcohol dehydrogenases (Adf) (132). Ethanol is oxidized to acetate via a NADP-dependent alcohol dehydrogenase (4). Although the growth on alcohols is poor compared to that on H_2, it is an important exception to the generalization that methanogens can not directly metabolize most organic compounds. Even in this case, where the substrate is obviously assimilated, the oxidation is incomplete, and methane is derived from CO_2 reduction.

Two species have been shown to utilize CO as a reductant for methanogenesis from CO_2 (26, 87). In *Methanothermobacter thermoautotrophicus* and *Methanosarcina barkeri*, four molecules of CO are oxidized to CO_2 using CO dehydrogenase (CODH) before one molecule of CO_2 is reduced to methane (26). H_2 is an intermediate in this reaction and serves as the direct electron donor for the reduction of CO_2. Growth with CO is poor, and the doubling time is more than 200 h for *M. thermoautotrophicus* and 65 h for *M. barkeri*. In contrast, *Methanosarcina acetivorans* grows on CO by an entirely different pathway to be discussed below.

The second type of substrate is methyl-group containing compounds including methanol, methylated amines (monomethylamine, dimethylamine, trimethylamine, and tetramethylammonium), and methylated sulfides (methanethiol and dimethylsulfide). Methanogens that are able to use methylated compounds, or methylotrophic methanogens, are limited to the order *Methanosarcinales*, except for *Methanosphaera* species which belong to the order *Methanobacteriales*. During methanogenesis, the methyl-groups from methylated

compounds are transferred to a cognate corrinoid protein and then to coenzyme M (CoM) (Fig. 1-1B) (13, 36, 101). Methyl-CoM subsequently enters the methanogenesis pathway and is reduced to methane. The activation and transfer of the methyl-group requires substrate-specific methyltransferases. Interestingly, all known methylamine methyltransfereases contain a UAG (amber codon)-encoded L-pyrrolysine designated the 22nd genetically encoded amino acid. This implies a connection between the abilities of amber codon translation and methylamine utilization (47, 64, 78). In most methylotrophic methanogens, the electrons required for the reduction of the methyl groups to methane are obtained from the oxidation of additional methyl-groups to CO_2, which proceeds stepwise as the reverse of hydrogenotrophic methanogenesis. In methylotrophic methanogenesis, three methyl groups are reduced to methane for every molecule of CO_2 formed. This process is termed a disproportionation, since the oxidation of a portion of the substrate is used to reduce the remainder. Different from this mode of growth, the methylotrophic growth of *Methanomicrococcus blatticola* and *Methanosphaera* species is H_2-dependent (6, 40, 82, 112-114). They are obligate methylotrophic and hydrogenotrophic methanogens that are specialized to reduce methyl groups with H_2. The metabolism of *Methanosphaera* is restricted to methanol, while *M. blatticola* can use both methanol and methylamine.

The third type of substrate is acetate. Acetate is a major intermediate in the anaerobic food chain, and as much as two-thirds of the biologically generated methane is derived from

acetate. Surprisingly, only two genera are known to use acetate for methanogenesis: *Methanosarcina* and *Methanosaeta*. They carry out an aceticlastic reaction that splits acetate, oxidizing the carboxyl-group to CO_2 and reducing the methyl group to CH_4 (Fig. 1-1C). *Methanosarcina* is a relative generalist that prefers methanol and methylamine to acetate, and many species also utilize H_2. *Methanosaeta* is a specialist that uses only acetate. *Methanosaeta* is a superior acetate utilizer in that it can use acetate at concentrations as low as 5-20 μM, while *Methanosarcina* requires a minimum concentration of about 1 mM (54). The difference of acetate affinity is probably due to differences in the first step of acetate metabolism. *Methanosarcina* uses the low affinity acetate kinase (AK)-phosphotransacetylase (PTA) system to activate acetate to acetyl-CoA, while *Methanosaeta* uses the high affinity AMP-forming acetyl-CoA synthetase (54, 108, 110, 120). Moreover, based upon their genome sequences, these two genera probably have different modes of electron transfer and energy conservation, even though the main steps in the methanogenesis pathway are likely to be similar (110).

The metabolism of *Methanosarcina acetivorans* grown on CO is unconventional. It is distinct from the CO metabolism in *Methanosarcina barkeri* and *Methanothermobacter thermoautotrophicus*. First, although the oxidation of CO to CO_2 via CODH is commonly required for CH_4 production, H_2 is not generated as an intermediate in *M. acetivorans* (95). *M. acetivorans* is also unable to grow with H_2/CO_2 and lacks hydrogenases activities. Second, proteomic analyses suggest that CO-dependent methanogenesis in *M. acetivorans* requires an

unusual mechanism for energy conservation. Although the steps of CO_2 reduction to methyl groups are similar as those in hydrogenotrophic methanogens, a coenzyme $F_{420}H_2$:heterodisulfide oxidoreductase system is responsible for energy conservation (68, 96). This system is used in *Methanosarcina* during methanogenesis with methylated compounds in the absence H_2, but it has not been identified in CO_2-dependent methanogenesis. Third, novel methyltransferases, which are used in place of methyl-H_4MPT:CoM methyltransferase (Mtr), involve in the transfer of methyl group from tetrahydromethanopterin (H_4MPT) to coenzyme M (CoM) (68). Fourth, substantial amounts of acetate and formate are produced in addition to methane during the growth on CO in *M. acetivorans*. Mutational analysis suggests that acetate is formed via the AK-PTA system, which is the reverse of the initial steps of methanogenesis from acetate in *Methanosarcina*. Acetate production may generate ATP via substrate level phophorylation. Thus, the growth on CO in *M. acetivorans* may conserve more energy than that in *M. barkeri* and *M. thermoautotrophicus*, which can be an explanation of the faster growth of *M. acetivorans* on CO (doubling time about 24 h). The mechanism of formate production is unclear yet. Since the formate dehydrogenase activity is absent in *M. acetivorans*, novel reactions are presumably involved.

2. Systematics of methanogenic archaea

Despite of their restricted substrate range, methanogens are phylogenetically diverse. They are classified into five well established orders: *Methanobacteriales*, *Methanococcales*,

Methanomicrobiales, *Methanosarcinales*, and *Methanopyrales*. Organisms from different orders have less than 82 % 16S rRNA sequence similarity. Methanogens belonging to different orders also possess different cell envelope structure, lipid composition, substrate range, and other biological properties. The methanogen orders are further divided into 10 families and 31 genera. Organisms with less than 88-93 % and less than 93-95 % 16S rRNA sequence similarity are separated into different families and genera, respectively. Detailed descriptions of the systematics and characteristics of the methanogen taxa are reviewed in Bergey‘s Manual of Systematic Bacteriology (129) and The Prokaryotes (8, 42, 58, 127, 128). Some characteristics of the methanogenic taxa are listed in Table 1-3.

Recent culture-independent studies have revealed the presence of novel phylogenetic groups of methanogens. They are not closely related to known organisms and probably represent new orders. For instance, the Rice cluster I (RC-I), which is abundant in rice field soil, forms a separate lineage within the phylogenetic radiation of *Methanosarcinales* and *Methanomicrobiales*. The 16S rRNA sequences of RC-I have similarities of less than 82 % with known organisms (24, 35, 44, 73). Investigations of rumen methanogens have found a novel monophyletic group of at least two families (85). The 16S rRNA sequences of this group have similarities closest to, but less than 80 %, with those of *Methanosarcinales*. These studies illustrate our incomplete understanding of methanogen diversity.

2.1 *Methanobacteriales*

Members of the order *Methanobacteriales* generally produce methane using CO_2 as the elector acceptor and H_2 as the electron donor. Some species can use formate, CO, or secondary alcohols as electron donors. The genus *Methanosphaera* can only reduce methanol with H_2. In most genera, the cells are short to long rods with a length of 0.6 to 25 μm. They often form filaments up to 40 μm in length. The cell wall contains pseudomurein. The cellular lipids contain caldarchaeol, archaeol, and, in some species, hydoxyarchaeol as core lipids. The polar lipids can contain glucose, N-acetylglucosamine, *myo*-inositol, ethanolamine, and serine, depending on the species. Most species are nonmotile. However, members of the genus *Methanothermaceae* are motile via peritrichous flagella. They are widely distributed in anaerobic habitats, such as marine and freshwater sediments, soil, animal gastrointestinal tracts, anaerobic sewage digestors, and geothermal habitats.

The order of *Methanobacteriales* is divided into two families, *Methanobacteriaceae* and *Methanothermaceae*. The family *Methanobacteriaceae* contains three mesophilic genera, *Methanobacterium*, *Methanobrevibacter*, and *Methanosphaera*, and one extremely thermophilic genus *Methanothermobacter*. The family *Methanothermaceae* is represented by one hyperthermophilic genus, *Methanothermus*, which have only been isolated from thermal springs.

2.2 *Methanococcales*

Members of the order *Methanococcales* produce methane using CO_2 as the electron acceptor and H_2 or formate as the electron donor. The cells are irregular cocci with a diameter of

1-3 μm. The cell wall is composed of S-layer proteins. Glycoproteins and cell wall carbohydrates are generally absent or of low abundance. The cellular lipids contain archaeol, caldarchaeol, hydroxyarchaeol, and macrocyclic archaeal, depending upon the species. The polar lipids can contain glucose, N-acetylglucosamine, serine, and ethanolamine. They are motile by means of flagella. The temperature range for growth varies from mesophilic to hyperthermophilic. They have all been isolated from marine habitats and require sea salts for optimal growth.

The order of *Methanococcales* has been divided into two families distinguished by their growth temperatures. The family *Methanocaldococcaceae* includes two hyperthermophilic genera, *Methanocaldococcus* and *Methanotorris*. The family *Methanococcaceae* includes the mesophilic genus *Methanococcus* and the extremely thermophilic genus *Methanothermococcus*.

2.3 *Methanomicrobiales*

Members of the order *Methanomicrobiales* use CO_2 as the electron acceptor and H_2 as electron donor. Most species can use formate and many species also use secondary alcohols as alternative electron donors. Their morphology is diverse, including cocci, rods, and sheathed rods. Most cells have protein cell walls, and some cells are surrounded by a sheath containing glycoproteins. The cellular lipids contain archaeol and caldarchaeol as core lipids. Glucose, galactose, aminopentanetetrol, and glycerol are common polar lipids. Motility varies between species. They are widely distributed in anaerobic habitats, including marine and freshwater sediments, anaerobic sewage digestors, and animal gastrointestinal tracts.

The order of *Methanomicrobiales* is divided into three families, *Methanomicrobiaceae*, *Methanospirillaceae*, and *Methanocorpusculaceae*. The *Methanospirillaceae* is distinguished from the other two families by the curved rod shape of the cells. The *Methanomicrobiaceae* and *Methanocorpusculaceae* are difficult to distinguish by their physiological characteristics.

2.4 *Methanosarcinales*

Members of the order *Methanosarcinales* have the widest substrate range among methanogens. Most can produce methane by disproportionating methyl-group containing compounds or by splitting acetate. Some species can reduce CO_2 with H_2, but formate is not used as electron donor. Their cellular morphologies are diverse, including cocci, pseudosarcinae, and sheathed rods. Most cells have protein cell walls, and some cells are surrounded by a sheath or acidic heteropolysaccharides. The cellular lipids contain archaeol, hydroxyarchaeol, and caldarchaeol. Polar lipids can contain glucose, galactose, mannose, *myo*-inositol, ethanolamine, serine, and glycerol, depending upon the species. All cells are nonmotile. They are widely distributed in marine and freshwater sediments, anaerobic sewage digestors, and animal gastrointestinal tracts.

The order of *Methanosarcinales* is divided into two families, *Methanosarcinaceae* and *Methanosaetaceae*. All members of the family *Methanosarcinaceae* are able to grow with methyl-group containing compounds. The family *Methanosaetaceae* is represented by only one genus, *Methanosaeta*, and all cells produce methane by splitting acetate.

2.5 *Methanopyrales*

The order of *Methanopyrales* is represented by only one species, *Methanopyrus kandleri*. Cells reduce CO_2 with H_2 for methanogenesis. They are rod-shaped. Cell walls contain pseudomurein, and lipids contain archaeol. The cells are motile via flagella arranged as polar tufts. *M. kandleri* is hyperthermophile with a growth temperature range of 84-110 ^{o}C. It inhabits marine hydrothermal system.

3. Ecology of methanogens

Methanogens are abundant in habitats where electron acceptors such as O_2, NO_3^-, Fe^{3+}, and SO_4^{2-} are limiting. When electron acceptors other than CO_2 are present, methanogens are outcompeted by the bacteria that utilize them, such as sulfate-reducing bacteria, denitrifying bacteria, and iron-reducing bacteria. This phenomenon probably occurs because these compounds are better electron acceptors, and their reductions are thermodynamically more favorable than CO_2 reduction to methane. However, because CO_2 is generated during fermentations, it is seldom limiting in anaerobic environments. Besides methanogens, homoacetogens are another group of anaerobes that can reduce CO_2 for energy production. During acetate production or acetogenesis, CO_2 is reduced with H_2 or other substances, for instance sugars, alcohols, methylated compounds, CO, and organic acids. However, acetogenesis with H_2 is thermodynamically less favorable than methanogenesis. Therefore, homoacetogens do not compete well with methanogens in many habitats. However, homoacetogens outcompete

methanogens in some environments, such as the hindgut of certain termites and cockroaches. Possible explanations may be their metabolic versatility as well as lower sensitivity to O_2.

In methanogenic habitats, complex organic matter is degraded to methane by the cooperation of different groups of anaerobes. A general scheme of the anaerobic food chain is shown in Fig. 1-2. The organic polymers are initially degraded by specialized bacteria to simple sugars, lactate, volatile fatty acids, and alcohols. These products are further fermented by syntrophs and related bacteria to acetate, formate, H_2, and CO_2, which are substrates for methanogenesis. Methanogens catalyze the terminal step in the anaerobic food chain by converting methanogenic substrates to methane. The reactions catalyzed by the syntrophic bacteria, for instance the conversion of volatile fatty acids and alcohols to acetate, CO_2, and H_2, is only favorable at H_2 partial pressures below 10^2 Pa (136). When methanogens are present, H_2 is rapidly metabolized and maintained at concentrations below 10 Pa (48). Therefore, these syntrophic bacteria depend on the association with methanogens or another hydrogenotrophic organism for energy production. The interaction between H_2-producing organisms (e.g. propionate-oxidizing bacteria) and H_2-consuming organisms (e.g. hydrogenotrophic methanogens) is named interspecies hydrogen transfer.

3.1 Marine sediments

Methanogenesis in marine habitats is a significant process that produces between 75 and 320 Tg CH_4 $year^{-1}$, but nearly all the methane is anaerobically oxidized to CO_2 instead of

escaping to the atmosphere (122). Sulfate, which is commonly present at 20-30 mM in seawater, is an important factor that controls the distribution of marine methanogens (14). Sulfate-reducing bacteria outcompete methanogens in sulfate-rich marine sediments for H_2 and acetate. For instance, in the sediments of Cape Lookout Bight (North Carolina), the H_2 in the sulfate-rich sediments is mainly utilized by sulfate-reducing bacteria and kept at a level of 0.1-0.3 Pa, which is below the minimum values utilized by hydrogenotrophic methanogens (49, 50). Therefore in upper layers of sediments, or sulfate-reducing zones, methanogenesis is limited and accounts for less than 0.1% of total carbon turnover (14). In sediments with high input of organic matter, sulfate can be depleted with depth, and methanogenesis can become the predominant terminal process in the anaerobic food chain.

Based upon studies of carbon and hydrogen stable isotopes, CO_2-reduction by H_2 is a predominant source of methanogenesis in deep marine sediments (89, 125, 126). In methanogenic zones, which are usually beneath the sulfate-reducing zones, the dissolved bicarbonate pool is replenished from oxidation of carbon compounds in upper sediments and can obtain concentrations greater than 100 mM (125). CO_2-reducing methanogens in marine sediments include members within the orders *Methanococcales*, *Methanomicrobiales*, and *Methanobacteriales* (59, 61, 84). They gain energy strictly by CO_2 reduction coupled with H_2 or formate oxidation. Moreover, hydrogenotrophic methanogens belonging to *Methanomicrobiales*

can be detected from all depths of the sediments under certain circumstances (61). Possibly, these methanogens gain energy from syntrophic growth with H_2-producers (60).

Methylotrophic methanogens are major contributors to the limited methane production in sulfate-rich sediments. Identified organisms include members of the genera *Methanococcoides*, *Methanosarcina*, and *Methanolobus* (59, 61, 75). Methylated compounds are generated in marine sediments from osmolytes of marine bacteria, algae, phytoplankton and some plants. For instance, dimethylsulfide and trimethylamine are derived from dimethylsulfoniopropionate and betaine glycine, respectively. These compounds are not utilized efficiently by the sulfate-reducing bacteria and are termed noncompetitive substrates (88). Because of the presence of considerable amount of these substrates, obligately methylotrophic methanogens, such as *Methanococcoides*, can be cultivated from all depths in these sediments (61).

Acetate is a minor substrate for methanogenesis in most marine sediments (84, 126). Only a few aceticlastic methanogens belonging to *Methanosarcina* have been isolated (34, 111, 123). The minimum concentration of acetate utilized by *Methanosarcina* is typically 1 mM (136). However, pore water acetate concentrations in marine sediments are usually below 20 μM (59, 89). Therefore, the aceticlastic methanogens that have been isolated probably also use methylated compounds for methanogenesis under environmental conditions. As measured by isotopes, the rate of acetate oxidation to CO_2 exceeds that of CH_4 production by the aceticlastic

reaction in sulfate-reducing sediments (89). Therefore, in these sediments, acetate is mainly metabolized by acetate oxidizers, for instance sulfate-reducing bacteria.

3.2 Freshwater sediments

Freshwater environments have lower sulfate concentrations (100-200 μM) than marine sediments (14). Therefore methanogenesis in freshwater sediments proceeds uninhibited in anoxic zones and replaces sulfate reduction as the most important terminal process in the anaerobic degradation of organic matter. Due to the absence of competition by sulfate-reducing bacteria, the acetate pool is available for methanogenesis and is the dominant substrate. In most investigated freshwater environments, aceticlastic and hydrogenotrophic methanogenesis are responsible for about 70 % and 30% of the CH_4 production, respectively (22, 125). The relative contribution of acetate and H_2/CO_2 in methanogenesis is close to the theoretical expectation. The fermentation of hexose yields 4 H_2, 2 acetate, and 2 CO_2. In addition, 4 H_2 are required to reduce CO_2 to methane. Thus, the expected ratio of methane from H_2 and acetate is 1:2, respectively. Methanogenesis from methylated compounds is minor, possibly reflecting the absence of these substrates in freshwater sediments (14). The methanogenic communities are usually dominated by the aceticlastic family *Methanosaetaceae* and the hydrogenotrophic families *Methanomicrobiaceae* and *Methanobacteriaceae*. *Methanosarcinaceae* may also be present, and they may utilize either H_2/CO_2 or acetate (11, 16, 17, 43, 77).

A few factors have been investigated that affect the relative contribution of aceticlastic and hydrogenotrophic methanogenesis as well as the relative abundance of different types of methanogens in freshwater sediments. First, hydrogenotrophic methanogenesis decreases at low pH (91). For instance, in Lake Knaack sediments (pH 6.8), only 4 % of the CH_4 production is derived from H_2/CO_2 (91). In Lake Grosse Fuchskuhle (pH <5), only aceticlastic methanogens belonging to *Methanosarcinaceae* can be detected (15). Low pH provides a selective advantage to homoacetogens, which reduce CO_2 to acetate instead of methane. This limits hydrogenotrophic methanogenesis. Second, the relative contribution of hydrogenotrophic methanogenesis decreases with temperature, even though the absolute rate of aceticlastic methanogenesis also decreases (23, 43, 104, 105). A similar effect of temperature is also observed in rice paddies (19). This effect can be explained by better adaptation of homoacetogens to low temperatures (23, 104). Moreover, H_2 production by syntrophic bacteria decreases, as H_2-producing processes are less favorable at low temperature. Therefore, hydrogenotrophic methanogenesis is inhibited at low temperature due to an insufficient supply of substrates. Third, the relative contribution of hydrogenotrophic methanogenesis changes with depth in some cases. In Lake Dagow sediments, the relative contribution of hydrogenotrophic methanogenesis increases from 22 % to 38 % from 0 to 18 cm (16). Coincidently, the relative abundance of *Methanomicrobiales* increases slightly with depth, while the abundance of *Methanosaetaceae* decreases. In contrast, in Lake Rotsee sediments, hydrogenotrophic

methanogenesis is only observed in the upper 2 cm of the sediments (135). In this case, hydrogenotrophic methanogens possibly live as symbionts of ciliates. Fourth, the abundance of other H_2 and acetate-consumers greatly influences the methanogenic communities. In Lake Constance sediments, the presence of H_2-consuming sulfate-reducing bacteria and absence of acetate-consuming sulfate-reducing bacteria together with low temperature (4 ^{o}C) results in 100 % CH_4 production from aceticlastic methanogenesis (3, 104). In Lake Kinneret sediments, CH_4 is produced exclusively by hydrogenotrophic methanogens (*Methanomicrobiaceae* and *Methanobacteriaceae*) through syntrophic association with acetate-oxidizers (86).

3.3 Rice field soils

Rice fields are major anthropogenic sources of methane emission. In rice paddies, upon flooding, oxygen, nitrate, ferric iron, and sulfate are rapidly exhausted due to high input of plant carbon, developing the conditions favoring methanogenesis. Methanogenesis is a significant process in rice fields, and about 3-6 % of the photosynthetically fixed CO_2 is converted to methane (27). Methanogens inhabit both the soils and the root surfaces. Methane is emitted mostly through the vascular system of the rice plant, which also supplies O_2 to the roots and adjacent rhizosphere soil (106). Since rice field soils are transiently oxic and exposed to drying, soil methanogens are proposed to be more resistant to O_2 and desiccation than methanogens in aquatic habitats (37).

Methane in rice fields is derived from both H_2/CO_2 and acetate. Dominant methanogens are affiliated with *Methanomicrobiaceae*, *Methanobacteriaceae*, *Methanosarcinaceae*, *Methanosaetaceae*, and Rice Cluster I (RC-I) (20, 63, 72). A few factors have been suggested that affect methanogenesis and/or methanogenic populations in rice fields. First, the relative populations of methanogens remain constant upon flooding and seasonal drying (63, 74, 90, 106). However, hydrogenotrophic methanogenesis dominates immediately after flooding, while aceticlastic methanogenesis increases later, reaching a maximum at about 70-80 days after flooding (63, 98). This shift may be due to activation of hydrogenotrophic methanogens immediately upon flooding and not changes of the methanogenic populations. Second, the methanogen community structures on rice roots differ from those in the bulk soils. On rice roots, RC-I is usually the dominant organism, and CH_4 is mainly derived from H_2/CO_2 (60-80 %) (20, 72). In the bulk soil, aceticlastic methanogens are dominant, and CH_4 is mainly derived from acetate cleavage (50-83 %) (22, 57, 72, 97, 106). One possible reason for this difference is that the hydrogenotrophic methanogens on rice roots could be more resistant to O_2, which has a higher concentration on the roots than in the bulk soils. Third, the population of hydrogenotrophic methanogens increases with temperature ($\geq$ 30 ^{o}C) (18, 38). Fourth, phosphate ($\geq$ 20 mM) specifically inhibits aceticlastic methanogens (20, 25, 72).

RC-I methanogens, which have not yet been cultivated, form a distinct phylogenetic lineage within the radiation of *Methanosarcinales* and *Methanomicrobiales*, based upon analyses

of both 16S rRNA and *mcrA* genes (review in (24)). These hydrogenotrophs are ubiquitous and abundant in rice paddies, representing 20-50 % of the total methanogens. Incubations of rice roots or rice field soils with RC-I methanogens show that they are preferentially active at low H_2 concentrations, moderately high temperatures (45-50 ^{o}C), and with additional supplies of sugars or amino acids. Other speculations to explain their prevalence in rice fields include their superior adaptations to temporary drought and oxic conditions. Indeed, the genome sequence of RC-I suggests the presence of enzymes that detoxify highly reactive oxygen species (35). Interestingly, their genome also encodes enzymes of carbohydrate metabolism and assimilatory sulfate reduction, which are rare in methanogens (35).

3.4 Human and animal gastrointestinal tracts

In the human colon, organic substrates that have escaped digestion in the upper intestinal tract are fermented by anaerobic microbial communities into short chain fatty acids and CO_2. H_2 is produced for disposing of reducing equivalents and kept at very low partial pressures to meet the thermodynamic requirements for anaerobic fermentation processes. H_2 is mainly removed through re-utilization by hydrogenotrophic microorganisms. For instance, in some individuals about 1 L of H_2 is excreted in breath and flatus per day, while 16 L of H_2 is used to make 4 L of CH_4 per day (80). The predominant H_2-consuming populations in the human colons are methanogens, acetogens, and sulfate-reducing bacteria.

About one-third of healthy human adults are strong methane-producers and possess breathe methane levels > 1 ppm above the atmospheric methane level (69, 80). Most of the produced CH_4 gas is excreted as flatus and some is absorbed in the blood and excreted in breath. Methanogens number 10^8-10^{10} cells/g feces in these individuals. Individuals with low levels of methane in their breathe contain < 10^2-5 × 10^6 methanogen cells/g feces (33, 80). Acetogens predominate in these individuals, and the numbers of acetogens have a negative correlation with that of methanogens (5). Although acetogens offer nutritional benefits to the hosts by producing acetate, methanogens can successfully outcompete acetogens in the colon of some individuals, possibly due to their lower threshold of H_2 utilization (66). Sulfate-reducing bacteria outcompete methanogens in many other habitats, but they do not exclude methanogens in human feces (93, 115-117). Neither the cell numbers of sulfate-reducing bacteria nor the concentrations of sulfate and sulfide in feces are significantly different between methane-producing and non-producing individuals (93, 117). Moreover, methane-producing feces consumes H_2 more rapidly than non-producing feces, suggesting that methanogens can outcompete other H_2-consumers in the human colon (116-118). What determines methanogen abundance in feces is still a mystery. Methanogens are not detected in feces of children under 27 months of age; while in methane-producing adults, the levels of methanogens are stable over time (69, 99). The development of methanogens is not directly related to the introduction of particular foods (99). No significant autosomal genetic effects have yet been identified (39). Shared environment is one of the

determinants of methane production (39). Methanogenesis is negatively correlated with the frequency of bowel movements (69). Likewise, methanogen abundance is negatively correlated to the fecal concentrations of butyrate, but not to acetate or total short chain fatty acids (1). The lack of significant correlation between methanogen abundance and the concentration of acetate is unexpected, since low methanogen abundance enhances acetate production by hydrogenotrophic acetogens. Low acetate concentration in the colon is probably due to efficient absorption by the host and consumption by other anaerobes, such as butyrate-producing bacteria (30, 51, 76).

Methane produced in the human colon is mainly derived from H_2/CO_2. Aceticlastic methanogenesis is generally limited, because the short retention time of the intestine does not allow the slow growth of methanogens on acetate (80). Only two methanogens species have been isolated from human feces: *Methanobrevibacter smithii* and *Methanosphaera stadtmanae* (81, 83). Both of them belong to the order *Methanobacteriales*. *M. smithii* is the predominant methanogen species and constitutes up to 10 % of all anaerobes in the human colon (32, 80). It produces methane from H_2/CO_2 or formate but grows poorly with formate (83). *M. stadtmanae* is present in lower numbers than *M. smithii*. It can only produce methane by reducing methanol with H_2 and depends on acetate as a carbon source. Methanol in human gut is derived from pectin degradation by *Bacteroides* and other anaerobes (28, 53). The restricted metabolism of *M. stadtmanae* can be explained by that the absence of genes for CO dehydrogenase/acetyl-CoA synthase (CODH/ACS) and molybdopterin biosynthesis proteins, which are common among

other methanogens (40). The genome of both *M. smithii* and *M. stadtmanae* encode enzymes for the synthesis of surface glycans resembling the components of the mucosal layer of the hosts (100). Their genomes also encode adhesion-like proteins (100). These features are shared among bacteria in gastrointestinal tracts and may contribute to their adaptation to the human colon.

The rumen of herbivores is the primary location for microbial fermentation of plant material which can not be digested by the host enzymes. A wide variety of microorganisms, such as bacteria, fungi, and protozoa, ferment plant biomass into H_2, short chain fatty acids, CO_2, and CH_4. Methane production from the rumen contributes to up to 20 % of the global methane emissions to the atmosphere. In addition, 6-10 % of the energy value of the food ingested by host animal is lost as methane (124). Therefore, manipulation of methane production in rumen serves a way to limit methane emission from anthropogenic sources as well as improve animal production. Daily methane production is different among ruminant species. For instance, an adult cow produces about 200 L of CH_4 per day, while sheep under generous grazing conditions produce 35-50 L of CH_4 per day (80, 92).

In the rumen, hydrogenotrophic methanogens predominate. Methanogenesis limits hydrogenotrophic acetogenesis by lowering the H_2 concentration to below the minimal level required for acetogenesis (65). Methanogens in the bovine rumen typically number 10^8-10^{10} cells/g of rumen content, and the population densities of methanogens are influenced by the type of diet, especially the fiber content (55, 56). *Methanobrevibacter* species, including *M.*

ruminantium, *M. thaueri*, and *M. smithii*, are the predominant methanogens isolated and cultured from the bovine and ovine rumen (109) (Table 1-4). Recent 16S rRNA gene based studies reveal that, although *Methanobrevibacter* are usually dominant, a wide diversity of ruminal methanogens coexist in the rumen (70, 109, 133). *Methanosphaera* species similar to *M. stadtmanae* are likely to be common (109, 124). Methanogens belonging to the *Methanosarcinales* and *Methanococcales* are present in the rumen of some individuals, but they are not detectable in most individuals (70). Substantial numbers of the 16S rRNA sequences obtained from the rumen are not related to known methanogens and probably represent a novel order of archaea (85, 119, 133). Some of these uncultured microorganisms can be established on methanogen-selective medium with H_2/CO_2 but do not compete well with *Methanobrevibacter* (85). These studies indicate that uncultured methanogens may have significant population densities in the rumen.

The insect hindgut is another important habitat of methanogens. About 3 % of the total global methane emissions or 11% the methane emissions from natural sources are from the termite hindgut. Methanogenesis and acetogenesis occur simultaneously in the termite hindgut, and the relative activities are related to host diets. In wood-feeding termites, acetogenesis outpaces methanogenesis; by contrast, in soil-feeding and fungus-feeding termites, methanogenesis outpaces acetogenesis (10, 121). It is interesting that acetogens can outcompete methanogens in termite guts, though the mechanism is still under study and may vary between

different termite species. A few proposed mechanisms include (1) Acetogens are metabolically versatile and able to use organic substrates in addition to H_2. Their mixtrophic life styles give them competitive advantages over methanogens. However, it is necessary to explain why these advantages would not be applied in other habitats. (2) The H_2 levels in termite guts are not limiting for acetogenesis. For instance, in *Reticulitermes flavipes*, a wood-feeding lower termite, the H_2 partial pressure is about 5 kPa, which is two orders of magnitude higher than the minimum level of H_2 for acetogenesis (31). (3) Acetogens and methanogens may be spatially separated in different compartments of the termite gut to avoid direct competition for H_2. Termite guts are highly structured and characterized by steep gradients of O_2, H_2, and pH. Some regions may form microniches which favor acetogenesis (12, 121).

Methanogens identified from termite hindguts include members of the *Methanobacteriaceae* and *Methanosarcinaceae* (9, 29). The relationship between methanogen community compositions and termite diet is not clear yet. *Methanobacteriaceae* are predominant in most termite species, but in four studied termite species *Methanosarcinaceae* are the dominant methanogen group (9). The dominance of *Methanosarcinaceae* is uncommon in gastrointestinal tracts of animals. Possibly, their ability to use a variety of substrates, including H_2/CO_2, acetate, and methylated compounds, may provide an advantage in the termite hindgut.

3.5 Anaerobic digestors

Anaerobic digestors are widely used for the degradation of organic wastes such as animal manure and municipal wastewater to methane. Compared with aerobic treatments, the anaerobic treatments have the advantage of generating high quantities of renewable fuel in form of biogas. Moreover, they produce much less sludge, a costly byproduct of the aerobic process.

The anaerobic conversion of wastes to methane requires cooperation of at least three groups of microorganisms (134). The first step, hydrolysis, involves enzyme-mediated conversion of organic polymers such as polysaccharides, lipids, proteins, and fats into soluble organic monomers. This step is carried out by anaerobic bacteria such as *Bacterioides*, *Clostridium*, and *Streptococcus*. The second step, acidogenesis, involves anaerobic fermentation of monomers into acetate, H_2, CO_2, as well as short chain fatty acids (propionate and butyrate), which are subsequently converted to acetate and H_2. The third step, methanogenesis, involves conversion of acetate, H_2, and CO_2 into CH_4 by methanogens. Methanogenesis is considered the rate-limiting step, and high activity of the methanogens is important for maintaining efficient anaerobic digestion and avoiding the accumulation of H_2 and short chain fatty acids. Moreover, this step is most vulnerable to parameters such as temperature, pH, and inhibitory chemicals. Therefore, enhancement of methanogenesis is a major route for improving the performance of anaerobic digestors.

Acetate is a major product of the fermentation and accounts for two-thirds of the methane production in anaerobic digestors (136). Usually, only one aceticlastic methanogen group,

Methanosaeta or *Methanosarcina*, dominates each digestor, depending upon the type of waste and digestor (67). *Methanosaeta* have slower growth rates and higher affinity for acetate, while *Methanosarcina* have faster growth rates and lower affinity for acetate. The relative abundance of these two groups is not only regulated by acetate concentrations, as in other environments, but also by feeding rates (2, 21). *Methanosaeta* perform better at high feeding rate digestors, such as upward-flow anaerobic sludge blanket (UASB), presumably due to their efficient adhesion and granulation (45, 107). In contrast, *Methanosarcina* are more sensitive to turbulence and shear, and they frequently dominate in fixed- and stirred- tank digestors (62).

The H_2 partial pressures in anaerobic digestors range from 2 Pa to 1200 Pa (2). Low H_2 levels indicate efficient hydrogenotrophic methanogenesis and are usually associated with stable performance. High H_2 levels (> 10 Pa) lead to inhibition of the anaerobic fermentation, and accumulation of electron sinks as lactate, ethanol, propionate, and butyrate. Therefore, efficient interspecies hydrogen transfer is quite important for good performance of anaerobic digestors. Formation of granular sludge facilitates interspecies hydrogen transfer by reducing the distance between H_2-producing bacteria and H_2-consuming methanogens (46). A wide variety of hydrogenotrophic methanogens belonging to *Methanomicrobiales* and *Methanobacteriales* are detected in and cultured from anaerobic digestors (79, 136).

Temperature and pH are two main parameters that influence methanogenesis in anaerobic digestors. Slightly thermophilic temperatures (50-60 ^{o}C) are desired in certain anaerobic

digestors to increase reaction rates and decrease retention times. The most common hydrogenotrophic methanogens in thermophilic digestors include *Methanothermobacter thermoautotrophicus* and *Methanoculleus thermophilicum* (52, 136). Aceticlastic methanogens generally can not grow at temperatures higher than 65 ^{o}C, thus limiting the temperature range of digestors. The most common aceticlastic methanogens in thermophilic digestors include *Methanosarcina thermophila* and thermophilic *Methanosaeta* (136, 137). The pH is another important parameter. Increases of loading rates lead to increases in the concentration of fatty acids and decreases in pH. Most methanogens grow optimally under neutral to slightly alkaline conditions (pH 6.8 – 8.5). Thus, acid tolerant methanogens are desired to improve the stability of anaerobic digestion. *Methanobrevibacter acididurans*, a methanogen isolated from a sour anaerobic digestor, grows in the pH range of 5.0-7.5 (103). Additions of *M. acididurans* to acidic digestors show better methanogenesis and decreases in accumulation of fatty acids (102).

Conclusions

Methanogens are very diverse in terms of phylogeny and ecology. Their ability to use methanogenesis as an anaerobic respiration allows them to occupy a physiologically unique niche which is unavailable to the Bacteria. They play an important role in the anaerobic food chain, driving anaerobic fermentation through removal of excess H_2 and formate. Their physiological diversity make them truly cosmopolitan in anaerobic environments. The relative abundance of different types of methanogens is regulated by the availability of substrates and

other parameters, for instance temperature, pH, and salinity. The diversity of methanogens is underestimated as indicated by recent culture-independent studies. Further physiological and ecological investigations are required to fully reveal the diversity and importance of methanogens.

References

1. **Abell, G. C. J., M. A. Conlon, and A. L. McOrist.** 2006. Methanogenic archaea in adult human faecal samples are inversely related to butyrate concentration. Microb. Ecol. Health Dis. **18:**154-160

2. **Aiyuk, S., I. Forrez, D. K. Lieven, A. van Haandel, and W. Verstraete.** 2006. Anaerobic and complementary treatment of domestic sewage in regions with hot climates--A review. Bioresour. Technol. **97:**2225-2241.

3. **Bak, F., and N. Pfennig.** 1991. Sulfate-reducing bacteria in littoral sediment of Lake Constance. FEMS Microbiol. Lett. **85:**43-52.

4. **Berk, H., and R. K. Thauer.** 1997. Function of coenzyme F_{420}-dependent NADP reductase in methanogenic archaea containing an NADP-dependent alcohol dehydrogenase. Arch. Microbiol. **168:**396-402.

5. **Bernalier, A., M. Lelait, V. Rochet, J.-P. Grivet, G. Gibson, and M. Durand.** 1996. Acetogenesis from H_2 and CO_2 by methane- and non-methane-producing human colonic bacterial communities FEMS Microbiol. Ecol. **19:**193-202.

6. **Biavati, B., M. Vasta, and J. G. Ferry.** 1988. Isolation and characterization of "*Methanosphaera cuniculi*" sp. nov. Appl. Environ. Microbiol. **54:**768-771.

7. **Bleicher, K., G. Zellner, and J. Winter.** 1989. Growth of methanogens on cyclopentanol/CO_2 and specificity of alcohol dehydrogenase. FEMS Microbiol. Lett. **59:**307-312.

8. **Bonin, A., and D. Boone.** 2006. The Order *Methanobacteriales*, p. 231-243, The Prokaryotes.

9. **Brauman, A., J. Dore, P. Eggleton, D. Bignell, J. A. Breznak, and M. D. Kane.** 2001. Molecular phylogenetic profiling of prokaryotic communities in guts of termites with different feeding habits. FEMS Microbiol. Ecol. **35:**27-36.

10. **Brauman, A., M. D. Kane, M. Labat, and J. A. Breznak.** 1992. Genesis of acetate and methane by gut bacteria of nutritionally diverse termites. Science **257:**1384-1387.

11. **Briee, C., D. Moreira, and P. Lopez-Garcia.** 2007. Archaeal and bacterial community composition of sediment and plankton from a suboxic freshwater pond. Res. Microbiol. **158:**213-227.

12. **Brune, A.** 1998. Termite guts: the world's smallest bioreactors. Trends Biotechnol. **16:**16-21.

13. **Burke, S. A., and J. A. Krzycki.** 1997. Reconstitution of monomethylamine:coenzyme M methyl transfer with a corrinoid protein and two methyltransferases purified from *Methanosarcina barkeri*. J. Biol. Chem. **272:**16570-16577.

14. **Capone, D. G., and R. P. Kiene.** 1988. Comparison of microbial dynamics in marine and freshwater sediments: contrasts in anaerobic carbon catabolism. Limnol. Oceanogr. **33:**725-749.

15. **Casper, P., O. Chim Chan, A. L. S. Furtado, and D. D. Adams.** 2003. Methane in an acidic bog lake: The influence of peat in the catchment on the biogeochemistry of methane. Aquat. Sci. **65:**36-46.

16. **Chan, O. C., P. Claus, P. Casper, A. Ulrich, T. Lueders, and R. Conrad.** 2005. Vertical distribution of structure and function of the methanogenic archaeal community in Lake Dagow sediment. Environ. Microbiol. **7:**1139-1149.

17. **Chan, O. C., M. Wolf, D. Hepperle, and P. Casper.** 2002. Methanogenic archaeal community in the sediment of an artificially partitioned acidic bog lake. FEMS Microbiol. Ecol. **42:**119-129.

18. **Chin, K.-J., and R. Conrad.** 1995. Intermediary metabolism in methanogenic paddy soil and the influence of temperature. FEMS Microbiol. Ecol. **18:**85-102.

19. **Chin, K.-J., T. Lukow, and R. Conrad.** 1999. Effect of temperature on structure and function of the methanogenic archaeal community in an anoxic rice field soil. Appl. Environ. Microbiol. **65:**2341-2349.

20. **Chin, K. J., T. Lueders, M. W. Friedrich, M. Klose, and R. Conrad.** 2004. Archaeal community structure and pathway of methane formation on rice roots. Microb. Ecol. **47:**59-67.

21. **Conklin, A., H. D. Stensel, and J. Ferguson.** 2006. Growth kinetics and competition between *Methanosarcina* and *Methanosaeta* in mesophilic anaerobic digestion. Water Environ. Res. **78:**486-96.

22. **Conrad, R.** 1999. Contribution of hydrogen to methane production and control of hydrogen concentrations in methanogenic soils and sediments. FEMS Microbiol. Ecol. **28:**193-202.

23. **Conrad, R., F. Bak, H. J. Seitz, B. Thebrath, H. P. Mayer, and H. Schutz.** 1989. Hydrogen turnover by psychrotrophic homoacetogenic and mesophilic methanogenic bacteria in anoxic paddy soil and lake sediment. FEMS Microbiol. Lett. **62:**285-293.

24. **Conrad, R., C. Erkel, and W. Liesack.** 2006. Rice Cluster I methanogens, an important group of Archaea producing greenhouse gas in soil. Curr. Opin. Microbiol. **17:**262-267.

25. **Conrad, R., M. Klose, and P. Claus.** 2000. Phosphate inhibits acetotrophic methanogenesis on rice roots. Appl. Environ. Microbiol. **66:**828-831.

26. **Daniels, L., G. Fuchs, R. K. Thauer, and J. G. Zeikus.** 1977. Carbon monoxide oxidation by methanogenic bacteria. J. Bacteriol. **132:**118-126.

27. **Dannenberg, S., and R. Conrad.** 1999. Effect of rice plants on methane production and rhizospheric metabolism in paddy soil. Biogeochemistry **45:**53-71.

28. **Dongowski, G., A. Lorenz, and H. Anger.** 2000. Degradation of pectins with different degrees of esterification by *Bacteroides thetaiotaomicron* isolated from human gut flora. Appl. Environ. Microbiol. **66:**1321-1327.

29. **Donovan, S. E., K. J. Purdy, M. D. Kane, and P. Eggleton.** 2004. Comparison of Euryarchaea strains in the guts and food-soil of the soil-feeding termite *Cubitermes fungifaber* across different soil types. Appl. Environ. Microbiol. **70:**3884-3892.

30. **Duncan, S. H., A. Barcenilla, C. S. Stewart, S. E. Pryde, and H. J. Flint.** 2002. Acetate utilization and butyryl coenzyme A (CoA):acetate-CoA transferase in butyrate-producing bacteria from the human large intestine. Appl. Environ. Microbiol. **68:**5186-5190.

31. **Ebert, A., and A. Brune.** 1997. Hydrogen concentration profiles at the oxic-anoxic interface: a microsensor study of the hindgut of the wood-feeding lower termite *Reticulitermes flavipes* (Kollar). Appl. Environ. Microbiol. **63:**4039-4046.

32. **Eckburg, P. B., E. M. Bik, C. N. Bernstein, E. Purdom, L. Dethlefsen, M. Sargent, S. R. Gill, K. E. Nelson, and D. A. Relman.** 2005. Diversity of the human Intestinal microbial flora. Science **308:**1635-1638.

33. **El Oufir, L., B. Flourie, S. Bruley des Varannes, J. L. Barry, D. Cloarec, F. Bornet, and J. P. Galmiche.** 1996. Relations between transit time, fermentation products, and hydrogen consuming flora in healthy humans. Gut **38:**870-7.

34. **Elberson, M. A., and K. R. Sowers.** 1997. Isolation of an aceticlastic strain of *Methanosarcina siciliae* from marine canyon sediments and emendation of the species description for *Methanosarcina siciliae*. Int. J. Syst. Bacteriol. **47:**1258-1261.

35. **Erkel, C., M. Kube, R. Reinhardt, and W. Liesack.** 2006. Genome of Rice Cluster I Archaea--the key methane producers in the rice rhizosphere. Science **313:**370-372.

36. **Ferguson, D. J., Jr., N. Gorlatova, D. A. Grahame, and J. A. Krzycki.** 2000. Reconstitution of dimethylamine:coenzyme M methyl transfer with a discrete corrinoid protein and two methyltransferases purified from *Methanosarcina barkeri*. J. Biol. Chem. **275:**29053-29060.

37. **Fetzer, S., F. Bak, and R. Conrad.** 1993. Sensirivity of methanogenic bacteria from paddy soil to oxygen and desiccation. FEMS Microbiol. Ecol. **12:**107-115.

38. **Fey, A., K. J. Chin, and R. Conrad.** 2001. Thermophilic methanogens in rice field soil. Environ. Microbiol. **3:**295-303.

39. **Florin, T. H. J., G. Zhu, K. M. Kirk, and N. G. Martin.** 2000. Shared and unique environmental factors determine the ecology of methanogens in humans and rats. Am. J. Gastroenterol. **95:**2872-2879.

40. **Fricke, W. F., H. Seedorf, A. Henne, M. Kruer, H. Liesegang, R. Hedderich, G. Gottschalk, and R. K. Thauer.** 2006. The genome sequence of *Methanosphaera stadtmanae* reveals why this human intestinal archaeon is restricted to methanol and H_2 for methane formation and ATP synthesis. J. Bacteriol. **188:**642-658.

41. **Frimmer, U., and F. Widdel.** 1989. Oxidation of ethanol by methanogenic bacteria. Arch. Microbiol. **152:**479-483.

42. **Garcia, J.-L., B. Ollivier, and W. Whitman.** 2006. The Order *Methanomicrobiales*, p. 208-230, The Prokaryotes.

43. **Glissman, K., K. J. Chin, P. Casper, and R. Conrad.** 2004. Methanogenic pathway and archaeal community structure in the sediment of Eutrophic Lake Dagow: effect of temperature. Microb. Ecol. **48:**389-399.

44. **Gro kopf, R., S. Stubner, and W. Liesack.** 1998. Novel euryarchaeotal lineages detected on rice roots and in the anoxic bulk soil of flooded rice microcosms. Appl. Environ. Microbiol. **64:**4983-9.

45. **Grotenhuis, J. T., M. Smit, C. M. Plugge, Y. S. Xu, A. A. van Lammeren, A. J. Stams, and A. J. Zehnder.** 1991. Bacteriological composition and structure of granular sludge adapted to different substrates. Appl. Environ. Microbiol. **57:**1942-1949.

46. **Grotenhuis, J. T. C., M. Smit, A. A. M. van Lammeren, A. J. M. Stams, and A. J. B. Zehnder.** 1990. Effect of interspecies hydrogen transfer on the bacteriological structure of methanogenic granular sludge.

47. **Hao, B., W. Gong, T. K. Ferguson, C. M. James, J. A. Krzycki, and M. K. Chan.** 2002. A new UAG-dncoded residue in the structure of a methanogen methyltransferase. Science **296:**1462-1466.

48. **Hedderich, R., and W. Whitman.** 2006. Physiology and biochemistry of the methane-producing Archaea, p. 1050-1079, The Prokaryotes.

49. **Hoehler, T. M., M. J. Alperin, D. B. Albert, and C. S. Martens.** 2001. Apparent minimum free energy requirements for methanogenic Archaea and sulfate-reducing bacteria in an anoxic marine sediment. FEMS Microbiol. Ecol. **38:**33-41.

50. **Hoehler, T. M., M. J. Alperin, D. B. Albert, and C. S. Martens.** 1998. Thermodynamic control on hydrogen concentrations in anoxic sediments. Geochim. Cosmochim. Acta. **62:**1745-1756.

51. **Hold, G. L., A. Schwiertz, R. I. Aminov, M. Blaut, and H. J. Flint.** 2003. Oligonucleotide probes that detect quantitatively significant groups of butyrate-producing bacteria in human feces. Appl. Environ. Microbiol. **69:**4320-4324.

52. **Hori, T., S. Haruta, Y. Ueno, M. Ishii, and Y. Igarashi.** 2006. Dynamic transition of a methanogenic population in response to the concentration of volatile fatty acids in a thermophilic anaerobic digester. Appl. Environ. Microbiol. **72:**1623-1630.

53. **Jensen, N. S., and E. Canale-Parola.** 1986. *Bacteroides pectinophilus* sp. nov. and *Bacteroides galacturonicus* sp. nov.: two pectinolytic bacteria from the human intestinal tract. Appl. Environ. Microbiol. **52:**880-887.

54. **Jetten, M. S. M., A. J. M. Stams, and A. J. B. Zehnder.** 1992. Methanogenesis from acetate: a comparison of the acetate metabolism in *Methanothrix soehngenii* and *Methanosarcina* spp. FEMS Microbiol. Lett. **88:**181-197.

55. **Joblin, K.** 2005. Methanogenic archaea, p. 47-53, Methods in Gut Microbial Ecology for Ruminants.

56. **Johnson, K. A., and D. E. Johnson.** 1995. Methane emissions from cattle. J. Anim. Sci. **73:**2483-2492.

57. **Joulian, C., B. Ollivier, B. K. C. Patel, and P. A. Roger.** 1998. Phenotypic and phylogenetic characterization of dominant culturable methanogens isolated from ricefield soils. FEMS Microbiol. Ecol. **25:**135-145.

58. **Kendall, M., and D. Boone.** 2006. The Order *Methanosarcinales*, p. 244-256, The Prokaryotes.

59. **Kendall, M. M., and D. R. Boone.** 2006. Cultivation of methanogens from shallow marine sediments at Hydrate Ridge, Oregon. Archaea. **2:**31-8.

60. **Kendall, M. M., Y. Liu, and D. R. Boone.** 2006. Butyrate- and propionate-degrading syntrophs from permanently cold marine sediments in Skan Bay, Alaska, and description of *Algorimarina butyrica* gen. nov., sp. nov. FEMS Microbiol. Lett. **262:**107-114.

61. **Kendall, M. M., G. D. Wardlaw, C. F. Tang, A. S. Bonin, Y. Liu, and D. L. Valentine.** 2007. Diversity of Archaea in marine sediments from Skan Bay, Alaska, including cultivated methanogens, and description of M*ethanogenium boonei* sp. nov. Appl. Environ. Microbiol. **73:**407-414.

62. **Kobayashi, H. A., E. C. Demacario, R. S. Williams, and A. J. L. Macario.** 1988. Direct characterization of methanogens in 2 high-rate anaerobic biological reactors Appl. Environ. Microbiol. **54:**693-698.

63. **Kruger, M., P. Frenzel, D. Kemnitz, and R. Conrad.** 2005. Activity, structure and dynamics of the methanogenic archaeal community in a flooded Italian rice field. FEMS Microbiol. Ecol. **51:**323-331.

64. **Krzycki, J. A.** 2005. The direct genetic encoding of pyrrolysine. Curr. Opin. Microbiol. **8:**706-712.

65. **Le Van, T. D., J. A. Robinson, J. Ralph, R. C. Greening, W. J. Smolenski, J. A. 燴. Leedle, and D. M. Schaefer.** 1998. Assessment of reductive acetogenesis with indigenous ruminal bacterium populations and *Acetitomaculum ruminis*. Appl. Environ. Microbiol. **64:**3429-3436.

66. **Leclerc, M., A. Bernalier, G. Donadille, and M. Lelait.** 1997. H_2/CO_2 Metabolism in acetogenic bacteria isolated from the human colon. Anaerobe **3:**307-315.

67. **Leclerc, M., J.-P. Delgenes, and J.-J. Godon.** 2004. Diversity of the archaeal community in 44 anaerobic digesters as determined by single strand conformation polymorphism analysis and 16S rDNA sequencing. Environ. Microbiol. **6:**809-819.

68. **Lessner, D. J., L. Li, Q. Li, T. Rejtar, V. P. Andreev, M. Reichlen, K. Hill, J. J. Moran, B. L. Karger, and J. G. Ferry.** 2006. An unconventional pathway for reduction of CO2 to methane in CO-grown *Methanosarcina acetivorans* revealed by proteomics. Proc. Natl. Acad. Sci. USA. **103:**17921-6. Epub 2006 Nov 13.

69. **Levitt, M. D., J. K. Furne, M. Kuskowski, and J. Ruddy.** 2006. Stability of human methanogenic flora over 35 years and a review of insights obtained from breath methane measurements. Clin. Gastroenterol. Hepatol. **4:**123-9.

70. **Lin, C., L. Raskin, and D. A. Stahl.** 1997. Microbial community structure in gastrointestinal tracts of domestic animals: comparative analyses using rRNA-targeted oligonucleotide probes. FEMS Microbiol. Ecol. **22:**281-294.

71. **Lowe, D. C.** 2006. Global change: A green source of surprise. Nature **439:**148-149.

72. **Lu, Y., T. Lueders, M. W. Friedrich, and R. Conrad.** 2005. Detecting active methanogenic populations on rice roots using stable isotope probing. Environ. Microbiol. **7:**326-336.

73. **Lueders, T., K.-J. Chin, R. Conrad, and M. Friedrich.** 2001. Molecular analyses of methyl-coenzyme M reductase alpha-subunit (mcrA) genes in rice field soil and enrichment cultures reveal the methanogenic phenotype of a novel archaeal lineage. Environ. Microbiol. **3:**194-204.

74. **Lueders, T., and M. Friedrich.** 2000. Archaeal population dynamics during sequential reduction processes in rice field soil. Appl. Environ. Microbiol. **66:**2732-2742.

75. **Lyimo, T. J., A. Pol, H. J. M. Op den Camp, H. R. Harhangi, and G. D. Vogels.** 2000. *Methanosarcina semesiae* sp. nov., a dimethylsulfide-utilizing methanogen from mangrove sediment. Int. J. Syst. Evol. Microbiol. **50:**171-178.

76. **Macfarlane, G. T., and G. R. Gibson.** 1994. Metabolic activities of the normal colonic flora. *In* G. SAW (ed.), Human health. The contribution of microorganisms. Dpringer Verlag, London.

77. **MacGregor, B. J., D. P. Moser, E. W. Alm, K. H. Nealson, and D. A. Stahl.** 1997. Crenarchaeota in Lake Michigan sediment. Appl. Environ. Microbiol. **63:**1178-1181.

78. **Mahapatra, A., A. Patel, J. A. Soares, R. C. Larue, J. K. Zhang, W. W. Metcalf, and J. A. Krzycki.** 2006. Characterization of a *Methanosarcina acetivorans* mutant unable to translate UAG as pyrrolysine. Mol. Microbiol. **59:**56-66.

79. **McHugh, S., M. Carton, T. Mahony, and V. O'Flaherty.** 2003. Methanogenic population structure in a variety of anaerobic bioreactors. FEMS Microbiol. Lett. **219:**297-304.

80. **Miller, T., and M. Wolin.** 1986. Methanogens in human and animal intestinal tracts. System. Appl. Microbiol.**:**223-229.

81. **Miller, T. L., and M. J. Wolin.** 1985. *Methanosphaera stadtmaniae* gen. nov., sp. nov.—a species that forms methane by reducing methanol with hydrogen. Arch. Microbiol. **141:**116-122.

82. **Miller, T. L., and M. J. Wolin.** 1985. *Methanosphaera stadtmaniae* gen. nov., sp. nov.: a species that forms methane by reducing methanol with hydrogen. Arch. Microbiol. **141:**116-122.

83. **Miller, T. L., M. J. Wolin, E. C. de Macario, and A. J. Macario.** 1982. Isolation of *Methanobrevibacter smithii* from human feces. Appl. Environ. Microbiol. **43:**227-232.

84. **Newberry, C. J., G. Webster, B. A. Cragg, R. J. Parkes, A. J. Weightman, and J. C. Fry.** 2004. Diversity of prokaryotes and methanogenesis in deep subsurface sediments from the Nankai Trough, Ocean Drilling Program Leg 190. Environ. Microbiol. **6:**274-287.

85. **Nicholson, M., P. Evans, and K. Joblin.** 2007. Analysis of methanogen diversity in the rumen using Temporal Temperature Gradient Gel Electrophoresis: identification of uncultured methanogens. Microb. Ecol.

86. **Nusslein, B., K.-J. Chin, W. Eckert, and R. Conrad.** 2001. Evidence for anaerobic syntrophic acetate oxidation during methane production in the profundal sediment of subtropical Lake Kinneret (Israel). Environ. Microbiol. **3:**460-470.

87. **O'Brien, J. M., R. H. Wolkin, T. T. Moench, J. B. Morgan, and J. G. Zeikus.** 1984. Association of hydrogen metabolism with unitrophic or mixotrophic growth of *Methanosarcina barkeri* on carbon monoxide. J. Bacteriol. **158:**373-375.

88. **Oremland, R. S., and S. Polcin.** 1982. Methanogenesis and sulfate reduction: competitive and noncompetitive substrates in estuarine sediments. Appl. Environ. Microbiol. **44:**1270-1276.

89. **Parkes, R. J., B. A. Cragg, N. Banning, F. Brock, G. Webster, J. C. Fry, E. Hornibrook, R. D. Pancost, S. Kelly, N. Knab, B. B. Jorgensen, J. Rinna, and A. J. Weightman.** 2007. Biogeochemistry and biodiversity of methane cycling in subsurface marine sediments (Skagerrak, Denmark). Environ. Microbiol. **9:**1146-1161.

90. **Peter Mayer, H., and R. Conrad.** 1990. Factors influencing the population of methanogenic bacteria and the initiation of methane production upon flooding of paddy soil. FEMS Microbiol. Lett. **73:**103-111.

91. **Phelps, T. J., and J. G. Zeikus.** 1984. Influence of pH on terminal carbon metabolism in anoxic sediments from a mildly acidic lake. Appl. Environ. Microbiol. **48:**1088-1095.

92. **Pinares-Patino, C. S., M. J. Ulyatt, K. R. Lassey, T. N. Barry, and C. W. Holmes.** 2003 Persistence of differences between sheep in methane emission under generous grazing conditions J. Agric. Sci. **140:**227-233.

93. **Pochart, P., J. Dore, F. Lemann, I. Goderel, and J. C. Rambaud.** 1992. Interrelations between populations of methanogenic archaea and sulfate-reducing bacteria in the human colon. FEMS Microbiol. Lett. **77:**225-8.

94. **Prather, M., and D. Ehhalt.** 2001. Atmospheric chemistry and greenhouse gases, p. 239-287. *In* J. T. Houghton, Y. Ding, D. J. Griggs, M. Noguer, P. J. v. d. Linden, X. Dai, K. Maskell, and C. A. Johnson (ed.), Climate Change 2001: The sicentific basis. Cambridge Univ. Press, Cambridge.

95. **Rother, M., and W. W. Metcalf.** 2004. Anaerobic growth of *Methanosarcina acetivorans* C2A on carbon monoxide: An unusual way of life for a methanogenic archaeon. Proc. Natl. Acad. Sci. USA. **101:**16929-16934.

96. **Rother, M., E. Oelgeschläger, and W. W. Metcalf.** 2007. Genetic and proteomic analyses of CO utilization by *Methanosarcina acetivorans*. Arch. Microbiol.

97. **Rothfuss, F., and R. Conrad.** 1992. Vertical Profiles of CH_4 concentrations, dissolved substrates and processes involved in CH_4 production in a flooded Italian rice field. Biogeochemistry **18:**137-152.

98. **Roy, R., H. D. Kluber, and R. Conrad.** 1997. Early initiation of methane production in anoxic rice soil despite the presence of oxidants. FEMS Microbiol. Ecol. **24:**311-320.

99. **Rutili, A., E. Canzi, T. Brusa, and A. Ferrari.** 2006. Intestinal methanogenic bacteria in children of different ages. New Microbiol. **19:**227-234.

100. **Samuel, B. S., E. E. Hansen, J. K. Manchester, P. M. Coutinho, B. Henrissat, R. Fulton, P. Latreille, K. Kim, R. K. Wilson, and J. I. Gordon.** 2007. Genomic and metabolic adaptations of *Methanobrevibacter smithii* to the human gut. Proc. Natl. Acad. Sci. USA. **104:**10643-10648.

101. **Sauer, K., U. Harms, and R. K. Thauer.** 1997. Methanol:coenzyme M methyltransferase from *Methanosarcina barkeri*. Purification, properties and encoding genes of the corrinoid protein MT1. Eur. J. Biochem. **243:**670-677.

102. **Savant, D. V., and D. R. Ranade.** 2004. Application of *Methanobrevibacter acididurans* in anaerobic digestion. Water Sci. Technol. **50:**109-14.

103. **Savant, D. V., Y. S. Shouche, S. Prakash, and D. R. Ranade.** 2002. *Methanobrevibacter acididurans* sp. nov., a novel methanogen from a sour anaerobic digester. Int. J. Syst. Evol. Microbiol. **52:**1081-1087.

104. **Schulz, S., and R. Conrad.** 1996. Influence of temperature on pathways to methane production in the permanently cold profundal sediment of Lake Constance. FEMS Microbiol. Ecol. **20:**1-14.

105. **Schulz, S., H. Matsuyama, and R. Conrad.** 1997. Temperature dependence of methane production from different precursors in a profundal sediment (Lake Constance). FEMS Microbiol. Ecol. **22:**207-213.

106. **Schutz, H., W. Seiler, and R. Conrad.** 1989. Processes involved in formation and emission of methane in rice paddies. Biogeochemistry **7:**33-53.

107. **Sekiguchi, Y., Y. Kamagata, K. Nakamura, A. Ohashi, and H. Harada.** 1999. Fluorescence in situ hybridization using 16S rRNA-targeted oligonucleotides reveals localization of methanogens and selected uncultured bacteria in mesophilic and thermophilic sludge granules. Appl. Environ. Microbiol. **65:**1280-1288.

108. **Singh-Wissmann, K., and J. G. Ferry.** 1995. Transcriptional regulation of the phosphotransacetylase-encoding and acetate kinase-encoding genes (*pta* and *ack)* from *Methanosarcina thermophila*. J. Bacteriol. **177:**1699-1702.

109. **Skillman, L. C., P. N. Evans, C. Strompl, and K. N. Joblin.** 2006. 16S rDNA directed PCR primers and detection of methanogens in the bovine rumen. Lett. Appl. Microbiol. **42:**222-228.

110. **Smith, K. S., and C. Ingram-Smith.** 2007. *Methanosaeta*, the forgotten methanogen? Trends Microbiol. **15:**150-155.

111. **Sowers, K. R., S. F. Baron, and J. G. Ferry.** 1984. *Methanosarcina acetivorans* sp. nov., an acetotrophic methane-producing bacterium isolated from marine sediments. Appl. Environ. Microbiol. **47:**971-978.

112. **Sprenger, W. W., J. H. P. Hackstein, and J. T. Keltjens.** 2007. The competitive success of *Methanomicrococcus blatticola*, a dominant methylotrophic methanogen in the cockroach hindgut, is supported by high substrate affinities and favorable thermodynamics. FEMS Microbiol. Lett. **60:**266-275.

113. **Sprenger, W. W., J. H. P. Hackstein, and J. T. Keltjens.** 2005. The energy metabolism of *Methanomicrococcus blatticola*: physiological and biochemical aspects. Antonie Leeuwenhoek **87:**289-299.

114. **Sprenger, W. W., M. C. van Belzen, J. Rosenberg, J. H. P. Hackstein, and J. T. Keltjens.** 2000. *Methanomicrococcus blatticola* gen. nov., sp. nov., a methanol- and methylamine-reducing methanogen from the hindgut of the cockroach *Periplaneta americana*. Int. J. Syst. Evol. Microbiol. **50:**1989-1999.

115. **Stewart, J. A., V. S. Chadwick, and A. Murray.** 2006. Carriage, quantification, and predominance of methanogens and sulfate-reducing bacteria in faecal samples. Lett. Appl. Microbiol. **43:**58-63.

116. **Strocchi, A., J. Furne, C. Ellis, and M. D. Levitt.** 1994. Methanogens outcompete sulphate reducing bacteria for H_2 in the human colon. Gut **35:**1098-101.

117. **Strocchi, A., J. K. Furne, C. J. Ellis, and M. D. Levitt.** 1991. Competition for hydrogen by human faecal bacteria: evidence for the predominance of methane producing bacteria. Gut **32:**1498-1501.

118. **Strocchi, A., and M. D. Levitt.** 1992. Factors affecting hydrogen production and consumption by human fecal flora. The critical roles of hydrogen tension and methanogenesis. J. Clin. Invest. **89:**1304-11.

119. **Tajima, K., T. Nagamine, H. Matsui, M. Nakamura, and R. I. Aminov.** 2001. Phylogenetic analysis of archaeal 16S rRNA libraries from the rumen suggests the existence of a novel group of archaea not associated with known methanogens. FEMS Microbiol. Lett. **200:**67-72.

120. **Teh, Y. L., and S. Zinder.** 1992. Acetyl-coenzyme A synthetase in the thermophilic, acetate-utilizing methanogen *Methanothrix* sp. strain CALS-1. FEMS Microbiol. Lett. **98:**1-7.

121. **Tholen, A., and A. Brune.** 1999. Localization and in situ activities of homoacetogenic bacteria in the highly compartmentalized hindgut of soil-feeding higher termites (*Cubitermes* spp.). Appl. Environ. Microbiol. **65:**4497-4505.

122. **Valentine, D.** 2002. Biogeochemistry and microbial ecology of methane oxidation in anoxic environments: a review. Antonie Leeuwenhoek **81:**271-282.

123. **von Klein, D., H. Arab, H. Volker, and M. Thomm.** 2002. *Methanosarcina baltica*, sp. nov., a novel methanogen isolated from the Gotland Deep of the Baltic Sea. Extremophiles **6:**103-10.

124. **Whitford, M., R. Teather, and R. Forster.** 2001. Phylogenetic analysis of methanogens from the bovine rumen. BMC Microbiol. **1:**5.

125. **Whiticar, M. J.** 1999. Carbon and hydrogen isotope systematics of bacterial formation and oxidation of methane. Chem. Geol. **161:**291-314.

126. **Whiticar, M. J., E. Faber, and M. Schoell.** 1986. Biogenic methane formation in marine and freshwater environments: CO2 reduction vs. acetate fermentation--Isotope evidence. Geochim. Cosmochim. Acta. **50:**693-709.

127. **Whitman, W., T. Bowen, and D. Boone.** 2006. The Methanogenic Bacteria, p. 165-207, The Prokaryotes.

128. **Whitman, W., and C. Jeanthon.** 2006. *Methanococcales*, p. 257-273, The Prokaryotes.

129. **Whitman, W. B., D. R. Boone, Y. Koga, and J. Keswani.** 2001. Taxonomy of methanogeic archaea, p. 211-213. *In* D. R. Boone, R. W. Castenholtz, and G. M. Garrity (ed.), Bergey's Manual of Systematic Bacteriology, 2 ed, vol. Springer, New York.

130. **Widdel, F.** 1986. Growth of methanogenic bacteria in pure culture with 2-propanol and other alcohols as hydrogen donors. Appl. Environ. Microbiol. **51:**1056-1062.

131. **Widdel, F., P. E. Rouvière, and R. S. Wolfe.** 1988. Classification of secondary alcohol-utilizing methanogens including a new thermophilic isolate. Arch. Microbiol. **150:**477-481.

132. **Widdel, F., and R. S. Wolfe.** 1989. Expression of secondary alcohol dehydrogenase in methanogenic bacteria and purification of the F_{420}-specific enzyme from *Methanogenium thermophilum* strain TCI. Arch. Microbiol. **152:**322-328.

133. **Wright, A.-D. G., A. J. Williams, B. Winder, C. T. Christophersen, S. L. Rodgers, and K. D. Smith.** 2004. Molecular diversity of rumen methanogens from sheep in Western Australia. Appl. Environ. Microbiol. **70:**1263-1270.

134. **Yadvika, Santosh, T. R. Sreekrishnan, S. Kohli, and V. Rana.** 2004. Enhancement of biogas production from solid substrates using different techniques--a review. Bioresour. Technol. **95:**1-10.

135. **Zepp Falz, K., C. Holliger, R. Grosskopf, W. Liesack, A. N. Nozhevnikova, B. Muller, B. Wehrli, and D. Hahn.** 1999. Vertical distribution of methanogens in the anoxic sediment of Rotsee (Switzerland). Appl. Environ. Microbiol. **65:**2402-2408.

136. **Zinder, S. H.** 1993. Physiological ecology of methanogens, p. 128-206. *In* J. G. Ferry (ed.), Methanogenesis: ecology, physiology, biochemistry and genetics. Chapman and Hall, New York.

137. **Zinder, S. H., T. Anguish, and S. C. Cardwell.** 1984. Effects of temperature on methanogenesis in a thermophilic (58 ^{o}C) anaerobic digestor. Appl. Environ. Microbiol. **47:**808-813.

Table 1-1. Sources of global methane emissions from identified sources (modified from (71, 94))

Sources	Methane emission (Tg of CH_4 per year)	Percentage (%)[a]
Natural sources		
Wetlands	92-237	15-40
Termites	20	3
Ocean	10-15	2-3
Methane hydrates	5-10	1-2
Subtotal	127-282	21-47
Anthropogenic sources		
Ruminants	80-115	13-19
Energy generation[b]	75-110	13-18
Rice agriculture	25-100	7-17
Landfills	35-73	6-12
Biomass burning	23-55	4-9
Waste treatment	14-25	2-4
Subtotal	267-478	45-80
Total sources	500-600	

[a] Estimates of the relative contribution of methane emission from a source to the total global emissions of 600 Tg of CH_4 per year.

[b] Methane deposits released by coal mining, petroleum drilling, and petrochemical production.

Table 1-2. Free energies and typical organisms of methanogenesis reactions. (Modified from (48, 136))

Reaction	$\Delta G^{o'}$ [a] (kJ/mol CH_4)	Organisms
I. CO_2-type		
$4\ H_2 + CO_2 \rightarrow CH_4 + 2\ H_2O$	-135	Most methanogens
$4\ HCOOH \rightarrow CH_4 + 3\ CO_2 + 2\ H_2O$	-130	Many hydrogenotrophic methanogens
CO_2 + 4 isopropanol $\rightarrow CH_4$ + 4 acetone + $2\ H_2O$	-37	Some hydrogenotrophic methanogens
$4\ CO + 2H_2O \rightarrow CH_4 + 3\ CO_2$	-196	*Methanothermobacter* and *Methanosarcina*
II. Methylated C1 compounds		
$4\ CH_3OH \rightarrow 3\ CH_4 + CO_2 + 2\ H_2O$	-105	*Methanosarcina* and other methylotrophic methanogens
$CH_3OH + H_2 \rightarrow CH_4 + H_2O$	-113	*Methanomicrococcus blatticola* and *Methanosphaera*
$2\ (CH_3)_2$-S + $2\ H_2O \rightarrow 3\ CH_4 + CO_2$ + $2\ H_2S$	-49	Some methylotrophic methanogens
$4\ CH_3$-$NH_2 + 2\ H_2O \rightarrow 3\ CH_4 + CO_2$ + $4\ NH_3$	-75	Some methylotrophic methanogens
$2\ (CH_3)_2$-NH + $2\ H_2O \rightarrow 3\ CH_4$ + $CO_2 + 2\ NH_3$	-73	Some methylotrophic methanogens
$4\ (CH_3)_3$-N + $6\ H_2O \rightarrow 9\ CH_4$ + $3\ CO_2 + 4\ NH_3$	-74	Some methylotrophic methanogens
$4\ CH_3NH_3Cl + 2\ H_2O \rightarrow 3\ CH_4$ + $CO_2 + 4\ NH_4Cl$	-74	Some methylotrophic methanogens
III. Acetate		
$CH_3COOH \rightarrow CH_4 + CO_2$	-33	*Methanosarcina* and *Methanosaeta*

[a] The standard changes in free energies were calculated from the free energy of formation of the most abundant ionic species at pH 7. For instance, CO_2 is $HCO_3^- + H^+$ and HCOOH is $HCOO^- + H^+$.

Table 1-3. Properties of major taxonomic groups of methanogens.

			Methanogenesis Substrates [a]	Temperature Optimum (^{o}C)	Typical Habitats
Order *Methanobacteriales*					
Family	*Methanobacteriaceae*				
	Genus	*Methanobacterium*	H_2, (formate)	37-45	anaerobic digestors, freshwater sediments, marshy soils, rumen
		Methanobrevibacter	H_2, formate	37-40	animal gastrointestinal tracts, anaerobic digestors, rice paddies, decaying woody tissues
		Methanosphaera[b]	H_2 + methanol	37	animal gastrointestinal tracts
		Methanothermobacter	H_2, (formate)	55-65	anaerobic digestors
Family	*Methanothermaceae*				
	Genus	*Methanothermus*	H_2	80-88	hot springs
Order *Methanococcales*					
Family	*Methanococcaceae*				
	Genus	*Methanococcus*	H_2, formate	35-40	marine sediments
		Methanothermococcus	H_2, formate	60-65	marine geothermal sediments
Family	*Methanocaldococcaceae*				
	Genus	*Methanocaldococcus*	H_2	80-85	marine geothermal sediments
		Methanotorris	H_2	88	marine geothermal sediments

Order *Methanomicrobiales*					
Family	*Methanomicrobiaceae*				
	Genus	*Methanomicrobium*	H_2, formate	40	anaerobic digestors, ground water, rumen
		Methanoculleus	H_2, formate	20-55	anaerobic digestors, marine sediments, freshwater sediments, rice paddies, oil fields, hot springs
		Methanofollis	H_2, formate	37-40	anaerobic digestors
		Methanogenium	H_2, formate	15-57	marine sediments, freshwater sediments, rice paddies, animal gastrointestinal tracts
		Methanolacinia	H_2	40	marine sediments
		Methanoplanus	H_2, formate	32-40	oil fields
Family	*Methanospirillaceae*				
		Methanospirillum	H_2, formate	30-37	anaerobic digestors, marine sediments
Family	*Methanocorpusculaceae*				
	Genus	*Methanocorpusculum*	H_2, formate	30-40	anaerobic digestors, freshwater sediments
		Methanocalculus [b]	H_2, formate	30-40	oil fields
Order *Methanosarcinales*					
Family	*Methanosarcinaceae*				
	Genus	*Methanosarcina*	(H_2), $MeNH_2$, Acetate	35-60	anaerobic digestors, marine sediments, freshwater sediments, rumen

		Methanococcoides	$MeNH_2$	23-35	marine sediments
		Methanohalobium	$MeNH_2$	40-55	hypersaline sediments
		Methanohalophilus	$MeNH_2$	35-40	hypersaline sediments
		Methanolobus	$MeNH_2$	37	hypersaline sediments
		Methanomethylovorans	$MeNH_2$	20-50	freshwater sediments, anaerobic digestors
		Methanimicrococcus	$H_2 + MeNH_2$	39	animal gastrointestinal tracts
		Methanosalsum	$MeNH_2$	35-45	hypersaline sediments
Family	*Methanosaetaceae*				
	Genus	*Methanosaeta*	Acetate	35-60	anaerobic digestors, freshwater sediments
Order *Methanopyrales*					
Family	*Methanopyraceae*				
	Genus	*Methanopyrus*	H_2	98	marine geothermal sediments

[a] Major substrates utilized for methanogenesis. $MeNH_2$ is methylamine. Parentheses means utilized by some but not all species or strains.

[b] Placement in higher taxon is tentative.

Table 1-4. Methanogens cultured from human and animal gastrointestinal tracts

Hosts	**Representative methanogen species**
Human	*Methanobrevibacter smithii*; *Methanosphaera stadtmanae*
Bovine	*Methanobrevibacter ruminantium*; *Methanobrevibacter thaueri*; *Methanobrevibacter smithii*; *Methanosarcina barkeri*; *Methanobacterium formicicum*; *Methanobrevibacter millerae*; *Methanobacterium mobilis*
Ovine	*Methanosarcina barkeri*; *Methanobacterium formicicum*; *Methanobrevibacter olleyae*; *Methanobrevibacter wolinii*
Termite	*Methanobrevibacter cuticularis; Methanobrevibacter curvatus; Methanobrevibacter filiformis*; *Methanobacterium bryantii*
Cockroach	*Methanomicrococcus blatticola*

Figure 1-1. Pathways of methanogenesis. (**A)** Methanogenesis from H_2/CO_2 or formate. (**B)** Methanogenesis from methanol. (**C)** Methanogenesis from acetate. Abbreviations: Fd_{red}, reduced form of ferredoxin; Fd_{ox}; oxidized form of ferredoxin; $F_{420}H_2$, reduced form coenzyme F_{420}; MFR, methanofuran; H_4MPT, tetrahydromethanopterin; CoM-SH, coenzyme M; CoB-SH, coenzyme B; CoM-S-S-CoB, heterodisulfide of CoM and CoB; CoA-SH, coenzyme A. Enzymes: 1. formyl-MFR dehydrogenase (Fmd); 2. formyl-MFR:H_4MPT formyl-transferase (Ftr); 3. methenyl-H_4MPT cyclohydrolase (Mch); 4. methylene-H_4MPT dehydrogenase (Hmd); 5. methylene-H_4MPT reductase (Mer); 6. methyl-H_4MPT:HS-CoM methyltransferase (Mtr); 7. methyl-CoM reductase (Mcr); 8. heterodisulfide reductase (Hdr); 9. formate dehydrogenase (Fdh); 10. energy conserving hydrogenase (Ech); 11. F_{420}-reducing hydrogenases; 12. methyltransferase; 13. acetate kinase (AK)-phosphotransacetylase (PTA) system in *Methanosarcina*; AMP-forming acetyl-CoA synthetase in *Methanosaeta*; 14. CO dehydrogenase/acetyl-CoA synthase (CODH/ACS).

(A)

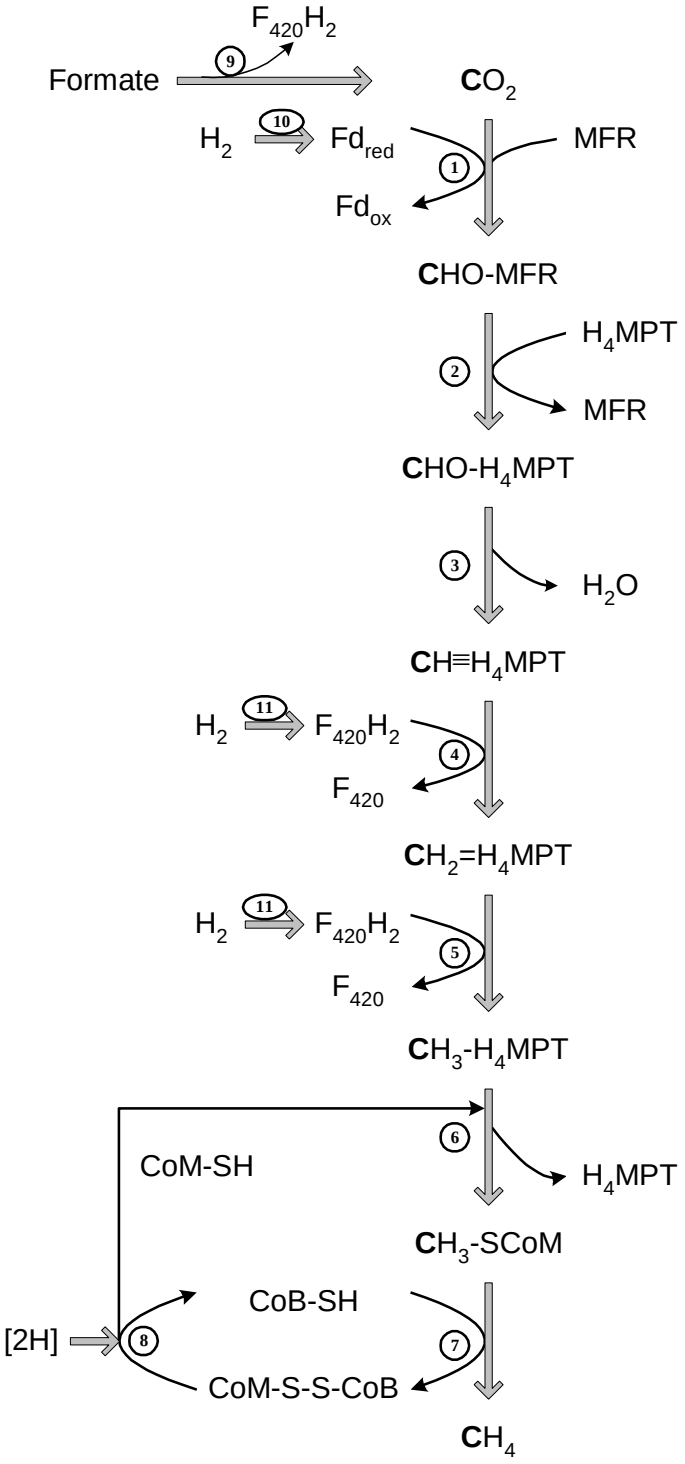
F420H2
9
Formate
CO2
H2
10
Fdred
MFR
1
Fdox
CHO-MFR
H4MPT
2
MFR
CHO-H4MPT
3
H2O
CH≡H4MPT
H2
11
F420H2
4
F420
CH2=H4MPT
H2
11
F420H2
5
F420
CH3-H4MPT
6
CoM-SH
H4MPT
CH3-SCoM
CoB-SH
[2H]
8
7
CoM-S-S-CoB
CH4

(B)

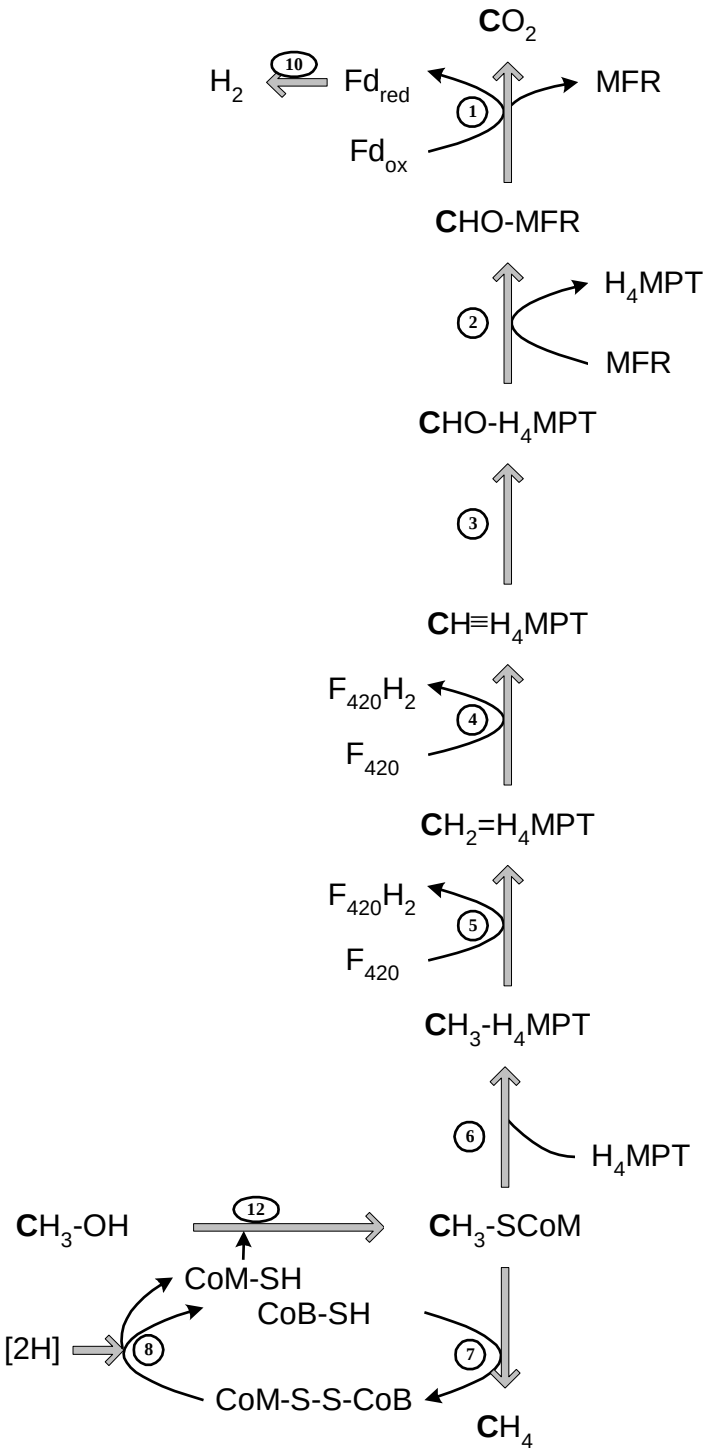
CO2
H2
10
Fdred
MFR
1
Fdox
CHO-MFR
H4MPT
2
MFR
CHO-H4MPT
3
CH≡H4MPT
F420H2
4
F420
CH2=H4MPT
F420H2
5
F420
CH3-H4MPT
6
H4MPT
CH3-OH
12
CH3-SCoM
CoM-SH
CoB-SH
[2H]
8
7
CoM-S-S-CoB
CH4

(C)

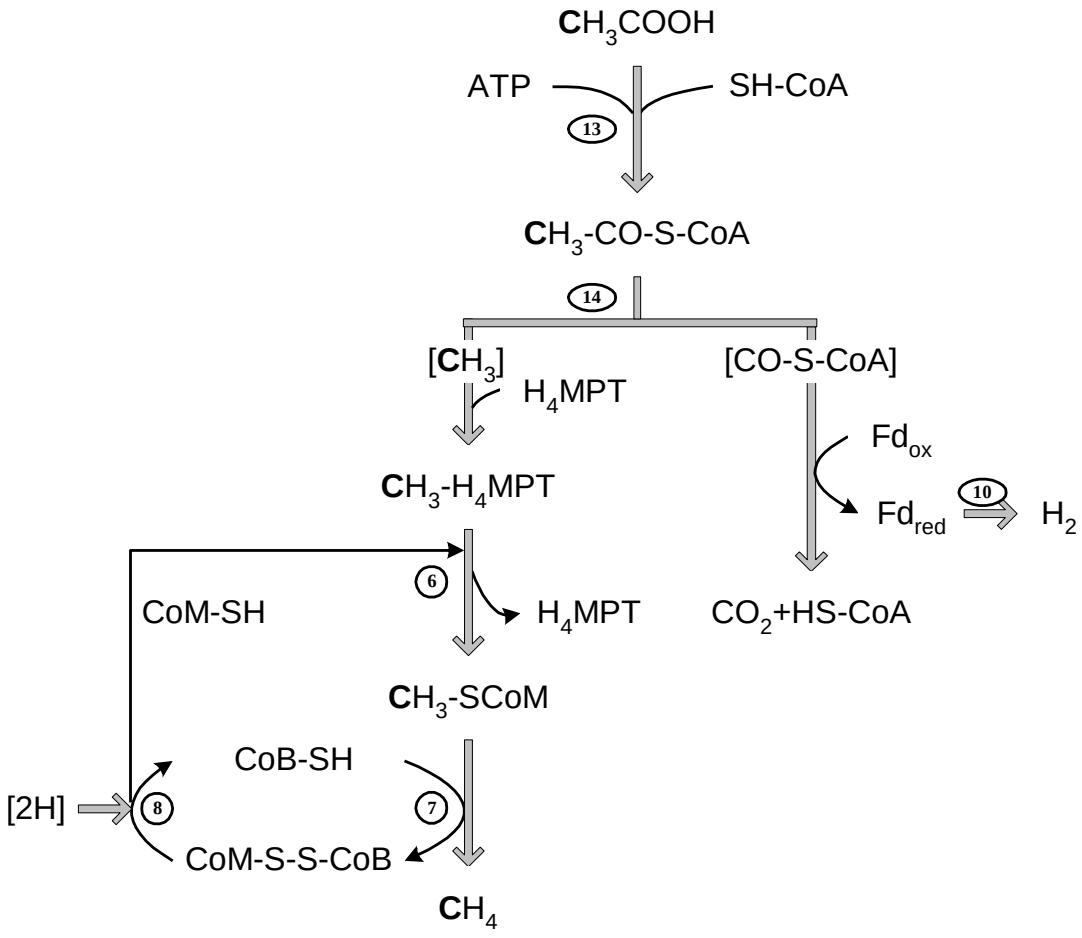
CH3COOH
ATP
SH-CoA
13
CH3-CO-S-CoA
14
[CH3]
[CO-S-CoA]
H4MPT
Fdox
CH3-H4MPT
Fdred
10
H2
6
CoM-SH
H4MPT
CO2+HS-CoA
CH3-SCoM
CoB-SH
[2H]
8
7
CoM-S-S-CoB
CH4

Figure 1-2. Anaerobic food chain for the conversion of organic matter to methane. Major microbial groups catalyzing the reactions are in ellipses.

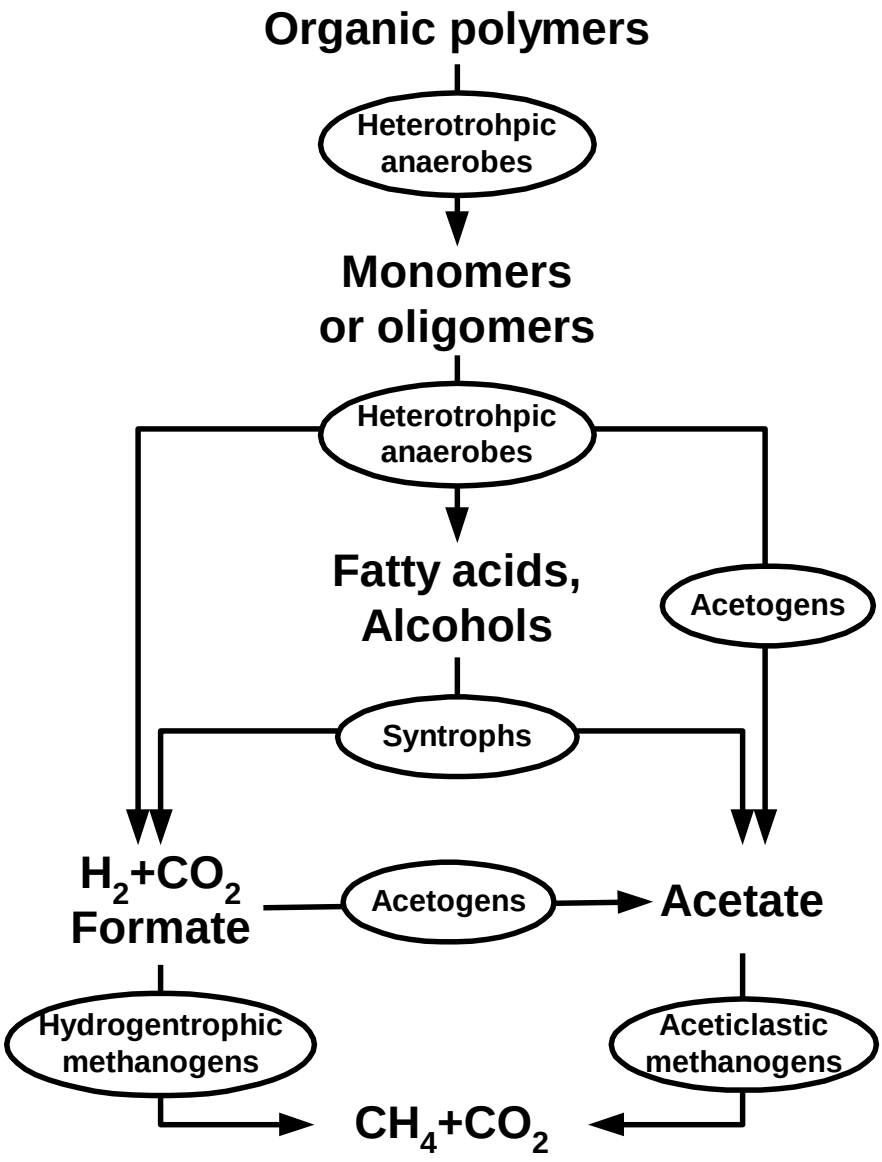
Organic polymers
Heterotrohpic anaerobes
Monomers or oligomers
Heterotrohpic anaerobes
Fatty acids, Alcohols
Acetogens
Syntrophs
H_2+CO_2 Formate
Acetogens
Acetate
Hydrogentrophic methanogens
Aceticlastic methanogens
CH_4+CO_2

CHAPTER 2

THE SAC10B HOMOLOG IN *METHANOCOCCUS MARIPALUDIS* BINDS DNA AT SPECIFIC SITES[2]

---

[2]Liu, Y., L. Guo, R. Guo, R. L. Wong, H. Hernandez, J. Hu, Y. Chu, I. J. Amster, W. B. Whitman, and L. Huang. 2009. The Sac10b Homolog in *Methanococcus maripaludis* Binds DNA at Specific Sites. J. Bacteriol. 191(7):2315-2329.

Abstract

The Sac10b protein family, also known as Alba, is widely distributed in Archaea. Sac10b homologs in thermophilic *Sulfolobus* species are very abundant. They bind both DNA and RNA with high affinity and without sequence specificity, and their physiological functions are still not fully understood. Mma10b from the euryarchaeote *Methanococcus maripaludis* is a mesophilic member of the Sac10b family. Mma10b is not abundant and constitutes only ~ 0.01% of the total cellular protein. Disruption of *mma10b* resulted in poor growth of the mutant in minimal medium at near the optimal growth temperature but had no detectible affect on growth in rich medium. Quantitative proteomics, real time RT-PCR, and enzyme assays revealed that the expression levels of some genes involved in CO_2 assimilation and other activities were changed in the Δ*mma10b* mutant. Chromatin immunoprecipitation suggested a direct association of Mma10b with an 18-bp DNA binding motif *in vivo*. Electrophoretic mobility shift assays and DNase I footprinting confirmed that Mma10b preferentially binds specific sequences of DNA with an apparent K_d in the 100 nM range. These results suggested that the physiological role of Mma10b in the mesophilic methanococci is greatly diverged from homologs in thermophiles.

Introduction

Proteins of the Sac10b protein family (also called Alba) are proposed to be a major type of chromosome-associated proteins in Archaea [reviewed in (33)]. Sac10b homologs have been identified in all archaea whose genomes have been sequenced except for the mesophilic euryarchaeotes belonging to *Halobacteria* and *Methanosarcinales* (9). The proteins from the hyperthermophilic archaea of the genus *Sulfolobus* have been extensively studied, but their physiological functions are not well established.

Sac10b homologs show high affinities for DNA and bind cooperatively to DNA without apparent sequence specificity (24, 44). The proteins are able to constrain DNA into negative supercoils, and this ability is dramatically enhanced at temperatures higher than 45^{o}C (50). Therefore, it is possible that the proteins affect DNA compaction at temperatures optimal for the growth of the hyperthermophiles. Given their DNA-binding properties and abundance in thermophiles, these proteins have been proposed to play a role in DNA protection and stability at high temperature (18, 50). Native Sso10b from *S. solfataricus* is acetylated on Lys16, and acetylation decreases the affinity of the protein for DNA (4). Thus, the Sac10b protein family is also referred to as ‗Alba', which stands for ―acetylation lowers binding affinity". The deacetylase Sir2 associates with Sso10b *in vivo* (4), and the transacetylase Pat acetylates Sso10b specifically on Lys16 *in vitro* (26). The presence of a reversible Sso10b acetylation system suggests a histone-like reversible modification of Sac10b homologs, which could be important for controlling DNA availability for replication, transcription, and recombination. A role of Sac10b homologs in transcriptional regulation is also supported by the observation that deacetylation of Sso10b by Sir2 mediated transcriptional repression in an *in vitro* transcription system (4). The Sir2/Pat system is absent in many euryarchaeotes including methanococci.

However, other acetyltransferases, e.g. Elp3 homologs, could be functional in the modification of Sac10b homologs and the regulation of DNA compaction (45).

Although originally identified as DNA-binding proteins, the Sac10b family proteins also bind RNA. The overall structure of Sso10b resembles the RNA-binding IF3-C fold (44). Moreover, phylogenetic analysis indicates that the Sac10b family is related to two eukaryotic protein families involved in RNA-binding (2). Ssh10b from *Sulfolobus shibatae* binds both DNA and RNA *in vitro*, and RNAs are bound *in vivo* (11). In addition, both DNase and RNase release Sso10b from cellular nucleic acid-protein complexes, suggesting that this protein is associated with both DNA and RNA *in vivo* (26).

Although genes encoding Sac10b homologs have been identified in mesophiles, none of these proteins has been biochemically characterized. Therefore, it is of interest to compare these homologs to their counterparts from the hyperthermophiles, especially in view of the suggestion that the latter may be involved in thermal adaptation. Methanococci are hydrogenotrophic methanogens belonging to the phylum Euryarchaeota and are classified into genera depending in part upon their growth temperatures. The genera *Methanococcus*, *Methanothermococcus*, and *Methanocaldococcus* have optimal growth temperatures of 35-40^{o}C, 60-65^{o}C, and 68-85^{o}C, respectively (46). The presence of Sac10b homologs in all these organisms permits a comparison of properties of the Sac10b homologs at different growth temperatures. In addition, the readily available genetic systems in mesophilic methanococci are of value for the investigation of the *in vivo* role of the Sac10b family. Heinicke *et al*. (13) constructed a deletion mutant of the mesophilic, heterotrophic *Methanococcus voltae* for the gene encoding a Sac10b homolog. While the mutation did not affect growth in complex medium, two-dimensional gel electrophoresis of the cellular proteins identified changes in the

expression of genes encoding a helx-turn-helix (HTH) DNA-binding protein, a cystathionine β-synthase (CBS) domain-containing protein, and pyruvate oxidoreductase subunit C (13).

In this study, Mma10b from *Methanococcus maripaludis* was characterized to elucidate the physiological properties of Sac10b homologs in mesophiles. The expression level of Mma10b, the Sac10b homolog from *M. maripaludis*, was the least abundant as compared to the Sac10b homologs from the extreme thermophile *Methanothermococcus thermolithotrophicus* and the hyperthermophile *Methanocaldococcus jannaschii*. Disruption of the gene encoding Mma10b in *M. maripaludis* limited autotrophic growth and resulted in changes of the expression of several genes. A ChIP assay detected specific associations of Mma10b with the coding regions of genes *in vivo*. The association of Mma10b with DNA was sequence-dependent *in vitro*. These results suggested that the role of Mma10b differs greatly from homologs in thermophiles.

Materials and Methods

Strains, media and culture conditions. The strans and plasmids used in this study are listed in Table 2-1. *M. maripaludis* was grown in 28-ml aluminum seal tubes with 275 kPa of H_2:CO_2 (80:20 [v:v]) at 37^{o}C in 5 ml of McN (minimal medium), McNA (McN + 10 mM sodium acetate), McNAla (McN + 1 mM alanine), McNY (McN + 0.2% [wt/vol] yeast extract), or McC (McNA + 0.2% [wt/vol] Casamino acids + 0.2% [wt/vol] yeast extract) as described previously (47). Antibiotics were not included when comparing the growth of the wild-type and mutants. The inocula were 0.1 ml of cultures grown in the same medium. The inocula for cultures of the mutant S590 and the strain S591 were started with frozen stocks for all experiments to ensure that a revertant at second loci had not been selected. Puromycin (2.5 μg/ml) was added when needed. The growth was determined by measuring the increase in

absorbance at 600 nm. In general, the exponential growth of methanococci was only observed at low cell densities or below an absorbance of 0.4, and cells entered a linear growth phase at higher cell densities due to the low solubility of H_2.

Protein expression and purification. The full-length genes for Sac10b homologs from *M. jannaschii*, *M. thermolithotrophicus*, *M. voltae*, and *M. maripaludis* were PCR amplified from genomic DNA (primer sequences are available upon request).

For the expression of Mja10b, the PCR product was digested with NdeI and BamHI, and ligated into pET11a (Novagen), yielding the expression vector pET11a-mja10b. *E. coli* BL21 (DE3) cells were transformed with pET11a-mja10b and grown at 37^{o}C in LB medium supplemented with 0.1 mg/ml ampicillin until the absorbance at 600 nm reached 0.8-1.0. The expression of Mja10b was induced for 3-4 hours by adding isopropyl-1-thio-β-D-galactopyranoside (IPTG) to a final concentration of 1 mM. Cells were harvested by centrifugation, resuspended in buffer A [30 mM potassium phosphate (pH 6.6), 0.1 mM EDTA and 1 mM DTT], and lysed by sonication. The lysate was centrifuged at 150,000 g for 30 min, and the supernatant was heated for 15 min at 75°C. After centrifugation, the supernatant was applied to a 1-ml Mono S column (Pharmacia). Proteins bound to the column were eluted with a KCl gradient from 0 to 1 M in buffer A. Fractions containing Mja10b were pooled and dialyzed against 10 mM potassium phosphate buffer (pH 7.0) and 10% glycerol (wt/vol).

For the expression of Mth10b, Mma10b, and Mvo10b, the PCR products were digested with restriction enzymes and ligated into pET15b containing a His-tag sequence (Novagen). Transformation and protein expression were carried out as described above for Mja10b. After harvesting, cells were resuspended in buffer B [20 mM potassium phosphate buffer (pH 7.4), 0.5 M NaCl, 1 mM DTT, and 10% glycerol (wt/vol)], and lysed by sonication. The lysates were

centrifuged at 150,000 g for 30 min, and the supernatants were applied to a 1-ml Histrap affinity column (Pharmacia). Proteins bound to the column were eluted with an imidazole gradient from 0.05 to 0.5 M. Protein fractions containing the Sac10b homolog were pooled and dialyzed against 10 mM potassium phosphate buffer (pH 7.0) and 10% glycerol (wt/vol). After purification, the N-terminal His-tag of the protein was cleaved using the THROMBIN CleanCleave^{TM} kit (Sigma).

The homogeneity of purified proteins was confirmed by SDS polyacrylamide gel electrophoresis (Supplementary figure S2-1).

Quantitative immunoblotting. Mja10b, Mth10b, and Mma10b, which were purified to homogeneity, were injected to rabbits to generate polyclonal antiserum. For the Western blot of Mma10b, crude extracts (containing ~400 μg protein) from *M. maripaludis* strain S2, S590, and S591 and recombinant Mma10b (25-200 ng) were loaded onto a 12% SDS polyacrylamide gel. After electrophoresis, proteins were electrophoretically transferred onto a PVDF membrane (Bio-Rad). The membrane was then incubated sequentially with rabbit anti-Mma10b antiserum and goat anti-rabbit IgG conjugated to horseradish peroxidase (Bio-Rad). The immunoblots were developed with SuperSignal West Femto Maximum Sensitivity Substrate (Pierce) and exposed to CL-XPosure film (Pierce). For the Western blot of Mja10b and Mth10b, crude extract (containing 60 and 200 μg of protein) from *M. jannaschii* and *M. thermolithotrophicus*, respectively, was loaded onto 12% SDS polyacrylamide gel, electrophoretically transferred onto a PVDF membrane (Bio-Rad), incubated sequentially with rabbit antiserum and goat anti-rabbit IgG conjugate to alkaline phosphatase (Bio-Rad), and visualized with nitroblue tetrazolium chloride and 5-bromo-4-chloro-3-indolyl phosphate (Promega).

Measurement of protein aggregation. Aggregation of Sac10b homologs following heat treatment was monitored by 90^{o} light scattering at 488 nm on a Shimadzu RF5301PC spectrofluorimeter. The proteins (0.1 mg/ml) were incubated at indicated temperatures for various lengths of time in 10 mM potassium phosphate buffer (pH 7.0) and 10% glycerol (wt/vol). The effect of salt on protein aggregation was determined by comparing incubations with no addition of salt and with 400 mM KCl.

Construction of the Δ*mma10b*::*pac* mutant. The mutant was made by transformation of the wild-type *M. maripaludis* strain S2 with pMma10b, which was constructed from the integration vector pIJA03. The plasmid pIJA03 lacks the origin of replication for methanococci and contains a *pac* cassette, which encodes puromycin resistance (10, 21). To construct pIJA03-mma10b, a 937 bp region upstream and a 969 bp region downstream of the *mma10b* gene was PCR amplified and cloned into MCS1 and MCS2 of pIJA03, respectively. The orientation of each insert was confirmed by restriction mapping.

pIJA03-mma10b was transformed into *M. maripaludis* strain S2 by the polyethylene glycol method (42). After transformation, cultures were plated on McC medium plus puromycin. Puromycin-resistant isolates were restreaked on the same medium, and isolated colonies were then transferred to broth cultures containing 5 ml McC medium plus puromycin. After growth, 2 ml of the culture were used for determination of the genotype and phenotype. The remaining culture was used for preparation of frozen stocks (41).

The genotype of the Δ*mma10b*::*pac* mutant (S590) was confirmed by Southern hybridization. Southern hybridizations were performed using the DIG High Prime DNA Labeling and Detection Starter Kit I (Roche, Mannheim, Germany). The DNA template of the probe was made by digestion of pIJA03-mma10b with *Kpn*I and *Nhe*I. These sites were in the

multiple cloning sites that flanked the downstream PCR products. The 972 bp fragment was purified by agarose gel electrophoresis and gel extraction using the QIAquick Gel Extraction Kit (Qiagen, CA, USA). The genomic DNA was digested with *Bgl*II and then hybridized with the probe. The hybridization with S2 and S590 genomic DNA generated expected products of ~2,300 bp and ~ 3,400 bp, respectively.

For complementation, the *mma10b* gene with the 100 bp upstream region was PCR amplified. The PCR products and the shuttle vector pMEV2 (21) were digested with XhoI and BglII and purified from gel. The cloning of the PCR products into the digested pMEV2 replaced the strong promoter PhmvA with the native promoter of *mma10b*. The resulting plasmid, pMEV2-mma10b, was transformed into S590 and screened on McC plates containing neomycin as previously described (21). The complementation strain was named S591.

Enzyme assays. The Por and CODH/ACS activities were determined as described (22). *M. maripaludis* strains S2, S590, and S591 were grown in McN medium to an absorbance at 600 nm of about 0.4. The cells from 100 ml cultures were harvested anaerobically by centrifugation and resuspended in assay buffer containing 100 mM potassium Tricine (pH 8.6), 5 mM $MgCl_2$, and 1 mM thiamine pyrophosphate. The cells were lysed by freezing at -20^{o}C. Unbroken cells were removed by centrifugation at 10,000 g for 10 min at room temperature. The protein concentrations were determined by Bradford protein assays (Bio-Rad). One unit of enzyme activity was defined as 1 μmol of methyl viologen reduced per minute.

Differential ^{14}N:^{15}N- labeling of proteins. To prepare differentially ^{14}N:^{15}N labeled proteins, the wild-type strain S2 and the Δ*mma*10b mutant S590 were grown in McNA medium containing either 4.6 mM unlabeled [^{14}N] ammonium sulfate or 4.6 mM ≥99% [^{15}N] ammonium sulfate in sidearm bottles. These bottles were manufactured from 160 ml serum bottles by fusing

a 28-ml aluminum seal tube to the side. They could be pressurized to 138 kPa and contained 10 ml of culture. To prevent contamination with other nitrogen compounds, glassware was immersed in 1 M HCl overnight, rinsed with deionized water and dried before use. Rubber stoppers were autoclaved for 20 min in 0.5 M NaOH and rinsed thoroughly with deionized water. Cultures were inoculated a day after adding sulfide and ammonium sulfate to the medium. The inocula were 0.1 ml of cultures grown in the same medium. After inoculation, cultures were initially pressurized to 138 kPa with H_2/ CO_2 gas (80:20 [vol/vol]) and repressurized twice daily. When S2 and S590 cultures reached an average absorbance at 600 nm of 0.54, four cultures of the unlabeled S2 and four cultures of ^{15}N-labeled S590 were mixed together to generate sample A. The reverse labeled cultures were mixed to generate sample B. Cells were harvested by centrifugation at 10,000 g for 30 min at 4^{o}C. The pellets were suspended in 0.5 ml of 100 mM ammonium bicarbonate buffer (pH 7.8), and 5 µl of 0.5 M PMSF was added to inhibit protease activity. The cells were lysed by freezing at -20^{o}C. Upon thawing, 10 U of DNase I were added to the cell lysate, and the crude extracts were incubated at room temperature for 1 hour. After DNA digestion, the crude extracts were centrifuged at 16,000 g for 30 min to remove unbroken cells. Because of the carry over of $^{14}NH_4Cl$ from the inocula, the proteins from cultures grown with [^{15}N] ammonium sulfate were ~98% enriched with [^{15}N].

Quantitative proteomics. The protein digestion, fractionation, and mass spectrometry were performed as described (48). The accurate mass of each peptide was obtained from the m/z of monoisotopic peaks. The number of nitrogen atoms in each peptide was determined from the mass separation between the monoisotopic peaks of the peptide and its ^{15}N- enriched counterpart. The identification of peptides was automated using the software as described (48). A measured mass peak was considered identified when it was within 10 ppm of the mass of a predicted

tryptic peptide that had the same nitrogen content. A protein (ORF) was considered identified when at least one unique peptide, i.e. predicted to be present in only one ORF, was identified.

Multiple peptide pairs from the same ORF were usually detected because more than one unique peptide was detected for many proteins, and most peptides were detected in multiple MALDI spots. The number of peptide pairs collected per ORF was designated as ~~"n~~". The relative signal intensity (peak height) of ^{14}N and ^{15}N peptide peaks in each peak pair was used as a measure of relative peptide level. Multiple measurements of one protein were averaged to obtain the relative protein level in S2 and S590. The average relative protein levels for all proteins were normalized to 1. Differential protein levels were regarded as significant if N was ≥ 2, the normalized relative protein levels were not between 0.7 and 1.5 (equivalent to > 1.5 fold changes), and the 95% confidence interval for the normalized ratio did not include the value 1.00.

Real time RT-PCR. To compare the levels of gene expression in the wild-type and mutant strains of *M. maripaludis*, total RNA was purified from 100 ml of cells, which had grown in McNA to an absorbance at 600 nm of about 0.4, using the TRIZOL LS reagent (Invitrogen). The purified RNA (20 μg) was incubated with RNase-free DNase (10 units) for 30 min at 37ºC to remove residual DNA. RT-PCR was performed with a mixture of 1 μg of template RNA, 200 U of M-MLV reverse transcriptase (Promega), 1 μM of the reverse primer for a tested gene or the 16S rRNA gene, and 30 U of RNase inhibitor (Promega) in a total volume of 25 μl. After 1 h at 42ºC, RNA was removed by incubation with 4 U of RNase H (Takara) for 30 min at 37ºC. Real-time PCR was performed in a ABI Prism 7000 Sequence Detection System (Applied Biosystems) with a 25 μl mixture containing 12.5 μl of 2 x SYBR Green PCR Master Mix (Applied Biosystems), 200 μM each of the primers for the tested gene and a dilution of the

reverse transcription products. Cycling conditions included incubation at 50 ºC for 2 min, 95ºC for 10 min, and 40 cycles of 95ºC for 30 sec and 60ºC for 1 min. The standard curves for quantification of the expression of the tested genes and the 16S rDNA were constructed with dilutions of PCR-amplified DNA fragments containing corresponding genes under the same conditions. Levels of expression of the tested genes were normalized against those of the 16S rRNA gene.

Chromatin ImmunoPrecipitaion (ChIP). The ChIP assays were performed with a Chromatin ImmunoPrecipitaion (ChIP) Assay kit (USB Corporation) as described by the manufacturer with the following modifications. Cells of *M. maripaludis* strains S2 and S590 were grown in 100 ml of McNA medium to OD 0.6-0.8. Crosslinking was performed by adding 2.7 ml of formaldehyde directly to the culture (1% final concentration) and incubating for 20 minutes at room temperature with gentle agitation. The crosslinking reaction was then quenched by adding glycine to a final concentration of 0.125 M. Cells were harvested and washed twice with chilled 1×PBS buffer. Cells were then resuspended in 3 ml of lysis buffer with addition of 1×protease inhibitor cocktail and passed twice through a French pressure cell at 100 Mpa to break the cells and shear DNA into short fragments. The cell extracts were centrifuged at 20,000 g for 10 min to remove debris, and then 700 µl of supernatant was incubated with 70 µl of pre-blocked Protein A agarose beads for 1 hour at 4 ^{o}C with gentle agitation. The mixture was centrifuged at 3,000 g for 5 minutes, and the supernatant was incubated with 7 µl of antiserum overnight at 4 ^{o}C with gentle agitation. Antibody was not added for the negative control reaction. The immune-complexes were captured with 70 µl of pre-blocked Protein A agarose beads, washed, and eluted as described by the manufacturer. The

immunoprecipitated DNA was purified with a DNA Clean & Concentrator kit (Zymo Research).

The purified DNA fragments were blunted with T4 DNA polymerase (New England Biolabs), ligated to linkers for PCR by blunt-end ligation, and PCR amplified as described (12). The amplified DNA fragments were cloned into pCR2.1-TOPO using a TOPO TA Cloning kit (Invitrogen). A 96 clone library was generated for each sample. The sequencing of the insert DNA fragments was performed by the Sequencing and Synthesis Facility at the University of Georgia.

Prediction of protein binding sites. The Mma10b binding site for DNA was predicted by the Gibbs Motif Sampler program (http://bayesweb.wadsworth.org/gibbs/gibbs.html) using DNA sequences of the fragments co-precipitated with Mma10b in the ChIP analysis. A diagram of the binding motif was created with the WebLogo program (http://weblogo.berkeley.edu/). The presence of binding motif in a DNA fragment or the whole genome was predicted using the Motif Locator program with a score cutoff of 9.0 (http://www.cmbl.uga.edu/software/motloc.html).

Electrophoretic mobility shift assays (EMSA). For gel shift assays in agarose gel, about 100 ng DNA was incubated with 0-15 μM of Mma10b for 30 min at 37 ^{o}C in 20 mM Tris-HCl (pH 7.6), 1 mM DTT, 100 μg/ml BSA, and 10% glycerol (wt/vol) in a total volume of 20 μl. DNA-protein complexes were resolved by electrophoresis in 0.7% or 1.2% agarose gels in 1×TAE buffer, which was comprised of 40 mM Tris-HCl, 20 mM acetic acid and 1 mM disodium EDTA. After electrophoresis, the gels were stained with ethidium bromide and visualized by UV.

EMSA in polyacrylamide gel were performed with a 58 or 60-bp double-stranded DNA or a 64-nt single-stranded RNA fragment. The 58-mer DNA corresponded to a sequence fragment in the wild-type *M. maripaludis* genome (positions 1,307,685-1,307,742) and contained the predicted Mma10b binding site. The sequence of one strand of the 60-mer DNA was 5'-GATCCCCCAATGCTTCGTTTCGTATCACACACCCCAAAGCCTTCTGCTTTGAATGCTGCC. The predicted Mma10b binding site was absent in this fragment. The sequence of the RNA fragment was 5'-GAAUACUCAAGCUUAUGCAUGCGGCCGCAUCUAGAGGGCCCGGAUCCCUCGAGGUCGACGAAUU. The DNA and RNA fragments were labeled at the 5'-end with [γ-^{32}P]-ATP using T4 polynucleotide kinase (Promega). The labeled 60 bp and 58 bp DNA fragments (20-30 nM) were incubated with Sac10b homologs (0-10 μM) at 22 ^{o}C and 37 ^{o}C, respectively, in 20 mM Tris-HCl (pH 7.6), 1 mM DTT, 100 μg/ml BSA, and 8% glycerol (wt/vol) in a total volume of 20 μl. The labeled RNA fragment was heated at 90 ^{o}C for 1 min and chilled on ice. Then 20-30 nM of the RNA fragment was incubated with Sac10b homologs (0-10 μM) for 10 min at 22 ^{o}C in 20 mM Tris-HCl (pH 7.6), 1 mM DTT, 100 μg/ml BSA, and 8% glycerol (wt/vol) in a total volume of 20 μl. DNA-protein or RNA-protein complexes were resolved by electrophoresis in 8% nondenaturing polyacrylamide gels. When KCl was added to the incubations, the electrophoresis was performed with 1×TBE buffer, which was comprised of 89 mM Tris, 89 mM boric acid, and 2 mM disodium EDTA.. For incubations without added salts, the electrophoresis was performed in 0.1×TBE. After electrophoresis, the gels were visualized by exposure to X-ray films.

DNase I footprinting. The DNase I footprinting method was modified from Yindeeyoungyeon *et al.* (51). DNA fragments were prepared by PCR using pB9 as the template

and primer pairs *B9F and B9R. The *B9F primer was labeled with 6-carboxyfluorescein (6-FAM*) at the 5‘ end. The PCR amplicon was an approximately 400 bp 6-FMA-labeled fragment and contained two predicted Mma10b binding sites. The PCR products were gel purified with a QuickClean DNA Gel Extraction kit (GenScript Corporation).

Approximately 450 ng of 6-FAM-labeled DNA (15 nM final concentration) and 9 μg of purified Mma10b (15 μM final concentration) were incubated in 20 mM Tris-HCl pH7.6, 1 mM DTT, 100 μg/ml BSA, and 10% glycerol (wt/vol) in a total volume of 60 μl. The samples without addition of Mma10b were supplemented with BSA to yield the same total protein concentration. After incubation at 37 ^{o}C for 1 hour, samples were digested with 15 μl DNase I (0.01 U/μl final concentration), which was freshly prepared by diluting the 10 U/μl stock of RQ1 RNase-free DNase (Promega). The digestion was performed at room temperature for 4 min, and then the reaction was stopped by adding 15 μl Stop Solution (20 mM EGTA, pH 8.0). The digested DNA was purified with a DNA Clean & Concentrator kit (Zymo Research, Orange, CA, USA). The DNA fragments were analyzed on the ABI 3730 Genetic Analyzer (Applied Biosystems) at the Sequencing and Synthesis Facility at the University of Georgia.

Results

Mma10b was expressed at low levels. The protein levels of Sac10b homologs from *Sulfolobus shibitae* (Ssh10b), *Methanocaldococcus jannaschii* (Mja10b), *Methanothermococcus thermolithotrophicus* (Mth10b), and *Methanococcus maripaludis* (Mma10b) were compared by quantitative Western blotting. The protein level of Mma10b was very low. In two independent measurements, Mma10b constituted 0.009-0.014% of the total cellular protein (Fig. 2-1A). In a separate experiment, the cellular concentration of Mvo10b was found to be below the level of detection, or <0.01% of the total cellular protein (data not shown). In contrast, the Sac10b

homologs were more abundant in thermophiles. Ssh10b, Mja10b, and Mth10b constituted 1.6%, 0.42%, and 0.12% of the total cellular protein, respectively (Fig. 2-1B). Thus, the protein levels of Sac10b homologs in methanococci were lower than that in *Sulfolobus* and negatively correlated with the methanococcal optimum growth temperatures.

Aggregation of Sac10b homologs with heat treatment. The heat-induced aggregation of Sac10b homologs was monitored by light scattering to indicate the irreversible denaturation of proteins at high temperature. Some proteins from the mesophilic methanococci are stable at high temperature, which may be evidence for a thermophilic origin of archaea (38). For instance, the temperature optimum of pyruvate oxidoreductase from *M. maripaludis* is 60 ^{o}C (22). Thus, it was of interest to determine whether the Sac10b homologs from the mesophiles were also resistant to heat. As shown in Fig. 2-2A, Mma10b and Mvo10b denatured faster than Mth10b and Mja10b at temperatures higher than 60 ^{o}C, suggesting that mesophilic Sac10b homologs were not as heat stable as thermophilic homologs.

The methanococci are marine organisms, and the intracellular concentration of K^+ in methanococci is 0.4-1.3 M (32, 36). Moreover, high ionic strengths are important for the full folding of archaeal histones and their function in negative supercoiling of DNA (35). Therefore, high ionic strengths may influence the stability of Sac10b homologs. As shown in Fig. 2-2B, protein aggregation with 0.4 M of KCl was reduced compared with an incubation without salt, but the rates of aggregation followed the same trend under both conditions, i.e. Mvo10b > Mma10b > Mth10b > Mja10b. The rapid denaturation of Mvo10b and Mma10b indicated that they were not functional at high temperatures, and Sac10b homologs were adapted to the organism‘s optimum growth temperature.

Large differences in the heat-induced aggregation suggested that Mma10b and Mvo10b were not closely related. Extensive phylogenetic analyses of the Sac10b homologs in the euryarchaeotes supported this conclusion (data not shown). In contrast to most proteins of the two mesophilic methanococci, the sequence of Mma10b was only 57 % identical to that of Mvo10b, and it was more similar to that of Mth10b (79 % identical) from the thermophile *M. thermolithotrophicus*. *Sulfolobus* and several other archaeal species encode two copies of the Sac10b homologs, Alba1 and Alba2, which are 30 %-40 % identical and very likely paralogs with different functions (18). The sequences of Mma10b, Mth10b, and Mja10b were more closely related to Alba1 (48 %-58 % identical), while Mvo10b was equidistant to Alba1 and Alba2 (40 % identical). Because of their low sequence similarity, Mma10b and Mvo10b may have been derived from paralogous lineages, which might explain their different responses to high temperatures.

Comparisons of affinities of Mma10b for DNA and RNA with other Sac10b homologs. Previous studies reported that the association of Sac10b homologs from *Sulfolobales* with DNA was sequence-independent (26). The affinity of Mma10b for oligonucleotide DNA was compared with other Sac10b homologs by EMSA. A ^{32}P-labeled 60-bp double-stranded DNA fragment was titrated with Sac10b homologs (Fig. 2-3A). The affinities of Mja10b and Mth10b for DNA were similar to that of Ssh10b. At low protein concentrations, they formed a series of low molecular weight protein-DNA complexes that were well resolved. At higher protein concentrations, they formed slowly migrating aggregates which were unable to enter the 8% gels. The aggregates presumably resulted from uncharacterized protein-protein and/or protein-DNA interactions. Unlike the thermophilic proteins, Mma10b and Mvo10b only formed high molecular weight complexes with DNA, suggesting different patterns of protein-DNA

interactions. The amount of Mma10b required to retard half of the input DNA (K_d) was about 600 nM.

The presence of salt affected the protein-DNA interaction. At 0.2 M of KCl, none of the Sac10b homologs was able to generate stable DNA shifts, but all formed aggregates at high protein concentrations (Fig. 2-3A). At 0.4 M of KCl, the apparent K_d of Mma10b increased by about 10-fold to 7 μM, and Mth10b was unable to form aggregates (Fig. 2-3A).

In contrast, the RNA binding patterns of these proteins were independent of the salt concentration, and the affinities for a 64-nt RNA fragment were only slightly lower with 0.4 M KCl than no salt (data not shown). All Sac10b homologs were able to form well-resolved complexes with the RNA in the presence of 0.4 M KCl (Fig. 2-3B). Ssh10b and Mja10b also formed high molecular aggregates at higher protein concentrations. In contrast, the other three proteins did not form aggregates even at protein concentrations as high as 10 μM. The protein concentrations that were required to retard half of the input RNA were about 10 nM for Ssh10b, 2.5 nM for Mja10b, 150 nM for Mth10b and Mma10b, and 600 nM for Mvo10b. Therefore, the mesophilic methanococcal Sac10b homologs possessed higher affinities for oligonucleotide RNA than DNA *in vitro*, especially in the presence of high salt.

Disruption of *mma10b* impaired autotrophic growth. Since mesophilic Sab10b homologs were expressed at low levels, they may perform a very different and possibly dispensable function compared to homologs in thermophiles. *M. maripaludis* was used here as a model to elucidate the physiological role of Sac10b homologs in mesophilic methanococci. The gene encoding Mma10b (Mmp1613) was deleted by gene replacement with the *pac* cassette, which encodes puromycin resistance in methanococci (Fig. S2-2). The deletion of *mma10b* was confirmed by Southern hybridization (data not shown) and Western blotting (Fig.

2-1A). Since the gene was transcribed on the opposite strand as its neighbors, this mutation was not expected to affect transcription of downstream genes.

When grown in minimal medium, the Δ*mma10b* mutant, strain S590, experienced a longer lag phase, slower growth rate during exponential phase, and lower maximum growth yield than the wild-type (Fig. 2-4). The differences in the growth of S590 and the wild-type S2 were consistent in three independent experiments. To confirm that these differences were due to the mutation, the complementation strain S591 was constructed by transforming the plasmid pMEV2-mma10b into S590. Because Mma10b was only expressed at low levels in the wild-type, the native promoter was used for the complementation. This resulted in the expression of Mma10b about 40% lower than that of the wild-type (Fig. 2-1A). The complementation partially restored growth. In a typical experiment, the durations of the lag phase of S2, S590, and S591 were about 3, 10, and 15 hours, respectively. The doubling times (means ± standard deviations of five cultures) of S2, S590, and S591 were 5.8 ± 0.7, 10.2 ± 0.6, and 6.7 ± 1.1 h, respectively. The maximum growth yields (means ± standard deviations of five cultures) of S2, S590, and S591 were 0.48 ± 0.00, 0.31 ± 0.01, and 0.45 ± 0.02 mg dry weight/ml of culture, respectively. Thus, at the lower levels of expression in the complemented strain, only the lag phase was severely affected. The longer lag phase may have been caused by the lower efficiency of *mma10b* expression from the shuttle vector and a requirement for more time to accumulate Mma10b sufficient for optimal growth.

When acetate, alanine, Casamino Acids, or yeast extract was added into the medium, the growth of S590 was indistinguishable from that of the wild-type strain (see below). Thus, the growth defect appeared to be restricted to minimal medium. A Δ*ehb* mutant of *M. maripaludis* has a similar phenotype. It is impaired in autotrophic growth and possesses high specific

activities of the key autotrophic enzymes, CO dehydrogenase/acetyl-CoA synthase (CODH/ACS) and pyruvate oxidoreductase (Por) (29). The specific activities of both enzymes from cells grown in minimal medium in exponential growth phase increased in S590 (Table 2-2). The differences between S2 and S590 were significant, with *P* values of <0.05. The complementation strain S591 had activities close to wild-type level.

To determine if Mma10b was involved in thermal adaptation, the growth response of the Δ*mma10b* mutant to temperature was characterized (Fig. 2-5). In minimal medium, the growth rate of S590 was less than that of the wild-type strain at near 37^{o}C, which was close to the temperature optimum (Fig. 2-5). Growth of S2 and S590 were similar at both lower and higher temperatures. In contrast, growth in media with abundant sources of reduced carbon was the same for S590 and S2 at all tested temperatures. Presumably, the process(es) affected in the mutant were only growth limiting at high growth rates under conditions where autotrophic CO_2 fixation was required. In any case, the similar growth of the mutant and wild-type at high temperatures did not support a role for Mma10b in thermoadaptation.

Quantitative proteomic analysis of protein expression patterns. To elucidate the influence of mma10b disruption on gene expression, the proteomes of the Δ*mma10b* mutant S590 and the wild-type S2 were compared. Both S590 and S2 were cultured in McNA medium and harvested during the exponential growth phase, conditions where their growth was indistinguishable. Proteins encoded by 442 of the 1722 ORFs were detected at least once, and 327 proteins were detected by multiple measurements (Supplementary Table S2-1). By the criteria described in methods, the levels of 8 of the 327 proteins increased significantly in S590 relative to the wild-type, and the levels of 6 proteins decreased significantly (Table 2-3).

The levels of several enzymes involved in carbon assimilation increased moderately in S590, including Por β subunit (PorB, Mmp1504), 2-ketoglutarate oxidoreductase α subunit (Mmp0003), pyruvate carboxylase subunit A (Mmp0341), and acetyl-CoA synthetase (Mmp0148). While the differences in protein levels were less than 1.5-fold, they were statistically significant. Por expression also increased in the Δ*mvo10b* mutant of *M. voltae* (13).

The changes in gene expression revealed by quantitative proteomics were confirmed by real time RT-PCR. Six potentially regulated ORFs were selected (Table 2-4). The direction of change in the steady state levels of mRNA in all cases agreed with proteomics. For all of the six ORFs, the extent of changes in mRNA levels were greater than the proteome, a trend that was consistent with previous observations with *M. maripaludis* (49).

Mma10b was associated with DNA *in vivo*. Mma10b bound DNA with a low affinity *in vitro*. The Chromatin ImmunoPrecipitaion (ChIP) assay was employed to determine if Mma10b was associated with chromosomal DNA *in vivo*. To confirm the specificity of the immunoprecipitation, Δ*mma10b* mutant (S590) cells were used as a control. PCR amplification of co-precipitated DNA from wild-type cells generated multiple DNA fragments ranging from 100 to 1,000 bp, while the immunoprecipitation with S590 cells did not yield enough DNA to be visible with ethidium bromide on agarose gels after PCR amplification (Fig. S2-3). Therefore, DNA purified from ChIP samples did not result from non-specific immunoprecipitation.

The sequences of 46 clones with inserts of DNA fragments that co-precipitated with Mma10b were determined (Table S2-2). Some of these fragments were part of the operons which encoded proteins that were differentially expressed in the Δ*mma10b* mutant. These included DNA-directed RNA polymerase subunits and genes involved in flagella biosynthesis. These results indicated that associations of Mma10b with coding regions of the genes might affect gene

expression. Mma10b was also associated with some genes that were not differentially expressed, such as MMP0383 which encoded the surface-layer protein (Table S2-1), indicating that the binding of Mma10b did not necessarily affect gene expression, at least under the conditions tested.

Mma10b bound DNA with sequence specificity. To identify potential Mma10b binding sites, the DNA sequences identified in the ChIP experiment were analyzed with the Gibbs Sampler program (40). This program predicted an 18 bp binding motif derived from 46 potential binding sites, in which the highly conserved A (5^{th} position) and T (14^{th} position) were separated by 8 bp (Fig. 2-6). The 2^{nd} and the 17^{th} position were also preferably T and A/T, respectively. Based upon this degenerate sequence, the presence and absence of a binding site in a DNA fragment was analyzed by the Motif Locator program at a cutoff score of 9.0 (27). The higher the cutoff score, the more stringent the binding site identification. The cutoff value was validated by EMSA in agarose gel with five different DNA fragments with lengths of 500-1,000 bp. For three fragments in which the predicted binding site was present at a cutoff of 9.0, the apparent K_d on agarose gels was < 1 μM (Fig. 2-7A and data not shown). For the two other fragments in which the predicted binding site was absent at a cutoff of 9.0, the apparent K_d was > 10 μM (Fig. 2-7A and data not shown). Because both fragments also contained one predicted binding site at a cutoff of 8.0, this cutoff value was not stringent enough to predict the presence of binding sites. Using the same criterion, the whole genome of *M. maripaludis* contained about 4,000 Mma10b binding sites. Among the 46 co-precipitated DNA fragments, 32 sequences contained at least one predicted binding site. All of the predicted binding sites were located in the protein coding regions (Table S2-2). Other binding sites not recognized by the sequence analyses may also exist, since some of the co-precipitated DNA fragments did not contain the degenerate motif.

Furthermore, the sequence-dependent association was not influenced by the DNA structure. For a plasmid containing four predicted binding sites, Mma10b bound equally well to the supercoiled plasmid and linear DNA (Fig. 2-7B). At a protein concentration of 0.8 μM, migration of both forms of the input DNAs were retarded. Moreover, at higher protein concentrations multiple protein-DNA bands formed, suggesting that more than one binding site may be occupied and Mma10b may bind cooperatively as oligomers. At the highest protein concentration of 15 μM, the complexes formed with both supercoiled DNA and linear DNA migrated faster than the protein-free DNA, suggesting that DNA may be condensed. The presence of high salt reduced the association of Mma10b with binding-motif containing DNA fragments. With 0.4 M of KCl, the plasmid DNA was not retarded by 15 μM of Mma10b in agarose gel (data not shown).

The sequence-dependent binding of Mma10b to short dsDNA was further examined by EMSA in polyacrylamide gels. This method may be more accurate for Sac10b homolog-binding to nucleic acids than agarose gels because smaller changes of mobility can be detected due to the small pore size of polyacrylamide gels and the lower ionic strength used during electrophoresis may stabilize binding. The affinities of Mma10b for two 58 bp dsDNA fragments were compared (Fig. 2-7C). For the DNA fragment possessing the binding motif sequence, the apparent K_d was about 120 nM by this method. For the DNA fragment with A and Ts at the 2^{nd}, 5^{th}, 14^{th}, and 17^{th} positions changed to G, the K_d was about 600 nM, which was close to that of a 60 bp dsDNA fragment that lacked a predicted binding site (Fig. 2-3A). Therefore, Mma10b associated with motif-containing DNA at least five-fold more strongly than with bulk DNA. Moreover, two discrete shifts, which may represent protein binding in different cooperative fashions, were observed (Fig. 2-7C). The cooperative association of Ssh10b with DNA was

described previously (7). In Fig. 2-7C, the first shift, which may have lower protein oligomerization state than the second shift, appeared at lower Mma10b concentrations in the presence of the binding site than in its absence.

The predicted DNA binding sites of Mma10b were further validated by DNase I footprinting analysis. A 389 bp DNA fragment with two predicted binding sites was used in this assay (Fig. 2-8A). Binding site ~~"a~~" had been previously shown to associate with Mma10b by EMSA (Fig. 2-7C). The electropherograms of the 389 bp DNA fragment after DNase I digestion clearly revealed that two regions were protected by incubation with Mma10b, and these two regions corresponded to the positions within the predicted binding sites (Fig. 2-8). A third region (around 130 nt position) was also protected, even though a binding motif was not identified in this region. These results suggested that Mma10b did not coat DNA but bound to specific loci.

Discussion

Proteins of the Sac10b family are abundant in the thermophilic archaea and have been proposed to play important roles in thermoadaption. Assuming a thermophilic origin for the archaea (38), these proteins could be molecular fossils in mesophiles like *M. maripaludis*. However, two lines of evidence suggest that this is not the case and that this protein has retained a function in the mesophiles. First, the mesophilic methanococcal proteins are labile to denaturation at high temperature. This result suggests that their amino acid composition has evolved under selection for a functional protein. Second, disruption of *mma10b* results in impaired autotrophic growth and changes in gene expression. Thus, the protein plays some role in cellular processes.

Comparisons between thermophilic and mesophilic Sac10b homologs. The physiological properties of thermophilic and mesophilic methanococcal Sac10b homologs are

remarkably different, indicating that the function of these proteins has diverged greatly. First, the expression levels of Sac10b homologs are much lower in mesophilic methanococci than in thermophiles. In the mesophile *M. maripaludis*, Mma10b only accounts for ~ 0.01% of the total protein. Second, *in vitro* the affinity of Mma10b for DNA is sequence-dependent, suggesting that Mma10b binds preferentially at specific loci *in vivo*. Third, the disruption of *mma10b* only affects growth in minimal medium, showing that this protein is not essential. Attempts to delete *ssh10b* in *S. shibitae* were not successful, indicating that disruption of *ssh10b* may lead to a lethal mutation. These differences indicate that the protein family has evolved from a more crucial role in thermophiles to a nonessential role in mesophiles. This is supported by the absence of Sac10b homologs in mesophilic *Methanosarcina* and *Halobacteria* species.

Mma10b binds to DNA with sequence specificity and has a lower affinity for DNA without a specific binding site. When a single sequence-specific binding site is available, the apparent K_d for short dsDNA is ~ 120 nM as determined by PAGE gel EMSA, which is about two times higher than recombinant Sso10b and similar to acetylated Sso10b (18). When the binding site is absent, the apparent K_d increases to ~ 600 nM. Two features of mesophilic Sac10b homologs (Mma10b and Mvo10b) probably contribute to their low nonspecific affinities for DNA. First, Lys16 (Sso10b numbering) is replaced with Asn and Glu in Mma10b and Mvo10b, respectively. Lys16 plays a key role in DNA-binding (4). In Sso10b, replacement of Lys16 with Ala reduces the affinity by 7-14 fold, and replacement with Glu reduces the affinity by ~ 40-fold. Therefore, the substitutions observed in the mesophilic methanococcal proteins are expected to lower their affinities for DNA. Second, the mesophilic Sac10b homologs are less highly charged than those from the thermophiles. For instance, the pIs calculated from the amino acid contents are: Ssh10b (pI=10.5) > Mja10b (pI=9.7) > Mth10b (pI=8.0) > Mvo10b (pI=7.9) > Mma10b

(pI=5.8). The intracytoplasmic pH of mesophilic methanococci is around 6.5-8 (8). Thus, Mma10b and Mvo10b are expected to be neutral or negatively charged *in vivo*. In contrast, Sso10b and most other chromatin proteins are highly basic and possess a positively charged DNA-binding surface. Presumably, the reduced positive charges on the mesophilic Sac10b homologs limit their nonspecific binding to nucleic acids.

Comparison of Mma10b with other DNA binding proteins. Mma10b is very different from typical transcription regulators. For instance, NrpR in *M. maripaludis* binds its operator sequences with a K_d of 0.3 nM (20). On the other hand, the low abundance of Mma10b makes it unlike common chromatin architectural proteins such as archaeal histones and MC1, which make up ~ 5% of total cellular protein. For instance, based upon a protein content of ~ 4.3×10^{-13} g of protein per cell and a molecular mass of Mma10b of 11.8 kDa, *M. maripaludis* contains ~2,200 copies of Mma10b per cell. If the cell contains only one copy of the chromosome and one dimer of Mma10b binds 18 bp of DNA, Mma10b could bind no more than 1% of the genome. *M. jannaschii* cells contain multiple copies of the chromosome (25). If *M. maripaludis* cells also contain multiple copies, Mma10b could only bind an even smaller proportion of the genome.

Even though Mma10b is not abundant enough to coat the entire genome, it could still modulate nucleoid architecture. The nucleoid in enteric bacteria is organized in loops of ~ 10 kb, which are connected and closed by DNA-binding proteins (30, 31). If the *M. maripaludis* chromosome is organized in the same manner, Mma10b is abundant enough to play a role in loop maintenance. Likewise, the cellular level of Mma10b is similar to that of Lrp in *E. coli*, which contains ~ 1,000 dimers per cell (1). The DNA-binding affinity of Mma10b is also close to that of LrpC in *Bacillus subtilis*, which binds intrinsically curved DNA with higher affinity (K_d ~ 80 nM) than non-curved DNA (K_d ~ 700 nM) (39). Therefore, the physiological role of

Mma10b could resemble that of Lrp in some bacteria, which contributes to nucleoid organization by wrapping and bridging DNA (5, 23, 31, 39).

Binding of DNA by Mma10b *in vivo*. The ChIP experiment identified association of Mma10b with some DNA regions *in vivo*. Sequence analysis with these regions identified an 18 bp binding-motif and indicated that the whole genome contains about 4000 Mma10b binding sites. Thus, there are about 0.3 molecules of the physiologically active dimer per binding site, and Mma10b dimer would have to act at below stoichiometric levels. About 99% of the predicted binding sites are located inside protein-coding regions. Therefore, the associations of Mma10b with DNA need to be reversible during transcription.

The K_d of the Mma10b association with a motif-containing 58 bp ds-DNA fragment was about 120 nM at low salt. While the presence of salt near physiological concentrations reduced its affinity, it would not necessarily eliminate the association of Mma10b with DNA. At intracellular concentrations of Mma10b (~ 2 μM) and DNA-binding sites (~ 4 μM, assuming one genome per cell), 70 % of the total amount of Mma10b would be associated with specific DNA-binding sites with K_ds of 1 μM. Moreover, the calculated ratio of Mma10b-DNA complexes to free Mma10b molecules might be underestimated, as the nucleoid is highly compacted in the living cells, and the local concentrations of Mma10b and DNA-binding sites could be much higher.

The oligomeric state of Mma10b when binding to DNA is not clear. The footprinting experiment suggested that Mma10b protected DNA regions about 10-20 bp in length. A model of DNA binding by Sac10b homologs proposes that the binding stoichiometry varies between 5-20 bp DNA per dimer, depending on the binding density (43, 44). This model suggests that within 10-20 bp DNA regions, Mma10b could bind either as a dimer, tetramer, or octamer.

Binding of RNA by Mma10b. Although no evidence was obtained for RNA binding by Mma10b *in vivo*, this possibility is not exluded. First, Mma10b and Mvo10b possess high affinities for RNA, even in the presence of physiological concentrations of salt. Second, the low abundance of Mma10b can not eliminate a role in mRNA or ribosome binding. Based upon the total amount of RNA in methanococci of 6-10 × 10^{-8} μg $cell^{-1}$ (16) and that 4 % of the total RNA is mRNA in growing cells (28), the mRNA content in methanococci is expected to be 1,400-2,400 molecules per cell. With 2,200 Mma10b monomers per cell, there are about 0.5 molecules of the physiologically active dimer per mRNA molecule. Similarly, *M. maripaludis* contains 1.0-2.3 × 10^{4} ribosomes $cell^{-1}$, or about twice the value reported for *E. coli* (15). Thus, there are about 0.1-0.2 molecules of Mma10b dimer per ribosome. This level is comparable to the levels of bacterial translation initiation factors (IF1, 2, and 3), which in *E. coli* are present at a level of 0.2-0.3 molecules per ribosome (6). Thus, the levels of Mma10b are consistent with a role in mRNA or rRNA binding, but only at nonstoichiometric levels.

Influence of Mma10b on gene expression. The influence of Mma10b on carbon assimilation is suggested by the poor growth in minimal medium and increased protein levels of carbon assimilation enzymes in the Δ*mma10b* mutant. In minimal medium, *M. maripaludis* reduces CO_2 to acetyl-CoA by ACS/CODH. Acetyl-CoA is then reductively carboxylated to pyruvate by Por (22, 34). Exogenous acetate and alanine are alternative sources for acetyl-CoA and pyruvate, respectively. Because the addition of acetate or alanine restores the growth of the Δ*mma10b* mutant to the wild-type level, the disruption of *mma10b* appears to impair an early step(s) of CO_2 fixation, such as converting CO_2 to acetyl-CoA or pyruvate. Compared with a Δ*ehb* mutant which is also defective in CO_2 assimilation, the expression of a similar group of proteins is affected but with smaller changes in the Δ*mma10b* mutant (29, 49). First, enzymes

involved in autotrophy, such as Por and ACS/CODH, are up-regulated in both mutants. Second, proteins of the *fla* operon are down-regulated in both mutants. The regulation of flagellar genes in *M. maripaludis* is complex and affected by levels of H_2 and phosphate as well as growth rate (15). The striking similarities between gene regulation in the Δ*mma10b* and the Δ*ehb* mutants suggest that the disruption of *mma10b* limits autotrophic CO_2 flux. However, there is no reason to propose a specific regulatory role for Mma10b. CO_2 fixation imposes large bioenergetic demands upon methanococci, and any mutation that lowers the growth efficiency could negatively impact this process.

Conclusions. The Sac10b homologs of the mesophilic methanococci are clearly functional. The proteins are expressed at low levels, suggesting that their function is very different from that of the hyperthermophilic proteins. The association of Mma10b with DNA *in vitro* is sequence-dependent, indicating that it binds to the chromosome at specific loci. However, the affinity is much lower than transcriptional regulators. Mutations that disrupt the gene alter the growth properties of the cells and change the expression levels of several genes. While the association of Mma10b at specific sites could change DNA structure, whether it acts in concert with other DNA binding proteins and directly affects gene expression remain an area for future investigations.

Acknowledgments

We thank Magdalena Sieprawska-Lupa for preparing protein samples for proteomic study. We thank Dr. Iris Porat for designing plasmid pIJA03-mma10b. We thank Dr. Timothy R. Hoover for help with the ChIP experiment. We thank Dr. Kenneth L. Jones and Dr. Travis C. Glenn for help with the DNase I footprinting experiment. We thank Dr. Jan Mrazek and Dr. Xiangxue Guo for help with sequence analysis for identification of binding motif.

This work was supported in part by grant DE-FG02-97ER20269 from DOE Energy Biosciences to W. B. Whitman, grant IR01RR019767-04 from NIH to J. I. Amster, and grants 2004CB719603 from National Basic Research Program of China, 30730003, 30621005 and 39925001 from the National Natural Science Foundation of China (NSFC), and KSCX2-YW-G-023 from the Chinese Academy of Sciences to L. Huang.

References

1. **Ali Azam, T., A. Iwata, A. Nishimura, S. Ueda, and A. Ishihama.** 1999. Growth phase-dependent variation in protein composition of the *Escherichia coli* nucleoid. J. Bacteriol. **181:**6361-6370.

2. **Aravind, L., L. M. Iyer, and V. Anantharaman.** 2003. The two faces of Alba: the evolutionary connection between proteins participating in chromatin structure and RNA metabolism. Genome Biol. **4:**R64.

3. **Balch, W. E., G. E. Fox, L. J. Magrum, C. R. Woese, and R. S. Wolfe.** 1979. Methanogens: reevaluation of a unique biological group. Microbiol. Mol. Biol. Rev. **43:**260-296.

4. **Bell, S. D., C. H. Botting, B. N. Wardleworth, S. P. Jackson, and M. F. White.** 2002. The interaction of Alba, a conserved archaeal chromatin protein, with Sir2 and its regulation by acetylation. Science **296:**148-51.

5. **Beloin, C., J. Jeusset, B. Revet, G. Mirambeau, F. Le Hegarat, and E. Le Cam.** 2003. Contribution of DNA conformation and topology in right-handed DNA wrapping by the *Bacillus subtilis* LrpC Protein. J. Biol. Chem. **278:**5333-5342.

6. **Bremer, H., and P. P. Dennis.** 1996. Modulation of chemical composition and other parameters of the cell by growth, p. 1553-1569. *In* F. C. Neidhardt, R. Curtiss, J. L. Ingraham, E. C. C. Lin, K. B. Low, B. Magasanik, W. S. Reznikoff, M. Riley, M. Schaechter, and H. E. Umbarger (ed.), *Escherichia coli* and *Salmonella*, vol. 2. ASM Press, Washington, D.C.

7. **Cui, Q., Y. Tong, H. Xue, L. Huang, Y. Feng, and J. Wang.** 2003. Two conformations of archaeal Ssh10b: the origin of its temperature-dependent interaction with DNA. J. Biol. Chem. **278:**51015-51022.

8. **Dybas, M., and J. Konisky.** 1992. Energy transduction in the methanogen *Methanococcus voltae* is based on a sodium current. J. Bacteriol. **174:**5575-5583.

9. **Forterre, P., F. Confalonieri, and S. Knapp.** 1999. Identification of the gene encoding archeal-specific DNA-binding proteins of the Sac10b family. Mol. Microbiol. **32:**669-70.

10. **Gernhardt, P., O. Possot, M. Foglino, L. Sibold, and A. Klein.** 1990. Construction of an integration vector for use in the archaebacterium *Methanococcus voltae* and expression of a eubacterial resistance gene. Mol. Gen. Genet. **221:**273-9.

11. **Guo, R., H. Xue, and L. Huang.** 2003. Ssh10b, a conserved thermophilic archaeal protein, binds RNA *in vivo*. Mol. Microbiol. **50:**1605-15.

12. **Hecht, A., S. Strahl-Bolsinger, and M. Grunstein.** 1996. Spreading of transcriptional represser SIR3 from telomeric heterochromatin. Nature **383:**92-96.

13. **Heinicke, I., J. Muller, M. Pittelkow, and A. Klein.** 2004. Mutational analysis of genes encoding chromatin proteins in the archaeon *Methanococcus voltae* indicates their involvement in the regulation of gene expression. Mol. Genet. Genomics **272:**76-87. Epub 2004 Jul 07.

14. **Hendrickson, E. L., R. Kaul, Y. Zhou, D. Bovee, P. Chapman, J. Chung, E. Conway de Macario, J. A. Dodsworth, W. Gillett, D. E. Graham, M. Hackett, A. K. Haydock, A. Kang, M. L. Land, R. Levy, T. J. Lie, T. A. Major, B. C. Moore, I. Porat, A. Palmeiri, G. Rouse, C. Saenphimmachak, D. Soll, S. Van Dien, T. Wang, W. B. Whitman, Q. Xia, Y. Zhang, F. W. Larimer, M. V. Olson, and J. A. Leigh.** 2004. Complete genome sequence of the genetically tractable hydrogenotrophic methanogen *Methanococcus maripaludis*. J. Bacteriol. **186:**6956-6969.

15. **Hendrickson, E. L., Y. Liu, G. Rosas-Sandoval, I. Porat, D. Soll, W. B. Whitman, and J. A. Leigh.** 2008. Global responses of *Methanococcus maripaludis* to specific nutrient limitations and growth rate. J. Bacteriol. **190:**2198-2205.

16. **Hennigan, A. N., and J. N. Reeve.** 1994. mRNAs in the methanogenic archaeon *Methanococcus vannielii*: numbers, half-lives and processing. Mol. Microbiol. **11:**655-70.

17. **Huber, H., M. Thomm, H. König, G. Thies, and K. O. Stetter.** 1982. *Methanococcus thermolithotrophicus*, a novel thermophilic lithotrophic methanogen. Arch. Microbiol. **132:**47-50.

18. **Jelinska, C., M. J. Conroy, C. J. Craven, A. M. Hounslow, P. A. Bullough, J. P. Waltho, G. L. Taylor, and M. F. White.** 2005. Obligate heterodimerization of the archaeal Alba2 protein with Alba1 provides a mechanism for control of DNA packaging. Structure **13:**963-971.

19. **Jones, W. J., J. A. Leigh, F. Mayer, C. R. Woese, and R. S. Wolfe.** 1983. *Methanococcus jannaschii* sp. nov., an extremely thermophilic methanogen from a submarine hydrothermal vent. Arch. Microbiol. **136:**254-261.

20. **Lie, T. J., G. E. Wood, and J. A. Leigh.** 2005. Regulation of *nif* expression in *Methanococcus maripaludis*: roles of the euryarchaeal repressor NrpR, 2-oxoglutarate, and two operators. J. Biol. Chem. **280:**5236-5241.

21. **Lin, W., and W. Whitman.** 2004. The importance of porE and porF in the anabolic pyruvate oxidoreductase of *Methanococcus maripaludis*. Arch. Microbiol. **181:**68-73.

22. **Lin, W. C., Y.-L. Yang, and W. B. Whitman.** 2003. The anabolic pyruvate oxidoreductase from *Methanococcus maripaludis*. Arch. Microbiol. **179:**444-456.

23. **Lopez-Torrejon, G., M. I. Martinez-Jimenez, and S. Ayora.** 2006. Role of LrpC from *Bacillus subtilis* in DNA transactions during DNA repair and recombination. Nucl. Acids Res. **34:**120-129.

24. **Lurz R., Grote M., Dijk J., Reinhardt R., and D. B.** 1986. Electron microscopic study of DNA complexes with proteins from the Archaebacterium *Sulfolobus acidocaldarius*. EMBO J. **5:**3715-3721.

25. **Malandrin, L., H. Huber, and R. Bernander.** 1999. Nucleoid structure and partition in *Methanococcus jannaschii*: an archaeon with multiple copies of the chromosome. Genetics **152:**1315-1323.

26. **Marsh, V. L., S. Y. Peak-Chew, and S. D. Bell.** 2005. Sir2 and the acetyltransferase, Pat, regulate the archaeal chromatin protein, Alba. J. Biol. Chem. **280:**21122-21128.

27. **Mrazek, J., S. Xie, X. Guo, and A. Srivastava.** 2008. AIMIE: a web-based environment for detection and interpretation of significant sequence motifs in prokaryotic genomes. Bioinformatics **24:**1041-1048.

28. **Neidhardt, F. C., and H. E. Umbarger.** 1996. Chemical composition of *Escherichia coli*, p. 143-17. *In* F. C. Neidhardt, R. Curtiss, J. L. Ingraham, E. C. C. Lin, K. B. Low, B. Magasanik, W. S. Reznikoff, M. Riley, M. Schaechter, and H. E. Umbarger (ed.), E*scherichia coli* and *Salmonella*, vol. 1. ASM Press, Washington, D.C.

29. **Porat, I., W. Kim, E. L. Hendrickson, Q. Xia, Y. Zhang, T. Wang, F. Taub, B. C. Moore, I. J. Anderson, M. Hackett, J. A. Leigh, and W. B. Whitman.** 2006. Disruption of the operon encoding Ehb hydrogenase limits anabolic CO_2 assimilation in the archaeon *Methanococcus maripaludis*. J. Bacteriol. **188:**1373-1380.

30. **Postow, L., C. D. Hardy, J. Arsuaga, and N. R. Cozzarelli.** 2004. Topological domain structure of the Escherichia coli chromosome. Genes & Development **18:**1766-1779.

31. **Remus, T. D.** 2005. The role of nucleoid-associated proteins in the organization and compaction of bacterial chromatin. Mol. Microbiol. **56:**858-870.

32. **Robertson, D. E., D. Noll, and M. F. Roberts.** 1992. Free amino acid dynamics in marine methanogens. beta-amino acids as compatible solutes. J. Biol. Chem. **267:**14893-14901.

33. **Sandman, K., and J. N. Reeve.** 2006. Archaeal histones and the origin of the histone fold. Curr. Opin. Microbiol. **9:**520-525.

34. **Shieh, J., and W. B. Whitman.** 1988. Autotrophic acetyl coenzyme A biosynthesis in *Methanococcus maripaludis*. J. Bacteriol. **170:**3072-3079.

35. **Soares, D., I. Dahlke, W. T. Li, K. Sandman, C. Hethke, M. Thomm, and J. N. Reeve.** 1998. Archaeal histone stability, DNA binding, and transcription inhibition above 90 degrees C. Extremophiles **2:**75-81.

36. **Sprott, G. D., and K. F. Jarrell.** 1981. K+, Na+, and Mg2+ content and permeability of *Methanospirillum hungatei* and *Methanobacterium thermoautotrophicum*. Can. J. Microbiol. **27:**444-51.

37. **Stathopoulos, C., W. Kim, T. Li, I. Anderson, B. Deutsch, S. Palioura, W. Whitman, and D. Soll.** 2001. Cysteinyl-tRNA synthetase is not essential for viability of the archaeon *Methanococcus maripaludis*. Proc. Natl. Acad. Sci. U S A **98:**14292-14297.

38. **Stetter, K. O.** 1994. The lesson of Archaeabacteria, p. 143-151. *In* S. Boengtson (ed.), Early life on earth. Columbia U.P., New York.

39. **Tapias, A., G. Lopez, and S. Ayora.** 2000. *Bacillus subtilis* LrpC is a sequence-independent DNA-binding and DNA-bending protein which bridges DNA. Nucl. Acids Res. **28:**552-559.

40. **Thompson, W., E. C. Rouchka, and C. E. Lawrence.** 2003. Gibbs Recursive Sampler: finding transcription factor binding sites. Nucl. Acids Res. **31:**3580-3585.

41. **Tumbula D. L., K., J., Shieh, J. S., Whitman, W. B.** 1995. Maintenance of methanogen stock cultures in glycerol at -70 ^{o}C, p. 85-87. *In* S. Robb F. T., K. R., DasSarma, S., Place, A. R., Schreier, H. J., Fleischmann, E. M. (ed.), Archaea-a laboratory manual. Cold Spring Harbor Laboratory Press, Cold Spring Harbor, N. Y.

42. **Tumbula, D. L., R. A. Makula, and W. B. Whitman.** 1994. Transformation of *Methanococcus maripaludis* and identification of a PstI-like restriction system. FEMS Microbiol. Lett. **121:**309-314.

43. **Wang, G., R. Guo, M. Bartlam, H. Yang, H. Xue, Y. Liu, L. Huang, and Z. Rao.** 2003. Crystal structure of a DNA binding protein from the hyperthermophilic euryarchaeon *Methanococcus jannaschii*. Protein Sci **12:**2815-2822.

44. **Wardleworth, B. N., R. J. M. Russell, S. D. Bell, G. L. Taylor, and M. F. White.** 2002. Structure of Alba: an archaeal chromatin protein modulated by acetylation. EMBO J. **21:**4654-4662.

45. **White, M. F., and S. D. Bell.** 2002. Holding it together: chromatin in the Archaea. Trends Genet. **18:**621-626.

46. **Whitman, W. B.** 2001. Genus I. *Methanococcus*-, p. 236-240. *In* D. R. Boone, R. W. Castenholz, and G. M. Garrity (ed.), Bergey's mannual of systematic bacteriology, vol. 1. Springer-Berlin Heidelberg, New York.

47. **Whitman, W. B., J. Shieh, S. Sohn, D. S. Caras, and U. Premachandran.** 1986. Isolation and characterization of 22 mesophilic methanococci. Syst. Appl. Microbiol. **7:**235-240.

48. **Wong, R. L., and I. J. Amster.** 2006. Combining low and high mass ion accumulation for enhancing shotgun proteome analysis by accurate mass measurement. J. Am. Soc. Mass Spectr. **17:**205-212.

49. **Xia, Q., E. L. Hendrickson, Y. Zhang, T. Wang, F. Taub, B. C. Moore, I. Porat, W. B. Whitman, M. Hackett, and J. A. Leigh.** 2006. Quantitative proteomics of the archaeon *Methanococcus maripaludis* validated by microarray analysis and real time PCR. Mol. Cell Proteomics **5:**868-881.

50. **Xue, H., R. Guo, Y. Wen, D. Liu, and L. Huang.** 2000. An Abundant DNA binding protein from the hyperthermophilic archaeon *Sulfolobus shibatae* affects DNA supercoiling in a temperature-dependent fashion. J. Bacteriol. **182:**3929-3933.

51. **Yindeeyoungyeon, W., and M. A. Schell.** 2000. Footprinting with an automated capillary DNA sequencer. Biotechniques. **29:**1034-6, 1038, 1040-1.

Table 2-1. Archaea strains and plasmids.

Strain or plasmid	Genotype or description	Source or reference
Methanococcus maripaludis		
S2	Wild-type	(47)
S590	Δ*mma10b*::*pac*	This work
S591	Δ*mma10b*::*pac*/pMEV2-mma10b	This work
Methanocaldococcus jannaschii JAL-1	Wild-type	(19)
Methanothermococcus thermolithotrophicus SN1	Wild-type	(17)
Methanococcus voltae PS	Wild-type	(3)
Plasmids		
pIJA03	Pur^r methanogen integration vector	(37)
pIJA03-mma10b	pIJA03 with the upstream and downstream regions of the *mma10b* gene (MMP1613)	This work
pMEV2	Neomycin shuttle vector	(21)
pMEV2-mma10b	pMEV2 with *mma10b* gene	This work
pET11a-mja10b	*M. jannaschii* MJ0212 cloned into pET11a	This work
pET15b-mth10b	*M. thermolithotrophicus* EF565170 cloned into pET11b	This work
pET15b-mvo10b	*M. voltae* CAF74922 cloned into pET11b	This work
pET15b-mma10b	*M. maripaludis* MMP1613 cloned into pET11b	This work
pB9	*M. maripaludis* genome fragment (position 1307469-1307986) cloned into pCR2.1-TOPO	This work

Table 2-2. POR and CODH-ACS activities of *M. maripaludis* strains S2, S590, and S591[a].

	Specific activity (U/mg) [a]	
Strains	POR	CODH-ACS
S2	304 ± 25	216 ± 21
S590	467 ± 59	305 ± 26
S591	273 ± 22	195 ± 16

[a] The cultures were grown in McN medium.

[b]Data were the averages and standard deviations for nine assays from three independent cultures. One unit of enzyme activity was defined as 1 μmol of methyl viologen reduced per minute.

Table 2-3. Changes in expression of certain proteins in the mutant S590 determined by quantitative proteomic analysis[a].

ORF	N[b]	Protein ratio[c]	S.E.[d]	Annotation[e]
Up-regulation in S590				
MMP0003[f]	4	1.38	0.11	2-oxoglutarate oxidoreductase alpha subunit, *korA*
MMP0092	2	1.66	0.10	DNA-directed RNA polymerase subunit F
MMP0148	3	1.36	0.12	acetyl-CoA synthetase, AMP-forming, *acsA*
MMP0276	2	1.57	0.06	conserved hypothetical protein
MMP0341	4	1.26	0.07	pyruvate carboxylase subunit A
MMP0414	6	1.51	0.03	threonyl-tRNA synthetase
MMP0594	2	1.53	0.11	conserved hypothetical archaeal protein
MMP0684	3	2.05	0.06	heat shock protein Hsp20
MMP0872	4	5.84	0.04	porphobilinogen deaminase
MMP0971	6	1.52	0.06	adenylosuccinate lyase
MMP1157	2	1.79	0.09	desulfoferrodoxin, ferrous iron-binding site
MMP1504	2	1.32	0.05	pyruvate oxidoreductase subunit beta
Down-regulation in S590				
MMP0196	5	0.76	0.11	ABC-type iron (III) transport system, periplasmic binding protein
MMP0197	4	0.77	0.08	ABC-type iron (III) transport system, permease component
MMP0944	2	0.60	0.02	hypothetical protein
MMP0956	7	0.66	0.18	DNA topoisomerase I
MMP1363	6	0.74	0.15	RNA polymerase, subunit A‘
MMP1364	5	0.74	0.10	RNA polymerase, subunit A‘‘
MMP1666	2	0.42	0.23	flagellin B1 precursor
MMP1667	3	0.36	0.38	flagellin B2
MMP1670	5	0.68	0.15	flagella accessory protein D
MMP1671	3	0.59	0.29	flagella accessory protein E

[a] The cultures for proteomic analysis were grown in McNA medium.

[b] Numbers of proteome measurements for the ORF.

[c] Mean of the S590/S2 ratio of protein levels.

[d] Standard error of the mean or the standard deviation / $\sqrt{N}$.

[e] From (14).

[f] Expression of the ORFs in italics changed only 1.25-1.5-fold, but the veracity of these changes were supported by changes of neighboring ORFs or other members of the same pathway.

Table 2-4. Relative transcript levels of genes of the mutant S590 determined by quantitative RT-PCR[a].

ORF	Transcript ratio[b]	Annotation[c]
MMP0684	6.82 ± 1.38	heat shock protein Hsp20
MMP0872	5.58 ± 1.15	porphobilinogen deaminase
MMP0092	3.56 ± 0.74	DNA-directed RNA polymerase subunit F
MMP1504	3.23 ± 0.64	pyruvate oxidoreductase subunit beta
MMP0944	0.54 ± 0.11	hypothetical protein
MMP0956	0.18 ± 0.05	DNA topoisomerase I

[a] The cultures for quantitative RT-PCR analysis were grown in McNA medium.

[a] S590/S2 mRNA ratio determined by quantitative RT-PCR. Data were the average and standard deviations of three measurements.

[b] From (14).

Figure 2-1. Expression level of Sac10b homologs determined by Western blotting. **A.** Western blotting of Mma10b. Proteins were separated with a 12% SDS polyacrylamide and then transferred onto a PVDF membrane. The membrane was incubated sequentially with rabbit anti-Mma10b antiserum and anti-rabbit IgG horseradish peroxidase conjugate. The proteins were detected with enhanced chemiluminescent substrates and exposed to CL-XPosure film for 5 seconds. Lane 1, 2, and 3, loaded with 400 μg of protein crude extracts of S2 (wild-type), S590 (the Δ*mma10b* mutant), and S591 (the complemented Δ*mma10b* mutant), respectively. Lane 4, loaded with 25 ng of recombinant Mma10b. **B.** Amount of Sac10b homologs in wild-type cells as determined by Western blotting. Percentages of Sac10b homologs in total cellular protein were the average of two independent measurements.

A

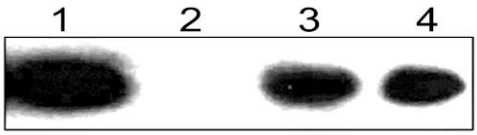
1
2
3
4

B

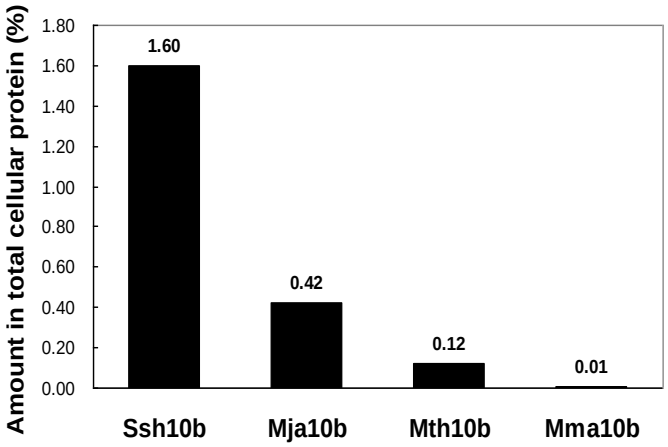
Amount in total cellular protein (%)
1.80
1.60
1.40
1.20
1.00
0.80
0.60
0.40
0.20
0.00
1.60
0.42
0.12
0.01
Ssh10b
Mja10b
Mth10b
Mma10b

Figure 2-2. Heat-induced aggregation of Sac10b homologs. Recombinant proteins Ssh10b, Mja10b, Mth10b, Mma10b, and Mvo10b were suspended at a concentration of 0.1 mg/ml in buffer containing 10 mM potassium phosphate (pH 7.0) and 10% (v/v) glycerol. Protein aggregation was monitored by 90^{o} light scattering at 488 nm on a Shimadzu RF5301PC spectrofluorimeter. **A.** Incubation without additions. **B.** Incubation with 0.4 M KCl. Error bars indicate standard deviations of ten measurements from one experiment.

A

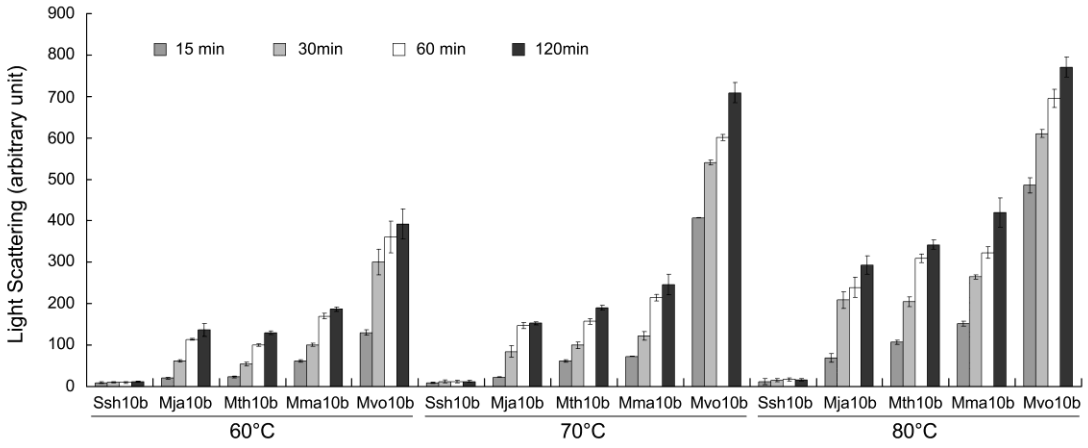
Light Scattering (arbitrary unit)
900
800
700
600
500
400
300
200
100
0
15 min
30min
60 min
120min
Ssh10b
Mja10b
Mth10b
Mma10b
Mvo10b
60°C
70°C
80°C

B

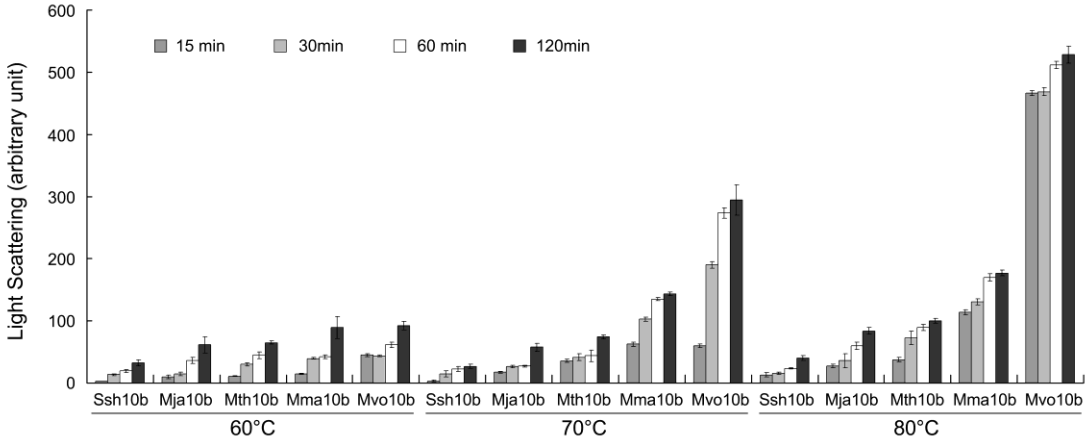
Light Scattering (arbitrary unit)
600
500
400
300
200
100
0
15 min
30min
60 min
120min
Ssh10b
Mja10b
Mth10b
Mma10b
Mvo10b
60°C
70°C
80°C

Figure 2-3. Analysis of binding of Sac10b homologs to DNA and RNA by EMSA. **A.** Binding of Sac10b homologs to a ^{32}P-labeled 60-bp double-stranded DNA fragment. The proteins were incubated with the DNA (20-30 nM) at 22^{o}C for 10 min in the presence of 0, 0.2 or 0.4 M KCl. Protein-DNA complexes were resolved by electrophoresis on an 8% non-denaturing polyacrylamide gel. The gel was exposed to X ray film. From lane 0 to 10, the protein concentrations were 0, 0.02, 0.04, 0.08, 0.16, 0.31, 0.63, 1.25, 2.5, 5, and 10 μM, respectively. **B.** Binding of Sac10b homologs to a ^{32}P-labeled 64-nt single-stranded RNA fragment. The proteins were incubated with RNA (20-30 nM) at 22^{o}C for 10 min in the presence of 0.4 M KCl. Protein-RNA complexes were resolved by electrophoresis on an 8% non-denaturing polyacrylamide gel. The gel was exposed to X ray film. From lane 0 to 10, the protein concentrations were 0, 4×10^{-5}, 1.6×10^{-4}, 6.3×10^{-4}, 2.5×10^{-3}, 0.01, 0.04, 0.16, 0.63, 2.5, and 10 μM, respectively.

A

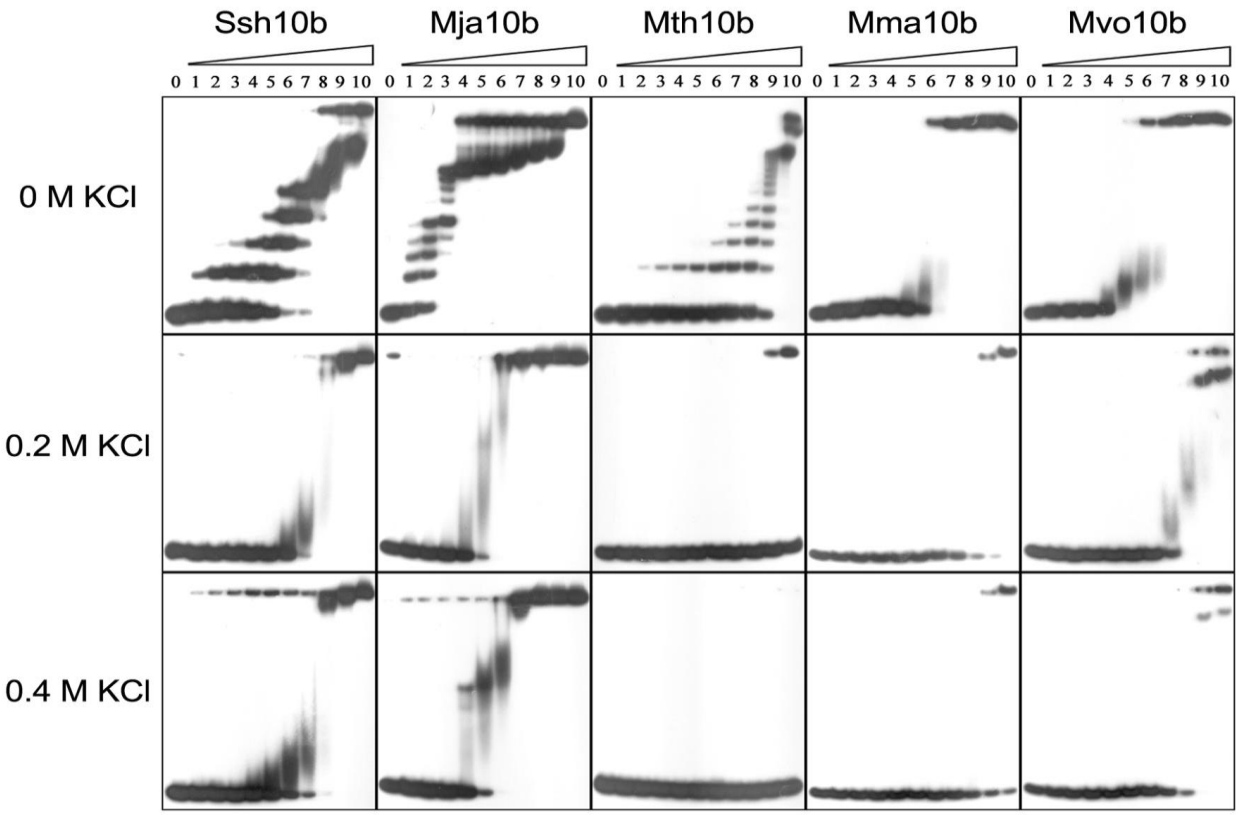
Ssh10b
Mja10b
Mth10b
Mma10b
Mvo10b
0 1 2 3 4 5 6 7 8 9 10
0 M KCl
0.2 M KCl
0.4 M KCl

B

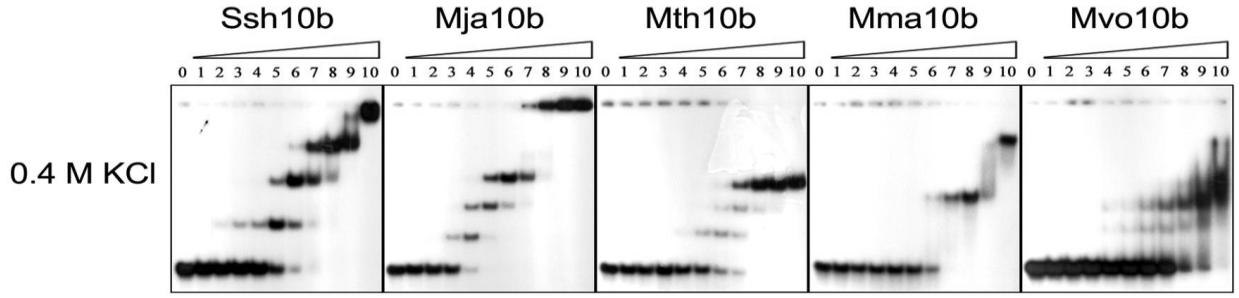
Ssh10b
Mja10b
Mth10b
Mma10b
Mvo10b
0 1 2 3 4 5 6 7 8 9 10
0.4 M KCl

Figure 2-4 Growth of the Δ*mma10b*::*pac* mutant S590 in minimal medium at 37°C. (■), wild-type strain S2; (□), the Δ*mma10b* mutant S590; (▲), the strain S591 (complementation of S590 with *mma10b* expressed from pMEV2-mma10b). Error bars are the standard deviations from twelve measurements of three independent experiments.

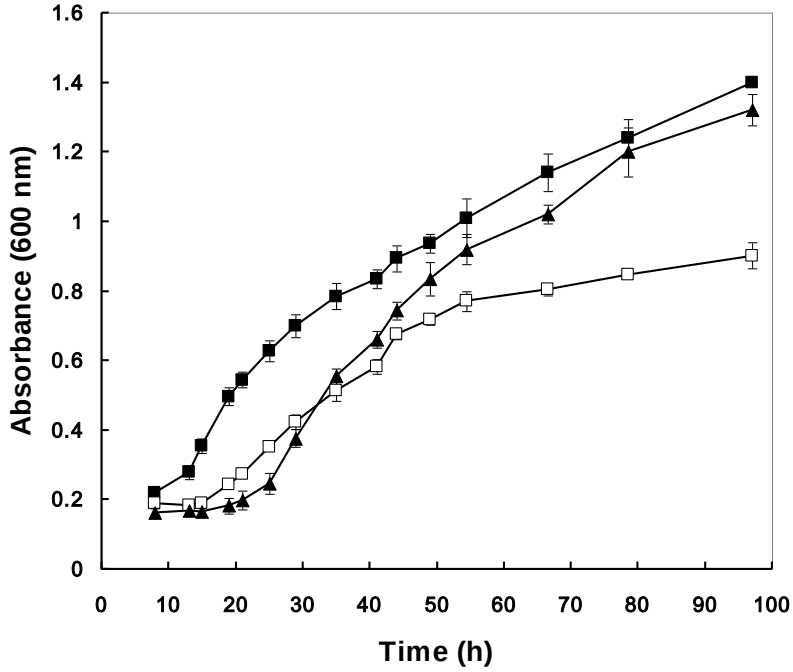
Absorbance (600 nm)
1.6
1.4
1.2
1
0.8
0.6
0.4
0.2
0
0
10
20
30
40
50
60
70
80
90
100
Time (h)

Figure 2-5. Effect of temperature on the growth of the Δ*mma10b*::*pac* mutant S590. (■), wild-type strain S2; (□), the mutant S590. The specific growth rates (μ) during the exponential phase were calculated from the slopes of the semilogarithmic plots. Representative error bars are the standard deviations from 8 measurements of two independent experiments. Growth rates in **A.** McN medium, **B.** McN medium plus acetate or McNA, **C.** McN medium plus alanine or McNAla, and **D.** McN medium plus yeast extract or McNY.

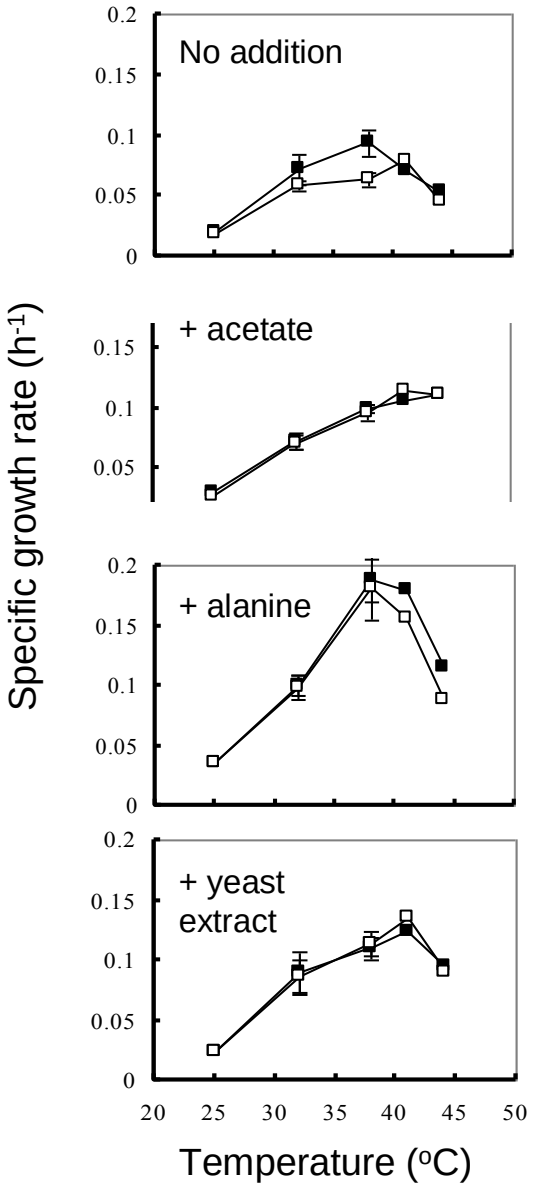
No addition
+ acetate
+ alanine
+ yeast extract
Specific growth rate (h-1)
Temperature (oC)
0.2
0.15
0.1
0.05
0
20
25
30
35
40
45
50

Figure 2-6. The consensus sequence of Mma10b binding site. The Mma10b binding site for DNA was predicted by the Gibbs Motif Sampler program using DNA sequences of the fragments associated with Mma10b in the ChIP analysis (Table S2-2). Diagram was created with the WebLogo program.


bits
2
1
0
5′
3′
1
2
3
4
5
6
7
8
9
10
11
12
13
14
15
16
17
18
weblogo.berkeley.edu

Figure 2-7. Analysis of sequence-dependent association of Mma10b with DNA by agarose (**A** and **B**) and PAGE gel (**C**) EMSA. **A.** Binding of Mma10b to linear DNA fragments with and without the binding-motif. The DNA concentration was 15 nM. Protein-DNA complexes were resolved by electrophoresis on 1.2 % agarose gels. From lanes 0 to 5, the protein concentrations were 0, 1, 2, 3.75, 7.5, and 15 μM, respectively. The presence or absence of Mma10b binding sites was predicted by the Motif Locator program with a score cutoff of 9.0. **B.** Binding of Mma10b to closed, circular supercoil and linear forms of the plasmid pB9. The linear plasmid was generated after digestion with HindIII. Based upon the Motif Locator program with a score cutoff of 9.0, the DNA sequences contained 4 potential Mma10b binding sites. The DNA concentration was 2 nM. Protein-DNA complexes were resolved by electrophoresis on 0.7 % agarose gels. From lane 0 to 5, the protein concentrations were 0, 1, 2, 3.75, 7.5, and 15 μM, respectively. **C.** Binding of Mma10b to ^{32}P-labeled 58-bp double-stranded DNA fragments. The DNA concentration was 20 nM. Protein-DNA complexes were resolved by electrophoresis on an 8 % non-denaturing polyacrylamide gel. The gel was exposed to X ray film. From lane 0 to 10, the protein concentrations were 0, 0.02, 0.04, 0.08, 0.16, 0.31, 0.63, 1.25, 2.5, 5, and 10 μM, respectively. The upper panel used DNA fragment with wild-type sequence (position in chromosome: 1307685- 1307742, which included ~~"b~~inding site a" in Fig. 2-8). The lower panel used a fragment where key bases in the motif were changed as indicated.

A

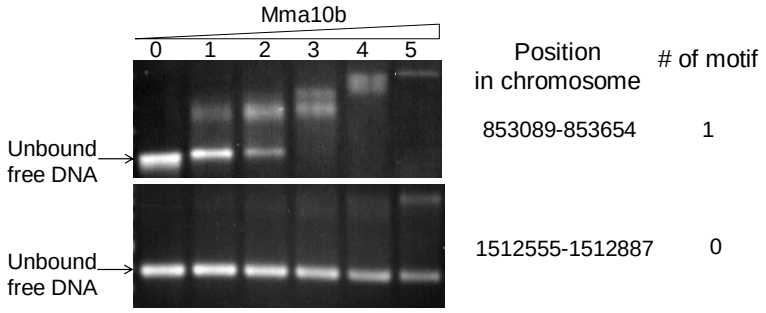
Mma10b
0 1 2 3 4 5
Position in chromosome
# of motif
Unbound free DNA
853089-853654
1
Unbound free DNA
1512555-1512887
0

B

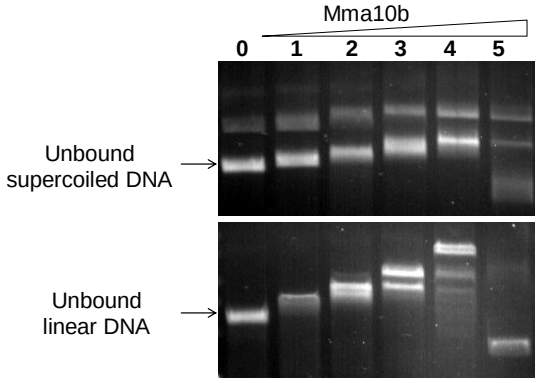
Mma10b
0 1 2 3 4 5
Unbound supercoiled DNA
Unbound linear DNA

C

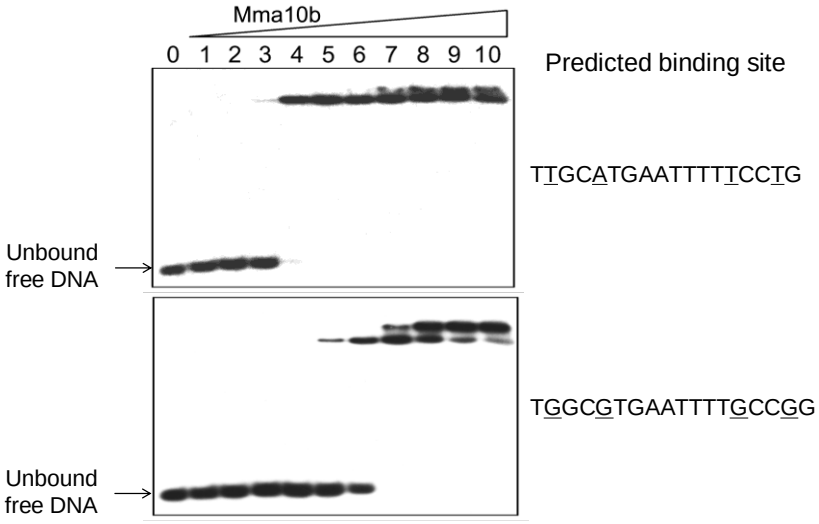
Mma10b
0 1 2 3 4 5 6 7 8 9 10
Predicted binding site
TTGCATGAATTTTTCCTG
Unbound free DNA
TGGCGTGAATTTTGCCGG
Unbound free DNA

Figure 2-8. Identification of DNA regions protected by Mma10b in DNase I footprinting analyses. **A.** Schematic diagram of the 389 bp DNA fragment (position in chromosome: 1307598-1307986) used in the footprinting reactions. One DNA strand was fluorescently labeled via PCR reactions with the primer B9F, which was labeled with 6-FAM at the 5‘ end. The DNA-binding sites (a and b), which were predicted by the program Motif Locator with consensus binding sequence, are indicated by shaded boxes. **B.** Electropherograms of fragments generated by footprinting reactions in the presence (15 μM) and absence of Mma10b. The patterns were viewed with the Peak Scanner software v1.0 (Applied Biosystems, Foster City, CA, USA). The regions that were protected by Mma10b during the digestion with DNase I are indicated as regions I and II. **C.** Expanded view of the region I from panel B. **D.** Expanded view of the site II from panel B. Red and blue lines represent reactions in the presence (15 μM) and absence of Mma10b, respectively. Specific sites that were protected by Mma10b are marked (•). The solid bars indicate the positions of the predicted binding sites a and b. The DNA sequences of sites a and b are shown below.

A


B9F
a
b
B9R
0
389
TTGCATGAATTTTTCCTG
271
288
CTATAGGAATATTTTCAA
343
360

B

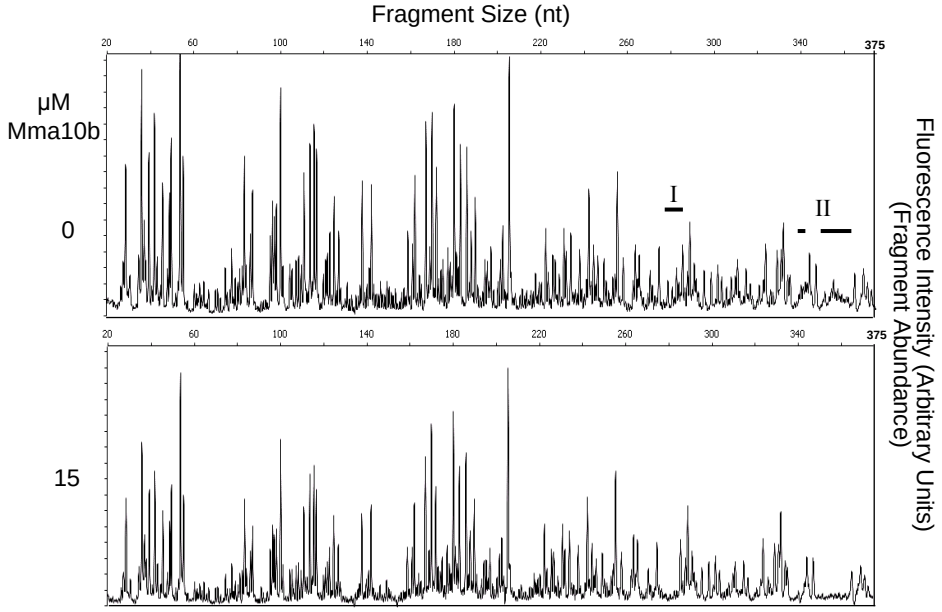
Fragment Size (nt)
20
60
100
140
180
220
260
300
340
375
μM Mma10b
0
15
I
II
Fluorescence Intensity (Arbitrary Units)
(Fragment Abundance)

C

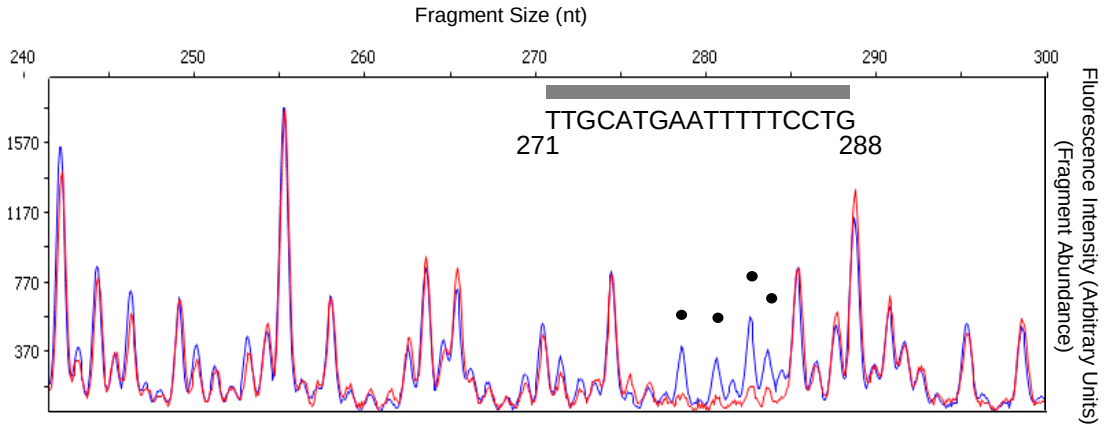
Fragment Size (nt)
240
250
260
270
280
290
300
1570
1170
770
370
TTGCATGAATTTTTCCTG
271
288
Fluorescence Intensity (Arbitrary Units)
(Fragment Abundance)

D

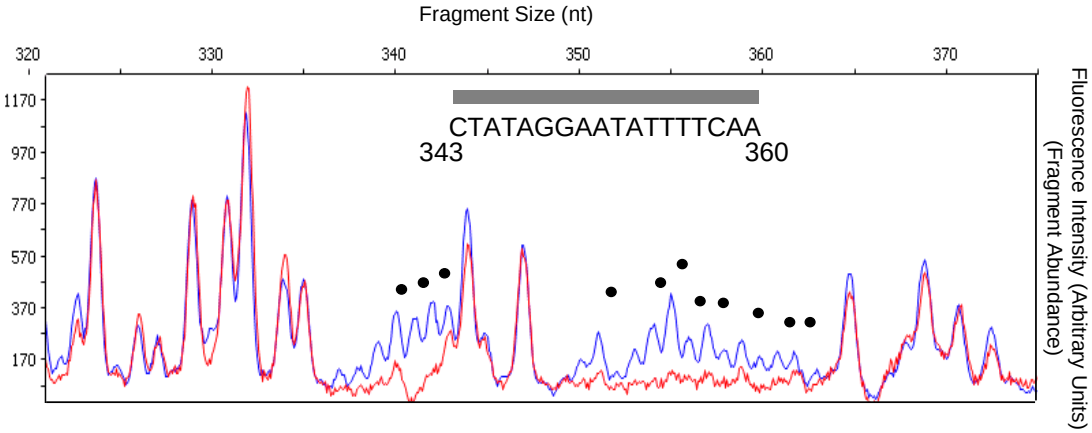
Fragment Size (nt)
320
330
340
350
360
370
1170
970
770
570
370
170
CTATAGGAATATTTTCAA
343
360
Fluorescence Intensity (Arbitrary Units)
(Fragment Abundance)

CHAPTER 3

METHANOCOCCI USE THE DIAMINOPIMELATE AMINOTRANSFERASE (DAPL) PATHWAY FOR LYSINE BIOSYNTHESIS[3]

---

[3]Liu, Y., R. H. White, and W. B. Whitman. Methanococci use the diaminopimelate aminotransferase (DapL) pathway for lysine biosynthesis. J. Bacteriol. 192(13):3304-3310. Reprinted here with permission of the publisher.

Abstract

The pathway of lysine biosynthesis in the methanococci has not been previously identified. A variant of the diaminopimelic acid (DAP) pathway uses diaminopimelate aminotransferase (DapL) to catalyze the direct conversion of tetrahydrodipicolinate (THDPA) to LL-DAP. Recently, the enzyme DapL (MTH52) was identified in *Methanothermobacter thermautotrophicus* and shown to belong to the DapL1 group. Although the *Methanococcus maripaludis* genome lacks a gene that can be unambiguously assigned a DapL function based upon sequence similarity, the open-reading frame MMP1527 shares 30 % amino acid sequence identity with MTH52. A deletion mutant, Δ*mmp1527*, was constructed and found to be a lysine auxotroph, suggesting that this DapL homolog in methanococci is required for lysine biosynthesis. In cell extracts of *M. maripaludis* wild-type strain, the specific activity of DapL using LL-DAP and α-ketoglutarate as substrates was 24.3 ± 2.0 nmol min^{-1} mg of $protein^{-1}$. The DapL homolog from *Methanocaldococcus jannaschii* (MJ1391) was cloned and expressed in *E. coli* and purified. Maximum activity of MJ1391 was observed at 70 ^{o}C and pH 8.0-9.0. The apparent K_ms of MJ1391 for LL-DAP and α-ketoglutarate were 82.8 ± 10 μM and 0.42 ± 0.02 mM, respectively. MJ1391 was not able to use succinyl-DAP or acetyl-DAP as a substrate. Phylogenetic analyses suggest two lateral gene transfers occurred within the DapL genes, one from the archaea to the bacteria in the DapL2 group, and one from the bacteria to the archaea in the DapL1 group. These results demonstrated that the DapL pathway is present in marine methanogens of the *Methanococcales*.

Introduction

Two separately evolved lysine biosynthesis pathways exist in nature, the diaminopimelic acid (DAP) and aminoadipic acid (AAA) pathways. The DAP pathway synthesizes L-lysine from aspartate and pyruvate, and diaminopimelic acid is an intermediate. This pathway is utilized by most bacteria, some archaea, some fungi, some algae, and plants (29, 30). The AAA pathway synthesizes L-lysine from α-ketoglutarate and acetyl-CoA, and α-aminoadipic acid is an intermediate. This pathway is utilized by most fungi, some algae, the bacterium *Thermus thermophilus*, and probably some archaea such as *Sulfolobus*, *Thermoproteus*, and *Pyrococcus* (28, 36). No organism is known to possess both pathways.

Four variations of the DAP pathway are known in bacteria: the succinylase, acetylase, aminotransferase, and dehydrogenase pathways (Fig. 3-1). They share the steps converting L-aspartate to L-2,3,4,5-tetrahydrodipicolinate (THDPA), but subsequent steps leading to the production of *meso*-diaminopimelate, the immediate precursor of L-lysine, are different. The succinylase pathway acylates THDPA with succinyl-CoA to generate *N*-succinyl-LL-2-amino-6-ketopimelate and forms *meso*-DAP by subsequent transamination, desuccinylation, and epimerization. This pathway is utilized by proteobacteria and many firmicutes and actinobacteria (4, 13, 15, 30). The acetylase pathway is analogous to the succinylase pathway but uses *N*-acetyl intermediates. This pathway is limited to certain *Bacillus* species, where the corresponding genes have not been identified (34, 39). The aminotransferase pathway converts THDPA directly to LL-DAP by diaminopimelate aminotransferase (DapL) without acylation. This pathway is shared by cyanobacteria (20), chlamydia (25), the archaeon *Methanothermobacter thermautotrophicus* (16, 19), and the plant *Arabidopsis thaliana* (20). The dehydrogenase pathway forms *meso*-DAP

directly from THDPA, NADPH, and NH_4^+ by diaminopimelate dehydrogenase (Ddh). This pathway is utilized by some *Bacillus* and *Brevibacterium* species and *Corynebacterium glutamicum* (26, 27, 40). Most bacteria use only one of the four variants, although certain bacteria, such as *C. glutamicum* and *Bacillus macerans*, possess both the succinylase and dehydrogenase pathways (3, 31).

The diaminopimelate aminotransferase (DapL) catalyzes the transfer of an amino group from L-glutamate to THDPA forming LL-DAP (20, 25). It uses pyridoxal 5‘-phosphate (PLP) as a coenzyme and has constrained substrate specificity. DapL is not closely related to the DapC/ArgD aminotransferase, which functions in the succinylase pathway. Comparative genomic analysis identified *dapL* homologs in both bacterial and archaeal genomes. Homologs of *dapD* and *dapE* are not found in genomes with *dapL* homologs, suggesting that transamination of THDPA does not require succinylation in these organisms (19). Phylogenetic analysis also suggests the classification of DapL into two groups, DapL1 and DapL2, which share ~30% amino acid sequence identity (19). Both groups exhibit DapL activity and cannot be differentiated by kinetic properties (19, 37). The distribution of the two groups is not obviously associated with specific prokaryotic lineages (19).

Methanogens are strictly anaerobic archaea that obtain all or most of their energy for growth from the production of large quantities of methane. All methanogens belong to *Euryarchaeota* and are currently classified into six orders: *Methanobacteriales*, *Methanococcales*, *Methanomicrobiales*, *Methanosarcinales*, *Methanopyrales*, and *Methanocellales* (24, 41, 42). Biochemical studies of *Methanocaldococcus jannaschii* and *Methanococcus voltae* belonging to *Methanococcales*, *Methanospirillum hungatei* belonging to *Methanomicrobiales*, and *Methanothermobacter thermautotrophicus* belonging to

Methanobacteriales suggested that these organisms derive their L-lysine from a DAP pathway but did not discriminate among the four DAP pathway variations (2, 10, 11, 33). Genome sequence analysis also suggested a DAP pathway in *Methanosarcina mazei* belonging to *Methanosarcinales* (9). Recent studies identified a *dapL* homolog belonging to the DapL1 group in *Methanothermobacter thermautotrophicus*. The gene product complemented an *Escherichia coli dapD-dapE* double mutant and catalyzed the transamination of DAP to THDPA, suggesting that *Methanobacteriales* use the DapL pathway for L-lysine biosynthesis (16, 19). Homologs of *asd*, *dapA*, *dapB*, *dapF*, and *lysA* have been identified in the genomes of *M. maripaludis* and *M. jannaschii* belonging to the *Methanococcales*, but homologs responsible for the conversion of THDPA to LL-DAP have not been annotated (5, 18). Here we identified methanococcal DapL homologs and demonstrate that the DapL pathway is present in *Methanococcales*.

Materials and Methods

Chemicals. A mixture of LL-, DD-, and *meso*-isomers of 2,6-diaminopimelic acid (DL-DAP) was purchased from Sigma-Aldrich. LL-DAP was a gift from Dr. André O. Hudson and Dr. Thomas Leustek.

A mixture of the different *N*-acetyl-diaminopimelic acid isomers was prepared by acetylation of DL-DAP with acetic anhydride. Thus, 150 µl of acetic anhydride was added to 3 ml of DL-DAP (190 mg, 1 mmol, dissolved in 1 M NaOH) with stirring. After 1 hr at room temperature, thin layer chromatography (TLC) analysis followed by detection of the amines with ninhydrin showed the presence of only two positive bands. Isolation of each band from the TLC plate and their conversion to the dimethyl trifluoroacetyl derivative showed that the bottom band was DAP, M^+ = 410 *m/z* with fragment ions at M^+ - 32 = 378 *m/z* and M^+-$COOCH_3$ at 351 *m/z*, and the upper band was the *N*-acetyl-DAP derivative with M^+ = 356 *m/z* with fragment ions at

M^+ - 31 = 325 *m/z* and M^+-$COOCH_3$ at 297 *m/z*. The sample was diluted with water, applied to a Dowex 50 H^+ column (1.5 x 16 cm), and eluted with a 400 ml gradient of HCl from 0 to 2 M. This resulted in the complete separation of DAP and *N*-acetyl-DAP. The *N*-acetyl-DAP was concentrated by lyophilization. A yield of 15% of soft, white non-crystalline solid was obtained. Despite the presence of multiple stereoisomers in each sample, only a single TLC spot was observed. The ^{1}H-NMR spectrum of the final product was also consistent with the authentic compound.

A mixture of the different *N*-succinyl-DAP isomers was prepared by the succinylation of DL-DAP as previously described for the preparation of *N*-succinyl-L-DAP (23). Analysis of the reaction mixture by TLC showed the presence of three compounds: the unreacted DAP, *N*-succinyl-DAP, and *N,N*-disuccinyl-DAP. The first two compounds formed ninhydrin positive spots after TLC. Despite the presence of multiple steroisomers, only a single spot was observed by TLC.

The TLC plates used for the analysis of amino acids were silica gel 60 F254 glass plates (5 × 20 cm) (EMD Chemicals, Inc., Darmstadt, Germany), and the solvent consisted of acetonitrile–water–formic acid (88%), (40:10:5 vol/vol/vol). In this solvent system, the compounds had the following R_f's: diaminopimelate, 0.107; aspartate, 0.30; *N*-acetyl-diaminopimelate, 0.35; *N*-succinyl-diaminopimelate, 0.35; α-glutamate, 0.40; *N*-disuccinyl-diaminopimelate, 0.43; and β-alanine, 0.45.

Strains, media, and culture conditions. *M. maripaludis* was grown in 28-ml aluminum seal tubes with 275 kPa of H_2:CO_2 (80:20 [v:v]) at 37°C in 5 ml of McNA (minimal medium + 10 mM sodium acetate), McNALys (McNA + 1 mM L-lysine), or McC (McNA + 0.2% [wt/vol] Casamino acids + 0.2% [wt/vol] yeast extract) as described previously (43). Antibiotics were not

included when comparing the growth of the wild-type and mutants. The inocula were 0.1 ml of cultures (~ 10^7 cells) grown in McC or McNALys medium. The inocula for cultures of the mutant S600 and the strain S601 were started with frozen stocks for all experiments to ensure that a revertant at second loci had not been selected. Puromycin (2.5 μg/ml) or neomycin (500 μg/ml in plates and 1 mg/ml in broth) was added when needed. Growth was determined by measuring the increase in absorbance at 600 nm.

Construction of the Δ*mmp1527*::*pac* mutant. The mutant was made by transformation of the wild-type *M. maripaludis* strain S2 with pIJA03-MMP1527, which was constructed from the integration vector pIJA03. The plasmid pIJA03 lacks an origin of replication for methanococci and contains a *pac* cassette, which encodes puromycin resistance (14, 22). To construct pIJA03-MMP1527, a 764 bp region upstream and a 766 bp region downstream of the MMP1527 gene were PCR amplified and cloned into the multiple cloning sites MCS1 and MCS2 of pIJA03, respectively. Primer sequences are available upon request. The orientation of each insert was confirmed by restriction mapping.

pIJA03-MMP1527 was transformed into *M. maripaludis* strain S2 by the polyethylene glycol method (35). After transformation, cultures were plated on McC medium plus puromycin. Puromycin-resistant isolates were restreaked on the same medium, and isolated colonies were then transferred to broth cultures containing 5 ml McC medium plus puromycin. After growth, 3 ml of the culture were used for determination of the genotype and phenotype. The remaining culture was used for preparation of frozen stocks (21). The genotype of the Δ*mmp1527*::*pac* mutant (S600) was confirmed by Southern hybridization (data not shown).

For complementation, the MMP1527 gene was PCR amplified. The primers introduced a *Nsi*I and a *Xba*I site at the 5'- and 3'- ends, respectively. The PCR products and the shuttle vector

pMEV2 (22) were digested with *Nsi*I and *Xba*I and gel purified. The cloning of the PCR products into pMEV2 placed MMP1527 downstream of the strong promoter PhmvA. The resulting plasmid, pMEV2-MMP1527, was transformed into S600 and screened on McC plates containing neomycin as previously described (22). The complemented strain was named S601.

Preparation of *M. maripaludis* cell-free extract. *M. maripaludis* was cultured in 100 ml of McC medium to an absorbance of ~0.4 at 600 nm. The cells were collected by centrifugation at 10,000 *g* for 30 min at 4 ^{o}C and resuspended in 2 ml of buffer containing 100 mM Tris (pH 8.5). The cells were lysed by freezing at -20 ^{o}C. Upon thawing, the cell lysate was incubated with 20 U of RQ1 DNase (Promega) at 37 ^{o}C for 15 min to digest DNA. Unbroken cells were removed by centrifugation at 8,000 *g* for 30 min at 4 ^{o}C. The protein concentrations were determined by BCA protein assay (Pierce) (32).

Cloning, expression, and purification of recombinant MJ1391 in *E. coli*. The *M. jannaschii* gene MJ1391 was amplified by PCR from genomic DNA. PCR was performed as described previously (17) using a 45 °C annealing temperature. The primers introduced a *Nde*I and a *Bam*HI site at the 5'- and 3'- ends, respectively. The amplified PCR product was purified with QIAQuick spin column (Invitrogen), digested with restriction enzymes *Nde*I and *Bam*HI, and then ligated into the compatible sites in the plasmid pT7-7 (Novagen) by bacteriophage T4 DNA ligase (Invitrogen) to make the plasmid pMJ1391. DNA sequences were verified by dye-terminator sequencing at the University of Iowa DNA facility. The resulting plasmid pMJ1391 was transformed into *E. coli* Origami 2(DE3)pLysS Singles (Novagen) cells. The transformed cells were grown in 1 L of Luria-Bertani medium supplemented with 100 μg/mL ampicillin at 37 °C with shaking until they reached an absorbance at 600 nm of 0.6~0.8. Isopropyl β-D-1-thiogalactopyranoside **(**IPTG) was added to a final concentration of 1 mM to induce the

recombinant protein production. After an additional overnight incubation at room temperature, the cells were harvested by centrifugation at 8,000 *g* for 20 min at 4 ^{o}C.

Cell-free extracts were prepared by sonication of the *E. coli* cell pellets, ~ 2 g wet weight, suspended in 10 mL of buffer (20 mM Tris/HCl, pH 7.6), followed by centrifugation at 10,000 *g* for 20 min at 4 ^{o}C. The *E. coli* proteins were denatured by heating the cell-free extract at 70 °C for 10 min, and the insoluble material was removed by centrifugation at 14,000 *g* for 20 min at 4 ^{o}C. About 5 mL of this extract was applied to a Mono Q 5/50 GL anion-exchange column (GE Healthcare) equilibrated with buffer A (20 mM Tris/HCl, pH 7.5). Bound protein was eluted with a 20 mL linear gradient from 0 to 0.5 M NaCl in buffer A at a flow rate of 2.0 mL/min, collecting 1 ml per fraction. Elution of the protein was monitored by UV absorbance at 280 nm. One major UV-absorbing peak eluted at 0.37 M NaCl and contained the desired protein, based on DapL activity measurement and SDS-PAGE analysis. Purified proteins were dialyzed against 10 mM potassium phosphate buffer (pH 7.0) and 10% glycerol (wt/vol) and stored at -20 ^{o}C until use. Protein concentrations were determined by BCA protein assay (Pierce) (32).

DapL activity assays. DapL activity was measured quantitatively in the physiologically reverse direction (LL-DAP→THDPA) based on the DAP-dependent formation of glutamate from α-ketoglutarate. The assay was coupled to the conversion of glutamate back to α-KG by glutamate dehydrogenase in the presence of $NADP^{+}$, and the production of NADPH was monitored with a Beckman DU640B spectrophotometer at 340 nm.

For enzyme assays of the *M. maripaludis* cell-free extract, 1 ml reaction mixtures contained 100 mM Tris (pH 8.5), 0.25 mg of protein, 2 mM α-KG, 2 mM DL-DAP or 0.5 mM LL-DAP, 10 mM $NADP^{+}$, 0.25 mM PLP, and 20 U L-glutamate dehydrogenase from bovine liver

(Sigma-Aldrich). The reactions were incubated at 37 ^{o}C, and the increase in absorbance at 340 nm was monitored continuously.

For enzyme assays of the purified recombinant MJ1391-derived protein, the DapL and glutamate dehydrogenase reactions were carried out separately due to the different temperature optima. The 0.9 ml DapL reaction mixture contained 100 mM Tris-HCl (pH 8.5), 5 μg MJ1391 protein, 2 mM α-KG, 2 mM DL-DAP or 0.5 mM LL-DAP, and 0.25 mM PLP. The reactions were incubated at 70 ^{o}C for 30 min. Since the recombinant MJ1391 protein showed no detectable activity below 45 ^{o}C, the DapL reaction was terminated by rapid cooling of the mixture in an ice-water bath. Then 10 mM $NADP^{+}$ and 20 U L-glutamate dehydrogenase were added to a final volume of 1 ml. The reactions were incubated for an additional 20 min at 37 ^{o}C, and the absorbance at 340 nm was measured. The amount of NADPH produced was calculated from the extinction coefficient of 6.22 $mM^{-1}cm^{-1}$ (8). The DapL reaction at room temperature served as a negative control.

To determine the pH optimum, 200 mM of the following buffers were used at the indicated pH values: BIS-Tris (bis[2-hydroxyethyl]-amino-tris[hydroxymethyl]-methane) hydrochloride for pH 5.5, 6.0, and 6.5, Tris-HCl for pH 7.0, 7.5, 8.0, and 8.5, and sodium CHES [2-(*N*-cyclohexylamino)ethanesulfonate] for pH 9.0, 9.5, and 10.0. The coupling reaction by L-glutamate dehydrogenase was not limiting in the pH range from 5.5 to 10.0.

The affects of salts on MJ1391 activity was determined by addition of 100 mM of each of the following salts: KCl, K_2SO_4, KH_2PO_4, NaCl, Na_2SO_4, NaH_2PO_4, $MgCl_2$, and $MgSO_4$. The reaction buffers contained 100 mM of Tris (pH 8.5), and the pH was adjusted with HCl, H_2SO_4, or H_3PO_4 to have the same anion as the salt added. The L-glutamate dehydrogenase coupling reaction was not limited by these salts.

Kinetic constants of MJ1391 were determined as described above except that the LL-DAP concentrations were 0.2, 0.4, 0.6, 0.8, and 1.0 mM and the α-KG concentrations were 0.25, 0.5, 1.0, 1.5, and 2.0 mM. The data were analyzed using SigmaPlot 10.0 with the Enzyme Kinetics module (Systat Software Inc.) fitted with a Ping-Pong Bi-Bi mechanism.

Fluorescence assay of PLP. PLP in the purified recombinant protein MJ1391 was identified and quantified from the fluorescence of the PLP-cyanide product as described by Adams (1). Fluorescence spectra were recorded on a Shimadzu RF-1501 spectrofluorometer.

Phylogenetic analysis. DapL homologs were identified using BLASTp searches against selected genomes. A phylogenetic tree was constructed by the MEGA4 program using the minimum evolution (ME) method with its default settings. For comparisons of ratios of evolutionary distances (RED) (12), the alignments were generated using the ClustalX program. Evolutionary distances (E_d) were calculated by the MEGA4 program using the PAM-t matrix with its default settings. The mean E_d of the genes encoding the large ribosomal subunit protein 2 (L2P), leucyl-tRNA synthetase, and SecY, was used as the control E_d (12).

Results and Discussion

The Δ*mmp1527* mutant of *M. maripaludis* is a lysine auxotroph. Sequence similarity searches identified DapL homologs in *Methanococcales* sharing 27-33% amino acid sequence identity with the DapL in *M. thermautotrophicus* (MTH52). Since DapL is an aminotransferase closely related to many enzymes with other catalytic activities (19), this level of relatedness was not sufficient to predict the function of the *Methanococcales* homologs. Therefore, the gene encoding the DapL homolog in *M. maripaludis* (MMP1527) was deleted by gene replacement with the *pac* cassette, which encodes puromycin resistance in methanococci. The deletion of MMP1527 was confirmed by Southern hybridization (data not shown). Since the

downstream genes were transcribed on the opposite strand from MMP1527, this mutation was not expected to be polar and affect transcription of downstream genes.

The Δ*mmp1527* mutant, strain S600, was unable to grow in the absence of exogenous L-lysine (Fig. 3-2). Unlike some amino acids, lysine can be readily taken up by methanococci from the medium (44). When 1 mM of L-lysine was added to McNA medium, S600 grew at a rate comparable to that of wild-type S2. Addition of the other 19 standard amino acids to McNA medium did not result in the growth. To confirm that these differences were due to the deletion of MMP1527, the complementation strain S601 was constructed by transforming the plasmid pMEV2-MMP1527 into S600. In this strain, MMP1527 was expressed from a strong methanococcal promoter. S601 grew in the absence of exogenous L-lysine (Fig. 3-2). These results indicated that MMP1527 was required for a L-lysine biosynthesis, and that MMP1527 was not essential for the biosynthesis of other amino acids.

DapL activity in *M. maripaludis* cell extract. The specific activities of DapL in cell extracts of *M. maripaludis* strains S2, S600, and S601 using 0.5 mM of LL-DAP as substrate were 24 ± 2, < 1, and 36 ± 2 nmol min^{-1} mg of $protein^{-1}$, respectively. These results confirmed the presence of DapL activity in *M. maripaludis* and its attribution to MMP1527.

The *M. maripaludis* wild-type S2 cell extract was examined for substrate specificity. When DAP was replaced in assays with acetyl-DAP (2 mM) and succinyl-DAP (2 mM), the specific activities were < 4 nmol min^{-1} mg of $protein^{-1}$. The absence of detectable activities suggested that *M. maripaludis* DapL did not use acetyl-DAP or succinyl-DAP as substrates.

The MJ1391 gene product catalyzed the diaminopimelate aminotransferase reaction. The DapL homolog from *M. jannaschii* (MJ1391) was expressed in *E. coli* and partially purified by heat denaturation of *E. coli* proteins followed by anion-exchange

chromatography to a purity of ~70%. The presence of PLP in the recombinant MJ1391 protein was confirmed by the fluorescent excitation and emission spectra of the PLP-cyanide product. Analysis of the spectra indicated the presence of 18.7 μmol of PLP/mg protein (data not shown). Considering the molecular mass of 47.9 kDa for the protomer, this corresponded to 0.89 PLP per protomer.

This recombinant MJ1391 protein catalyzed the transamination of LL-DAP as determined by the DapL activity assay (Fig. 3-3A). Moreover, the protein MJ1391 and substrates α-KG and LL-DAP were stable at 100 ^{o}C for at least 30 min (Fig. 3-3B). The activity with acetyl-DAP (2 mM) or succinyl-DAP (2 mM) as substrate was below the detection limit of ~ 0.05 μmol min^{-1} mg of protein^{-1} (data not shown).

The DapL activity of MJ1391-derived enzyme was examined with different reaction conditions. The optimum temperature of the DapL activity of MJ1391 was ~70 ^{o}C, and no activity was detectable at temperatures below 45 ^{o}C (Fig. 3-4A). At 85 ^{o}C, the optimum growth temperature of *M. jannaschii*, the DapL activity was 85% of the maximum activity. The optimum pH was ~8.5. About 40 and 50% of the maximum activity were observed at pH 7.0 and 10.0, respectively (Fig. 3-4B). All subsequent assays were performed at 70 ^{o}C and pH 8.5. Monovalent anions are frequently stimulatory to enzymes from the methanococci (45). However, addition of 100 mM of KCl, K_2SO_4, KH_2PO_4, NaCl, Na_2SO_4, NaH_2PO_4, $MgCl_2$, and $MgSO_4$ had no effect on the enzyme activity (data not shown).

The kinetic constants of MJ1391 were within the range for DapL homologs from other sources (19, 25). The K_ms for LL-DAP and α-KG were 82.8 ± 10 μM (6-116 μM from other organisms) and 0.42 ± 0.02 mM (0.3-2.6 mM from other organisms), respectively. The V_{max} was

0.39 ± 0.01 μmol min^{-1} mg of $protein^{-1}$ (0.25-10.6 μmol min^{-1} mg of $protein^{-1}$ from other organisms). The k_{cat} for MJ1391 was 18.3 min^{-1} after correction for the purity of 70 %.

Phylogenetic analysis of *dapL* homologs. Phylogenetic analysis of DapL identified homologs in all sequenced genomes of the *Methanococcales*: *M. jannaschii*, *Methanocaldococcus infernus*, *Methanocaldococcus fervens*, *Methanocaldococcus vulcanius*, *M. maripaludis*, *Methanococcus voltae*, *Methanococcus aeolicus*, and *Methanococcus vannielii*. They shared 74-89% amino acid sequence identity. According to the phylogenetic tree topology, these methanococcal DapL homologs clustered apart from the DapL1 and DapL2 groups, with which they shared 29-33% and 30-42% amino acid sequence identity, respectively (Fig. 3-5A).

The methanococcal enzymes are also distinguished from the DapL1 and DapL2 groups by comparison of conserved amino acid residues. Based upon the crystal structure of DapL from *Arabidopsis thaliana*, three conserved residues in DapL1, Glu97, Asn309, and Lys129, are important for LL-DAP and glutamate binding (37). Lys129, which is found at similar positions in aspartate aminotransferases, is conserved in all DapL homologs. DapL2 lacks the other two residues, Glu97 and Asn309 (19). Methanococcal DapL contains only Glu97. Further study will be needed to understand how the substrates bind to DapL2 and methanococcal DapL.

The phylogeny of the bacterial and archaeal DapL in the ME tree was not correlated with the 16S-rRNA-based phylogeny, indicating that lateral gene transfers (LGTs) may have made substantial contributions to the evolution of DapL in some lineages. The evolutionary history of DapL homologs was evaluated by comparisons of ratios of their evolutionary distances (RED) with control genes which were believed to have undergone primarily vertical evolution (12). If the evolutionary rate of DapL was constant and LGTs have not occurred, then

a plot of the DapL evolutionary distances (E_d) against the control E_ds will be linear. As shown in Fig. 3-5B, the intra-domain comparisons within each DapL group were close to a trend line indicative of a constant rate of DapL evolution relative to that of the control genes. Moreover, comparisons between the bacterial DapL1, the archaeal DapL2, and the methanococcal DapL lay on the same trend line, indicating that these groups did not obtain the gene from a LGT. However, the inter-domain comparisons between bacteria and archaea within each of the DapL1 and DapL2 groups had lower E_ds than expected, and bacterial and archaeal intra-domain comparisons between each of the groups had higher E_ds than expected for normal vertical evolution. These results suggested that inter-domain LGTs occurred within both groups, one transfer from the archaeal DapL2 group to form the bacterial DapL2 group and one transfer from the bacterial DapL1 group to form the archaeal DapL1 group (Fig. 3-5C). Lastly, comparisons between the bacterial DapL2 and the archaeal DapL1 groups are on the central trend line because each resulted from LGTs but in the opposite directions. In toto, these results suggested that DapL evolution, while marked by two LGT events, did not undergo discontinuities in the rate of evolution or formation of paralogous gene families.

RED analyses including the uncharacterized DapL paralogs of *E.coli* (b2379) and *B. subtilis* (BSU37690) found that they had lower E_d with archaeal DapL2 and methanococcal DapL groups and higher E_d with bacteria DapL than expected, suggesting that these paralogs may have an archaeal origin (data not shown).

The selective pressure for some organisms to obtain and maintain the DapL pathway instead of the acylation pathways is unclear. THDPA is unstable at neutral pH and at equilibrium forms a mixture of the cyclic THDPA and acylic L-α-keto-ε-aminopimelate (6, 7). The equilibrium favors cyclic THDPA, while the acyclic form containing the keto-group is the

substrate for transamination. Therefore, acylation may facilitate the transamination by exposing the keto-group at the expense of one succinyl-CoA or acetyl-CoA (16, 19, 20). However, whether cyclic THDPA is the actual substrate of DapL or DapL catalyzes the ring-opening reaction await further investigation (37, 38).

In conclusion, methanococci use the DapL pathway for L-lysine biosynthesis, as a deletion mutation of the *dapL* homolog in *M. maripaludis* resulted in a lysine auxotrophy and the purified homologous protein in *M. jannaschii* catalyzed the DAP aminotransferase reaction. Moreover, the activities with succinylated and acetylated DAP were not observed for *M. maripaludis* cell extract and the recombinant *M. jannaschii* protein, suggesting that the succinylase and acetylase pathways are not used by methanococci.

Acknowledgments

We thank Dr. André O. Hudson and Dr. Thomas Leustek for the kind gift of LL-DAP. We thank Kim Harich for assistance with GC/MS analyses. This work was supported by grants from the U. S. Department of Energy to W.B.W, MCB0722787 from the U.S. National Science Foundation to R.H.W, and a dissertation completion grant from the University of Georgia to Y.L.

References

1. **Adams, E.** 1979. Fluorometric determination of pyridoxal phosphate in enzymes. Methods Enzymol. **62:**407-410.

2. **Bakhiet, N., F. Forney, D. Stahly, and L. Daniels.** 1984. Lysine biosynthesis in *Methanobacterium thermoautotrophicum* is by the diaminopimelic acid pathway. Curr. Microbiol. **10:**195-198.

3. **Bartlett, A. T. M., and P. J. White.** 1985. Species of *Bacillus* that make a vegetative peptidoglycan containing lysine lack diaminopimelate epimerase but have diaminopimelate dehydrogenase. J. Gen. Microbiol. **131:**2145-2152.

4. **Blanchard, J. S., and R. Ledwidge.** 1999. The dual biosynthetic capability of *N*-acetylornithine aminotransferase in arginine and lysine biosynthesis. Biochemistry **38:**3019-3024.

5. **Bult, C. J., O. White, G. J. Olsen, L. Zhou, R. D. Fleischmann, G. G. Sutton, J. A. Blake, L. M. FitzGerald, R. A. Clayton, J. D. Gocayne, A. R. Kerlavage, B. A. Dougherty, J.-F. Tomb, M. D. Adams, C. I. Reich, R. Overbeek, E. F. Kirkness, K. G. Weinstock, J. M. Merrick, A. Glodek, J. L. Scott, N. S. M. Geoghagen, J. F. Weidman, J. L. Fuhrmann, D. Nguyen, T. R. Utterback, J. M. Kelley, J. D. Peterson, P. W. Sadow, M. C. Hanna, M. D. Cotton, K. M. Roberts, M. A. Hurst, B. P. Kaine, M. Borodovsky, H.-P. Klenk, C. M. Fraser, H. O. Smith, C. R. Woese, and J. C. Venter.** 1996. Complete genome sequence of the methanogenic archaeon, *Methanococcus jannaschii*. Science **273:**1058-1073.

6. **Caplan, J., A. Sutherland, and J. C. Vederas.** 2001. The first stereospecific synthesis of L-tetrahydrodipicolinic acid; a key intermediate of diaminopimelate metabolism. J. Chem. Soc. Perkin Trans. 1**:**2217–2220.

7. **Chrystal, E. J. T., L. Couper, and D. J. Robins.** 1995. Synthesis of a key intermediate in the diaminopimelate pathway to L-Lysine: 2,3,4,5-tetrahydrodipicolinic acid. Tetrahedron **51:**10241-10252.

8. **Dawson, R. M. C., D. C. Elliott, W. H. Elliott, and K. M. Jones.** 1986. Spectral data and pKa values for purines, pyrmidine, nucleosides and nucleotides p. 103-114. *In* R. M. C. Dawson, D. C. Elliott, W. H. Elliott, and K. M. Jones (ed.), Data for biochemical research 3rd ed. Oxford University Press, New York.

9. **Deppenmeier, U., A. Johann, T. Hartsch, R. Merkl, R. A. Schmitz, R. Martinez-Arias, A. Henne, A. Wiezer, S. Baumer, C. Jacobi, H. Bruggemann, T. Lienard, A. Christmann, M. Bomeke, S. Steckel, A. Bhattacharyya, A. Lykidis, R. Overbeek, H. P. Klenk, R. P. Gunsalus, H. J. Fritz, and G. Gottschalk.** 2002. The genome of *Methanosarcina mazei*: evidence for lateral gene transfer between bacteria and archaea. J Mol Microbiol Biotechnol **4:**453-61.

10. **Ekiel, I., K. F. Jarrell, and G. D. Sprott.** 1985. Amino acid biosynthesis and sodium-dependent transport in *Methanococcus voltae*, as revealed by ^{13}C NMR. Eur. J. Biochem. **149:**437-444.

11. **Ekiel, I., I. C. Smith, and G. D. Sprott.** 1983. Biosynthetic pathways in *Methanospirillum hungatei* as determined by ^{13}C nuclear magnetic resonance. J. Bacteriol. **156:**316-326.

12. **Farahi, K., G. D. Pusch, R. Overbeek, and W. B. Whitman.** 2004. Detection of lateral gene transfer events in the prokaryotic tRNA synthetases by the ratios of evolutionary distances method. J. Mol. Evol. **58:**615-631.

13. **Fuchs, T. M., B. Schneider, K. Krumbach, L. Eggeling, and R. Gross.** 2000. Characterization of a *Bordetella pertussis* diaminopimelate (DAP) biosynthesis locus identifies *dapC*, a novel gene coding for an *N*-succinyl-L,L-DAP aminotransferase. J. Bacteriol. **182:**3626-3631.

14. **Gernhardt, P., O. Possot, M. Foglino, L. Sibold, and A. Klein.** 1990. Construction of an integration vector for use in the archaebacterium *Methanococcus voltae* and expression of a eubacterial resistance gene. Mol. Gen. Genet. **221:**273-279.

15. **Gilvarg, C.** 1961. *N*-Succinyl-α-amino-6-ketopimelic Acid. J. Biol. Chem. **236:**1429-1431.

16. **Graham, D. E., and H. K. Huse.** 2008. Methanogens with pseudomurein use diaminopimelate aminotransferase in lysine biosynthesis. FEBS letters **582:**1369-1374.

17. **Graupner, M., H. Xu, and R. H. White.** 2000. Identification of an archaeal 2-hydroxy acid dehydrogenase catalyzing reactions involved in coenzyme biosynthesis in methanoarchaea. J. Bacteriol. **182:**3688-3692.

18. **Hendrickson, E. L., R. Kaul, Y. Zhou, D. Bovee, P. Chapman, J. Chung, E. Conway de Macario, J. A. Dodsworth, W. Gillett, D. E. Graham, M. Hackett, A. K. Haydock, A. Kang, M. L. Land, R. Levy, T. J. Lie, T. A. Major, B. C. Moore, I. Porat, A. Palmeiri, G. Rouse, C. Saenphimmachak, D. Soll, S. Van Dien, T. Wang, W. B. Whitman, Q. Xia, Y. Zhang, F. W. Larimer, M. V. Olson, and J. A. Leigh.** 2004. Complete genome sequence of the genetically tractable hydrogenotrophic methanogen *Methanococcus maripaludis*. J. Bacteriol. **186:**6956-6969.

19. **Hudson, A. O., C. Gilvarg, and T. Leustek.** 2008. Biochemical and phylogenetic characterization of a novel diaminopimelate biosynthesis pathway in prokaryotes identifies a diverged form of LL-diaminopimelate aminotransferase. J Bacteriol. **190:**3256-3263.

20. **Hudson, A. O., B. K. Singh, T. Leustek, and C. Gilvarg.** 2006. An LL-diaminopimelate aminotransferase defines a novel variant of the lysine biosynthesis pathway in plants. Plant Physiol. **140:**292-301.

21. **L., T. D., J. Keswani, J. S. Shieh, and W. B. Whitman.** 1995. Maintenance of methanogen stock cultures in glycerol at -70 ^{o}C, p. 85-87. *In* S. Robb F. T., K. R., DasSarma, S., Place, A. R., Schreier, H. J., Fleischmann, E. M. (ed.), Archaea-a laboratory manual. Cold Spring Harbor Laboratory Press, Cold Spring Harbor, N. Y.

22. **Lin, W., and W. Whitman.** 2004. The importance of porE and porF in the anabolic pyruvate oxidoreductase of *Methanococcus maripaludis*. Arch. Microbiol. **181:**68-73.

23. **Lin, Y. K., R. Myhrman, M. L. Schrag, and M. H. Gelb.** 1988. Bacterial *N*-succinyl-L-diaminopimelic acid desuccinylase. Purification, partial characterization, and substrate specificity. J. Biol. Chem. **263:**1622-1627.

24. **Liu, Y.** 2010. Taxonomy of methanogens, p. 550-558. *In* K. N. Timmis, T. McGenity, J. R. v. d. Meer, and V. d. Lorenzo (ed.), Handbook of hydrocarbon and lipid microbiology, vol. 1. Springer-Verlag Berlin, Heidelberg.

25. **McCoy, A. J., N. E. Adams, A. O. Hudson, C. Gilvarg, T. Leustek, and A. T. Maurelli.** 2006. L,L-diaminopimelate aminotransferase, a trans-kingdom enzyme shared by *Chlamydia* and plants for synthesis of diaminopimelate/lysine. Proc. Natl. Acad. Sci. USA **103:**17909-17914.

26. **Misono, H., H. Togawa, T. Yamamoto, and K. Soda.** 1979. Meso-α,ε-diaminopimelate D-dehydrogenase: distribution and the reaction product. J. Bacteriol. **137:**22-27.

27. **Misono, H., H. Togawa, T. Yamamoto, and K. Soda.** 1976. Occurrence of meso-α,ε-diaminopimelate dehydrogenase in *Bacillus sphaericus*. Biochem. Biophys. Res. Commun. **72:**89-93.

28. **Nishida, H., M. Nishiyama, N. Kobashi, T. Kosuge, T. Hoshino, and H. Yamane.** 1999. A prokaryotic gene cluster involved in synthesis of lysine through the amino adipate pathway: a key to the evolution of amino acid biosynthesis. Genome Res. **9:**1175-1183.

29. **Patte, J.-C.** 1996. Biosynthesis of threonine and lysine, p. 528-541. *In* F. C. Neidhardt, R. Curtiss III, J. L. Ingraham, E. C. C. Lin, K. B. Low, B. Magasanik, W. S. Reznikoff, M. Riley, M. Schaechter, and H. E. Umbarger (ed.), *Escherichia coli* and *Salmonella*: cellular and molecular biology, 2nd ed. ASM Press, Washington, DC.

30. **Scapin, G., and J. S. Blanchard.** 1998. Enzymology of bacterial lysine biosynthesis. Adv. Enzymol. Relat. Areas Mol. Biol. **72:**279-324.

31. **Schrumpf, B., A. Schwarzer, J. Kalinowski, A. Puhler, L. Eggeling, and H. Sahm.** 1991. A functionally split pathway for lysine synthesis in *Corynebacterium glutamicium*. J. Bacteriol. **173:**4510-4516.

32. **Smith, P. K., R. I. Krohn, G. T. Hermanson, A. K. Mallia, F. H. Gartner, M. D. Provenzano, E. K. Fujimoto, N. M. Goeke, B. J. Olson, and D. C. Klenk.** 1985. Measurement of protein using bicinchoninic acid. Anal. Biochem. **150:**76-85.

33. **Sprott, G. D., I. Ekiel, and G. B. Patel.** 1993. Metabolic pathways in *Methanococcus jannaschii* and other methanogenic bacteria. Appl. Environ. Microbiol. **59:**1092-1098.

34. **Sundharadas, G., and C. Gilvarg.** 1967. Biosynthesis of α, ε-diaminopimelic acid in *Bacillus megaterium*. J. Biol. Chem. **242:**3983-3984.

35. **Tumbula, D. L., R. A. Makula, and W. B. Whitman.** 1994. Transformation of *Methanococcus maripaludis* and identification of a PstI-like restriction system. FEMS Microbiol. Lett. **121:**309-314.

36. **Velasco, A. M., J. I. Leguina, and A. Lazcano.** 2002. Molecular evolution of the lysine biosynthetic pathways. J. Mol. Evol. **55:**445-449.

37. **Watanabe, N., M. M. Cherney, M. J. van Belkum, S. L. Marcus, M. D. Flegel, M. D. Clay, M. K. Deyholos, J. C. Vederas, and M. N. James.** 2007. Crystal structure of LL-diaminopimelate aminotransferase from *Arabidopsis thaliana*: a recently discovered enzyme in the biosynthesis of L-lysine by plants and *Chlamydia*. J. Mol. Biol. **371:**685-702. Epub 2007 May 26.

38. **Watanabe, N., M. D. Clay, M. J. van Belkum, M. M. Cherney, J. C. Vederas, and M. N. G. James.** 2008. Mechanism of substrate recognition and PLP-induced conformational changes in LL-diaminopimelate aminotransferase from *Arabidopsis thaliana*. J. Mol. Biol. **384:**1314-1329.

39. **Weinberger, S., and C. Gilvarg.** 1970. Bacterial distribution of the use of succinyl and acetyl blocking groups in diaminopimelic acid biosynthesis. J. Bacteriol. **101:**323-324.

40. **White, P. J.** 1983. The essential role of diaminopimelate dehydrogenase in the biosynthesis of lysine by *Bacillus sphaericus*. J. Gen. Microbiol. **129:**739-749.

41. **Whitman, W., T. Bowen, and D. Boone.** 2006. The Methanogenic bacteria, p. 165-207. *In* M. Dworkin, Falkow, S., Rosenberg, E., Schleifer K.-H., Stackebrandt E. (ed.), The Prokaryotes, 3rd ed. Springer-Verlag, New York.

42. **Whitman, W. B., D. R. Boone, Y. Koga, and J. Keswani.** 2001. Taxonomy of methanogenic archaea, p. 211-213. *In* D. R. Boone, Castenholtz, R. W., Garrity, G. M. (ed.), Bergey's mannual of systematic bacteriology, 2nd ed, vol. 1. Springer-Verlag, New York.

43. **Whitman, W. B., J. Shieh, S. Sohn, D. S. Caras, and U. Premachandran.** 1986. Isolation and characterization of 22 mesophilic methanococci. Syst. Appl. Microbiol. **7:**235-240.

44. **Whitman, W. B., S. Sohn, S. Kuk, and R. Xing.** 1987. Role of amino acids and vitamins in nutrition of mesophilic *Methanococcus* spp. Appl. Environ. Microbiol. **53:**2373-2378.

45. **Xing, R. Y., and W. B. Whitman.** 1991. Characterization of enzymes of the branched-chain amino acid biosynthetic pathway in *Methanococcus* spp. J. Bacteriol. **173:**2086-2092.

Figure 3-1. Variations of the DAP pathway for lysine biosynthesis: ① succinylase pathway, ② acetylase pathway, ③ aminotransferase pathway, and ④ dehydrogenase pathway. Acronyms in the diagram include DAP, diaminopimelate; THDPA, L-2,3,4,5-tetrahydrodipicolinate; LL-DAP, LL-2,6-diaminopimelate; *meso*-DAP, *meso*-2,6-diaminopimealte; LysC, aspartate kinase; Asd, aspartate semialdehyde dehydrogenase; DapA, dihydrodipicolinate synthase; DapB, dihydrodipicolinate reductase; DapD, THDPA succinylase; DapC, succinyl-DAP aminotransferase; DapE, succinyl-DAP desuccinylase; DapF, DAP epimerase; LysA, DAP decarboxylase; DapL, LL-DAP aminotransferase; Ddh, DAP dehydrogenase.

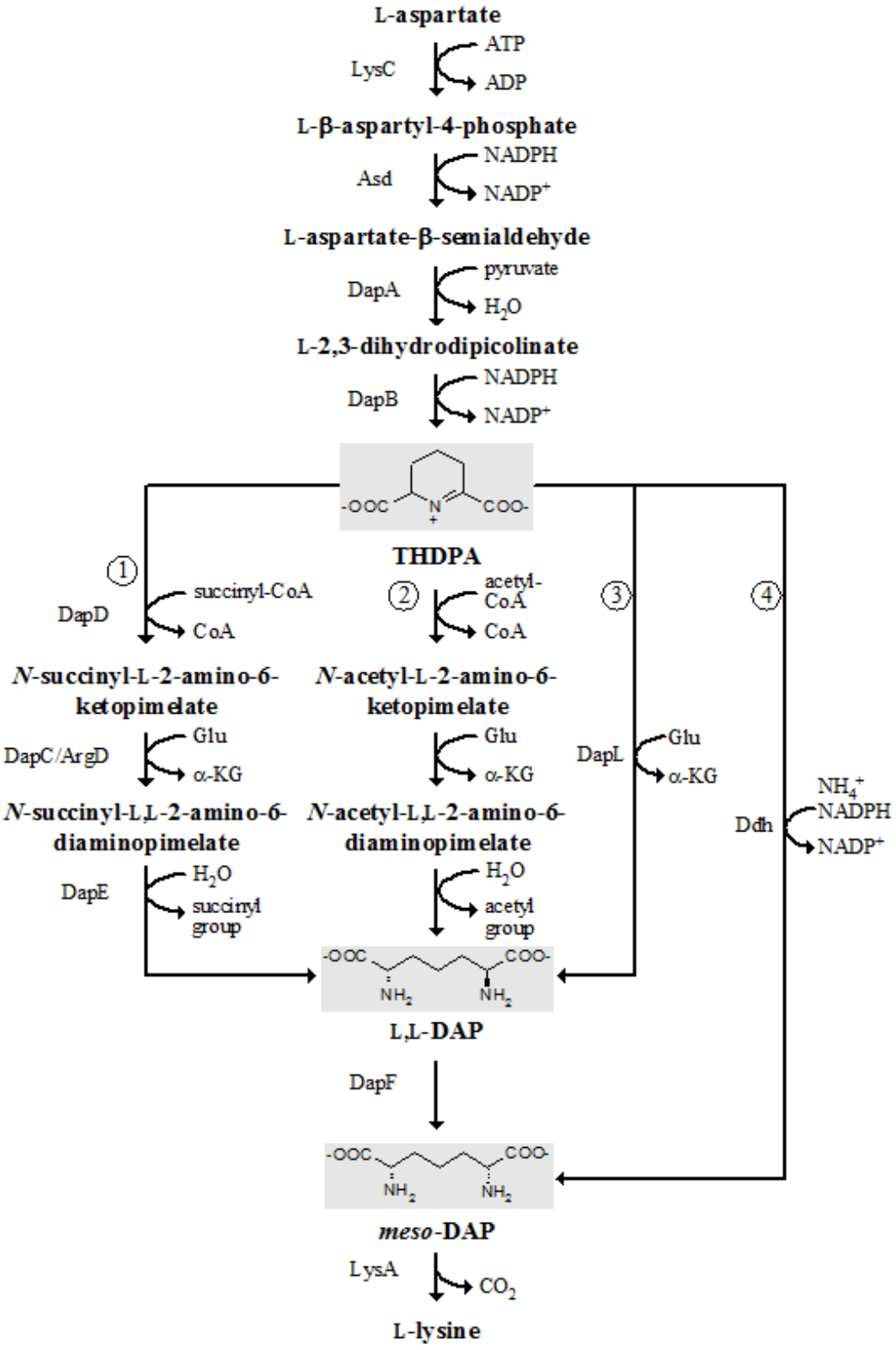
L-aspartate
LysC
ATP
ADP
L-β-aspartyl-4-phosphate
Asd
NADPH
NADP+
L-aspartate-β-semialdehyde
DapA
pyruvate
H2O
L-2,3-dihydrodipicolinate
DapB
NADPH
NADP+
-OOC
N
COO-
THDPA
1
DapD
succinyl-CoA
CoA
2
acetyl-CoA
CoA
3
4
N-succinyl-L-2-amino-6-ketopimelate
N-acetyl-L-2-amino-6-ketopimelate
DapC/ArgD
Glu
α-KG
DapL
Glu
α-KG
Ddh
NH4+
NADPH
NADP+
N-succinyl-L,L-2-amino-6-diaminopimelate
N-acetyl-L,L-2-amino-6-diaminopimelate
DapE
H2O
succinyl group
H2O
acetyl group
NH2
L,L-DAP
DapF
meso-DAP
LysA
CO2
L-lysine

Figure 3-2. Growth requirement of the Δ*mmp1527*::*pac* mutant S600 for lysine. Growth in (A) McNA medium and (B) McNA+lysine (1 mM) medium. (●), wild-type strain S2; (○), the ΔMmp1527 mutant S600; (▲), the strain S601 (complementation of S600 with Mmp1527 expressed from pMEV2-Mmp1527). Growth curves are representative of experiments that were independently replicated three times. All values are the averages of triplicate cultures.

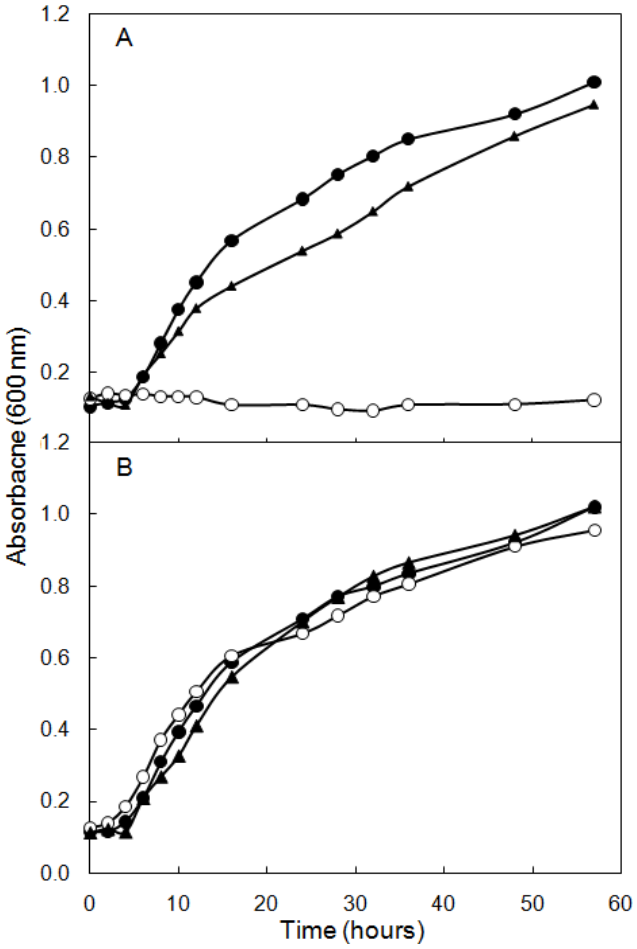
A
B
Absorbacne (600 nm)
Time (hours)
0.0
0.2
0.4
0.6
0.8
1.0
1.2
0
10
20
30
40
50
60

Figure 3-3. DapL activity (A) and heat stability (B) of MJ1391. (A) DapL assay was performed at 70 ^{o}C for 0-60 min before termination and measurement of the product glutamate. (B) The temperature stabilities of MJ1391 and the substrates α-KG and LL-DAP were examined by pre-incubation of the protein MJ1391 (white bars), the substrates (grey bars), or the protein and the substrates (incubated separately; black bars) at 70-100 ^{o}C in Tris-HCl buffer (pH 8.5) for 30 min before the DapL activity assay at 70 ^{o}C. The 100% activity was 0.30 μmol min^{-1} mg of protein^{-1} that was observed without pre-incubation. The error bars represents the standard deviation of three assays.

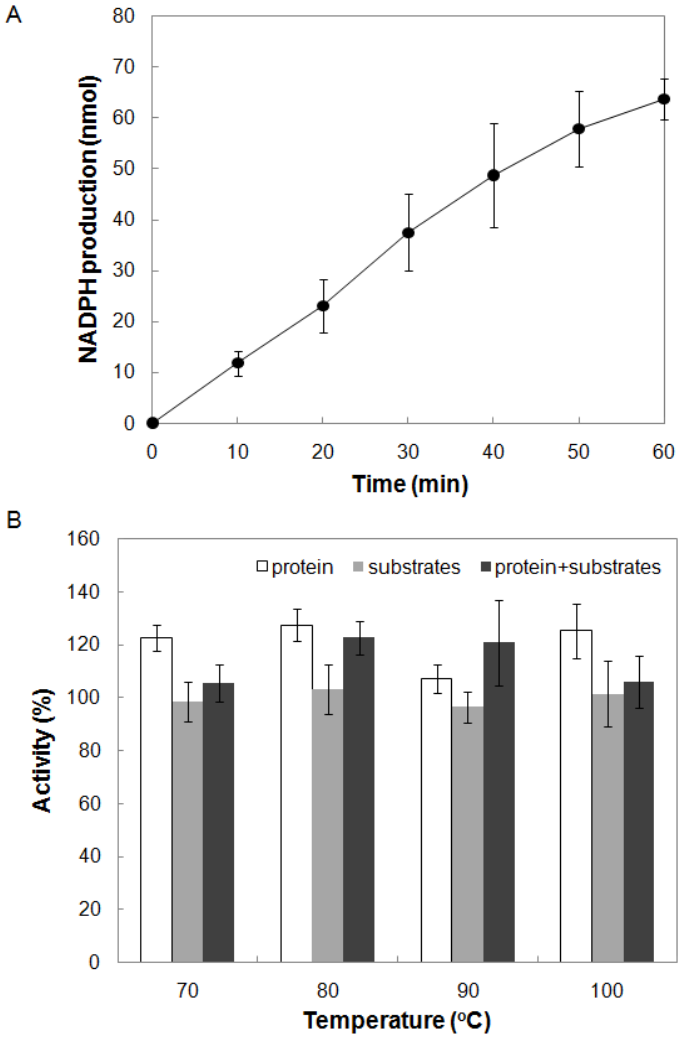
A
NADPH production (nmol)
Time (min)
B
protein
substrates
protein+substrates
Activity (%)
Temperature (°C)

Figure 3-4. Optimum temperature (A) and pH (B) of MJ1391. Assays were conducted for 30 min. The 100% activity was 0.33 μmol min^{-1} mg of $protein^{-1}$ and was observed at 70 ^{o}C, pH 8.5. (A) Assays were conducted at pH 8.5. (B) Assays were conducted at 70 ^{o}C.

A

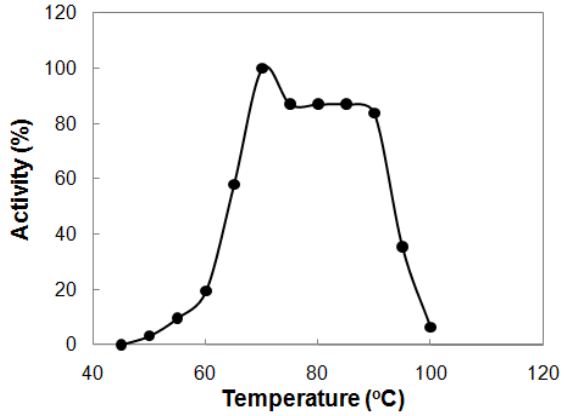
120
100
80
60
40
20
0
Activity (%)
40
60
80
100
120
Temperature (°C)

B

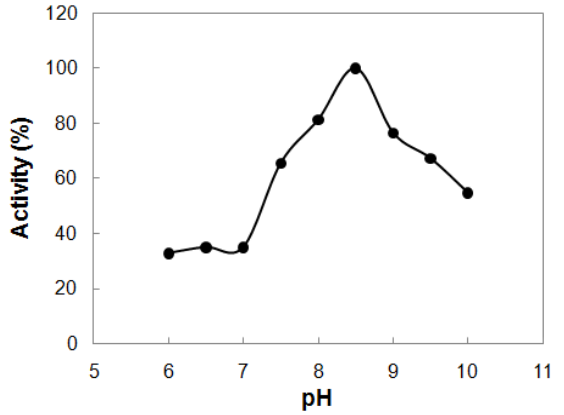
120
100
80
60
40
20
0
Activity (%)
5
6
7
8
9
10
11
pH

Figure 3-5. Phylogenetic analyses of the DapL homologs. The colors represent: red, bacterial DapL1; blue, bacterial DapL2; orange, archaeal DapL1; green, archaeal DapL2; cyan, methanococcal DapL. (A) The phylogenetic tree was constructed with the minimum evolution method using the program MEGA4. The scale bar represents 0.1 amino acid substitutions per site. Enzymes with biochemically confirmed DapL activities are indicated by an asterisk (19, 25). Closed circles at the branch points indicate ≥70% replication with 1,000 bootstraps. The grouping of DapL1 and DapL2 is based on (19). Several aminotransferases from *E. coli*, *B. subtilis*, *Bordetella parapertussis*, and *Corynebacterium glutamicum*, organisms that are known to lack DapL activity, were included to provide an overall context. Locus tag of all sequences used in the phylogenetic analysis are as follows: *Protochlamydia*, pc0685; *Chlamydia*, CT390; *E. coli* 1, b2379; *E. coli* 2, b3359; *Gloeobacter*, glr4108; *B. subtilis* 1, BSU37690; *B. subtilis* 2, BSU13580; *B. subtilis* 3, BSU11220; *B. subtilis* 4, BSU03900; *Bacteroides,* BF2666; *Bordetella* 1, BPP2543; *Bordetella* 2, BPP1996; *Synechocystis*, sll0480; *Leptospira*, LIC12841; *Methanococcoides*, Mbur1013; *Methanosarcina barkeri*, Mbar_A2605; *Methanosphaera*, Msp0924; *Methanospirillum*, Mhun2943; *Moorella*, Moth0889; *Archaeoglobus*, AF0409; *Methanosarcina acetivorans*, MA1712; *Methanosarcina mazei*, MM2649; *Methanosaeta*, Mthe0801; *Methanothermobacter*, MTH52; *Corynebacterium* 1, NCgl1343; *Corynebacterium* 2, NCgl1058; *Desulfitobacterium*, Dhaf1761; *Arabidopsis*, AT4G33680; *Syntrophobacter*, Sfum0054; *Methanocorpusculum*, Mlab0633; *Methanoculleus*, Memar1915; *Methanobrevibacter*, Msm1455; methanogen RCI, RCIX1962; *Methanoregula*, Mboo2096; *Methanococcus aeolicus*, Maeo1494; *Methanococcus vannielii*, Mevan0840; *Methanococcus maripaludis*, MMP1527; *Methanocaldococcus jannaschii*, MJ1391; and *Methanococcus voltae*, Mvol0315. (B) RED plot of DapL homologs. Intra-domain comparisons within each DapL

subgroups are represented by diamonds of a single color. Comparisons between different subgroups are represented by diamonds of two colors. (C) Hypothetical gene tree illustrating the proposed evolutionary history of DapL homologs. The solid-line tree represents the organismal phylogeny in the absence of LGT. The dashed-line tree represents the gene tree of DapL. T1 represents the acquisition of bacterial DapL1 by archaea, and T2 represents the acquisition of archaeal DapL2 by bacteria.

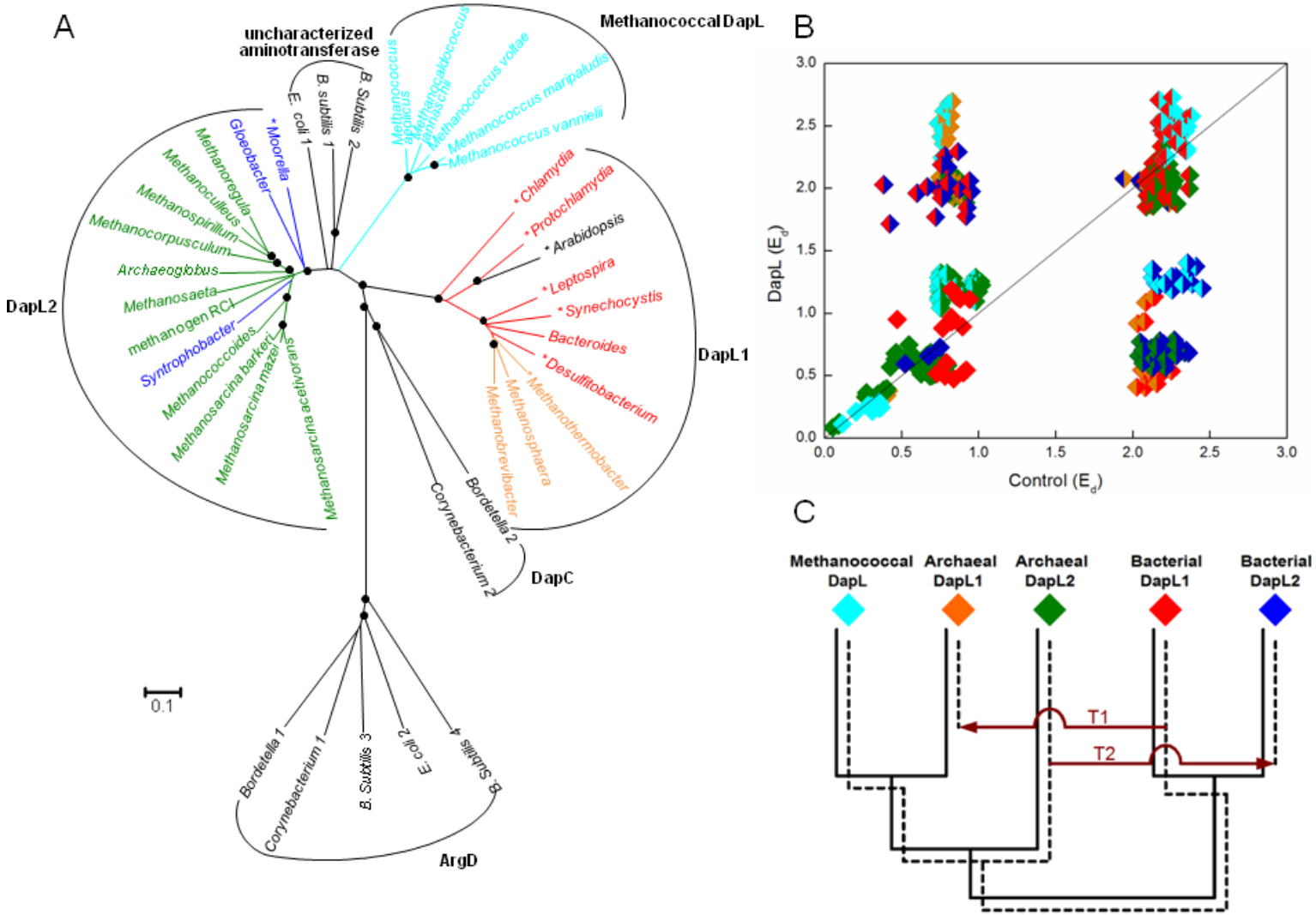
A
uncharacterized aminotransferase
Methanococcal DapL
DapL2
DapL1
DapC
ArgD
E. coli 1
B. subtilis 1
B. Subtilis 2
Methanococcus aeolicus
Methanocaldococcus jannaschii
Methanococcus voltae
Methanococcus maripaludis
Methanococcus vannielii
Gloeobacter
*Moorella
Methanoregula
Methanoculleus
Methanospirillum
Methanocorpusculum
Archaeoglobus
Methanosaeta
methanogen RC-I
Syntrophobacter
Methanococcoides
Methanosarcina barkeri
Methanosarcina mazei
Methanosarcina acetivorans
*Chlamydia
*Protochlamydia
*Arabidopsis
*Leptospira
*Synechocystis
Bacteroides
*Desulfitobacterium
*Methanothermobacter
Methanosphaera
Methanobrevibacter
Corynebacterium 2
Bordetella 2
0.1
Bordetella 1
Corynebacterium 1
B. Subtilis 3
E. coli 2
B. Subtilis 4
B
DapL (E_d)
Control (E_d)
0.0
0.5
1.0
1.5
2.0
2.5
3.0
C
Methanococcal DapL
Archaeal DapL1
Archaeal DapL2
Bacterial DapL1
Bacterial DapL2
T1
T2

CHAPTER 4

ROLE OF THIOSULFATE IN CYSTEINE BIOSYNTHESIS IN *METHANOCOCCUS MARIPALUDIS*[4]

[4]Liu, Y. and W.B. Whitman. To be submitted to *J. Bacteriol*.

Abstract

Cysteine in methanococci is synthesized primarily via the tRNA-dependent SepRS/SepCysS pathway. Sulfide can function as an *in vitro* sulfur source for this process, but the nature of the proximal sulfur donor awaits further characterization. The structure of SepCysS is analogous to cysteine desulfurase, indicating that a protein persulfide group may be the direct sulfur donor for cysteine biosynthesis. In *Methanococcus maripaludis* cell extracts, sulfide and thiosulfate can donate sulfur for tRNA-dependent cysteine biosynthesis. The activity with thiosulfate was 3.2 ± 0.3 nmol/min/mg protein, which was ~ 2.5-fold higher than that with sulfide, 1.2 ± 0.1 nmol/min/mg protein. Addition of sulfite increased the cysteine production activity with sulfide by ~ 2-fold, but sulfite alone was not used as a sulfur source. In contrast, addition of dithiothreitol inhibited cysteine production with sulfide but not thiosulfate. Therefore, an oxidized form of sulfur, presumably thiosulfate, is possibly an intermediate for sulfur incorporation into cysteine. Sulfide was oxidized to thiosulfate with F_{420} as the electron acceptor in *M. maripaludis* cell extracts. Moreover, persulfide (sulfane sulfur) was generated from thiosulfate through rhodanese (thiosulfate:cyanide sulfurtransferase) activities. Based upon these observations, a rhodanese-like, protein-mediated sulfur transfer is proposed to be involved in the sulfur assimilation for cysteine biosynthesis.

Introduction

Cysteine is an essential amino acid involved in metal-coordination, protein structure and folding, redox and non-redox catalysis, and regulatory processes through posttranslational modifications and formation of disulfide bonds (6). Two major cysteine biosynthetic pathways have been identified in bacteria and eukaryotes (Fig. 4-1) (2, 30). (i) For the serine sulfhydrylation pathway, serine is activated in the form of *O*-acetylserine (OAS) and then converted to cysteine by *O*-acetylserine sulfhydrylase (OASS) (21). Most bacteria use sulfide as the direct sulfur donor (30); in enteric bacteria, either sulfide (under aerobic condition) or thiosulfate (under anaerobic condition) is the sulfur donor (14). (ii) For the reverse transsulfuration pathway, cystathionine as an intermediate is synthesized from homocysteine and serine by cystathionine β-synthase (CBS) and then converted to cysteine by cystathionine γ-lyase (CGL) (10). In mammals and some bacteria, such as *Lactococcus lactis* (25) and *Pseudomonas putida* (29), the sulfur group in cysteine is derived from methionine, which is converted to homocysteine through the intermediate *S*-adenosylmethionine (10); in *Saccharomyces cerevisiae*, the overall sulfur donor is sulfide, which reacts with *O*-acetylhomoserine to form homocysteine by *O*-acetylhomoserine sulfhydrylase (OAHS) (28). The bacterium *Mycobacterium tuberculosis* possesses both the sulfhydrylation pathway using thiocarboxylate as the direct sulfur donor (19) and the reverse sulfhydrylation pathway using methionine as the sulfur source (32).

Both the sulfhydrylation and the reverse transsulfuration pathways for cysteine biosynthesis are present in archaea. The sulfhydrylation pathway with *O*-acetylserine as the precursor is present in *Methanosarcina* species, and functional homologs of OASS have been characterized in *Methanosarcina thermophila* and *Methanosarcina barkeri* (3, 4, 13). A variation

of the sulfhydrylation pathway is present in *Aeropyrum pernix*, which uses *O*-phosphoserine instead of *O*-acetylserine (20). The reverse transsulfuration pathway is proposed to be present in *Sulfolobus acidocaldarius* and *Halobacterium marismortui*, because ^{34}S-labeled methionine is incorporated into cellular cysteine (34).

Homologs of OASS, CBS, and CGL are absent from the genomes of most *Methanococcales* species, *Methanothermobacter thermautotrophicus*, and *Methanopyrus kandleri* (Table 4-1). A two-step tRNA-dependent pathway is present for cysteine production *de novo* in these and other methanogens (Fig. 4-1) (22). In the first step, $tRNA^{Cys}$ is aminoacylated with *O*-phosphoserine (Sep) by *O*-phosphoseryl-tRNA synthetase (SepRS). In the second step, the Sep moiety on Sep-$tRNA^{Cys}$ is converted to cysteine with a sulfur source to form Cys-$tRNA^{Cys}$ by Sep-tRNA:Cys-tRNA synthase (SepCysS). Homologs of SepRS and SepCysS always coexist and are encoded in completely sequenced genomes of *Archaeoglobus* species and all methanogens except *Methanosphaera* and *Methanobrevibacter* species (18). In addition to this pathway, many methanogens, including *M. maripaludis*, possess a canonical cysteinyl-tRNA synthetase (CysRS), which aminoacylates $tRNA^{Cys}$ with cysteine (Fig. 4-1) (15, 26). The deletion of SepRS (Δ*sepS*) in *M. maripaludis* resulted in a cysteine auxotroph, suggesting that the two-step tRNA-dependent pathway is the primary pathway for cysteine biosynthesis in methanococci (22).

The nature of the physiological sulfur donor for the tRNA-dependent cysteine biosynthesis remains unknown. Sodium sulfide, thiophosphate, and cysteine can function as *in vitro* sulfur donors in reactions with recombinant SepCysS, and sodium sulfide provides the highest activity (11, 22). However, the catalytic efficiency (k_{cat}/K_m) with sulfide for conversion

of Sep-tRNA^{Cys} to Cys-tRNA^{Cys} by SepCysS is ~ 500-fold lower than that of phophoserylation of tRNA^{cys} by SepRS, suggesting that sulfide is unlikely to be the sulfur donor used *in vivo* (11).

A persulfide group is proposed to be the physiological sulfur source for cysteine production based upon the structure of SepCysS (7, 18, 23). SepCysS is a pyridoxal 5‘-phosphate (PLP)-dependent enzyme and structurally analogous to cysteine desulfurase (7), which forms a persulfide group (R-S-SH) on a cysteinyl residue at the expense of one free cysteine and functions as the direct sulfur donor for Fe-S cluster biosynthesis (17). Three conserved cysteinyl residues are located at the active site of SepCysS, and one of them may be essential for forming a persulfidic intermediate (18, 23). If a persulfide group is the genuine sulfur donor for cysteine biosynthesis in the tRNA-dependent pathway, it needs to be generated in a cysteine-independent manner.

Here we present evidence that, in *M. maripaludis* cell extracts, thiosulfate can be the sulfur donor for cysteine biosynthesis. Moreover, persulfide groups can be generated from thiosulfate through rhodanese activities. Therefore, thiosulfate and rhodanese-like proteins are possibly involved in sulfur incorporation into cysteine.

Materials and Methods

Strains, media, and culture conditions. The *M. maripaludis* wild-type strain S2 was grown in McNA medium (a minimal medium with 10 mM sodium acetate) reduced with 3 mM dithiothreitol (DTT) (33). The 5 ml cultures were grown in 28 ml aluminum seal tubes pressurized to 276 kPa with H_2:CO_2 (4:1, v/v). The 100 ml cultures were grown in 1 L bottles pressurized to 138 kPa with H_2:CO_2 (4:1, v/v). Before inoculation, 3 mM of sodium sulfide was added as the sulfur source. The *Escherichia coli* strain K-12 MG1655 was grown aerobically in Luria-Bertani (LB) medium.

Preparation of cell-free extracts. *M. maripaludis* and *E. coli* cells grown in 100 ml of media were cultured to an absorbance of ~0.4 at 600 nm. The cells were collected by centrifugation at 10,000 *g* for 30 min at 4 ^{o}C and resuspended in 1 ml of buffer containing 0.1 M HEPES (pH 7.5). The *M. maripaludis* cells were lysed by repeated (2×) freezing (-20 °C) and thawing, and the *E. coli* cells were lysed by passage through a French pressure cell at 100 Mpa. The cell lysates were incubated with 20 U of RQ1 DNase (Promega) at 37 ^{o}C for 15 min to digest DNA. Unbroken cells were removed by centrifugation at 8,000 *g* for 30 min at 4 ^{o}C. The cell-free extracts were passed through a 2-ml Sephadex G-25 column (Aldrich) to remove low molecular weight compounds. The protein concentrations were determined by BCA protein assay (Pierce) (24).

Purification of F_{420}. Coenzyme F_{420} was purified as described (27). About 10 g of *M. mariaplduis* cells (wet weight) were resuspended in 100 ml of anoxic H_2O, mixed with 100 ml of cold acetone, and stirred for 30 min at 4 ^{o}C with a magnetic stir bar. The mixture was centrifuged anaerobically at 20,000 *g* for 20 min at 4 ^{o}C. The pellet was extracted twice with 100 ml of 50% cold acetone. The supernatant (~400 ml) was combined, mixed with 800 ml of buffer A [0.3 M NaCl and 50 mM Tris-Cl (pH 7.5)], and passed through a Millipore 0.2 μm GNWP filter. The filtrate was loaded onto a 1 × 10 cm QAE-Sephadex A-25 column (Sigma), which was equilibrated with buffer A. F_{420} was eluted with a 50 ml 0-100% linear gradient of buffer B [1 M NaCl and 50 mM Tris-Cl (pH 7.5)] and collected in 2-ml fractions. Fractions containing F_{420} were identified by their absorbance at 420 nm, pooled, and lyophilized. The purified F_{420} was resuspended in 50 mM Tris-Cl (pH 7.5), and the concentration was determined by the absorbance at 400 nm with $\varepsilon = 25\ mM^{-1} \cdot cm^{-1}$ (5). The final yield was ~ 100 nmol of F_{420} per gram wet weight of cells.

Enzyme activity assays. Cysteine biosynthesis activities in *M. maripaludis* cell extracts were determined by the production of cysteine with an adaptation of the acid-ninhydrin method (8). Assays were conducted in the anaerobic chamber with an atmosphere of 95% of N_2 and 5% of H_2. In a total volume of 150 µl, assays contained 0.1 M HEPES (pH 8.0), 50 mM NaCl, 0.2 mM $ZnCl_2$, 20 mM $MgCl_2$, 10 mM serine, 50 mM ATP, 50 µM PLP, and cell-free extracts (0.15 mg of total protein). The reactions were initiated by the addition of 10 mM of a sulfur source and incubated for 30 min at 37 ^oC. The reactions were stopped by addition of 150 µl glacial acetic acid and 150 µl of 2.5% (w/v) ninhydrin in 60% (v/v) acetic acid and 40% (v/v) HCl. The samples were heated in boiling water for 10 min for color development, and the absorbance was determined at 560 nm. Reactions without addition of sulfur source were used as negative controls. In reactions testing the RNA-dependency of the activities, cell extracts were pre-incubated with 5 mg/ml RNaseA (Sigma) at 37 ^oC for 1 hr before initiation of the assay. Solutions of cysteine were used as standards. Kinetic constants in cell extracts were determined with 0.1, 0.2, 0.5, 1, 2, 5, and 10 mM sodium sulfide, sodium thiosulfate, or sodium sulfite (in the presence of 10 mM sodium sulfide). The data were analyzed using SigmaPlot 10.0 with the Enzyme Kinetics module (Systat Software Inc.) fitted with the Michaelis-Menten equation.

The sulfide oxidation activities in *M. maripaludis* cell extracts were determined anaerobically under a N_2 atmosphere at 37 ^oC. The assay mixture of 1 ml contained 0.1 M HEPES (pH 7.5), *M. maripaludis* cell-free extracts (0.5 mg of total protein), and electron acceptors (100 µM FMN, 100 µM FAD, or 10 µM F_{420}). The reactions were initiated by addition of 100 µM sodium sulfide, and the reduction of the electron acceptors were followed continuously spectrophotometrically. The extinction coefficients ($mM^{-1} \cdot cm^{-1}$) of ε_{450}= 11 and ε_{400} = 25 were used for FMN and FAD (16) and coenzyme F_{420} (5), respectively. At the end of

the reaction with F_{420}, 100 µl of 37 % formaldehyde was added for quenching, and the production of thiosulfate was determined by an adaptation of the cold cyanolysis method, based upon the reaction of thiosulfate with cyanide at room temperature in the presence of a copper(II) catalyst (12). In 500 µl reaction mixtures, 100 µl of 0.1 M $CdCl_2$ was added to precipitate unreacted sulfide, followed by centrifugation at 17,000 *g* for 10 min. The supernatant was transferred to a new microcentrifuge tube, and then 40 µl of 0.25 M KCN, 60 µl of 0.1 M $CuSO_4$, and 300 µl of ferric nitrate reagent [10 g of $Fe(NO_3)_3 \cdot 9H_2O$ and 20 ml of 65 % HNO_3 per 150 ml] were added sequentially. The absorbance was measured at 460 nm. Reactions with formaldehyde added prior to the addition of sodium sulfide were used as negative controls. Solutions of sodium thiosulfate were used as standards.

Rhodanese assays were conducted in the anaerobic chamber with an atmosphere of 95% of N_2 and 5% of H_2, and the production of thiocyanate was determined as described (31). The assay mixture, in a total volume of 350 µl, contained 0.1 M Tris-acetate (pH 7.5), 10 mM sodium thiosulfate, and *M. maripaludis* (0.4 mg of total protein) or *E. coli* (0.1 mg of total protein) cell-free extracts. The reactions were initiated by addition of 50 mM KCN, incubated for 30 min at 37 ^{o}C, and then quenched by addition of 150 µl 15 % formaldehyde. For negative controls, formaldehyde was added before incubation. The color was then developed by addition of 0.5 ml of ferric nitrate reagent. The iron-thiocyanate complex was quantified by its absorbance at 460 nm, with $\varepsilon = 4.2\ mM^{-1} \cdot cm^{-1}$.

Results and Discussion

Cysteine biosynthesis activities in *M. maripaludis* cell extracts. While sulfide can function as the sole sulfur source for the growth of *M. maripaludis*, oxidized species of sulfur are required for some biosynthetic pathways. For instance, sulfite is presumably the sulfur source for

the biosynthesis of the sulfonate group of coenzyme M (2-mecaptoethanesulfonic acid) (9). Three lines of evidence suggested that thiosulfate is involved in cysteine biosynthesis.

First, thiosulfate was a more favorable sulfur source than sulfide for cysteine synthesis. The cysteine biosynthesis activities in cell extracts were examined with sulfide, thiosulfate, sulfite, and sulfate as sulfur sources. Only sulfide and thiosulfate resulted in measurable cysteine production, and the activity with thiosulfate was ~ 2.5-fold higher than that with sulfide (Table 4-2). This activity was due to the RNA-dependent pathway. Preincubation of the cell-free extracts with RNaseA reduced the activity by ~ 80% (Table 4-3). Similarly, the activity required both serine and ATP. When either one was omitted from the assay, the activity was below the detection limit of 0.3 nmol/min/mg protein. Sulfide and thiosulfate had similar $K_{0.5}$ (substrate concentration for 0.5 V_{max} of the overall reaction) for cysteine production, but the V_{max} with thiosulfate was ~ 2-fold higher (Table 4-2).

Second, although sulfite by itself could not be used as a sulfur source to support cysteine production, the presence of 0.1 mM sulfite (15 nmol in the reaction) increased the activity with sulfide (10 mM) by ~ 2-fold. During the reaction, 25 nmol of cysteine was produced, suggesting that sulfite stimulated cysteine production from sulfide but was not directly used as a sulfur source. Moreover, increasing of the sulfite concentration from 0.1 mM to 10 mM did not further increase the activity with sulfide, suggesting that if an enzyme was involved in the activation, it would possess a high affinity (in μM range) to sulfite.

Third, dithiothreitol (DTT) was inhibitory to cysteine production with sulfide. When 1 mM DTT was present, the cysteine biosynthesis activity was reduced by ~ 50%, and 10 mM DTT inhibited completely (Fig. 4-2). In contrast, DTT did not affect the cysteine production

activity with thiosulfate (Fig. 4-2). Therefore, DTT may inhibit the oxidation of sulfide to thiosulfate, or thiosulfate could protect the oxidized form of sulfur from reduction by DTT.

F_{420}-dependent sulfide oxidation. Since an oxidized form of sulfur is possibly involved in cysteine biosynthesis, the process of sulfide oxidation in *M. maripaludis* cell extracts was examined. Thiosulfate production from sulfide oxidation was measured with various electron acceptors (10 mM each), including air, NAD^+, $NADP^+$, flavin mononucleotide (FMN), flavin adenine dinucleotide (FAD), coenzyme F_{420}, glutathione disulfide, DTT disulfide, CoM disulfide, and cystine. Only FMN, FAD, and F_{420} resulted in detectable thiosulfate production (> 0.1 nmol/min/mg protein) during one hour reactions. F_{420} had the highest activity (Table 4-4). With 100 μM of sulfide and 10 μM of F_{420}, the specific activity of F_{420} reduction was 2.2 ± 0.5 nmol/min/mg protein. Although the reduction of FMN (E_0‘ = -0.19 V) and FAD (E_0‘ = -0.22 V) are thermodynamically more favorable electron acceptors than F_{420} (E_0‘ = -0.35 V), the activity of FMN or FAD was much lower, suggesting that F_{420} was more likely to be the physiological electron acceptor.

The coupling of thiosulfate production to F_{420}-dependent sulfide oxidation was further examined. Two oxidations are necessary to generate thiosulfate from sulfide: [1] $S^{2-} + 3\ H_2O \rightarrow SO_3^{2-} + 6\ H^+ + 6\ e^-$ (E_0‘ = -0.12 V); [2] $S^{2-} + SO_3^{2-} \rightarrow SSO_3^{2-} + 2\ e^-$ (E_0‘ = -0.40 V). If F_{420} reduction is coupled to the first oxidation, the reaction would be thermodynamically unfavorable (ΔG_0‘ = 126 kJ·mol^{-1}). Therefore, only the second oxidation, where ΔG_0‘ = -10 kJ·mol^{-1}, is likely. This oxidation requires sulfite as a co-substrate. Supporting this proposal, in three independent assays, the ratio of F_{420} reduction ($F_{420}/F_{420}H_2$) to thiosulfate production was 0.90 ± 0.02, indicating that only one molecule of F_{420} was reduced to generate one molecule of thiosulfate. If the reaction in fact requires sulfite, the measured activity would depend on sulfite

contamination in either cell extracts or sulfide solutions. The dependency and source of SO_3^{2-} for thiosulfate production is still under investigation.

Generation of persulfide groups from thiosulfate by rhodanese (thiosulfate:cyanide sulfurtransferase) activities. A persulfide group was proposed to be the physiological sulfur source for the tRNA-dependent cysteine biosynthesis (7, 18, 23). Rhodanese-like proteins are a protein superfamily that generate persulfide groups either from thiosulfate or from the persulfide groups of cysteine desulfurases (17). When thiosulfate is the sulfur donor, sulfite is produced as a byproduct. The rhodanese activity in *M. maripaludis* cell extracts with thiosulfate as the sulfur donor and cyanide as the sulfur acceptor was 0.37 ± 0.02 nmol/min/mg protein, suggesting that persulfide groups were generated with thiosulfate as the sulfur source. The activity in *M. maripaludis* was 32 times lower than that in *E. coli* (11.8 ± 0.4 $nmol \cdot min^{-1} \cdot mg^{-1}$ protein), which was similar to the previously reported values in *E. coli* cell extracts (1). Although the activity in *M. maripaludis* was lower than that required for the sulfur assimilation for cysteine biosynthesis (~ 1 $nmol \cdot min^{-1} \cdot mg^{-1}$ protein), cyanide is not the natural sulfur acceptor and the physiological activities from rhodanese-like proteins may still be high enough to support cysteine biosynthesis.

Proposed mechanism of the sulfur incorporation into cysteine. The activities in *M. maripaludis* cell-free extracts showed that (1) thiosulfate exhibited higher activity than sulfide for cysteine biosynthesis, suggesting that an oxidized form of sulfur (presumably thiosulfate) was an intermediate; (2) sulfite, at low concentrations, stimulated cysteine production with sulfide but was not sufficient as a sulfur source, suggesting that sulfite was involved in the generation of the oxidized form of sulfur but was not consumed in the overall reaction; (3) sulfide, presumably in the presence of sulfite, was oxidized to thiosulfate with F_{420} as the electron acceptor; and (4) persulfide groups were generated using thiosulfate as the sulfur donor,

suggesting that the rhodanese activity, which generates a persulfide intermediate and sulfite from thiosulfate, was present in *M. maripaludis*. Because that persulfide groups are commonly involved in sulfur passage from one sulfur carrier protein to another (17) and a persulfide group may be formed on SepCysS (7), a model of sulfur assimilation for cysteine biosynthesis is proposed (Fig. 4-3): (1) sulfide is oxidized into thiosulfate, in the presence of sulfite, with F_{420} as the electron acceptor; (2) the initial persulfide group is generated with thiosulfate as the sulfur source through a rhodanese-like protein, and sulfite is produced as a byproduct and therefore recycled in this process; (3) the persulfide group is transferred from the rhodanese-like protein to SepCysS; and finally (4) the persulfide group on SepCysS is used as the direct sulfur donor for cysteine biosynthesis.

Acknowledgements

This work was supported by grants from the U. S. Department of Energy to W.B.W and a dissertation completion award from the University of Georgia to Y.L.

References

1. **Alexander, K., and M. Volini.** 1987. Properties of an *Escherichia coli* rhodanese. J. Biol. Chem. **262:**6595-6604.

2. **Ambrogelly, A., S. Kamtekar, A. Sauerwald, B. Ruan, D. Tumbula-Hansen, D. Kennedy, I. Ahel, and D. Söll.** 2004. Cys-tRNA^{Cys} formation and cysteine biosynthesis in methanogenic archaea: two faces of the same problem? Cell. Mol. Life Sci. **61:**2437-2445.

3. **Borup, B., and J. G. Ferry.** 2000. Cysteine biosynthesis in the Archaea: *Methanosarcina thermophila* utilizes O-acetylserine sulfhydrylase. FEMS Microbiol. Lett. **189:**205-10.

4. **Borup, B., and J. G. Ferry.** 2000. O-acetylserine sulfhydrylase from *Methanosarcina thermophila*. J. Bacteriol. **182:**45-50.

5. **Eirich, L. D., G. D. Vogels, and R. S. Wolfe.** 1979. Distribution of coenzyme F_{420} and properties of its hydrolytic fragments. J. Bacteriol. **140:**20-27.

6. **Fomenko, D. E., S. M. Marino, and V. N. Gladyshev.** 2008. Functional diversity of cysteine residues in proteins and unique features of catalytic redox-active cysteines in thiol oxidoreductases. Mol. Cells. **26:**228-235.

7. **Fukunaga, R., and S. Yokoyama.** 2007. Structural insights into the second step of RNA-dependent cysteine biosynthesis in archaea: crystal structure of Sep-tRNA:Cys-tRNA synthase from *Archaeoglobus fulgidus*. J. Mol. Biol. **370:**128-141.

8. **Gaitonde, M. K.** 1967. A spectrophotometric method for the direct determination of cysteine in the presence of other naturally occurring amino acids. Biochem. J. **104:**627-633.

9. **Graham, D. E., H. Xu, and R. H. White.** 2002. Identification of coenzyme M biosynthetic phosphosulfolactate synthase. J. Biol. Chem. **277:**13421-13429.

10. **Griffith, O. W.** 1987. Mammalian sulfur amino acid metabolism: an overview. Methods Enzymol. **143:**366-376.

11. **Hauenstein, S. I., and J. J. Perona.** 2008. Redundant synthesis of cysteinyl-tRNA^{Cys} in *Methanosarcina mazei*. J. Biol. Chem. **283:**22007-22017.

12. **Kelly, D. P., and A. P. Wood.** 1994. Synthesis and determination of thiosulfate and polythionates. Methods Enzymol. **243:**475-501.

13. **Kitabatake, M., M. W. So, D. L. Tumbula, and D. Söll.** 2000. Cysteine biosynthesis pathway in the archaeon *Methanosarcina barkeri* encoded by acquired bacterial genes? J. Bacteriol. **182:**143-145.

14. **Kredich, N. M.** 1996. Biosynthesis of cysteine, p. 514-527. *In* F. C. Neidhardt, R. Curtiss, J. L. Ingraham, E. C. C. Lin, K. B. Low, B. Magasanik, W. S. Reznikoff, M. Riley, M. Schaechter, and H. E. Umbarger (ed.), E*scherichia coli* and *Salmonella*, vol. 2. ASM Press, Washington, D.C.

15. **Li, T., D. E. Graham, C. Stathopoulos, P. J. Haney, H.-s. Kim, U. Vothknecht, M. Kitabatake, K.-w. Hong, G. Eggertsson, A. W. Curnow, W. Lin, I. Celic, W. Whitman, and D. Söll.** 1999. Cysteinyl-tRNA formation: the last puzzle of aminoacyl-tRNA synthesis. FEBS Lett. **462:**302-306.

16. **Lin, W. C., Y.-L. Yang, and W. B. Whitman.** 2003. The anabolic pyruvate oxidoreductase from *Methanococcus maripaludis*. Arch. Microbiol. **179:**444-456.

17. **Mueller, E. G.** 2006. Trafficking in persulfides: delivering sulfur in biosynthetic pathways. Nat. Chem. Biol. **2:**185-194.

18. **O'Donoghue, P., A. Sethi, C. R. Woese, and Z. A. Luthey-Schulten.** 2005. The evolutionary history of Cys-tRNA^{Cys} formation. Proc. Natl. Acad. Sci. U S A. **102:**19003-19008.

19. **O'Leary, S. E., C. T. Jurgenson, S. E. Ealick, and T. P. Begley.** 2008. *O*-Phospho-L-serine and the thiocarboxylated sulfur carrier protein CysO-COSH are substrates for CysM, a cysteine synthase from *Mycobacterium tuberculosis*. Biochemistry **47:**11606-11615.

20. **Oda, Y., K. Mino, K. Ishikawa, and M. Ataka.** 2005. Three-dimensional structure of a new enzyme, *O*-phosphoserine sulfhydrylase, involved in L-cysteine biosynthesis by a hyperthermophilic archaeon, *Aeropyrum pernix* K1, at 2.0 Å resolution. J. Mol. Biol. **351:**334-344.

21. **Rabeh, W. M., and P. F. Cook.** 2004. Structure and mechanism of *O*-acetylserine sulfhydrylase. J. Biol. Chem. **279:**26803-26806.

22. **Sauerwald, A., W. Zhu, T. A. Major, H. Roy, S. Palioura, D. Jahn, W. B. Whitman, J. R. Yates, 3rd, M. Ibba, and D. Söll.** 2005. RNA-dependent cysteine biosynthesis in archaea. Science **307:**1969-1972.

23. **Sheppard, K., J. Yuan, M. J. Hohn, B. Jester, K. M. Devine, and D. Söll.** 2008. From one amino acid to another: tRNA-dependent amino acid biosynthesis. Nucl. Acids Res. **36:**1813-1825.

24. **Smith, P. K., R. I. Krohn, G. T. Hermanson, A. K. Mallia, F. H. Gartner, M. D. Provenzano, E. K. Fujimoto, N. M. Goeke, B. J. Olson, and D. C. Klenk.** 1985. Measurement of protein using bicinchoninic acid. Anal. Biochem. **150:**76-85.

25. **Sperandio, B., P. Polard, D. S. Ehrlich, P. Renault, and E. Guedon.** 2005. Sulfur amino acid metabolism and its control in *Lactococcus lactis* IL1403. J. Bacteriol. **187:**3762-3778.

26. **Stathopoulos, C., W. Kim, T. Li, I. Anderson, B. Deutsch, S. Palioura, W. Whitman, and D. Söll.** 2001. Cysteinyl-tRNA synthetase is not essential for viability of the archaeon *Methanococcus maripaludis*. Proc. Natl. Acad. Sci. U S A. **98:**14292-14297.

27. **Stemke, D. J.** 1995. Isolation of F_{420} from *Methanobacterium thermoautotrophicum*, p. 212-213. *In* F. T. Robb, A. R. Place, K. R. Sowers, H. J. Schreier, S. DasSarma, and E. M. Fleischmann (ed.), Archaea: a laboratory manual, vol. 2. Cold Spring Harbor Laboratory Press, New York.

28. **Thomas, D., and Y. Surdin-Kerjan.** 1997. Metabolism of sulfur amino acids in *Saccharomyces cerevisiae*. Microbiol. Mol. Biol. Rev. **61:**503-532.

29. **Vermeij, P., and M. A. Kertesz.** 1999. Pathways of assimilative sulfur metabolism in *Pseudomonas putida*. J. Bacteriol. **181:**5833-5837.

30. **Wada, M., and H. Takagi.** 2006. Metabolic pathways and biotechnological production of L-cysteine. Appl. Microbiol. Biotechnol. **73:**48-54.

31. **Westley, J.** 1981. Thiosulfate: cyanide sulfurtransferase (rhodanese). Methods Enzymol. **77:**285-291.

32. **Wheeler, P. R., N. G. Coldham, L. Keating, S. V. Gordon, E. E. Wooff, T. Parish, and R. G. Hewinson.** 2005. Functional demonstration of reverse transsulfuration in the *Mycobacterium tuberculosis* complex reveals that methionine is the preferred sulfur source for pathogenic mycobacteria. J. Biol. Chem. **280:**8069-8078.

33. **Whitman, W. B., J. Shieh, S. Sohn, D. S. Caras, and U. Premachandran.** 1986. Isolation and characterization of 22 mesophilic methanococci. Syst. Appl. Microbiol. **7:**235.

34. **Zhou, D., and R. H. White.** 1991. Transsulfuration in archaebacteria. J. Bacteriol. **173:**3250-3251.

Table 4-1. Presence (locus tag) or absence (-) of homologs of cysteine biosynthetic protein homologs and CysRS in methanogens.[a]

Organism	OASS/CBS[b]	CGL/OAHS[c]	CysRS[d]
Methanobacteriales			
Methanothermobacter thermautotrophicus	-	-	-
Methanobrevibacter smithii	Msm_0271	Msm_0174, 0265	Msm_0268
Methanosphaera stadtmanae	Msp_0499	Msp_0677	Msp_0124
Methanococcales			
Methanocaldococcus jannaschii	-	-	-
Methanococcus aeolicus	-	-	Maeo_1376
Methanococcus maripaludis	-	-	MMP1060
Methanococcus vannielii	Mevan_0178	Mevan_0171	Mevan_0382, 0170
Metahnococcus voltae	-	-	Mvol_1505
Methanomicrobiales			
Methanocorpusculum labreanum	-	Mlab_0544	-
Methanoculleus marisnigri	Memar_0452	-	-
Methanospirillum hungatei	Mhun_2182	Mhun_2181	Mhun_2176
Candidatus Methanoregula boonei	Mboo_1983, 0420	Mboo_2044, 1994, 1991, 1995	Mboo_1992
Candidatus Methanosphaerula palustris	Mpal_1219	Mpal_1208, 1162, 1156, 1142, 0648	Mpal_1158
Methanosarcinales			
Methanococcoides burtonii	Mbur_0413	Mbur_0797	-
Methanosarcina acetivorans	MA2720	MA2532, 2715	MA0749
Methanosarcina barkeri	Mbar_A2422	Mbar_A3023, 2427	Mbar_A1653
Methanosarcina mazei	-	MM3085	MM1911
Methanosarcina thermophila[e]	AAG01804	Nd	Nd
Methanopyrales			
Methanopyrus kandleri	-	-	-
Methanocellales			
Methanocella sp. RC-I	-	RCIX1554	RRC371

[a]The shaded area corresponds to the methanogens missing gene homologs for both the sulfhydrylation and the transsulfuration cysteine biosynthesis pathways.

[b]OASS and CBS are closely related enzymes, and homology searches differentiate them. Homologs were identified using BLASTp with *E. coli* OASS (CysK, b2414; CysM, b2421) and *S. cerevisiae* CBS (YGR155W) as queries.

[c]CGL, OAHS, and cystathionine γ-synthase (CGS) are closely related enzymes, and homology searches do not differentiate them. Homologs were identified using BLASTp with *S. cerevisiae* CGL (YAL012W) and OAHS (YLR303W) as queries.

[d]CysRS homologs were determined using BLASTp with *M. maripaludis* (MMP1060) as query.

[e]OASS in *Methanosarcina thermophila* TM-1 was experimentally isolated and characterized (3, 4). Nd, not determined.

Table 4-2. Cysteine biosynthesis activities in *M. maripaludis* cell extracts.

S-source	sp. act. (nmol/min/mg protein)[a]	$K_{0.5}$ (mM)[b]	V_{max} (nmol/min/mg protein)	R^{2}[e]
S^{2-}	1.2 ± 0.1	4.7 ± 1.1	1.8 ± 0.2	0.99
SSO_3^{2-}	3.2 ± 0.3	3.8 ± 0.8	4.4 ± 0.4	0.99
SO_3^{2-}	< 0.3	Nd[c]	Nd	Nd
SO_4^{2-}	< 0.3	Nd	Nd	Nd
$S^{2-} + SO_3^{2-}$	2.6 ± 0.3	0.03 ± 0.01[d]	2.6 ± 0.2	0.92

[a]Values were mean ± standard deviation of three assays. The concentration of the sulfur-containing compounds was 10 mM. The detection limit was 0.3 nmol/min/mg protein.

[b]$K_{0.5}$ represents the substrate concentration for 0.5 V_{max} of the overall reaction.

[b]Nd, not determined.

[c]$K_{0.5}$ of SO_3^{2-} determined in the presence of 10 mM Na_2S.

[d]R^2 of the Michaelis-Menten equation.

Table 4-3. RNA-dependency of the cysteine production activities in *M. maripaludis* cell extracts.

	sp. act. (nmol/min/mg protein)[a]	
S-source	- RNase A[b]	+ RNase A[c]
S^{2-}	1.8 ± 0.1	0.3 ± 0.2
$S_2O_3^{2-}$	3.3 ± 0.1	0.7 ± 0.2

[a]Values were mean ± standard deviation of three assays.

[b]Without RNase A treatment.

[c]The cell extracts were pre-incubated with 5 mg/ml RNaseA at 37 ^{o}C for 1 hr before the assays.

Table 4-4. Sulfide-dependent reduction of FMN, FAD, and F_{420} in *M. maripaludis* cell extracts.

e acceptor	sp. ac. (nmol/min/mg protein)[a]
FMN	0.9 ± 0.1
FAD	0.6 ± 0.1
F_{420}	2.2 ± 0.5

[a]Values were mean ± standard deviation of three assays. The concentration of FMN or FAD was 100 μM, and the concentration of F_{420} was 10 μM.

Figure 4-1. Cysteine biosynthesis pathways: (i) the sulfhydrylation pathway; (ii) the reverse transsulfuration pathway; and (iii) the tRNA-dependent pathway. The sulfhydrylation pathway is utilized by higher plants and many bacteria, such as enteric bacteria and actinobacteria. The reverse transsulfuration pathway is utilized by mammals, *Saccharomyces cerevisiae*, and some bacteria, such as *Lactococcus lactis* (25) and *Pseudomonas putida* (29). The tRNA-dependent pathway is utilized by methanogenic archaea. Abbreviations: SAT, serine *O*-acetyltransferase; OASS, *O*-acetylserine sulfhydrylase; CBS, cystathionine β-synthase; CGL, cystathionine γ-lyase; OAHS, *O*-acetylhomoserine sulfhydrylase; Sep, *O*-phosphoserine; SepRS, *O*-phosphoseryl-tRNA synthetase; SepCysS, Sep-tRNA:Cys-tRNA synthase; CysRS, cysteinyl-tRNA synthetase.

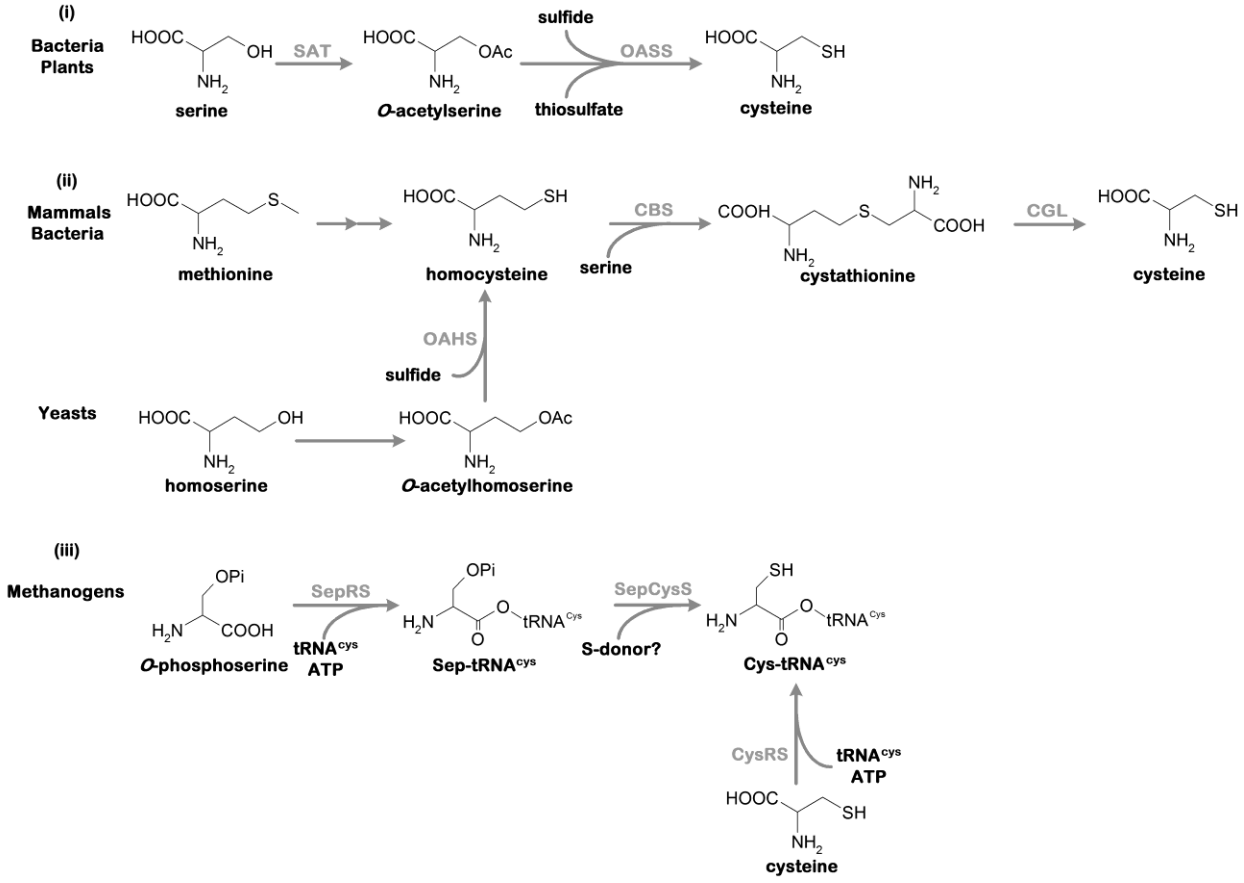
(i)
Bacteria
Plants
HOOC
OH
NH2
serine
SAT
HOOC
OAc
NH2
O-acetylserine
sulfide
thiosulfate
OASS
HOOC
SH
NH2
cysteine
(ii)
Mammals
Bacteria
HOOC
S
NH2
methionine
HOOC
SH
NH2
homocysteine
CBS
serine
COOH
NH2
S
NH2
COOH
cystathionine
CGL
HOOC
SH
NH2
cysteine
OAHS
sulfide
Yeasts
HOOC
OH
NH2
homoserine
HOOC
OAc
NH2
O-acetylhomoserine
(iii)
Methanogens
OPi
H2N
COOH
O-phosphoserine
SepRS
tRNACys
ATP
OPi
H2N
O
O
tRNACys
Sep-tRNACys
SepCysS
S-donor?
SH
H2N
O
O
tRNACys
Cys-tRNACys
CysRS
tRNACys
ATP
HOOC
SH
NH2
cysteine

Figure 4-2. The inhibition of the cysteine biosynthesis by DTT. (●) the reactions with Na_2S as the sulfur source; (○) the reactions with $Na_2S_2O_3$ as the sulfur source.

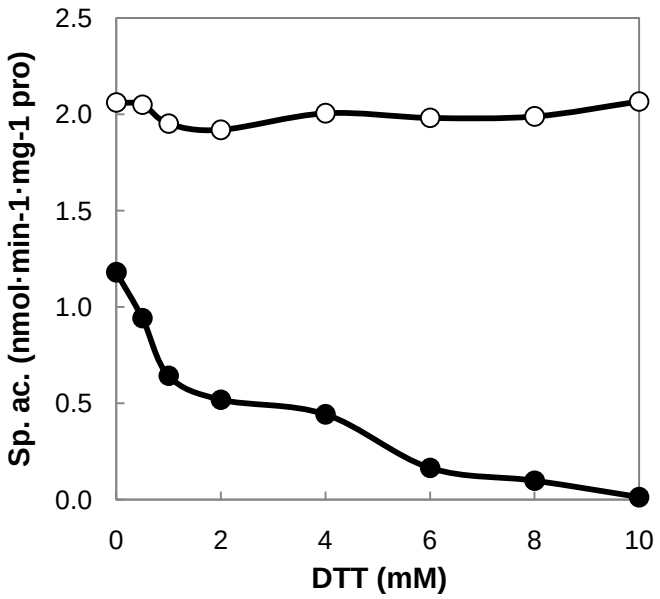
2.5
2.0
1.5
1.0
0.5
0.0
Sp. ac. (nmol·min-1·mg-1 pro)
0
2
4
6
8
10
DTT (mM)

Figure 4-3. Proposed mechanism for the sulfur assimilation into cysteine in *M. maripaludis*. The sulfur molecule being transferred was underlined. Sep, *O*-phosphoserine; Rhd, rhodanese-like proteins; and SepCysS, Sep-tRNA:Cys-tRNA synthase.

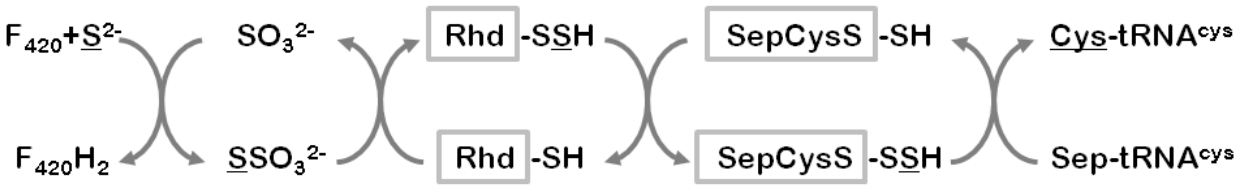
F420+S2-
F420H2
SO32-
SSO32-
Rhd -SSH
Rhd -SH
SepCysS -SH
SepCysS -SSH
Cys-tRNAcys
Sep-tRNAcys

CHAPTER 5

CYSTEINE IS NOT THE SULFUR SOURCE FOR IRON-SULFUR CLUSTER AND METHIONINE BIOSYNTHESES IN THE METHANOGENIC ARCHAEON *METHANOCOCCUS MARIPALUDIS*[5]

[5]Liu, Y., M. Sieprawska-Lupa, W.B. Whitman, and R.H. White. Submitted to *J. Biol. Chem.*

Abstract

Three multi-protein systems are known for iron-sulfur (Fe-S) cluster biogenesis in bacteria and eukaryotes: the NIF (nitrogen fixation), the ISC (iron-sulfur cluster), and the SUF (mobilization of sulfur) systems. In all three, cysteine is the physiological sulfur source, and the sulfur is transferred from cysteine desulfurase through a persulfidic intermediate to a scaffold protein. However, the biochemical nature of the sulfur source for Fe-S cluster assembly in archaea is not known, and many archaea lack homologs of cysteine desulfurases. *Methanococcus maripaludis* is a methanogenic archaeon that contains a high amount of protein-bound Fe-S clusters (45 nmol/mg protein). Cysteine in this archaeon is synthesized primarily via the tRNA-dependent SepRS/SepCysS pathway. When a Δ*sepS* mutant (a cysteine auxotroph) was grown with ^{34}S-labeled sulfide and unlabeled cysteine, < 3% of the cysteine, > 99% of the methionine, and > 93% of the the sulfur in the Fe-S clusters in proteins was labeled, suggesting that the sulfur in methionine and Fe-S clusters was derived predominantly from exogenous sulfide instead of cysteine. Therefore, this investigation challenges the prior knowledge that cysteine is always the sulfur source for Fe-S cluster biosynthesis *in vivo* and suggests that Fe-S clusters are derived from sulfide in organisms living in sulfide-rich habitats.

Introduction

Iron-sulfur (Fe-S) clusters play critical roles in a broad range of biological processes, such as electron transfer reactions, substrate binding, non-redox catalysis, sulfur donation, and sensing of redox status for regulatory processes (2, 12). Fe-S clusters can be synthesized *in vitro* on an apoprotein with iron salts and sulfide under anaerobic conditions (17, 21). However, due to their toxicity, the cellular concentrations of free iron and sulfide are usually much lower than the levels required for abiotic cluster formation. *In vivo* Fe-S cluster assembly uses several complex protein systems, which construct nascent clusters on scaffold proteins and then transfer them into recipient apo-proteins. Three Fe-S cluster assembly systems, NIF (nitrogen fixation), ISC (iron-sulfur cluster), and SUF (mobilization of sulfur), are conserved among bacteria, and many organisms possess more than one system (14, 24).

Cysteine is the sulfur source for Fe-S clusters in bacteria and eukaryotic mitochondria and chloroplasts. Cysteine desulfurase, a pyridoxal 5‘-phosphate (PLP)-dependent enzyme, initiates Fe-S cluster formation by mobilizing the sulfur atom from cysteine and transferring it to Fe-S clusters. A persulfide intermediate is formed on a conserved cysteinyl residue at the active site and functions as the direct sulfur donor for Fe-S cluster biosynthesis. Four cysteine desulfurase homologs are known: NifS, IscS, SufS, and CsdA (13, 24).

The sulfur source for Fe-S cluster biosynthesis in archaea awaits further investigation. The methanogenic archaeon *Methanococcus maripaludis* produces cysteine primarily on $tRNA^{Cys}$ via the SepRS/SepCysS pathway (37). This organism possesses two pathways for charging $tRNA^{Cys}$. When exogenous cysteine is available, $tRNA^{Cys}$ is aminoacylated with cysteine by a canonical cysteinyl-tRNA synthetase (CysRS) (29, 41). In a second pathway, cysteine is synthesized *de novo* in two steps (37). In the first step, $tRNA^{Cys}$ is acylated with *O*-

phosphoserine (Sep) by *O*-phosphoseryl-tRNA synthetase (SepRS). In the second step, Sep-tRNA^{Cys} is converted to Cys-tRNA^{Cys} by Sep-tRNA:Cys-tRNA synthase (SepCysS). However, the sulfur source for this reaction is not known. A Δ*sepS* mutant is a cysteine auxotroph (37). This raises two questions. First, do cells contain an alternative pathway to generate free cysteine? Second, if not, what is the sulfur source for the biosynthesis of Fe-S clusters and other sulfur-containing compounds in cells? Moreover, homologs of cysteine desulfurase are absent in many *Methanococcus* species, other *Methanococcales*, and many non-methanogenic archaea (Fig. 5-1). Therefore, no characterized enzymes are currently known that specifically catalyze the release of sulfur from cysteine in these organisms.

Here we demonstrate that, unlike in all other previously studied organisms, the sulfur in Fe-S clusters in the methanogenic archaeon *Methanococcus maripaludis* does not originate from cysteine. Instead, it is derived from sulfide, which is abundant in the anaerobic environment where the organism was isolated (25). This discovery also sheds light on the Fe-S cluster biogenesis in other organisms living in sulfide-rich environments and early life forms on the anoxic earth when sulfide was abundant.

Materials and Methods

Strains, media, and growth conditions. Two *M. maripaludis* strains, the wild-type strain S2 and the Δ*sepS* mutant (a cysteine auxotroph lacking the *O*-phosphoseryl-tRNA synthetase (37)), were used in this study. Cultures were grown in McNA medium (a minimal medium with 10 mM sodium acetate) reduced with 3 mM cysteine or dithiothreitol (DTT) as indicated (50). The 5 ml cultures were grown in 28 ml aluminum seal tubes pressurized to 276 kPa with H_2:CO_2 (4:1, v/v). The 100 ml cultures were grown in 1 L bottles pressurized to 138 kPa with H_2:CO_2 (4:1, v/v). Before inoculation, 3 mM of sodium sulfide was added as the sulfur

source. The *Escherichia coli* strain K-12 MG1655 was grown aerobically in Luria-Bertani (LB) medium.

Quantification of protein-bound inorganic sulfide, iron, and cysteinyl and methionyl residues. The inorganic acid-labile sulfide content in cell extracts was determined by an adaptation of the methylene blue method (3, 11). The assays were carried out in the anaerobic chamber with an atmosphere of 95% of N_2 and 5% of H_2. Cell-free extracts in 0.1 M potassium phosphate (pH 8.0) were filtered twice through a 2-ml Sephadex G-25 column (Aldrich) to remove non-protein-bound sulfide. Precipitated FeS complexes from the medium were also trapped at the top of the column. To measure the sulfide content, 0.3 ml of 1% (w/v) freshly prepared zinc acetate and 10 μl of 12% sodium hydroxide were added and mixed with 200 μl cell extract (0.2-0.4 mg protein of *M. maripaludis* or 1-2 mg protein of *E. coli*) in microcentrifuge tubes. The tubes were closed and left at room temperature for 20 min. Then 0.1 ml of 1% of *N*,*N*-dimethylphenylenediamine (DMPD) in 5 M of HCl and 40 μl of 11.5 mM of $FeCl_3$ in 1.2 M of HCl were added, and the solution was mixed rapidly. The samples were centrifuged at 16,000 g for 10 min to remove denatured proteins. The absorbance of the supernatant was determined at 670 nm. Solutions of sodium sulfide (0-20 nmol) were used as standards.

The iron content was determined by an adaptation of the *o*-phenanthroline method (18, 31). The Sephadex G-25 filtered cell extracts (0.1-0.2 mg protein of *M. maripaludis* or 1-2 mg protein of *E. coli*) were deproteinized with 5% (w/v, final concentration) of trichloroacetic acid (TCA). The supernatant (100 μl) was transferred to a microcentrifuge tube, and then 0.1 ml of 1 M sodium acetate-acetic acid buffer (pH 4.0), 0.1 ml of 0.3% (w/v) *o*-phenanthroline, and 0.1 ml of 10% (w/v) hydroxylamine hydrochloride were added. The mixture was incubated at 37 ^{o}C for

30 min. The absorbance was measured at 512 nm. Solutions of $FeCl_3 \cdot 6H_2O$ (0-20 nmol) were used as standards.

The content of cysteinyl and methionyl residues in *M. maripaludis* proteins were determined at the UC Davis amino acid analysis facility after acid hydrolysis with 6M HCl for 24 hrs at 110 ^oC. The protein concentrations were determined by BCA protein assay (Pierce) (40).

Quantification of intracellular free cysteine, homocysteine, coenzyme M, and cystathionine. The *M. maripaludis* wild-type (strain S2) cells were grown in 100 ml McNA medium (reduced with 3 mM DTT) to an absorbance of ~ 0.35 at 600 nm. Cells were harvested anaerobically by centrifugation at 3,000 *g* for 15 min at room temperature. The following steps were carried out in anaerobic chamber with an atmosphere of 95% of N_2 and 5% of H_2. The pellet was suspended in 1.5 ml 10 mM of acetic acid, incubated on ice for 15 min to lyse the cells, and the suspension was centrifuged in microcentrifuge tubes at 16,000 *g* for 10 min. The supernatant (~1.3 ml) was collected and divided into two 0.5 ml samples, to which 40 µl of buffer (1 M HEPES, 50 mM EDTA, pH 8.2) were added. One sample that served as a negative control was supplemented with 4 mM of *N*-ethylmaleimide (NEM). Thiols were quantified by a modification of the monobromobimane (mBBr) derivatization method (10). To each sample (~500 µl), 20 µl of 50 mM of mBBr (in acetonitrile) was added to a final concentration of 2 mM, and the solution was incubated for 5 min in the dark at room temperature. Samples were then deproteinized by addition of 0.6 ml of acetonitrile and incubated for 15 min at 60 ^oC. To stop the mBBr reaction, glacial acetic acid was added to the final concentration of 1% (v/v), and the samples were cooled on ice. The excess of unreacted mBBr was removed by extraction with 0.2 ml of chloroform, and the aqueous phase was collected. In this step, the sample was concentrated

by extraction of acetonitrile into the chloroform fraction. Samples (20 μl) were analyzed on a Waters 2695 Separation HPLC System. The samples were separated on an Altima C-18 reversed phase column at 30 ^{o}C using a linear gradient of 5 to 95% of methanol with 0.25% acetic acid. Fluorescence detection was performed with a Shimadzu- RF – 10A XL detector, using an excitation of 390 nm and emission at 480 nm. The standard curves were prepared with cysteine, homocysteine, and CoM.

The quantification of cystathionine in the free amino acid pool was performed as described (20) at the UC Davis amino acid analysis facility.

Measurement of the incorporation of [3,3-$^{2}H_2$]cysteine into cellular proteins. *M. maripaludis* wild-type strain S2 and the Δ*sepS* mutant were grown in 5 ml McNA medium with 3 mM DTT, 3 mM sodium sulfide, and 1.5 mM DL-[3,3,3‘,3‘-$^{2}H_4$]cystine to an absorbance of ~ 0.5 at 600 nm. The cells were collected by centrifugation at 2,460 *g* for 20 min at room temperature. The cell pellet was suspended, incubated with 0.4 ml of 5% TCA for 10 min at room temperature, and then centrifuged to collect denatured proteins. This process was repeated two more times to insure the complete removal of free cysteine from the precipitated proteins. The resulting sample was dissolved in 200 μl of 0.5 M Tris-HCl buffer (pH 8.6) containing 6 M urea and 16 mM DTT, and then the protein bound cysteinyl residues were alkylated with 10 μl of methyl iodide. The samples were then dialyzed for 15 hr against 3 × 1 L of water and evaporated. This process removed urea and also any remaining free cysteine and methionine not removed in the TCA washing. The protein samples were then acid hydrolyzed (6 M HCl, 110° for 12 hr under nitrogen), and the *S*-methylcysteine was assayed by gas chromatography-mass spectrometry (GC-MS) as previously described (46).

Measurement of the incorporation of [^{34}S]sulfide into thiol-containing amino acids and Fe-S clusters. Elemental sulfur with the following isotopic abundances: ^{32}S, 3.48 atom %; ^{33}S, 2.23 atom %; ^{34}S, 92.59 atom %; ^{36}S, 1.70 atom % (Monsanto Research Corp.) was used in the synthesis of [^{34}S]sulfide by reduction with DTT. ^{34}S (4 mg) was heated to 120 °C for 10 minutes in an aluminum seal tube containing 2 ml of McNA medium with 0.2 M DTT. To volatilize the sulfide, 2 ml of 1 M HCl was added, and the solution was incubated for 30 min. After the removal of the liquid, the H_2S gas was trapped in 0.5 ml of 0.5 M NaOH. Final concentration of sulfide was determined upon reaction with 1 mM 5,5'-dithio-bis(2-nitrobenzoic acid) (DTNB). An extinction coefficient of ε_{412}= 14.15 $mM^{-1}cm^{-1}$ was used for calculations (9).

The Δ*sepS* mutant was grown in McNA medium containing 1.5 mM [^{34}S]sulfide and 3 mM cysteine containing the natural abundance of [^{34}S]sulfide (4.2 atom % ^{34}S). All the following steps were carried out anaerobically. Cells from 40 ml of overnight grown cultures were harvested by centrifugation at 2,460 *g* for 20 min at room temperature and washed twice with McNA medium reduced with 3 mM CoM. The cell pellets were suspended in 0.5 ml of 50 mM PIPES buffer (pH 6.8) containing 1 mM DTT. Cells (~10 mg dry wt) were lysed by repeated (2 ×) freezing (-20°C) and thawing. A few crystals of DNAse were added to digest genomic DNA. The cell extract was passed through a 2-ml Sephadex G-25 column to remove free sulfide, insoluble iron sulfides, and other low molecular weight compounds. The cell extract (~1 ml) was then concentrated using a Centricon 10 kD filtration unit (Millipores). The concentrated samples (70 µl) were transferred to 1.5 ml microcentrifuge tubes, which were placed in 10 ml glass serum bottles, closed with butyl stoppers, sealed, flushed with N_2 for 5 min, and frozen at -20 ^{o}C. As controls, 1 ml of media was collected immediately after inoculation of culture and again after harvesting the cells. To test the possibility that homocysteine or cystathionine supplied the sulfur

for the Fe-S clusters, Δ*sepS* cells were grown with 3 mM homocysteine plus 3 mM cysteine plus 1.5 mM [^{34}S]sulfide or 5 mM cystathionine plus 1.5 mM [^{34}S]sulfide.

The ^{34}S isotopic abundance in Fe-S clusters was analyzed by GC-MS. The acid-labile sulfide was released by treatment of the sample with 1 M HCl and trapped in 1 M NaOH as described (43). The resulting sulfide was converted into dibenzyl sulfide and assayed by GC-MS to determine the isotopic abundance of the ^{32}S/^{34}S in the M^+ = 214 *m/z* ion as described (48). The apparatus for trapping the sulfide used a septate 1.0 ml glass vial containing a 2 × 4 mm glass test tube and a stirring bar. The septate vial was flushed with argon, and 50-200 μl sample was injected into the bottom of the vial. Then 15 μl 1 M NaOH was added to the absorbent tube, followed by addition of 0.1 volume of 1 M HCl. After stirring at room temperature for 1 hr, 40 μl of 50% methanol in water was added to the absorbent tube, and the sample was transferred to the 1 ml septate glass vial flushed with Ar. Then 2 μl of distilled benzyl chloride was added, and the vial was heated for 1 hr at 60 °C. The samples were then evaporated to dryness with a stream of nitrogen gas and extracted with 0.5 ml of methylene chloride. The methylene chloride was separated from water by passing the solution through a small plug of absorbent cotton and concentrated by evaporation to 3-6 μl for GC-MS analysis.

The proteins remaining in the acidified samples were dissolved in 400 μl of Tris-HCl buffer (pH 8.6) containing 6 M urea and 16 mM DTT, and the cysteinyl residues were alkylated with methyl iodide as described above. The methylcysteine and methionine in proteins was assayed for ^{34}S abundance as previously described (47).

Enzyme assays. All enzyme assays were carried out in anaerobic chamber with an atmosphere of 95% of N_2 and 5% of H_2. The protein concentrations were determined by BCA protein assay (Pierce) (40).

Cystathionine γ-cleavage activity in *M. maripaludis* cell extracts were determined by following the production of cysteine by reaction with the acid-ninhydrin reagent (16). Assay mixture in a total volume of 0.3 ml contained 0.1 M Tris-HCl (pH 8.0), 10 μM PLP, and cell-free extract (0.3 mg of total protein). The reactions were initiated by the addition of 10 mM L-cystathionine and incubated for 30 min at 37 ^{o}C. The reactions were stopped by addition of 0.3 ml glacial acetic acid and 0.3 ml of 2.5% (w/v) ninhydrin in 60% (v/v) acetic acid and 40% (v/v) concentrated HCl. The samples were heated in boiling water for 10 min for color development, and the absorbance was determined at 560 nm after cooling. Solutions of cysteine (0-40 nmol) were used as standards. Kinetic constants in cell extracts were determined with 0.5, 1, 2, 4, 8, and 10 mM L-cystathionine.

Cystathionine β-cleavage activity was determined by following the production of homocysteine (Hcy) by reaction with DTNB (9). Assay mixture in a total volume of 0.2 ml contained 0.1 M Tris-HCl (pH 8.0), 10 μM PLP, and cell-free extract (0.2 mg of total protein). The reactions were initiated by the addition of 10 mM L-cystathionine and incubated for 30 min at 37 ^{o}C. The reactions were stopped by heating in boiling water for 10 min, followed by reaction with 50 μl of 0.1 M DTNB. The samples (20 μl) were analyzed for Hcy and Cys on an Altima C-18 reversed phase column with a Waters 2695 Separation HPLC System at 25 ^{o}C using a linear gradient of 5 to 95% of methanol with 0.25% acetic acid, and the peaks of the 2-nitro-5-thiobenzoate derivatives of Hcy and Cys were monitored at 330 nm. Kinetic constants in cell extracts were determined with 1.25, 2.5, 5, 7.5, and 10 mM L-cystathionine.

Cysteine desulfurase activity was determined by the methylene blue method (11). Assay mixtures in a total volume of 0.8 ml contained 0.1 M Tris-HCl (pH 8.0), 0.2 M NaCl, 1 mM DTT, 50 μM PLP, and cell-free extract (0.2 mg of total protein). The reactions were initiated by the addition of 1 mM L-cysteine and incubated for 30 min at 37 ^{o}C. The reactions were stopped by the addition of 100 μl of 1% DMPD in 5 M of HCl and 100 μl of 11.5 mM of $FeCl_3$ in 1.2 M HCl. The samples were centrifuged at 16,000 *g* for 10 min, and the absorbance of the supernatant was determined at 670 nm. Kinetic constants in cell extracts were determined with 0.05, 0.1, 0.2, 0.5, and 1 mM of cysteine and DTT.

Homoserine sulfhydrylase activity was determined by following the production of homocysteine (Hcy) after the reaction with DTNB (9). Assay mixture in a total volume of 0.2 ml contained 0.25 M Tris-HCl (pH 8.0), 10 mM $MgSO_4$, 0.2 M KCl, 10 mM homoserine, 50 mM ATP, 50 mM acetyl-CoA or succinyl-CoA, 10 μM PLP, and cell-free extract (0.2 mg of total protein). The reactions were initiated by the addition of 10 mM sodium sulfide and incubated for 1 hr at 37 ^{o}C. The reactions were stopped by heating in boiling water for 10 min, followed by reaction with DTNB and separation with HPLC as described above for the cystathionine β-cleavage activity assay.

The kinetic data were analyzed using SigmaPlot 10.0 with the Enzyme Kinetics module (Systat Software Inc.) fitted with the Michaelis-Menten equation for cystathionine cleavage activities and a Ping-Pong Bi-Bi mechanism for cysteine desulfurase activity.

Results

Fe-S clusters are abundant in methanococci. A prior bioinformatics analysis suggested that Fe-S cluster-containing proteins were abundant in methanogens (32). To test this hypothesis, the amount of Fe-S clusters in *M. maripaludis* was determined by measurements of protein-

bound inorganic sulfide and iron and compared to that found in aerobically grown *E. coli* (Table 5-1). The inorganic sulfide content agreed with the measurement in *Methanocaldococcus jannashcii* (31 nmol/mg protein) (46), and the iron content agreed with that in whole cells of *Methanococcus voltae* (30-94 nmol/mg protein) (49). Therefore, methanococci possessed ~15-fold higher amounts of Fe-S clusters than aerobically grown *E. coli*. If the Fe-S clusters were mostly low potential [4Fe-4S] and [2Fe-2S] clusters (33) and coordinated by cysteinyl residues at a 1:1 stoichiometry, ~ 40% of the total cysteinyl residues in *M. maripaludis* would be associated with Fe-S clusters.

The SepRS/SepCysS pathway is the primary pathway for cysteine biosynthesis. The Δ*sepS* mutant of *M. maripaludis* is a cysteine auxotroph, suggesting that this pathway is necessary for cysteine biosynthesis (37). However, it is possible that the mutant is a pseudoauxotroph and possesses an alternative cysteine biosynthetic pathway that is insufficient to support growth (39). Three lines of evidence demonstrated that the SepRS/SepCysS pathway provides the predominant, if not sole, source of cysteine.

First, exogenous ^{2}H-labeled cysteine was incorporated into cellular proteins with little dilution in the Δ*sepS* mutant. When wild-type cells were grown with sulfide, DTT, and [3,3,3‘,3‘-$^{2}H_4$]cystine, ~ 45% of the cysteine in cellular proteins was ^{2}H-labeled. Thus, about half of the cysteine was biosynthesized by the cells and half was assimilated directly from the medium. By contrast, in the Δ*sepS* mutant cells, > 99% of the cysteine in proteins was ^{2}H-labeled, suggesting that the mutant synthesized < 1% of its cysteine.

Second, in the Δ*sepS* mutant, ^{34}S-labeled sulfide was poorly incorporated into cysteinyl residues in the cellular proteins. Presumably, if the cells could synthesize cysteine *de novo* from sulfide, the cysteinyl residues would contain high levels of ^{34}S. The Δ*sepS* mutant was grown in

medium containing ^{34}S-enriched sulfide (92.6 atom % of ^{34}S) and cysteine with the natural abundance of ^{34}S (4.2 atom % of ^{34}S). Cysteine recovered from the medium after growth, retained its isotopic signatures and did not interchange its sulfur atoms with sulfide during cultivation (data not shown). Similarly, at the beginning of growth the measured enrichment of ^{34}S-labeled sulfide in the medium was 95 ± 2%, and it decreased to 82 ± 8% after growth. This decrease could be explained by the release of a small amount of unlabeled sulfide from cysteine, possibly via cysteine desulfurase (see below) or cysteine desulfidase activity, which cleaves cysteine into pyruvate, ammonia, and sulfide (43). In cellular proteins, only a small amount of ^{34}S was incorporated into cysteine (Table 5-2). Considering the abundance of ^{34}S in cysteine and sulfide used as substrates for growth, less than 1.7-3.0% of the cysteinyl residues of the Δ*sepS* mutant were derived from sulfide.

Third, the activity of cysteine production from L-cystathionine cleavage was examined. L-Cystathionine is an important intermediate in transsulfuration, and cysteine production from cystathionine γ-cleavage is employed by mammals, yeasts, fungi, and many bacteria such as actinomycetes (34). *M. jannaschii* cell extracts had activities of both cystathionine β- (produces homocysteine that is a precursor of methionine) and γ- (produces cysteine) cleavage (46), suggesting that transsulfuration with cystathionine could be an intermediate in the interconversion and biosynthesis of cysteine and methionine. Supporting this assumption, high levels of L-cystathionine (≥ 2 mM) can substitute for cysteine in the growth of the Δ*sepS* mutant (Fig. 5-2). When the Δ*sepS* mutant was grown with ^{34}S-enriched sulfide and unenriched cystathionine, neither the cysteinyl nor the methionyl residues in proteins were ^{34}S-enriched (Table 5-2), suggesting that cystathionine provided the sulfur for the biosynthesis of both of these amino acids under this growth condition. Therefore, cystathionine can be assimilated by

the cells and function as an intermediate of sulfur metabolism. To examine the physiological significance of these reactions, the intracellular amount of cystathionine in wild-type cells grown without exogenous cystathionine was determined (Table 5-3). Assuming that proteins account for 60 % of the cell dry wt and cells contain 2.5 µl of water per mg dry wt (5), the intracellular cystathionine concentration would be ~0.1 mM. In *M. maripaludis* cell extracts, cystathionine γ-cleavage activity had an apparent K_m (cystathionine) of 8.7 ± 0.5 mM and V_{max} of 7.8 ± 0.3 nmol/min/mg protein (Table 5-4). Accordingly, at the physiological concentration of cystathionine, the cysteine biosynthetic activity would be ~0.1 nmol/min/mg protein, which was 10-fold lower than the activity required for cysteine biosynthesis (1 nmol/min/mg protein) during growth. Therefore, cysteine production from cystathionine at physiological conditions was insignificant and would only generate a small amount of free cysteine, possibly as part of an organic sulfur salvage pathway in this organism. On the other hand, the homocysteine biosynthetic activity from cystathionine β-cleavage had an apparent K_m (cystathionine) of 5 ± 1 mM and V_{max} of 40 ± 5 nmol/min/mg protein (Table 5-4). With the physiological concentration of 0.1 mM cystathionine, the activity would be ~1 nmol/min/mg protein, which was about half of the activity required for methionine biosynthesis (~2 nmol/min/mg protein). Therefore, cystathionine β-cleavage may play a more important role in methionine biosynthesis.

Free cysteine pool and cysteine desulfurase activity in *M. maripaludis*. If cysteine was synthesized primarily on tRNA via the SepRS/SepCysS pathway, the intracellular levels of free cysteine would be expected to be very low. The free cysteine content was determined to be 0.05 nmol/mg dry wt (Table 5-3). Therefore, the intracellular concentration of free L-cysteine would be ~20 µM. As an internal control for the loss in thiols during these measurements, the levels of coenzyme M were determined at the same time. The levels of coenzyme M were similar to those

that had been previously reported (1). The expected intracellular concentration of free cysteine in bacteria ranges between 100-200 μM (26). Therefore, while free cysteine was present in *M. maripaludis*, the levels were much lower than those common in bacteria. Presumably, the free cysteine may be formed from L-cystathionine cleavage or hydrolysis of Cys-tRNA^{cys} and proteins.

Although cysteine desulfurase homologs have not been identified in the *M. maripaludis* genome, cysteine desulfurase activity was detected in cell-free extracts with cysteine and DTT as substrates. The specific activity was 0.20 ± 0.02 nmol/min/mg protein, which was about half of the activity measured in aerobically grown *E. coli* cell extracts (0.45 ± 0.04 nmol/min/mg protein). This activity may come from an uncharacterized enzyme. This reaction in cell extracts had an apparent K_m (cysteine) of 25 ± 3 μM and V_{max} of 0.28 ± 0.05 nmol/min/mg protein. Therefore, the activity at the physiological concentration of cysteine (20 μM) would be about 0.1 nmol/min/mg protein and insufficient to support Fe-S cluster biosynthesis required for growth (~0.5 nmol/min/mg protein). However, cysteine desulfurase activity would still be sufficient to serve as a major sulfur source for tRNA modification and vitamin biosynthesis.

Origin of sulfur in Fe-S clusters and methionine. Even though a small pool of free cysteine exists in *M. maripaludis*, two lines of evidence indicated that cysteine is not the origin of sulfur in Fe-S clusters and methionine. First, when the Δ*sepS* mutant was grown with limiting amount of cysteine (0.01 mM) in McNA medium, 80 μmol of cysteine was required for growth of one gram cell dry wt. This value agreed well with the cysteine content of the whole cells of 102 μmol/g protein (or 61 μmol/g dry wt) (Table 5-1). In contrast, if cysteine was a general intermediate in sulfur assimilation, greater than 200 μmol cysteine would be required for cysteine, Fe-S cluster, and methionine biosynthesis. Second, the incorporation of ^{34}S-labeled

sulfide into Fe-S clusters and methionine in the Δ*sepS* mutant demonstrated that cysteine was a minor sulfur source for these compounds. Cells were grown with ^{34}S-enriched sulfide and unlabeled cysteine as described above. The acid-labile sulfide, which was released from the Fe-S clusters present in cellular proteins, was highly ^{34}S-enriched (Table 5-2). Based upon the atom % of ^{34}S, at least 93% of the sulfide released from Fe-S clusters originated from ^{34}S-enriched sulfide, suggesting that the sulfur in Fe-S clusters was mainly derived from exogenous sulfide instead of cysteine. Similarly, > 99% of the sulfur in methionyl residues in proteins was also derived from sulfide.

Whether sulfide could be a sulfur source for methionine biosynthesis through the direct sulfhydrylation of homoserine derivatives was examined. Yeast, fungi, and some bacteria can directly synthesize homocysteine from sulfhydrylation of acylated homoserine. Thus, they bypass cystathionine of the transsulfuration pathway for methionine biosynthesis (28). The homocysteine biosynthesis activities in *M. maripaludis* cell extracts with sulfide and homoserine plus succinyl-CoA, acetyl-CoA, or ATP as substrates were below the detection limit of 0.1 nmol/min/mg protein, suggesting that sulfide is probably not a direct sulfur source for homocysteine biosynthesis. This observation agreed with the previous report that even though homocysteine can be synthesized from *O*-phosphohomoserine in *M. jannaschii* cell extracts, this reaction does not use sulfide as a sulfur source (46).

The possibility of homocysteine and cystathionine as sulfur sources for Fe-S cluster biosynthesis was also examined. When the Δ*sepS* mutant was grown with ^{34}S-labeled sulfide and unlabeled cystathionine instead of cysteine, at least 90% of the sulfur in Fe-S clusters was derived from sulfide (Table 5-2). Homocysteine could not replace cysteine for the growth of Δ*sepS* (Fig. 5-2). Addition of unlabeled homocysteine to cells grown with ^{34}S-enriched sulfide

and unlabeled cysteine did not dilute the enrichment of ^{34}S in Fe-S clusters (Table 5-2). Therefore, neither L-cystathionine nor L-homocysteine provided the sulfur for Fe-S cluster formation.

Discussion

In summary, sulfur in Fe-S clusters and methionine in *M. maripaludis* originated from sulfide instead of cysteine. Moreover, sulfur assimilation in methanococci is different from that in previously studied bacteria in four respects.

First, bacteria normally maintain cellular sulfide concentrations in the range of 20-160 μM (26). In contrast, methanococci inhabit anaerobic environments with high levels of sulfide (8) and are normally cultivated with 3-5 mM Na_2S (49). At neutral pH, one third of the sulfide remains in non-ionized form (H_2S), which may freely diffuse across cell membrane (44). Therefore, the intracellular sulfide concentrations of methanococci are likely in the millimolar range. Methanococci are adapted to high sulfide-tolerant life style (30, 45), and they lack many targets for sulfide toxicity, such as the α,β-unsaturated fatty acid biosynthetic intermediates and cytochromes (7, 44). Considering that sulfide at millimolar concentrations is used frequently *in vitro* for the enzymatic and non-enzymatic reactions, methanococci may use sulfide as a direct sulfur source in some reactions.

Second, enteric bacteria and plants synthesize cysteine via direct sulfhydrylation of *O*-acetylserine by *O*-acetylserine sulfhydrylase (36), and sulfide is the physiological sulfur donor for this reaction with K_m-values in the micro-molar range (23, 42). In contrast, even though sulfide is presumably present at high levels in methanococci, it is probably not the direct sulfur donor for cysteine biosynthesis. Cysteine in methanococci is synthesized primarily on $tRNA^{Cys}$ via the SepRS/SepCysS pathway, and a persulfide group is proposed to be a direct sulfur donor

based upon the structural similarity of SepCysS and cysteine desulfurases (15, 19, 38). If persulfide groups were derived from cysteine *in vivo*, it would be a futile cycle to synthesize cysteine from persulfide groups. Therefore, methanococci presumably use a new biochemical process to generate persulfide groups for sulfur incorporation into cysteine.

Third, the known Fe-S cluster assembly system is incomplete in methanococci and many other archaea. It is especially interesting that methanococci and some other archaea living in solfataric hydrothermal systems lack homologs of cysteine desulfurases (Fig. 5-1), indicating that they may use a different mechanism for sulfur incorporation into Fe-S clusters. Indeed, only the *sufBC* and *apbC*/*nbp35* genes involved in Fe-S biogenesis are conserved across archaea with completely sequenced genomes. Like the bacterial and eukaryotic ApbC/Nbp35 homologs, the *M. maripaludis* protein forms Fe-S clusters *in vitro* and may function as a Fe-S cluster carrier protein in cells (4). The *suf* system in bacteria is important under iron starvation and oxidative stress conditions, and it is the only Fe-S cluster assembly system in certain bacteria, such as *Thermatoga maritima*, *Mycobacterium tuberculosis*, and cyanobacteria (22, 24), suggesting that *suf* can function as the sole Fe-S cluster assembly system in some organisms. Recent biochemical studies showed that SufC is an ABC-type ATPase (6) and SufB is a persulfide acceptor, but it may also function as a scaffold protein (27). In most archaea *sufB* and *sufC* are arranged as neighboring genes. Mutagenesis of *sufB* (MMP1169) and *sufC* (MMP1168) in *M. maripaludis* was only successful with *sufBC* expressed in trans on a shuttle vector (data not shown), indicating that this protein may be essential in methanococci. However, identification of other assembly components is required to understand the nature of the direct sulfur donor and how *sufBC* could function without other known Fe-S cluster biogenesis proteins.

Fourth, bacteria synthesize homocysteine, the precursor of methionine, by either transsulfuration with cystathionine as an intermediate or direct sulfhydrylation of *O*-succinylhomoserine or *O*-acetylhomoserine (28, 51). None of the homologs of homocysteine biosynthetic genes are present in the *M. maripaludis* genome. The transsulfuration route uses cysteine as a sulfur source for cystathionine biosynthesis. Since cysteine is not the sulfur source for methionine biosynthesis in *M. maripaludis*, this route either plays a minor part in methionine biosynthesis or there is a new reaction independent of cysteine for cystathionine biosynthesis. The sulfhydrylation route uses sulfide as a sulfur source for homocysteine biosynthesis. However, the direct sulfhydrylation activity with sulfide and homoserine derivatives as substrates was below the detection limit in *M. maripaludis* cell extracts. Therefore, a new biochemical process should be responsible for homocysteine and methionine biosynthesis in methanococci.

Acknowledgements

This research was supported by the U.S. National Science Foundation grant MCB 0231319 to R.H.W., a DOE grant to W.B.W, and a Doctoral Completion Award from the Univ. of Georgia Graduate School to Y.L. We thank Kim Harich for assistance with MS analysis and Walter Niehaus for assistance with editing this manuscript.

References

1. **Balch, W. E., and R. S. Wolfe.** 1979. Specificity and biological distribution of coenzyme M (2-mercaptoethanesulfonic acid). J. Bacteriol. **137:**256-63.

2. **Beinert, H.** 2000. Iron-sulfur proteins: ancient structures, still full of surprises. J. Biol. Inorg. Chem. **5:**2-15.

3. **Beinert, H.** 1983. Semi-micro methods for analysis of labile sulfide and of labile sulfide plus sulfane sulfur in unusually stable iron-sulfur proteins. Anal. Biochem. **131:**373-378.

4. **Boyd, J. M., R. M. Drevland, D. M. Downs, and D. E. Graham.** 2009. Archaeal ApbC/Nbp35 homologs function as iron-sulfur cluster carrier proteins. J. Bacteriol. **191:**1490-1497.

5. **Dybas, M., and J. Konisky.** 1992. Energy transduction in the methanogen *Methanococcus voltae* is based on a sodium current. J. Bacteriol. **174:**5575-5583.

6. **Eccleston, J. F., A. Petrovic, C. T. Davis, K. Rangachari, and R. J. M. Wilson.** 2006. The kinetic mechanism of the SufC ATPase. J. Biol. Chem. **281:**8371-8378.

7. **Edgcomb, V. P., S. J. Molyneaux, M. A. Saito, K. Lloyd, S. Boer, C. O. Wirsen, M. S. Atkins, and A. Teske.** 2004. Sulfide ameliorates metal toxicity for deep-sea hydrothermal vent archaea. Appl. Environ. Microbiol. **70:**2551-2555.

8. **Edmond, J. M., K. L. Von Damm, R. E. McDuff, and C. I. Measures.** 1982. Chemistry of hot springs on the East Pacific Rise and their effluent dispersal. Nature **297:**187-191.

9. **Ellman, G. L.** 1959. Tissue sulfhydryl groups. Arch. Biochem. Biophys. **82:**70-77.

10. **Fahey, R. C., G. L. Newton, R. Dorian, and E. M. Kosower.** 1981. Analysis of biological thiols: quantitative determination of thiols at the picomole level based upon derivatization with monobromobimanes and separation by cation-exchange chromatography. Anal. Biochem. **111:**357-365.

11. **Fogo, J. K., and M. Popowsky.** 1949. Spectrophotometric determination of hydrogen sulfide. Anal. Chem. **21:**732-734.

12. **Fontecave, M.** 2006. Iron-sulfur clusters: ever-expanding roles. Nat. Chem. Biol. **2:**171-174.

13. **Fontecave, M., and S. Ollagnier-de-Choudens.** 2008. Iron-sulfur cluster biosynthesis in bacteria: Mechanisms of cluster assembly and transfer. Arch. Biochem. Biophys. **474:**226-237.

14. **Frazzon, J., J. R. Fick, and D. R. Dean.** 2002. Biosynthesis of iron-sulphur clusters is a complex and highly conserved process. Biochem. Soc. Trans. **30:**680-685.

15. **Fukunaga, R., and S. Yokoyama.** 2007. Structural insights into the second step of RNA-dependent cysteine biosynthesis in Archaea: crystal structure of Sep-tRNA:Cys-tRNA synthase from *Archaeoglobus fulgidus*. J. Mol. Biol. **370:**128-141.

16. **Gaitonde, M. K.** 1967. A spectrophotometric method for the direct determination of cysteine in the presence of other naturally occurring amino acids. Biochem. J. **104:**627-633.

17. **Hagen, K. S., J. G. Reynolds, and R. H. Holm.** 1981. Definition of reaction sequences resulting in self-assembly of $[Fe_4S_4(SR)_4]^{2-}$ clusters from simple reactants. J. Am. Chem. Soc. **103:**4054-4063.

18. **Harvey, A. E., J. A. Smart, and E. S. Amis.** 1955. Simultaneous spectrophotometric determination of iron(II) and total iron with 1,10-phenanthroline. Anal. Chem. **27:**26-29.

19. **Hauenstein, S. I., and J. J. Perona.** 2008. Redundant synthesis of cysteinyl-tRNA^{Cys} in *Methanosarcina mazei*. J. Biol. Chem. **283:**22007-22017.

20. **Hendrickson, E. L., Y. Liu, G. Rosas-Sandoval, I. Porat, D. Söll, W. B. Whitman, and J. A. Leigh.** 2008. Global responses of *Methanococcus maripaludis* to specific nutrient limitations and growth rate. J. Bacteriol. **190:**2198-2205.

21. **Herskovitz, T., B. A. Averill, R. H. Holm, J. A. Ibers, W. D. Phillips, and J. F. Weiher.** 1972. Structure and properties of a synthetic analogue of bacterial iron--sulfur proteins. Proc. Natl. Acad. Sci. U S A. **69:**2437-2441.

22. **Huet, G., M. Daffe, and I. Saves.** 2005. Identification of the *Mycobacterium tuberculosis* SUF machinery as the exclusive mycobacterial system of [Fe-S] cluster assembly: evidence for its implication in the pathogen's survival. J. Bacteriol. **187:**6137-6146.

23. **Huwang, C. C., E. U. Woehl, D. E. Minter, M. F. Dunn, and P. F. Cook.** 1996. Kinetic isotope effects as a probe of the β-elimination reaction catalyzed by *O*-acetylserine Sulfhydrylase. Biochemistry **35:**6358-6365.

24. **Johnson, D. C., D. R. Dean, A. D. Smith, and M. K. Johnson.** 2005. Structure, function, and formation of biological iron-sulfur clusters. Annu. Rev. Biochem. **74:**247-281.

25. **Jones, W. J., M. J. B. Paynter, and R. Gupta.** 1983. Characterization of *Methanococcus maripaludis* sp. nov., a new methanogen isolated from salt marsh sediment. Arch. Microbiol. **135:**91-97.

26. **Kessler, D.** 2006. Enzymatic activation of sulfur for incorporation into biomolecules in prokaryotes. FEMS Microbiol. Rev. **30:**825-880.

27. **Layer, G., S. A. Gaddam, C. N. Ayala-Castro, S. Ollagnier-de Choudens, D. Lascoux, M. Fontecave, and F. W. Outten.** 2007. SufE transfers sulfur from SufS to SufB for iron-sulfur cluster assembly. J. Biol. Chem. **282:**13342-13350.

28. **Lee, H. S., and B. J. Hwang.** 2003. Methionine biosynthesis and its regulation in *Corynebacterium glutamicum*: parallel pathways of transsulfuration and direct sulfhydrylation. Appl. Microbiol. Biotechnol. **62:**459-467.

29. **Li, T., D. E. Graham, C. Stathopoulos, P. J. Haney, H.-s. Kim, U. Vothknecht, M. Kitabatake, K.-w. Hong, G. Eggertsson, A. W. Curnow, W. Lin, I. Celic, W. B. Whitman, and D. Söll.** 1999. Cysteinyl-tRNA formation: the last puzzle of aminoacyl-tRNA synthesis. FEBS Lett. **462:**302-306.

30. **Lloyd, K. G., V. P. Edgcomb, S. J. Molyneaux, S. Boer, C. O. Wirsen, M. S. Atkins, and A. Teske.** 2005. Effects of dissolved sulfide, pH, and temperature on growth and survival of marine hyperthermophilic Archaea. Appl. Environ. Microbiol. **71:**6383-6387.

31. **Mahler, H. R., and D. G. Elowe.** 1954. Studies on metalloflavoproteins: II. the role of iron in diphosphopyridine nucleotide cytochrome *c* reductase. J. Biol. Chem. **210:**165-179.

32. **Major, T. A., H. Burd, and W. B. Whitman.** 2004. Abundance of 4Fe-4S motifs in the genomes of methanogens and other prokaryotes. FEMS Microbiol. Lett. **239:**117-123.

33. **Meyer, J.** 2008. Iron–sulfur protein folds, iron–sulfur chemistry, and evolution. J. Biol. Inorg. Chem. **13:**157-170.

34. **Nagasawa, T., H. Kanzaki, and H. Yamada.** 1984. Cystathionine γ-lyase of *Streptomyces phaeochromogenes*. The occurrence of cystathionine γ-lyase in filamentous bacteria and its purification and characterization. J. Biol. Chem. **259:**10393-10403.

35. **Neidhardt, F. C., and H. E. Umbarger.** 1996. Chemical composition of *Escherichia coli*, p. 13-16. *In* F. C. Neidhardt, R. Curtiss, J. L. Ingraham, E. C. C. Lin, K. B. Low, B. Magasanik, W. S. Reznikoff, M. Riley, M. Schaechter, and H. E. Umbarger (ed.), E*scherichia coli* and *Salmonella*, vol. 1. ASM Press, Washington, D.C.

36. **Rabeh, W. M., and P. F. Cook.** 2004. Structure and mechanism of *O*-acetylserine sulfhydrylase. J. Biol. Chem. **279:**26803-26806.

37. **Sauerwald, A., W. Zhu, T. A. Major, H. Roy, S. Palioura, D. Jahn, W. B. Whitman, J. R. Yates, 3rd, M. Ibba, and D. Söll.** 2005. RNA-dependent cysteine biosynthesis in archaea. Science **307:**1969-1972.

38. **Sheppard, K., J. Yuan, M. J. Hohn, B. Jester, K. M. Devine, and D. Söll.** 2008. From one amino acid to another: tRNA-dependent amino acid biosynthesis. Nucl. Acids Res. **36:**1813-1825.

39. **Shieh, J., M. Mesbah, and W. B. Whitman.** 1988. Pseudoauxotrophy of *Methanococcus voltae* for acetate, leucine, and isoleucine. J. Bacteriol. **170:**4091-4096.

40. **Smith, P. K., R. I. Krohn, G. T. Hermanson, A. K. Mallia, F. H. Gartner, M. D. Provenzano, E. K. Fujimoto, N. M. Goeke, B. J. Olson, and D. C. Klenk.** 1985. Measurement of protein using bicinchoninic acid. Anal. Biochem. **150:**76-85.

41. **Stathopoulos, C., W. Kim, T. Li, I. Anderson, B. Deutsch, S. Palioura, W. Whitman, and D. Söll.** 2001. Cysteinyl-tRNA synthetase is not essential for viability of the archaeon *Methanococcus maripaludis*. Proc. Natl. Acad. Sci. U S A. **98:**14292-14297.

42. **Tai, C. H., S. R. Nalabolu, T. M. Jacobson, D. E. Minter, and P. F. Cook.** 1993. Kinetic mechanisms of the A and B isozymes of O-acetylserine sulfhydrylase from *Salmonella typhimurium* LT-2 using the natural and alternative reactants. Biochemistry **32:**6433-6442.

43. **Tchong, S.-I., H. Xu, and R. White.** 2004. Cysteine desulfidase: An [4Fe-4S] Enzyme Isolated from *Methanocaldococcus jannaschii* that catalyzes the Breakdown of Cysteine into Pyruvate, Ammonia and Sulfide. Biochemistry **44:**1659-1670.

44. **Truong, D. H., M. A. Eghbal, W. Hindmarsh, S. H. Roth, and P. J. O'Brien.** 2006. Molecular mechanisms of hydrogen sulfide toxicity. Drug Metab. Rev. **38:**733-744.

45. **Visser, A.** 1996. Competition of methanogenic and sulfidogenic bacteria. Wat. Sci. Tech. **33:**99-110.

46. **White, R. H.** 2003. The biosynthesis of cysteine and homocysteine in *Methanococcus jannaschii*. Biochim. Biophys. Acta. **1624:**46-53.

47. **White, R. H.** 1981. A method for the measurement of the abundance of sulfur-34 in protein-bound cysteine and methionine. Anal. Biochem. **114:**349-354.

48. **White, R. H.** 1983. Origin of the labile sulfide in the iron-sulfur proteins of *Escherichia coli*. Biochem. Biophys. Res. Commun. **112:**66-72.

49. **Whitman, W. B., E. Ankwanda, and R. S. Wolfe.** 1982. Nutrition and carbon metabolism of *Methanococcus voltae*. J. Bacteriol. **149:**852-863.

50. **Whitman, W. B., J. Shieh, S. Sohn, D. S. Caras, and U. Premachandran.** 1986. Isolation and characterization of 22 mesophilic methanococci. Syst. Appl. Microbiol. **7:**235.

51. **Yamagata, S.** 1989. Roles of *O*-acetyl-L-homoserine sulfhydrylases in micro-organisms. Biochimie. **71:**1125-1143.

Table 5-1. The levels of protein-bound inorganic sulfide and iron and cysteinyl and methionyl residues in *M. maripaludis*.

	Amount in the cell (nmol/mg protein)[a]	
Chemicals	*M. maripaludis*[b]	*E. coli*[c]
Inorganic sulfide	45 ± 9	2.5 ± 0.4
Iron	50 ± 3	6.7 ± 0.7
Cysteinyl residue	102 ± 7	158[d]
Methionyl residue	202 ± 11	265[d]

[a]Values were mean ± one standard deviation obtained from measurements of three independent cultures.

[b] *M. maripaludis* strain S2 was grown anaerobically at 37 °C in McNA medium.

[c] *E.coli* strain K-12 MG1655 was grown aerobically at 37 °C in LB medium.

[d] Values from (35).

Table 5-2. Incorporation of [^{34}S]sulfide into Fe-S clusters and cysteinyl and methionyl residues in the *M. maripaludis* Δ*sepS* mutant.

Sulfur sources in the growth medium [a]	Atom % of ^{34}S		
	Fe-S	Cys	Met
[^{32}S]Cys + [^{34}S]Na_2S[b]	87 ± 4	8 ± 2	92 ± 3
[^{32}S]Cystathionine + [^{34}S]Na_2S[c]	84	5	5
[^{32}S]Cys + [^{32}S]Hcy + [^{34}S]Na_2S	92	5	ND[d]

[a] Cells were grown in media containing 1.5 mM [^{34}S]sulfide, 3 mM L-cysteine, 5 mM L-cystathionine, and/or 3 mM L-homocysteine as indicated. The numbers represented the measured atom % of ^{34}S in the derivatives of the indicated molecules. The ^{34}S enrichment of Na_2S used as the substrate was 92.6%. The natural abundance of ^{34}S in the sulfur-containing amino acids was 4.2%.

[b] Values were mean of three independent experiments ± one standard deviation.

[c] Medium contained 1.5 mM CoM as a reductant.

[d] ND, not determined.

Table 5-3. Contents of free sulfur-containing amino acids and coenzyme M in cells of *M. maripaludis*.

Compounds	Amount in the cell (nmol/mg dry wt)[a]
Cysteine	0.05 ± 0.01
Homocysteine	0.023 ± 0.004
Cystathionine	0.31 ± 0.01
Coenzyme M	0.43 ± 0.04

[a] Values were mean ± one standard deviation obtained from two to five independent measurements. The free thiol contents (cysteine, homocysteine, and Coenzyme M) were determined by derivatization with monobromobimane (mBBr) and fluorescence detection after HPLC separation. The free cystathionine content was determined using a Li citrate-based amino acid analyzer.

Table 5-4. Kinetic constants of L-cystathionine cleavage in *M. maripaludis* wild-type strain S2 cell extracts.

Reaction	Product determined	K_m (L-cystathionine, mM)	V_{max} (nmol/min/mg protein)	R^{2a}
γ-cleavage	Cysteine	8.7 ± 0.5	7.8 ± 0.3	0.99
β-cleavage	Homocysteine	5 ± 1	40 ± 5	0.98

[a] R^2 of Michaelis-Menten equation.

Figure 5-1. Distribution of Fe-S cluster biogenesis genes in archaea. The phylogenetic tree was based upon 16S rRNA sequences. The tree was constructed with the Minimum Evolution (ME) algorithm in MEGA4. Bootstrap analysis was performed with 1,000 replicates, and values greater than 70 % are labeled on the nodes. The hyperthermophilic bacteria *Thermotoga* and *Aquifex* represent the outgroup. CSD, cysteine desulfurse; U-type, U-type scaffold proteins; A-type, A-type scaffold proteins; ApbC/Nbp35, a potential Fe-S cluster carrier protein. The recombinant CSD homolog from *Methanothermobacter thermautotrophicus* (MTH1389) was shown not to possess cysteine desulfurase activity (unpublished data).

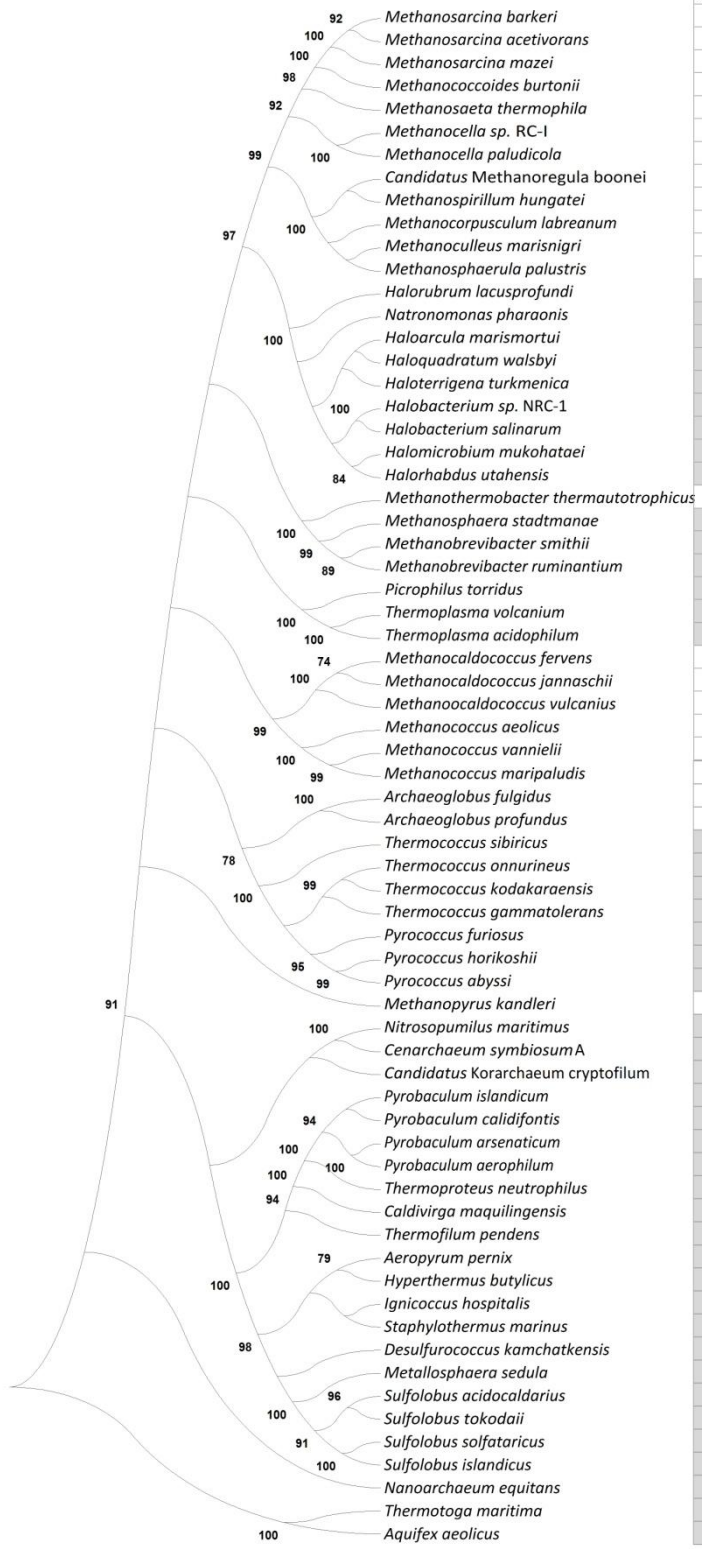

	SepRS/ SepCysS	CysRS	CSD	SufB/D	SufC	U-type	A-type	ApbC/ Nbp35
Methanosarcina barkeri	+	+	+	+	+	+	+	+
Methanosarcina acetivorans	+	+	+	+	+	+	+	+
Methanosarcina mazei	+	+	+	+	+	+	+	+
Methanococcoides burtonii	+	-	+	+	+	+	+	+
Methanosaeta thermophila	+	-	+	+	+	+	+	+
Methanocella sp. RC-I	+	+	+	+	+	+	+	+
Methanocella paludicola	+	+	+	+	+	+	+	+
Candidatus Methanoregula boonei	+	+	+	+	+	+	-	+
Methanospirillum hungatei	+	+	+	+	+	+	-	+
Methanocorpusculum labreanum	+	-	+	+	+	+	-	+
Methanoculleus marisnigri	+	-	+	+	+	+	-	+
Methanosphaerula palustris	+	+	+	-	+	+	-	+
Halorubrum lacusprofundi	-	+	+	+	+	+	+	+
Natronomonas pharaonis	-	+	+	+	+	+	+	+
Haloarcula marismortui	-	+	+	+	+	+	+	+
Haloquadratum walsbyi	-	+	+	+	+	+	+	+
Haloterrigena turkmenica	-	+	+	+	+	+	+	+
Halobacterium sp. NRC-1	-	+	+	+	+	+	-	+
Halobacterium salinarum	-	+	+	+	+	+	-	+
Halomicrobium mukohataei	-	+	+	+	+	+	+	+
Halorhabdus utahensis	-	+	+	+	+	+	-	+
Methanothermobacter thermautotrophicus	+	-	+	+	+	-	-	+
Methanosphaera stadtmanae	-	+	+	+	+	+	-	+
Methanobrevibacter smithii	-	+	+	+	+	+	-	+
Methanobrevibacter ruminantium	-	+	+	+	+	+	-	+
Picrophilus torridus	-	+	-	+	+	-	-	+
Thermoplasma volcanium	-	+	-	+	+	-	-	+
Thermoplasma acidophilum	-	+	-	+	+	-	-	+
Methanocaldococcus fervens	+	-	-	+	+	-	-	+
Methanocaldococcus jannaschii	+	-	-	+	+	-	-	+
Methanoocaldococcus vulcanius	+	-	-	+	+	-	-	+
Methanococcus aeolicus	+	+	-	+	+	-	-	+
Methanococcus vannielii	+	+	+	+	+	+	-	+
Methanococcus maripaludis	+	+	-	+	+	-	-	+
Archaeoglobus fulgidus	+	+	+	+	+	+	-	+
Archaeoglobus profundus	+	+	-	+	+	-	-	+
Thermococcus sibiricus	-	+	+	+	+	-	-	+
Thermococcus onnurineus	-	+	+	+	+	-	-	+
Thermococcus kodakaraensis	-	+	+	+	+	-	-	+
Thermococcus gammatolerans	-	+	+	+	+	-	-	+
Pyrococcus furiosus	-	+	+	+	+	-	-	+
Pyrococcus horikoshii	-	+	-	+	+	-	-	+
Pyrococcus abyssi	-	+	+	+	+	-	-	+
Methanopyrus kandleri	+	-	+	+	+	-	-	+
Nitrosopumilus maritimus	-	+	+	+	+	+	+	+
Cenarchaeum symbiosum A	-	+	+	+	+	+	+	+
Candidatus Korarchaeum cryptofilum	-	+	+	+	+	+	-	+
Pyrobaculum islandicum	-	+	-	+	+	-	-	+
Pyrobaculum calidifontis	-	+	-	+	+	-	-	+
Pyrobaculum arsenaticum	-	+	-	+	+	-	-	+
Pyrobaculum aerophilum	-	+	-	+	+	-	-	+
Thermoproteus neutrophilus	-	+	-	+	+	-	-	+
Caldivirga maquilingensis	-	+	-	+	+	-	-	+
Thermofilum pendens	-	+	+	+	+	-	-	+
Aeropyrum pernix	-	+	+	+	+	-	-	+
Hyperthermus butylicus	-	+	-	+	+	-	-	+
Ignicoccus hospitalis	-	+	-	+	+	-	-	+
Staphylothermus marinus	-	+	+	+	+	-	-	+
Desulfurococcus kamchatkensis	-	+	+	+	+	-	-	+
Metallosphaera sedula	-	+	-	+	+	-	-	+
Sulfolobus acidocaldarius	-	+	-	+	+	-	-	+
Sulfolobus tokodaii	-	+	-	+	+	-	-	+
Sulfolobus solfataricus	-	+	-	+	+	-	-	+
Sulfolobus islandicus	-	+	-	+	+	-	-	+
Nanoarchaeum equitans	-	+	-	+	+	-	-	+
Thermotoga maritima	-	+	+	+	+	+	-	+
Aquifex aeolicus	-	+	+	-	-	+	+	+

Figure 5-2. Growth of Δ*sepS* with (●) 0.05 mM L-cysteine, (○) 5 mM L-cystathionine, (Δ) 5 mM L-homocysteine, and (×) no addition. The inoculums size was ~ 10^7 cells per 5-ml cultures. All values are the averages of five cultures.

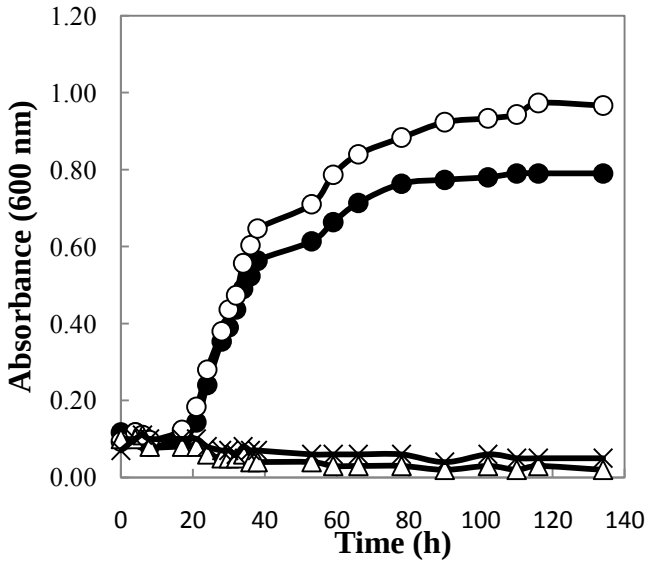
1.20
1.00
0.80
0.60
0.40
0.20
0.00
Absorbance (600 nm)
0
20
40
60
80
100
120
140
Time (h)

CHAPTER 6

PERSULFIDE MODIFICATION OF THE THII HOMOLOG IN THE METHANOGENIC ARCHAEON *METHANOCOCCUS MARIPALUDIS*[6]

[6]Liu, Y., X. Zhu, R. Orlando, and W.B. Whitman. To be submitted to *J. Biol. Chem.*

Abstract

ThiI in *Escherichia coli* is a rhodanese-like protein involved in sulfur transfer for the biosyntheses of 4-thiouridine and thiamine. During sulfur transfer, a conserved cysteinyl residue (Cys456 in *E. coli* ThiI) at the C-terminal rhodanese domain forms a persulfide intermediate. ThiI homologs are encoded in most archaeal genomes, although none have been biochemically characterized. Most of the archaeal homologs lack the rhodanese-domain, which is required for the thiosulfate:cyanide sulfurtransferase (rhodanese) activity. A *thiI* homolog (*mmp1354*) was identified in the *Methanococcus maripaludis* genome, which shares ~30 % amino acid identity with the *E. coli thiI* but lacks the rhodanese domain. The recombinant MMP1354 was cloned and expressed in *E. coli* and purified. The purified protein catalyzed the sulfur transfer from thiosulfate to cyanide with a specific activity of 6 nmol/min/mg protein. A persulfide group on Cys79 with thiosulfate as the sulfur donor was identified by mass spectrometry. Mutagenesis of *thiI* in *M. maripaludis* did not affect growth with either sulfide or elemental sulfur as the sulfur source, suggesting that it is not an essential gene under the tested growth conditions. Thiamine and cysteine were not required for growth of the Δ*mmp1354* mutant, suggesting that the ThiI homolog in *M. maripaludis* is dispensible for sulfur transfer for thiamine and cysteine biosyntheses.

Introduction

The protein persulfide group (R-S-SH), which contains sulfane sulfur, is a versatile biomolecule for sulfur delivery that provides sulfur for the biosyntheses of iron-sulfur clusters, thiamine, molybdopterin, biotin, and lipoic acid, and thionucleosides in tRNA (7, 36). Protein persulfide groups can be enzymatically generated on a cysteinyl residue by cysteine desulfurases (cysteine:[enzyme cysteine] sulfurtransferase) or rhodanese-like proteins (thiosulfate:cyanide sulfurtransferase) (7). Cysteine desulfurases are pyridoxal 5‘-phosphate (PLP)-dependent enzymes that form persulfide groups at the expense of free cysteine (34). Four cysteine desulfurases are known in bacteria: NifS, IscS, SufS, and CsdA. All of them are sulfur donors for Fe-S cluster biosynthesis (20, 28, 29, 43, 61, 62). IscS is also an intermediate sulfur donor for thiamine (24, 43), molybdopterin (60), and thionucleoside biosyntheses (16, 22, 24) and a selenium donor for selenoprotein and selenonucleoside biosyntheses (35). Rhodanese-like proteins catalyze the transfer of the terminal sulfur of thiosulfate or 3-mercaptopyruvate to cyanide through the formation of a persulfide intermediate (4, 42). The physiological functions of only a few rhodanese-like proteins are known: the *E. coli* ThiI is essential for the biosyntheses of 4-thiouridine (s^4U) (37) and thiamine (48); the human enzyme MOCS3 is involved in sulfur incorporation into molybdopterin (32); and the *E. coli* YbbB replaces a sulfur atom in 2-thiouridine in tRNA with selenium (57). For ThiI and MOCS3, the persulfide group from cysteine desulfurase is the physiological sulfur donor (18, 31), and for YbbB, selenophosphate is the selenium donor (57).

ThiI in *E. coli* consists of four domains. The N-terminal ferredoxin-like domain (NFLD) and the THUMP domain are responsible for tRNA binding (23, 47, 52). The PP-loop ATP pyrophosphatase domain activates uridine at position 8 in tRNA by adenylation at the expense of

ATP (38). The C-terminal rhodanese-like domain (RLD) transfers sulfur from the persulfide on IscS to the activated uridine to generate s^4U (17, 37, 40). s^4U acts as a photosensor for near-UV light by crosslinking with cytosine at position 13 (3, 8, 9). The crosslinked tRNAs are poor substrates for aminoacylation, therefore uncharged tRNAs accumulate and arrest growth (19, 49). Deletion of *thiI* in *Salmonella typhimurium* (53) and *E. coli* (48) also causes thiamine auxotrophy, suggesting that ThiI is also a sulfur carrier for the biosynthesis of thiamine. During the sulfur transfer, the catalytically essential Cys456 at the rhodanese-like domain of *E. coli* ThiI forms a persulfide intermediate. After donation of sulfur, it forms a disulfide bond with Cys344 (39, 40, 58). Presumably, the disulfide bond needs to be reduced to complete the enzymatic cycle. In many other bacteria such as *Bacillus subtilis*, the ThiI homologs lack the C-terminal rhodanese domain. Presumably, ThiI partners with a separate rhodanese-like protein during sulfur transfer (36).

ThiI is widespread in archaea, however, the rhodanese-like domain of ThiI is absent in most archaea. Although thiamine (26) and s^4U (33) are present in *Methanococcales*, whether ThiI is involved in the biosyntheses of these molecules is unknown. Here we demonstrated that the ThiI homolog in the methanogenic archaeon *Methanococcus maripaludis* possesses the thiosulfate:cyanide sulfurtransferase activity and a persulfide group can be generated on Cys79 in the N-terminal ferredoxin-like domain using thiosulfate as the sulfur source. Moreover, ThiI in *M. maripaludis* is not required for thiamine biosynthesis, and whether it is required for s^4U biosynthesis is under investigation.

Materials and Methods

Strains, media, and culture conditions. *M. maripaludis* was grown in 28-ml aluminum seal tubes with 275 kPa of H_2:CO_2 (80:20 [v:v]) at 37°C in 5 ml of McNA (minimal medium +

10 mM sodium acetate, reduced with 3 mM L-cysteine), McNACoM (McNA reduced with 3 mM coenzyme M instead of cysteine), McNACoM+Cys (McNACoM + 1 mM L-cysteine), or McC (McNA + 0.2% [wt/vol] Casamino acids + 0.2% [wt/vol] yeast extract) media as described previously (56). The 100 ml cultures were grown in McNACoM in 1 L bottles pressurized to 138 kPa with H_2:CO_2 (4:1, v/v). Antibiotics were not included when comparing the growth of the wild-type and mutants. The inocula were 0.01 ml of cultures (~ 10^6 cells) grown in McNA or McNACoM+Cys medium. The inocula for cultures of the mutant S620 and the strain S623 were started with frozen stocks for all experiments to ensure that a revertant had not been selected. Puromycin (2.5 μg/ml) or neomycin (500 μg/ml in plates and 1 mg/ml in broth) was added when needed. Growth was determined by measuring the increase in absorbance at 600 nm. Before inoculation, 3 mM of sodium sulfide was added as the sulfur source. When grown with elemental sulfur as the sulfur source, 0.1 g of S^0 was added to 5 ml of medium before autoclaving.

Cloning, expression, and purification of recombinant MMP1354 in *E. coli*. The gene MMP1354 was amplified by PCR from the *M. maripaludis* S2 genomic DNA with Herculase Enhanced DNA polymerase (Stratagene). The primers introduced a *Nde*I and a *Hind*III site at the 5'- and 3'- ends, respectively. Primer sequences are available upon request. The PCR product was digested with restriction enzymes *Nde*I and *Hind*III, gel purified, and then ligated into the compatible sites in the pQE2 vector (Qiagen), which introduced an N-terminal 6×histidine tag. The resulting plasmid pQE2-MMP1354 was transformed into the *E. coli* strain SG13009[pREP4] (14). The transformed cells were grown in 1 L of Luria-Bertani (LB) medium supplemented with 100 μg/ml ampicillin and 25 μg/ml kanamycin at 37 °C with shaking until they reached an absorbance at 600 nm of 0.6~0.8. Isopropyl β-D-1-thiogalactopyranoside **(**IPTG) was added to a final concentration of 0.5 mM to induce the production of the recombinant protein. After an

additional overnight incubation at room temperature, the cells were harvested by centrifugation at 8,000 *g* for 20 min at 4 ^{o}C.

E. coli cells (~ 2 g wet weight) were collected by centrifugation at 10,000 *g* for 20 min at 4 ^{o}C, resuspended in 10 ml of buffer A (20 mM sodium phosphate, 0.5 M NaCl, 20 mM imidazole, pH 7.4), and lysed by sonication. The cell lysate was centrifuged at 10,000 *g* for 20 min at 4 ^{o}C, and then the supernatant was filtered with the 0.22-μm syringe filter (Millipore) and applied to an 1 ml HisTrap HP column (GE Healthcare) equilibrated with buffer A. Proteins bound to the column were eluted with a 10 ml linear gradient from 0 to 100% of buffer B (20 mM sodium phosphate, 0.5 M NaCl, 1M imidazole, pH 7.4) at a flow rate of 1.0 ml/min. Elution of the protein was monitored by UV absorbance at 280 nm. One major UV-absorbing peak eluted at 0.2 M imidazole and contained the desired protein, based on SDS-PAGE analysis. Purified proteins were dialyzed against 20 mM of sodium phosphate buffer (pH 7.4) containing 10% glycerol (v/v) and stored at -20 ^{o}C until use. Protein concentrations were determined with the biuret method (30).

Expression of MMP1354 in the *E. coli* Δ*thiI* mutant. The *E. coli* Δ*thiI* mutant strain JW0413 (purchased from the Coli Genetic Stock Center at Yale) was transformed with the plasmid pQE2-MMP1354. The transformants were grown in LB or M9+thiamine pyrophosphate (1mM) medium supplemented with 100 μg/ml ampicillin. The expression of MMP1354 was induced with 1 mM IPTG and confirmed with Western blotting with the monoclonal mouse anti-His-tag antibody (Sigma).

Preparation of *M. maripaludis* cell-free extracts. *M. maripaludis* cells grown in 100 ml medium were cultured to an absorbance of ~0.4 at 600 nm. The cells were collected by centrifugation at 10,000 *g* for 30 min at 4 ^{o}C and resuspended in 1 ml of buffer containing 0.1 M

HEPES (4-[2-hydroxyethyl]-1-piperazineethanesulfonic acid), pH 7.5. The *M. maripaludis* cells were lysed by repeated (2×) freezing (-20 °C) and thawing, and the cell lysates were incubated with 20 U of RQ1 DNase (Promega) at 37 ^{o}C for 15 min to digest DNA. Unbroken cells were removed by centrifugation at 8,000 *g* for 30 min at 4 ^{o}C. The protein concentrations were determined by BCA protein assay (Pierce) (45).

Enzyme activity assays. The thiosulfate:cyanide sulfurtransferase (rhodanese) activity assays were conducted in the anaerobic chamber with an atmosphere of 95% of N_2 and 5% of H_2, and the production of thiocyanate was determined as described (55). The assay mixture in a total volume of 350 µl contained 0.1 M Tris-acetate (pH 7.5), 50 mM sodium thiosulfate, and recombinant MMP1354 (50 µg) or *M. maripaludis* cell-free extracts (0.4 mg of total protein). The reactions were initiated by addition of 50 mM KCN, incubated for 30 min at 37 ^{o}C, and then quenched by addition of 150 µl 15 % formaldehyde. Color was developed by addition of 0.5 ml ferric nitrate reagent. The iron-thiocyanate complex was quantified by its absorbance at 460 nm, with $\varepsilon = 4.2\ mM^{-1} \cdot cm^{-1}$. Measurements were corrected for spontaneous rates by omission of enzyme in reactions with recombinant MMP1354 or addition of formaldehyde before the cyanide substrate in reactions with cell extracts (1, 54).

To determine the pH optimum, 200 mM of the following buffers were used at the indicated pH values: BIS-Tris (bis[2-hydroxyethyl]-amino-tris[hydroxymethyl]-methane) hydrochloride for pH 6.0, 6.5, and 7.0, Tris-HCl for pH 7.0, 7.5, 8.0, 8.5, and 9.0, and sodium CHES [2-(*N*-cyclohexylamino)ethanesulfonate] for pH 9.0, 9.5, and 10.0.

Kinetic constants of MMP1354 were determined with 0.5, 1.0, 1.5, 2.5, and 5.0 mM of sodium thiosulfate and potassium cyanide. The data were analyzed using SigmaPlot 10.0 with the Enzyme Kinetics module (Systat Software Inc.) fitted with a Ping-Pong Bi-Bi mechanism.

For single turnover experiments, MMP1354 (~10 nmol) was incubated anaerobially with 10 mM thiosulfate in 0.2 M Tris-acetate buffer (pH 7.2) at 37 ^{o}C for 1 hr, and excess thiosulfate was removed by passage through the 0.5 ml Zeba Desalt Spin Column (Thermo Scientific). Then the sample was incubated with 5 mM DTT at 30 ^{o}C for 20 min. In control samples, thiosulfate was omitted. The amount of protein was determined with BCA protein assay (Pierce) standardized with the biuret method (30). The amount of free sulfide generated by reduction with DTT was determined by an adaptation of the methylene blue method (2, 10). Each sample (~ 200 µl) was mixed with 0.3 ml of 1% (w/v) freshly prepared zinc acetate and 10 µl of 12% sodium hydroxide in a microcentrifuge tube. The tube was closed and left at room temperature for 20 min. Then 0.1 ml of 1% of *N,N*-dimethylphenylenediamine (DMPD) in 5 M of HCl and 40 µl of 11.5 mM of $FeCl_3$ in 1.2 M of HCl were added, and the solution was mixed rapidly. The samples were centrifuged at 16,000 g for 10 min to remove denatured protein. The absorbance of the supernatant was determined at 670 nm. Solutions of sodium sulfide served as standards.

Cysteine biosynthesis activities in *M. maripaludis* cell extracts were determined by the production of cysteine with an adaptation of the acid-ninhydrin method (12). Assays were conducted in the anaerobic chamber with an atmosphere of 95% of N_2 and 5% of H_2. The assay mixture in a total volume of 150 µl contained 0.1 M HEPES (pH 8.0), 50 mM NaCl, 0.2 mM $ZnCl_2$, 20 mM $MgCl_2$, 10 mM serine, 50 mM ATP, 50 µM PLP, and cell-free extract (0.15 mg of total protein). The reactions were initiated by the addition of 10 mM sodium sulfide or sodium thiosulfate as the sulfur source and incubated for 30 min at 37 ^{o}C. The reactions were stopped by addition of 150 µl glacial acetic acid and 150 µl of 2.5% (w/v) ninhydrin in 60% (v/v) acetic acid and 40% (v/v) HCl. The samples were heated in boiling water for 10 min for color development,

and the absorbance was determined at 560 nm. Reactions without addition of sulfur source were used as blank controls. Solutions of cysteine served as standards.

Identification of the persulfide modification on ThiI by mass spectrometry (MS). The purified recombinant MMP1354 (130 µl, at a concentration of 1 mg/ml in buffer containing 20 mM sodium phosphate, pH 7.4, and 10% glycerol) was incubated with 1 mM dithiothreitol (DTT) for 1 hr at room temperature in the anaerobic chamber with an atmosphere of 95% of N_2 and 5% of H_2. The buffer was then exchanged with 0.2 M Tris-acetate (pH 7.2) by passage through the 0.5 ml Zeba Desalt Spin Column (Thermo Scientific). To form the persulfide, 30 µl of sample (~1 nmol of protein) was incubated anaerobically with 10 mM sodium thiosulfate for 1 hr at room temperature. The control samples were incubated under the same conditions without sodium thiosulfate. After the reaction, the buffer was exchanged with 0.1 M ammonium bicarbonate-formic acid buffer (pH 7.2) by passage through the desalting column. The protein was digested with 20 µg/ml trypsin (Promega) at 37 ^{o}C overnight. The digestion was stopped with 1% formic acid (v/v), and the samples were dried in vacuum.

The peptide samples obtained from the trypsin digestion were resuspended in 30 µl deionized H_2O containing 3% acetonitrile and 0.1% formic acid, and 8 µl of sample was analyzed on an Agilent 1100 Capillary LC (Palo Alto, CA) interfaced directly to a linear ion trap (LTQ) mass spectrometer (Thermo Electron, San Jose, CA). Mobile phases A and B were H_2O-0.1% formic acid and acetonitrile-0.1% formic acid, respectively. Peptides eluted from the C18 column were injected into the mass spectrometer during a 60 min linear gradient from 5 to 60% mobile phase B at a flow rate of 4 µl/min. The instrument was set to acquire MS/MS spectra on the nine most abundant precursor ions from each MS scan with a repeat count of 3 and repeat duration of 5 s. Dynamic exclusion was enabled for 60 s. Generated raw tandem mass spectra

were converted into the mzXML format and then into the PKL format using ReAdW followed by mzMXL2Other (41). The peak lists were then searched using the Mascot 2.2 software (Matrix Science, Boston, MA) against the NCBI database with the following parameters: full tryptic enzymatic cleavage with two possible missed cleavages, peptide tolerance of 1000 parts-per-million, fragment ion tolerance of 0.6 Da, and variable modifications with oxidation of methionyl residues (+16 Da) and persulfide modification of cysteinyl residues (+32 Da).

Construction of the Δ*mmp1354*::*pac* mutant. The mutant was made by transformation of the wild-type *M. maripaludis* strain S2 with pIJA03-MMP1354, which was constructed from the integration vector pIJA03. The plasmid pIJA03 lacks an origin of replication for methanococci and contains a *pac* cassette, which encodes puromycin resistance (13, 27). To construct pIJA03-MMP1354, a 1036 bp region upstream and a 959 bp region downstream of the MMP1354 gene were PCR amplified and cloned into the multi-cloning sites MCS1 and MCS2 of pIJA03, respectively. The orientation of each insert was confirmed by restriction mapping.

pIJA03-MMP1354 was transformed into *M. maripaludis* strain S2 by the polyethylene glycol method (51). After transformation, cultures were plated on McC medium plus puromycin. Puromycin-resistant isolates were restreaked on the same medium, and isolated colonies were then transferred to broth cultures containing 5 ml McC medium plus puromycin. After growth, 3 ml of the culture were used for determination of the genotype and phenotype. The remaining culture was used for preparation of frozen stocks (50). The genotype of the Δ*mmp1354*::*pac* mutant (S620) was confirmed by Southern hybridization (data not shown).

For complementation, the MMP1354 gene was PCR amplified. The primers introduced a *Nsi*I and a *Bgl*II site at the 5'- and 3'- ends, respectively. The PCR products and the shuttle vector pMEV2 (27) were digested with *Nsi*I and *Bgl*II and gel purified. The cloning of the PCR

products into pMEV2 placed MMP1354 downstream of the strong promoter PhmvA. The resulting plasmid, pMEV2-MMP1354, was transformed into S620 and screened on McC plates containing neomycin as previously described (27). The complementation strain was named S623.

Phylogenetic analysis. ThiI homologs were identified using BLASTp searches against selected genomes. The alignments were performed with the ClustalX 2.0 program (21) and edited with the GeneDoc version 2.6 program (http://www.nrbsc.org/gfx/genedoc/ebinet.htm). The phylogenetic tree was constructed by the MEGA4 program (46) using the minimum evolution (ME) method with its default settings.

Results and Discussion

Phylogenetic distribution and conserved cysteinyl residues of ThiI homologs in archaea. ThiI homologs are conserved in all archaea with completely sequenced genomes except *Cenarchaeum symbiosum* A, *Nitrosopumilus maritimus*, *Halorubrum lacusprofundi*, *Haloquadratum walsbyi*, and *Metallosphaera sedula*. Most archaeal ThiI homologs do not have Cys456 of the *E. coli* ThiI (b0423), which forms the persulfide intermediate and is essential for rhodanese activity (Fig. 6-1). However, Cys344 of b0423, which forms a disulfide bond with C456 during sulfur delivery, is conserved in most archaeal homologs (Fig. 6-1). Furthermore, two other Cys residues (C266 and C269 of MMP1354) in a consensus sequence of C(I/L/V)(F/L/V)C(K/R)(K/R) are conserved in ThiI homologs from all methanogens and *Archaeoglobus*, *Pyrococcus*, *Thermococcus*, and *Staphylothermus* species. These two Cys residues are replaced with G261 and L264, respectively, in b0423 at the corresponding positions. Finally, ThiI homologs from *Methanococcales* and several other archaea have a conserved Cys residue (C79 in *M. mairplaudis* ThiI) in the NFLD domain (Fig. 6-1).

Purification of the recombinant *M. maripaludis* ThiI (MMP1354). For purification of MMP1354, the corresponding gene was cloned into the pQE2 vector, resulting in an N-terminal 6×His-tagged recombinant protein, for heterologous expression in *E. coli*. The protein was purified with nickel Sepharose chromatography and displayed as a single band on Coomassie blue-stained SDS gels (Fig. 6-2A). The protein had an apparent mass of 50 kDa determined by SDS-PAGE, close to its expected mass of 45 kDa.

***M. maripaludis* ThiI cannot complement an *E. coli* Δ*thiI* mutant.** To determine whether MMP1354 can function in sulfur delivery in *E. coli* cells, a complementation study of an *E. coli* Δ*thiI* mutant strain (JW0413) with MMP1354 was performed. The expression of MMP1354 in the complementation strain (JW0413-MMP1354) was confirmed by Western blotting (data not shown). However, the complementation strain still required thiamine pyrophosphate for growth, suggesting that MMP1354 was unable to replace *E. coli* ThiI for thiamine biosynthesis. The failure to complement could result from many factors, including an inability of MMP1354 either to receive an active persulfide group from a sulfur donor in *E. coli* or to transfer sulfur to ThiS, which forms a thiocarboxylate group and acts as the direct sulfur source for the biosynthesis of the thiazole moiety of thiamine (25, 59).

MMP1354 displays thiosulfate:cyanide sulfurtransferase activity. The sulfurtransferase (rhodanese) activity of MMP1354 was measured with thiosulfate as the sulfur donor and cyanide as the sulfur acceptor. As shown in Fig. 6-2B, MMP1354 catalyzed the production of thiocyanate, indicating that this enzyme had thiosulfate:cyanide sulfurtransferase activity and was able to undergo multiple turnovers. The maximum activity was observed at pH 6.5-8.0 (Fig. 6-2C), which was lower than the pH of 8.5 commonly used in sulfurtransferase activity assays (1). The K_ms for thiosulfate and cyanide were 0.8 ± 0.1 and 4.2 ± 0.2 mM,

respectively. These values were ~ 6-fold lower than those reported for *E. coli* rhodanese (K_m thiosulfate, 5 mM; K_m cyanide, 24 mM) (1). The K_{cat} was 0.25 min^{-1}, which was similar to the rhodanese-like protein YnjE in *E. coli*, which has a K_{cat} of 0.35 min^{-1} (15), but lower than that observed for many other rhodaneses (5). The catalytic efficiency (K_{cat}/K_m thiosulfate) of MMP1354 was 0.3 $min^{-1}\cdot mM^{-1}$, which was ~50-fold higher than that of YnjE (0.006 $min^{-1}\cdot mM^{-1}$) (15) and three orders of magnitude lower than that of PspE (23.7 $s^{-1}\cdot mM^{-1}$), which contributes 85 % of the total rhodanese activity in *E. coli* (5).

The low catalytic efficiency of MMP1354 indicated that thiosulfate and/or cyanide may not be the physiological substrate(s) for this enzyme. In *E. coli*, IscS is the sulfur donor, which derives sulfur from cysteine to generate a persulfide group and subsequently transfers it to ThiI. IscS is the only cysteine desulfurase in *E. coli* that is able to donate sulfur to ThiI (17, 18, 22, 24). However, homologs of IscS or other cysteine desulfurases are absent in most methanococcal and many other archaeal genomes. Therefore, in these organisms, other types of enzymes or thiosulfate itself may act as the sulfur donor in a persulfuration reaction.

MMP1354 generates a persulfide group on Cys79. To examine whether a persulfide group was an intermediate during sulfur transfer, MMP1354 was incubated with thiosulfate for a single turnover experiment and then reduced with DTT. Presumably, if a persulfide group is formed from thiosulfate, free sulfide would be released upon reduction with DTT. In two independent assays, 6.9 and 7.1 nmol of sulfide was released from 10 nmol of thiosulfate-treated MMP1354, suggesting that ~70 % of MMP1354 was converted to the persulfurated form.

To identify the cysteinyl residue that was modified, the tryptic peptides of thiosulfate-treated MMP1354 were mapped by ESI-MS. A mass shift of 32 Da was observed for the peptide $_{70}$VPGIVSFSPCYYIDPDIEQIKK$_{91}$, with one missed cleavage. The unmodified peptide was

also detected, suggesting that part of the recombinant protein did not react. In the control samples without thiosulfate treatment, only the unmodified peptide was detected, suggesting that the persulfide modification was not present on the recombinant protein before reaction with thiosulfate. Analysis of the MS/MS spectra confirmed the expected amino acid sequence and a persulfide modification at Cys79 (Fig. 6-3). A persulfide modification was not observed for the peptides containing the other three conserved Cys residues (data not shown): Cys266 and Cys269 (in the CxxCK/R motif) and Cys349 (corresponding to Cys344 of b0423).

The position of the active site cysteine (Cys79) in MMP1354, which forms the persulfide intermediate, is different from *E. coli* ThiI. Both MMP1354 and *E. coli* ThiI are multi-domain proteins containing the N-terminal ferredoxin-like (NFLD), the THUMP, and the PP-loop domains. The active site cysteine of *E. coli* ThiI is present within the C-terminal rhodanese-like domain (RLD). The RLD is absent in MMP1354. Instead, the active site cysteine is present within the NFLD. The NFLD of *E. coli* thiI is involved in recognizing and binding of the acceptor-stem region of tRNA (47). The position of the active site cysteine in MMP1354 suggests a possible role of NFLD in sulfur transfer. Moreover, the active site loop sequence of ThiI in proteobactera, CxxGxx (4), is not conserved in MMP1354, suggesting that MMP1354 may have a different substrate specificity. The amino acids (GIVS[F/Y]SP) upstream of the active site cysteine are conserved in methanococcal ThiI, suggesting that they may be important for substrate binding and activity (Fig. 6-3C).

Mutagenesis of *thiI* in *M. maripaludis*. ThiI in *E. coli* is required for the biosynthesis of s^4U and thiamine, suggesting that it is shared by multiple sulfur incorporation processes. The physiological function of ThiI in *M. maripaludis* was investigated by construction and characterization of a Δ*mmp1354* mutant (S620). The mutation had no apparent affect on growth

in McNA medium with either sulfide or S^0 as the sulfur source, suggesting that MMP1354 was not an essential enzyme under the tested growth conditions. Moreover, thiamine was not needed for the growth of S620, suggesting that MMP1354, unlike the *E. coli* thiI, was not required for thiamine biosynthesis.

The total rhodanese activity in *M. maripaludis* cell extracts was not significantly affected by disruption of MMP1354 (Table 6-1), suggesting that other rhodanese-like proteins were abundant. Based upon sequence analyses, only the open reading frame *mmp0900* possesses homology to known rhodanese-like domains. This ORF possesses the active site loop motif (CXRGGXRS) of YbbB, which encodes 2-selenouridine synthase and catalyzes the replacement of a sulfur atom in 2-thiouridine in tRNA with selenium (57). However, the *E. coli* YbbB does not have detectable rhodanese activity, possibly because selenophosphate instead of thiosulfate is the physiological substrate (57). Therefore, other proteins with uncharacterized rhodanese domains may contribute to the rhodanese activity in *M. maripaludis*.

Rhodanese has been proposed to be involved in cysteine biosynthesis. Disruption of *cysA* in *Saccharopolyspora erythraea*, which encodes a rhodanese-like protein, results in cysteine auxotrophy (6). Moreover, a persulfide group has been proposed to be the sulfur donor for the tRNA-dependent cysteine biosynthesis in methanogens (11, 44). Since ThiI contains two tRNA-binding domains (NFLD and THUMP), it was thought to act as the sulfur donor for the tRNA-dependent cysteine biosynthesis. However, the Δ*mmp1354* mutant showed a similar phenotype as the wild type strain for growth without cysteine. When the inoculum size was small (~ 10^5 cells for 5-ml cultures), both the wild type and the Δ*mmp1354* strains frequently fail to grow at all in the McNA medium without cysteine. When the inoculums size was ~ 10^6 cells, a >30 hr lag phase was observed for both the wild type and Δ*mmp1354* strain (Fig. 6-4). Moreover, the

cysteine biosynthesis activities in Δ*mmp1354* and the wild type strain cell extracts were not significantly different (Table 6-2). Therefore, mutation of MMP1354 had no apparent affect on cysteine biosynthesis.

In conclusion, the ThiI homolog (MMP1354) in *M. maripaludis* has the rhodanese activity that transfers the sulfur from thiosulfate to cyanide *in vitro*. A persulfide group is formed on Cys79 in the N-terminal ferredoxin-like domain during sulfur transfer. MMP1354 is not required for thiamine biosynthesis, and whether it is required for s^4U biosynthesis is under investigation. Since a cysteine desulfurase is not encoded in the *M. maripaludis* genome, MMP1354 would have a physiological sulfur donor different from characterized ThiI. Whether thiosulfate acts as the physiological sulfur donor remains to be determined.

Acknowledgements

We thank Melissa Warren and Dr. Jon Amster for help with the mass spectrometry analysis of MMP1354 and Randon Prather for cloning of pQE2-MMP1354. This work was supported by grants from the U. S. Department of Energy to W.B.W and a Dissertation Completion Award from the University of Georgia to Y.L.

References

1. **Alexander, K., and M. Volini.** 1987. Properties of an *Escherichia coli* rhodanese. J. Biol. Chem. **262:**6595-6604.

2. **Beinert, H.** 1983. Semi-micro methods for analysis of labile sulfide and of labile sulfide plus sulfane sulfur in unusually stable iron-sulfur proteins. Anal. Biochem. **131:**373-378.

3. **Bergstrom, D. E., and N. J. Leonard.** 1972. Photoreaction of 4-thiouracil with cytosine. Relation to photoreactions in *Escherichia coli* transfer ribonucleic acids. Biochemistry **11:**1-9.

4. **Bordo, D., and P. Bork.** 2002. The rhodanese/Cdc25 phosphatase superfamily. Sequence-structure-function relations. EMBO Rep. **3:**741-746.

5. **Cheng, H., J. L. Donahue, S. E. Battle, W. K. Ray, and T. J. Larson.** 2008. Biochemical and genetic characterization of PspE and GlpE, two single-domain sulfurtransferases of *Escherichia coli*. Open Microbiol. J. **2:**18-28.

6. **Donadio, S., A. Shafiee, and C. R. Hutchinson.** 1990. Disruption of a rhodaneselike gene results in cysteine auxotrophy in *Saccharopolyspora erythraea*. J. Bacteriol. **172:**350-360.

7. **Dorothea, K.** 2006. Enzymatic activation of sulfur for incorporation into biomolecules in prokaryotes. FEMS Microbiol. Rev. **30:**825-840.

8. **Favre, A., A. M. Michelson, and M. Yaniv.** 1971. Photochemistry of 4-thiouridine in *Escherichia coli* transfer RNA1Val. J. Mol. Biol. **58:**367-379.

9. **Favre, A., M. Yaniv, and A. M. Michels.** 1969. The photochemistry of 4-thiouridine in *Escherichia coli* t-RNAVal1. Biochem. Biophys. Res. Commun. **37:**266-271.

10. **Fogo, J. K., and M. Popowsky.** 1949. Spectrophotometric determination of hydrogen sulfide. Anal. Chem. **21:**732-734.

11. **Fukunaga, R., and S. Yokoyama.** 2007. Structural insights into the second step of RNA-dependent cysteine biosynthesis in archaea: crystal structure of Sep-tRNA:Cys-tRNA synthase from *Archaeoglobus fulgidus*. J. Mol. Biol. **370:**128-141.

12. **Gaitonde, M. K.** 1967. A spectrophotometric method for the direct determination of cysteine in the presence of other naturally occurring amino acids. Biochem. J. **104:**627-633.

13. **Gernhardt, P., O. Possot, M. Foglino, L. Sibold, and A. Klein.** 1990. Construction of an integration vector for use in the archaebacterium *Methanococcus voltae* and expression of a eubacterial resistance gene. Mol. Gen. Genet. **221:**273-279.

14. **Gottesman, S., E. Halpern, and P. Trisler.** 1981. Role of *sulA* and *sulB* in filamentation by lon mutants of *Escherichia coli* K-12. J. Bacteriol. **148:**265-273.

15. **Häzelmann, P., J. U. Dahl, J. Kuper, A. Urban, U. Müller-Theissen, S. Leimkühler, and H. Schindelin.** 2009. Crystal structure of YnjE from *Escherichia coli*, a sulfurtransferase with three rhodanese domains. Protein Sci. **18:**2480-2491.

16. **Ikeuchi, Y., N. Shigi, J.-i. Kato, A. Nishimura, and T. Suzuki.** 2006. Mechanistic insights into sulfur relay by multiple sulfur mediators involved in thiouridine biosynthesis at tRNA wobble positions. Mol. Cell **21:**97-108.

17. **Kambampati, R., and C. T. Lauhon.** 2000. Evidence for the transfer of sulfane sulfur from IscS to ThiI during the *in vitro* biosynthesis of 4-thiouridine in *Escherichia coli* tRNA. J. Biol. Chem. **275:**10727-10730.

18. **Kambampati, R., and C. T. Lauhon.** 1999. IscS is a sulfurtransferase for the *in vitro* biosynthesis of 4-thiouridine in *Escherichia coli* tRNA. Biochemistry **38:**16561-16568.

19. **Kramer, G. F., J. C. Baker, and B. N. Ames.** 1988. Near-UV stress in *Salmonella typhimurium*: 4-thiouridine in tRNA, ppGpp, and ApppGpp as components of an adaptive response. J. Bacteriol. **170:**2344-2351.

20. **Kurihara, T., H. Mihara, S.-i. Kato, T. Yoshimura, and N. Esaki.** 2003. Assembly of iron-sulfur clusters mediated by cysteine desulfurases, IscS, CsdB and CSD, from *Escherichia coli*. Biochim. Biophys. Acta. **1647:**303-309.

21. **Larkin, M. A., G. Blackshields, N. P. Brown, R. Chenna, P. A. McGettigan, H. McWilliam, F. Valentin, I. M. Wallace, A. Wilm, R. Lopez, J. D. Thompson, T. J. Gibson, and D. G. Higgins.** 2007. Clustal W and Clustal X version 2.0. Bioinformatics **23:**2947-2948.

22. **Lauhon, C. T.** 2002. Requirement for IscS in biosynthesis of all thionucleosides in *Escherichia coli*. J. Bacteriol. **184:**6820-6829.

23. **Lauhon, C. T., W. M. Erwin, and G. N. Ton.** 2004. Substrate specificity for 4-thiouridine modification in *Escherichia coli*. J. Biol. Chem. **279:**23022-23029.

24. **Lauhon, C. T., and R. Kambampati.** 2000. The *iscS* gene in *Escherichia coli* is required for the biosynthesis of 4-thiouridine, thiamin, and NAD. J. Biol. Chem. **275:**20096-20103.

25. **Lehmann, C., T. P. Begley, and S. E. Ealick.** 2005. Structure of the *Escherichia coli* ThiS-ThiF complex, a key component of the sulfur transfer system in thiamin biosynthesis. Biochemistry **45:**11-19.

26. **Leigh, J. A.** 1983. Levels of water-soluble vitamins in methanogenic and non-methanogenic bacteria. Appl. Environ. Microbiol. **45:**800-803.

27. **Lin, W., and W. Whitman.** 2004. The importance of porE and porF in the anabolic pyruvate oxidoreductase of *Methanococcus maripaludis*. Arch. Microbiol. **181:**68-73.

28. **Loiseau, L., S. Ollagnier-de-Choudens, L. Nachin, M. Fontecave, and F. Barras.** 2003. Biogenesis of Fe-S cluster by the bacterial Suf system. J. Biol. Chem. **278:**38352-38359.

29. **Loiseau, L., S. Ollagnier-de Choudens, D. Lascoux, E. Forest, M. Fontecave, and F. Barras.** 2005. Analysis of the heteromeric CsdA-CsdE cysteine desulfurase, assisting Fe-S cluster biogenesis in *Escherichia coli*. J. Biol. Chem. **280:**26760-26769.

30. **Lowry, O. H., N. J. Rosebrough, A. L. Farr, and R. J. Randall.** 1951. Protein measurement with the folin phenol reagent. J. Biol. Chem. **193:**265-275.

31. **Marelja, Z., W. Stöcklein, M. Nimtz, and S. Leimkühler.** 2008. A novel role for human Nfs1 in the cytoplasm. J. Biol. Chem. **283:**25178-25185.

32. **Matthies, A., K. V. Rajagopalan, R. R. Mendel, and S. Leimkühler.** 2004. Evidence for the physiological role of a rhodanese-like protein for the biosynthesis of the molybdenum cofactor in humans. Proc. Natl. Acad. Sci. U S A. **101:**5946-5951.

33. **McCloskey, J. A., D. E. Graham, S. Zhou, P. F. Crain, M. Ibba, J. Konisky, D. Soll, and G. J. Olsen.** 2001. Post-transcriptional modification in archaeal tRNAs: identities and phylogenetic relations of nucleotides from mesophilic and hyperthermophilic *Methanococcales*. Nucl. Acids Res. **29:**4699-4706.

34. **Mihara, H. Mihara, Esaki, and N. Esaki.** 2002. Bacterial cysteine desulfurases: their function and mechanisms. Appl. Microbiol. Biotechnol. **60:**12-23.

35. **Mihara, H., S.-i. Kato, G. M. Lacourciere, T. C. Stadtman, R. A. J. D. Kennedy, T. Kurihara, U. Tokumoto, Y. Takahashi, and N. Esaki.** 2002. The iscS gene is essential for the biosynthesis of 2-selenouridine in tRNA and the selenocysteine-containing formate dehydrogenase H. Proc. Natl. Acad. Sci. U S A. **99:**6679-6683.

36. **Mueller, E. G.** 2006. Trafficking in persulfides: delivering sulfur in biosynthetic pathways. Nat. Chem. Biol. **2:**185-194.

37. **Mueller, E. G., C. J. Buck, P. M. Palenchar, L. E. Barnhart, and J. L. Paulson.** 1998. Identification of a gene involved in the generation of 4-thiouridine in tRNA. Nucl. Acids Res. **26:**2606-2610.

38. **Mueller, E. G., and P. M. Palenchar.** 1999. Using genomic information to investigate the function of ThiI, an enzyme shared between thiamin and 4-thiouridine biosynthesis. Protein Sci. **8:**2424-2427.

39. **Mueller, E. G., P. M. Palenchar, and C. J. Buck.** 2001. The role of the cysteine residues of ThiI in the generation of 4-thiouridine in tRNA. J. Biol. Chem. **276:**33588-33595.

40. **Palenchar, P. M., C. J. Buck, H. Cheng, T. J. Larson, and E. G. Mueller.** 2000. Evidence that ThiI, an enzyme shared between thiamin and 4-thiouridine biosynthesis, may be a sulfurtransferase that proceeds through a persulfide intermediate. J. Biol. Chem. **275:**8283-8286.

41. **Pedrioli, P. G. A., J. K. Eng, R. Hubley, M. Vogelzang, E. W. Deutsch, B. Raught, B. Pratt, E. Nilsson, R. H. Angeletti, R. Apweiler, K. Cheung, C. E. Costello, H. Hermjakob, S. Huang, R. K. Julian, E. Kapp, M. E. McComb, S. G. Oliver, G. Omenn, N. W. Paton, R. Simpson, R. Smith, C. F. Taylor, W. Zhu, and R. Aebersold.** 2004. A common open representation of mass spectrometry data and its application to proteomics research. Nat. Biotech. **22:**1459-1466.

42. **Rita, C., A. Paolo, and V. Paolo.** 2007. Common themes and variations in the rhodanese superfamily. IUBMB Life **59:**51-59.

43. **Schwartz, C. J., O. Djaman, J. A. Imlay, and P. J. Kiley.** 2000. The cysteine desulfurase, IscS, has a major role in *in vivo* Fe-S cluster formation in *Escherichia coli*. Proc. Natl. Acad. Sci. U S A. **97:**9009-9014.

44. **Sheppard, K., J. Yuan, M. J. Hohn, B. Jester, K. M. Devine, and D. Söll.** 2008. From one amino acid to another: tRNA-dependent amino acid biosynthesis. Nucl. Acids Res. **36:**1813-1825.

45. **Smith, P. K., R. I. Krohn, G. T. Hermanson, A. K. Mallia, F. H. Gartner, M. D. Provenzano, E. K. Fujimoto, N. M. Goeke, B. J. Olson, and D. C. Klenk.** 1985. Measurement of protein using bicinchoninic acid. Anal. Biochem. **150:**76-85.

46. **Tamura, K., J. Dudley, M. Nei, and S. Kumar.** 2007. MEGA4: Molecular Evolutionary Genetics Analysis (MEGA) software version 4.0. Mol. Biol. Evol. **24:**1596-1599.

47. **Tanaka, Y., S. Yamagata, Y. Kitago, Y. Yamada, S. Chimnaronk, M. Yao, and I. Tanaka.** 2009. Deduced RNA binding mechanism of ThiI based on structural and binding analyses of a minimal RNA ligand. RNA **15:**1498-1506.

48. **Taylor, S. V., N. L. Kelleher, C. Kinsland, H.-J. Chiu, C. A. Costello, A. D. Backstrom, F. W. McLafferty, and T. P. Begley.** 1998. Thiamin biosynthesis in *Escherichia coli*. J. Biol. Chem. **273:**16555-16560.

49. **Thomas, G., and A. Favre.** 1975. 4-Thiouridine as the target for near-ultraviolet light induced growth delay in *Escherichia coli*. Biochem. Biophys. Res. Commun. **66:**1454-1461.

50. **Tumbula, D. L., J. Keswani, J. S. Shieh, and W. B. Whitman.** 1995. Maintenance of methanogen stock cultures in glycerol at -70 ^{o}C, p. 85-87. *In* S. Robb F. T., K. R., DasSarma, S., Place, A. R., Schreier, H. J., Fleischmann, E. M. (ed.), Archaea-a laboratory manual. Cold Spring Harbor Laboratory Press, Cold Spring Harbor, N. Y.

51. **Tumbula, D. L., R. A. Makula, and W. B. Whitman.** 1994. Transformation of *Methanococcus maripaludis* and identification of a PstI-like restriction system. FEMS Microbiol. Lett. **121:**309-314.

52. **Waterman, D. G., M. Ortiz-Lombardía, M. J. Fogg, E. V. Koonin, and A. A. Antson.** 2006. Crystal structure of *Bacillus anthracis* ThiI, a tRNA-modifying enzyme containing the predicted RNA-binding THUMP domain. J. Mol. Biol. **356:**97-110.

53. **Webb, E., K. Claas, and D. M. Downs.** 1997. Characterization of thiI, a new gene involved in thiazole biosynthesis in *Salmonella typhimurium*. J. Bacteriol. **179:**4399-4402.

54. **Westley, J.** 1973. Rhodanese. Adv. Enzymol. **39:**327-368.

55. **Westley, J.** 1981. Thiosulfate: cyanide sulfurtransferase (rhodanese). Methods Enzymol. **77:**285-291.

56. **Whitman, W. B., J. Shieh, S. Sohn, D. S. Caras, and U. Premachandran.** 1986. Isolation and characterization of 22 mesophilic methanococci. Syst. Appl. Microbiol. **7:**235.

57. **Wolfe, M. D., F. Ahmed, G. M. Lacourciere, C. T. Lauhon, T. C. Stadtman, and T. J. Larson.** 2004. Functional diversity of the rhodanese homology domain. J. Biol. Chem. **279:**1801-1809.

58. **Wright, C. M., G. D. Christman, A. M. Snellinger, M. V. Johnston, and E. G. Mueller.** 2006. Direct evidence for enzyme persulfide and disulfide intermediates during 4-thiouridine biosynthesis. Chem. Commun.**:**3104-3106.

59. **Xi, J., Y. Ge, C. Kinsland, F. W. McLafferty, and T. P. Begley.** 2001. Biosynthesis of the thiazole moiety of thiamin in *Escherichia coli*: identification of an acyldisulfide-linked protein-protein conjugate that is functionally analogous to the ubiquitin/E1 complex. Proc. Natl. Acad. Sci. U S A. **98:**8513-8518.

60. **Zhang, W., A. Urban, H. Mihara, S. Leimkühler, T. Kurihara, and N. Esaki.** 2010. IscS functions as a primary sulfur-donating enzyme by interacting specifically with MoeB and MoaD in the biosynthesis of molybdopterin in *Escherichia coli*. J. Biol. Chem. **285:**2302-2308.

61. **Zheng, L., R. H. White, V. L. Cash, and D. R. Dean.** 1994. Mechanism for the desulfurization of L-cysteine catalyzed by the nifS gene product. Biochemistry **33:**4714-4720.

62. **Zheng, L., R. H. White, V. L. Cash, R. F. Jack, and D. R. Dean.** 1993. Cysteine desulfurase activity indicates a role for NIFS in metallocluster biosynthesis. Proc. Natl. Acad. Sci. U S A. **90:**2754-2758.

Table 6-1. Thiosulfate sulfurtransferase (rhodanese) activities in *M. maripaludis* cell extracts.

Strain	sp. act. (nmol/min/mg protein)[a]
S2 (wild-type)	0.18 ± 0.03
S620 (Δ*mmp1354*)	0.15 ± 0.03
S623 (complemented)	0.32 ± 0.04

[a]Specific activities were determined by measurements of the production of thiocyanate. Values were mean ± standard deviation of three assays.

Table 6-2. Cysteine production activities with Na_2S or $Na_2S_2O_3$ as sulfur source in *M. maripaludis* cell extracts.

	sp. act. (nmol/min/mg protein)[a]	
Strain	Na_2S	$Na_2S_2O_3$
S2 (wild-type)	1.28 ± 0.03	2.16 ± 0.05
S620 (Δ*mmp1354*)	1.16 ± 0.09	1.85 ± 0.06
S623 (complemented)	1.11 ± 0.08	1.95 ± 0.05

[a]Specific activities were determined by measurements of the production of cysteine. Values were mean ± standard deviation of three assays.

Figure 6-1. Architecture and phylogenetic distribution of ThiI homologs. (A) Schematic representation of the domain structure of ThiI homologs. The representations are drawn approximately to scale, with the phylogenetic distribution of the homologs shown on the right. The N-terminal ferredoxin-like (NFLD; yellow); thiouridine synthases, methylases, and pseudouridine synthases (THUMP; grey); PP-loop pyrophosphatase (PP-loop; blue); and rhodanese-like (RLD; red) domains as well as the conserved PP-loop motif (SGGxDS) and Cys residues are indicated. C344 (forming a disulfide bond with C456) and C456 (forming a persulfide group) represent the enzymatically active Cys residues in *E. coli* ThiI (b0423). C79 represents the Cys residue forming a persulfide group in *M. maripaludis* ThiI. (B) Phylogenetic distribution of ThiI homologs in archaea. The phylogenetic tree was constructed with the minimum evolution method using the program MEGA4. The scale bar represents 0.1 amino acid substitutions per site. Bootstrap analysis was performed with 1,000 replicates, and values greater than 70 % are labeled on the nodes. The colors of the branches correspond to the scheme in Fig. 6-1A. Two ThiI homologs are encoded in the genomes of *Thermococcus onnurineus*, *Thermococcus sibiricus*, *Methanospirillum hungatei*, and uncultured methanogenic archaeon RC-I. Locus tag of all sequences used in the phylogenetic analysis are as follows (from top to bottom): *Pyrobaculum arsenaticum*, Pars1882; *Pyrobaculum aerophilum*, PAE3421; *Pyrobaculum calidifontis*, Pcal1042; *Thermoproteus neutrophilus*, Tneu1312; *Pyrobaculum islandicum*, Pisl0972; *Caldivirga maquilingensis*, Cmaq0014 ; *Thermofilum pendens*, Tpen0320; *Aeropyrum pernix*, APE0465; *Hyperthermus butylicus*, Hbut0566; *Desulfurococcus kamchatkensis*, DKAM0691; *Ferroplasma acidarmanus*, FaciDRAFT1546; *Picrophilus torridus*, PTO0483; *Thermoplasma acidophilum*, Ta0506; *Thermoplasma volcanium*, TVG0805746; *Sulfolobus islandicus*, LD85 2027; *Sulfolobus solfataricus*, SSO0333; *Sulfolobus*

acidocaldarius, Saci2336; *Sulfolobus tokodaii*, ST2225; *Halobacterium salinarum*, OE2858F; *Halobacterium sp*., VNG1299C; *Halorhabdus utahensis*, Huta0512; *Halomicrobium mukohataei*, Hmuk2307; *Haloarcula marismortui*, rrnAC1234; *Haloterrigena turkmenica*, Htur1671; *Natrialba magadii*, NmagDRAFT1820; *Natronomonas pharaonis*, NP3782A; *Halogeometricum borinquense* HborDRAFT3191; *Methanopyrus kandleri*, MK0908; *Methanospirillum hungatei*-1, Mhun0070; *Methanoculleus marisnigri*, Memar1613; *Methanocorpusculum labreanum*, Mlab_0367; *Methanobrevibacter ruminantium*, mru0494; *Methanobrevibacter smithii*, Msm0617; *Methanothermobacter thermoautotrophicum*, MTH1685; *Methanosphaera stadtmanae*, Msp0160; Uncultured methanogenic archaeon RC-I, RCIX1548, RCIX732; *Methanocella paludicola*, MCP2657; *Methanococcoides burtonii*, Mbur1320; *Methanosarcina barkeri*, Mbar_A0010; *Methanosarcina acetivorans*, MA1466; *Methanosarcina mazei*, MM2517; *Methanosaeta thermophila*, Mthe0892; *Methanoregula boonei*, Mboo2042; *Methanosphaerula palustris*, Mpal1206; *Methanospirillum hungatei*-2, Mhun2184; *Archaeoglobus profundus*, Arcpr0189; *Korarchaeum cryptofilum*, Kcr1198; *Pyrococcus furiosus*, PF1288; *Thermococcus sibiricus*-1, TSIB1723; *Thermococcus onnurineus*-1, TON0853; *Archaeoglobus fulgidus*, AF0879; *Thermococcus kodakaraensis*, TK0368; *Thermococcus onnurineus*-2, TON1008; *Thermococcus gammatolerans*, TGAM1481; *Thermococcus sibiricus*-2, TSIB0351; *Pyrococcus abyssi*, PAB0226; *Pyrococcus horikoshii*, PH1786; *Methanococcus vannielii*, Mevan0664; *Methanococcus maripaludis*, MMP1354; *Methanococcus voltae*, MvolDRAFT1005; *Methanococcus aeolicus*, Maeo0796; *Methanocaldococcus infernus*, MetinDRAFT1337; *Methanocaldococcus vulcanius*, Metvu1747; *Methanocaldococcus fervens*, Mefer0763; *Methanocaldococcus jannaschii*, MJ0931; *Staphylothermus marinus*, Smar0447; *Nanoarchaeum equitans*, NEQ423.

A

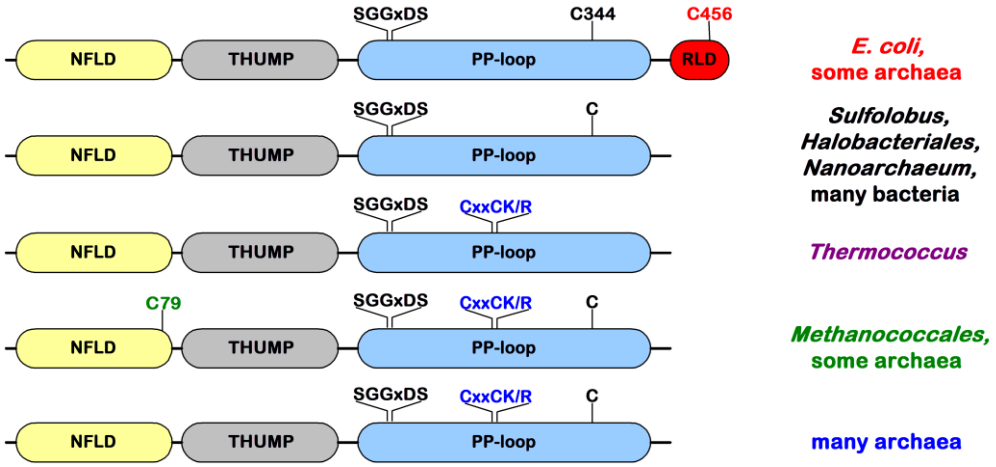
SGGxDS
C344
C456
NFLD
THUMP
PP-loop
RLD
E. coli,
some archaea
SGGxDS
C
Sulfolobus,
Halobacteriales,
Nanoarchaeum,
many bacteria
SGGxDS
CxxCK/R
Thermococcus
C79
Methanococcales,
some archaea
many archaea

B

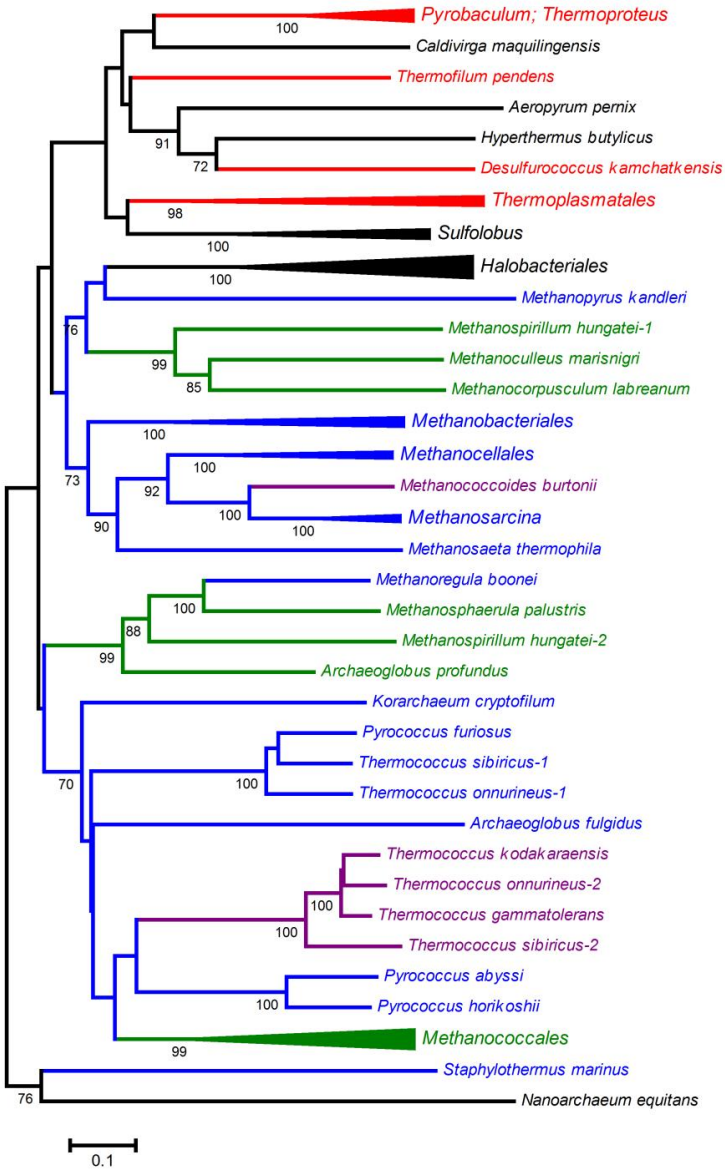
Pyrobaculum; Thermoproteus
Caldivirga maquilingensis
Thermofilum pendens
Aeropyrum pernix
Hyperthermus butylicus
Desulfurococcus kamchatkensis
Thermoplasmatales
Sulfolobus
Halobacteriales
Methanopyrus kandleri
Methanospirillum hungatei-1
Methanoculleus marisnigri
Methanocorpusculum labreanum
Methanobacteriales
Methanocellales
Methanococcoides burtonii
Methanosarcina
Methanosaeta thermophila
Methanoregula boonei
Methanosphaerula palustris
Methanospirillum hungatei-2
Archaeoglobus profundus
Korarchaeum cryptofilum
Pyrococcus furiosus
Thermococcus sibiricus-1
Thermococcus onnurineus-1
Archaeoglobus fulgidus
Thermococcus kodakaraensis
Thermococcus onnurineus-2
Thermococcus gammatolerans
Thermococcus sibiricus-2
Pyrococcus abyssi
Pyrococcus horikoshii
Methanococcales
Staphylothermus marinus
Nanoarchaeum equitans
0.1

Figure 6-2. Purification and the thiosulfate sulfurtransferase activity of MMP1354. (A) SDS-polyacrylamide gel (12 %) analysis of purified recombinant MMP1354. The gel was stained with Coomassie brilliant blue R. Lane 1, molecular mass marker (Fermentas); lane 2, 20 μg of purified recombinant MMP1354. (B) Time dependency of the thiocyanate formation catalyzed by MMP1354 (50 μg) with 50 mM thiosulfate and 50 mM cyanide. The error bars represents the standard deviation of three assays. (C) Optimum pH of MMP1354. The 100% activity was 5.5 nmol/min/mg of protein observed at pH 7.0. Reactions were carried out in Bis-Tris-Cl (pH 6.0-7.0; dashed line), Tris-Cl (pH 7.0-9.0; solid line), and Na-CHES (pH 9.0-10.0; dotted line) buffers.

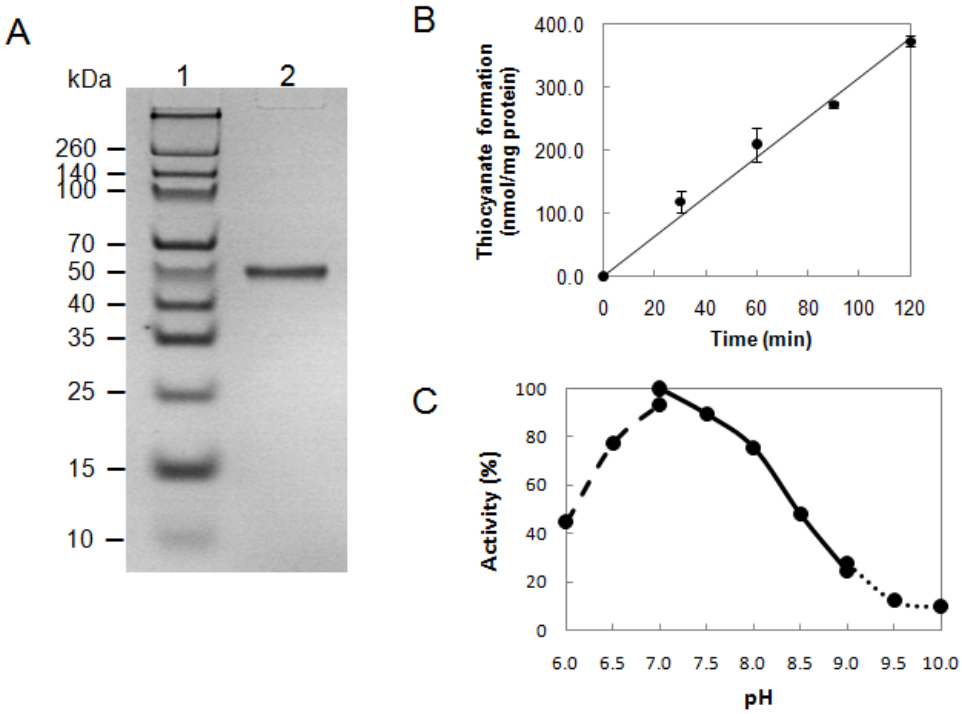
A
kDa
1
2
260
140
100
70
50
40
35
25
15
10
B
Thiocyanate formation (nmol/mg protein)
400.0
300.0
200.0
100.0
0.0
0
20
40
60
80
100
120
Time (min)
C
Activity (%)
100
80
60
40
20
0
6.0
6.5
7.0
7.5
8.0
8.5
9.0
9.5
10.0
pH

Figure 6-3. MS/MS analysis of the persulfide modification on the recombinant MMP1354. (A) MS/MS spectra of the tryptic peptide $_{70}$VPGIVSFSPCYYIDPDIEQIKK$_{91}$ derived from the recombinant MMP1354. Fragment b- and y-ions containing C79 are indicated by green and red dashed lines, respectively. The upper and lower panel represents the spectrum derived from the sample without and with thiosulfate incubation, respectively. The *in vitro* persulfide modification on C79 (+32 Da) is indicated by +32 m/z shifts for b^+ ions and +16 m/z shifts for b^{++} and y^{++} ions. (B) A multiple sequence alignment of ThiI homologs from *Methanococcales* (*Methanococcus maripaludis*, MMP1354; *Methanococcus vannielii*, Mevan0664; *Methanococcus voltae*, Mvol1005; *Methanococcus aeolicus*, Maeo0796; *Methanocaldococcus jannaschii*, MJ0931; *Methanocaldococcus fervens*, Mefer0763; *Methanocaldococcus infernus*, Metin1337; *Methanocaldococcus vulcanius*, Metvu1747), *E. coli* (b0423), and *Bacillus anthracis* (BA4899). The alignment was constructed with ClustalX 2.0. The cysteinyl residue (C79) that exhibits persulfide modification in MMP1354 is shaded in blue. The conserved sequence GIVS(F/Y)SP upstream of C79 is shaded in yellow.

A

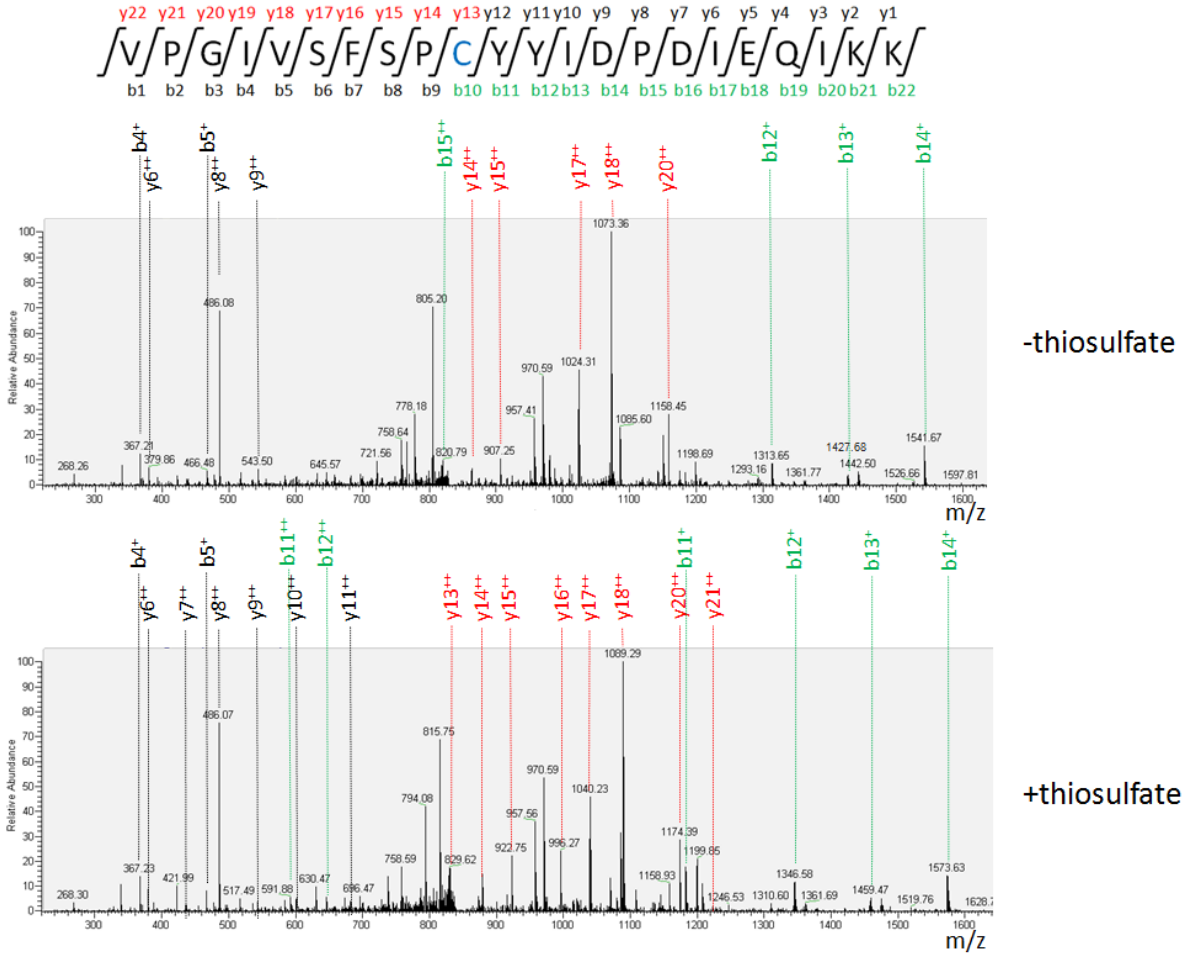
y22 y21 y20 y19 y18 y17 y16 y15 y14 y13 y12 y11 y10 y9 y8 y7 y6 y5 y4 y3 y2 y1
V P G I V S F S P C Y Y I D P D I E Q I K K
b1 b2 b3 b4 b5 b6 b7 b8 b9 b10 b11 b12 b13 b14 b15 b16 b17 b18 b19 b20 b21 b22
Relative Abundance
m/z
-thiosulfate
+thiosulfate

B

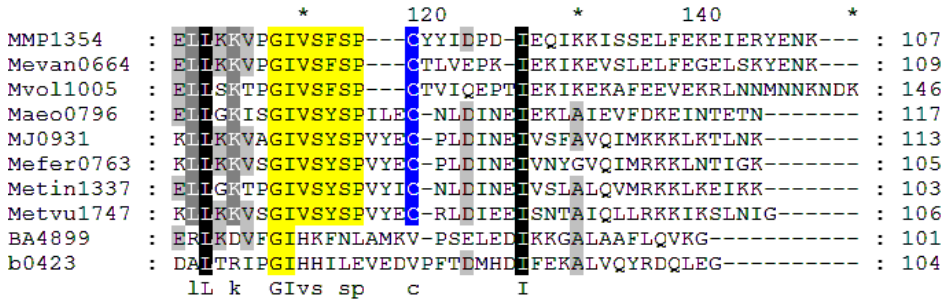
MMP1354 : ELLKKVPGIVSFSP---CYYIDPD-IEQIKKISSELFEKEIERYENK--- : 107
Mevan0664 : ELLKKVPGIVSFSP---CTLVEPK-IEKIKEVSLELFEGELSKYENK--- : 109
Mvol1005 : ELLSKTPGIVSFSP---CTVIQEPTIEKIKEKAFEEVEKRLNNMNNKNDK : 146
Maeo0796 : ELLGKISGIVSYSPILEC-NLDINEIEKLAIEVFDKEINTETN------- : 117
MJ0931 : KLLKKVAGIVSYSPVYEC-PLDINEIVSFAVQIMKKKLKTLNK------- : 113
Mefer0763 : KLLKKVSGIVSYSPVYEC-PLDINEIVNYGVQIMRKKLNTIGK------- : 105
Metin1337 : ELLGKTPGIVSYSPVYIC-NLDINEIVSLALQVMRKKLKEIKK------- : 103
Metvu1747 : KLLKKVSGIVSYSPVYEC-RLDIEEISNTAIQLLRKKIKSLNIG------ : 106
BA4899 : ERLKDVFGIHKFNLAMKV-PSELEDIKKGALAAFLQVKG---------- : 101
b0423 : DALTRIPGIHHILEVEDVPFTDMHDIFEKALVQYRDQLEG---------- : 104
lL k GIvs sp c I

Figure 6-4. Cysteine is not required for growth of the Δ*mmp1354* mutant. Wild-type strain S2 grown in McNACoM+Cys (●) or McNACoM (○) medium; the Δ*mmp1354* mutant strain S620 grown in McNACoM+Cys (■) or McNACoM (○) medium; the complemented strain S623 grown in McNACoM+Cys (▲) or McNACoM (△) medium. The inoculums size was ~ 10^6 cells per 5-ml cultures. All values are the averages of five cultures.

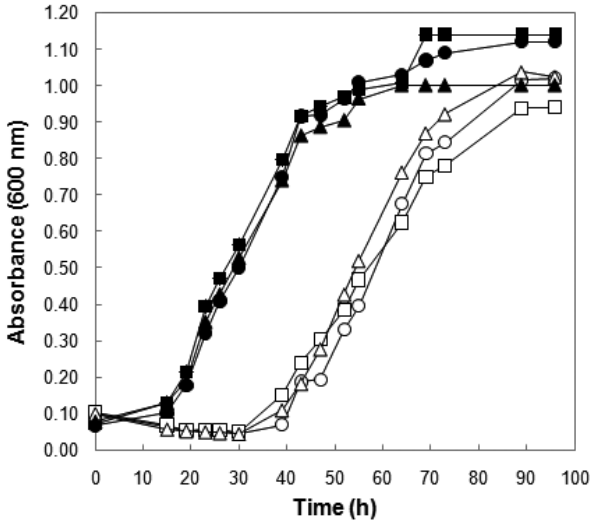
Absorbance (600 nm)
1.20
1.10
1.00
0.90
0.80
0.70
0.60
0.50
0.40
0.30
0.20
0.10
0.00
0
10
20
30
40
50
60
70
80
90
100
Time (h)

CHAPTER 7

CONCLUSION

Methanococcus maripaludis is an obligate anaerobic, mesophilic methanogen. Based upon 16S rRNA phylogeny, it is presumably evolved from an ancient hyperthermophilic anaerobe similar to *Methanocaldococcus jannaschii*. For that reason, proteins involved in thermoadaptation may be greatly modified. Moreover, ancient pathways prior to the evolution of O_2 may be present in methanococci.

First, the Sac10b homolog in *M. maripaludis* (Mma10b) binds DNA at specific sites, which may be an adaptation to the mesophilic lifestyle. The Sac10b protein family is widely distributed in Archaea. In hyperthermphilic *Sulfolobus* species, the Sac10b homologs are very abundant and bind DNA without sequence specificity. Disruption of Sac10b homologs in *Sulfolobus* is not possible, indicating that they may play essential roles. The Sac10b homologs are proposed to be involved in DNA compaction in these hyperthermophilic organisms. In contrast, Mma10b in *M. maripaludis* is not abundant and constitutes only ~ 0.01% of the total cellular protein. Moreover, the association of Mma10b with DNA *in vitro* is sequence-dependent, indicating that it binds to the chromosome at specific loci. Disruption of *mma10b* results in poor growth of the mutant in minimal medium at near the optimal growth temperature but has no detectable affect on growth in rich medium. These results suggest that the physiological role of Mma10b in the mesophilic methanococci is greatly diverged from homologs in thermophiles.

Second, methanococci biosynthesize lysine through the DapL pathway, which uses diaminopimelate aminotransferase (DapL) to catalyze the direct transfer of an amino group from L-glutamate to L-tetrahydrodipicolinate (THDPA), forming LL-diaminopimelate (LL-DAP). Many bacteria including proteobacteria, firmicutes, and actinobacteria convert THDPA to LL-DAP in three steps: succinylation or acetylation, transamination, and desuccinylation or deacetylation. The DapL pathway was previously identified in cyanobacteria, chlamydia, the archaeon *Methanothermobacter thermautotorphicus*, and the plant *Arabidopsis thaliana*. In *M. maripaludis*, the disruption of the DapL homolog (MMP1354) results in lysine auxotrophy. Moreover, succinyl-DAP or acetyl-DAP cannot be used as a substrate for the reverse reaction to generate THDPA. These results suggest that the DapL pathway is the sole pathway for lysine biosynthesis in methanococci. The selective pressure for methanococci to obtain and maintain the DapL pathway instead of the acylation pathways is unclear. Acylation pathways may facilitate the transamination reaction by exposing the keto-group. However, the DapL pathway eliminates the expense of succinyl-CoA or acetyl-CoA and may represent a more primitive mode for lysine biosynthesis.

Finally, the sulfur metabolism in *M. maripaludis* is different from previously studied organisms in three aspects, which may be an adaptation to growth with high sulfide concentration and the methanogenic life style. (1) Enteric bacteria and plants synthesize cysteine via direct sulfhydrylation of *O*-acetylserine by *O*-acetylserine sulfhydrylase, and sulfide is the physiological sulfur donor for this reaction with K_m-values in the micro-molar range. In contrast, even though sulfide is presumably present at high levels in methanococci, it is probably not the direct sulfur donor for cysteine biosynthesis. Cysteine in methanococci is synthesized primarily on $tRNA^{Cys}$ via the SepRS/SepCysS pathway, and thiosulfate and persulfide groups are probably

intermediates for sulfur incorporation into cysteine. (2) All known organisms use cysteine as the sulfur source for Fe-S cluster biosynthesis by cysteine desulfurase. Methanococci lack homologs of cysteine desulfurases and do not use cysteine for Fe-S cluster biosynthesis. (3) Bacteria synthesize homocysteine, the precursor of methionine, by either transsulfuration with cystathionine as an intermediate or direct sulfhydrylation of *O*-succinylhomoserine or *O*-acetylhomoserine. None of the homologs of homocysteine biosynthetic genes are present in the *M. maripaludis* genome. The transsulfuration route uses cysteine as a sulfur source for cystathionine biosynthesis. Since cysteine is not the sulfur source for methionine biosynthesis in *M. maripaludis*, this route either plays a minor part in methionine biosynthesis or there is a new reaction independent of cysteine for cystathionine biosynthesis. The sulfhydrylation route uses sulfide as a sulfur source for homocysteine biosynthesis. However, the direct sulfhydrylation activity with sulfide and homoserine derivatives as substrates is below the detection limit in *M. maripaludis* cell extracts. Therefore, a new biochemical process should be responsible for homocysteine and methionine biosynthesis in methanococci. The unique sulfur metabolism in methanococci may represent ancient pathways that were once common in an anoxic world with high levels of sulfide.

APPENDIX A

CHAPTER 2 SUPPLEMENTARY MATERIAL[1]

---

[1]Supporting online material for:

Liu, Y., L. Guo, R. Guo, R. L. Wong, H. Hernandez, J. Hu, Y. Chu, I. J. Amster, W. B. Whitman, and L. Huang. 2009. The Sac10b Homolog in *Methanococcus maripaludis* Binds DNA at Specific Sites. J. Bacteriol. 191:2315-2329.

Reprinted here with permission of the publisher.

Figure S2-1 SDS polyacrylamide gel electrophoresis of purified Sac10b homologs. Recombinant proteins of Ssh10b, Mja10b, Mth10b, Mma10b, and Mvo10b were expressed and purified from *E. coli*. About 5 μg of proteins were loaded onto each lane. The proteins were separated on 15% SDS-PAGE gel with 100V for 2 hours and visualized by staining with Commassie Blue R250.

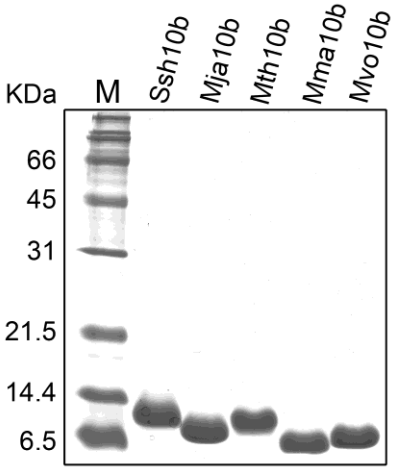
KDa
M
Ssh10b
Mja10b
Mth10b
Mma10b
Mvo10b
66
45
31
21.5
14.4
6.5

Figure S2-2 Construction of the Δ*mma10b*::*pac* mutant. The inner portion of *mma*10b was replaced by the *pac* cassette via two homologous recombination events. The ORFs Mmp1612 and Mmp1614 were annotated as hypothetical protein and histidyl-tRNA synthetase, respectively.

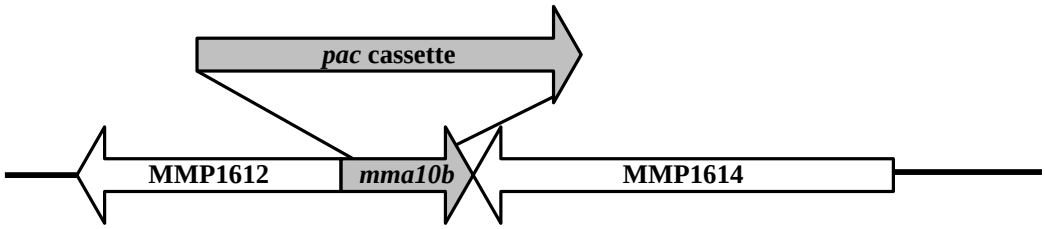
pac cassette
MMP1612
mma10b
MMP1614

Figure S2-3 Chromatin ImmunoPrecipitation assays with anti-Mma10b antiserum. DNA fragments associated with Mma10b were captured with antibodies attached to Protein A agarose beads, purified, blunt ended, ligated to oligonucleotide linkers, and PCR amplified. Lane 1, 100 bp DNA ladder (New England BioLabs); lane 2, PCR amplification of DNA fragments immunoprecipitated from wild-type (S2) cells; lane 3, PCR amplification of DNA fragments immunoprecipitated from Δ*mma10b* (S590) cells.

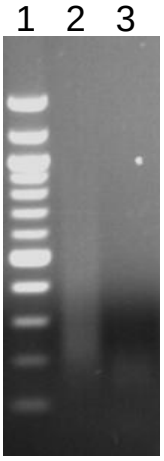
1 2 3

Table S1-1. Quantitative proteomic analysis of S2 and S590.

ORF	N[a]	Protein ratio[b]	S.E.[c]	Annotation
MMP0002	2	1.41	0.07	L-seryl-tRNA selenium transferase related protein
MMP0003	4	1.38	0.11	2-oxoglutarate oxidoreductase alpha subunit, *korA*
MMP0004	2	1.07	0.13	kinase related protein
MMP0013	2	0.96	0.16	Argininosuccinate lyase
MMP0014	4	0.62	0.63	conserved hypothetical protein
MMP0023	3	1.38	0.08	conserved hypothetical protein
MMP0025	9	0.98	0.06	hypothetical protein
MMP0028	2	0.89	0.11	cobyric acid synthase related protein
MMP0031	3	1.24	0.01	conserved hypothetical archeal protein
MMP0044	5	0.89	0.18	conserved hypothetical protein
MMP0045	3	1.02	0.10	bifunctional short chain isoprenyl diphosphate synthase
MMP0050	6	1.05	0.05	riboflavin synthase, subunit beta
MMP0054	5	1.16	0.04	conserved hypothetical protein
MMP0058	16	1.14	0.04	coenzyme F_{420}-dependent N^5,N^{10}-methylenetetrahydromethanopterin reductase
MMP0060	6	1.15	0.10	ribosomal L10 protein
MMP0063	2	1.08	0.01	acetylglutamate kinase
MMP0073	7	0.87	0.07	argininosuccinate synthase
MMP0080	6	0.94	0.12	glutamate synthase; large subunit; archaeal subunit 1
MMP0081	8	1.10	0.07	glutamate synthase; large subunit; archaeal subunit 2
MMP0082	3	1.20	0.02	glutamate synthase; large subunit; archaeal subunit 3
MMP0087	3	1.06	0.23	hydroxymethylglutaryl-coenzyme reductase:3-hydroxy-3-methylglutaryl coenzyme A reductase
MMP0090	2	0.99	0.11	glycosyl transferase
MMP0092	2	1.66	0.10	DNA-directed RNA polymerase, subunit F
MMP0093	2	0.84	0.05	ribosomal protein L21e
MMP0103	6	1.08	0.07	conserved hypothetical protein
MMP0107	2	0.72	0.25	hypothetical protein
MMP0119	2	0.99	0.01	biotin--protein ligase, *birA*
MMP0122	2	0.98	0.00	conserved hypothetical protein
MMP0127	7	1.09	0.09	H_2-forming N^5,N^{10}-methylenetetrahydromethanopterin dehydrogenease
MMP0128	2	1.02	0.10	conserved hypothetical protein
MMP0130	9	0.75	0.11	fumarate hydratase, *fumA*
MMP0132	2	0.89	0.14	aminotransferase (subgroup III) similar to branched-chain amino acid aminotransferase
MMP0133	6	1.03	0.08	IMP dehydrogenase
MMP0135	5	0.96	0.09	threonine synthase
MMP0139	4	0.70	0.10	formate dehydrogenase, subunit beta

MMP0142	3	1.03	0.22	thiamine pyrophosphate-dependent enzyme related to acetolactate synthase
MMP0148	3	1.36	0.12	acetyl-CoA synthetase, AMP-forming, *acsA*
MMP0149	8	0.74	0.16	conserved hypothetical protein
MMP0154	3	0.95	0.14	conserved hypothetical archaeal protein
MMP0156	9	0.93	0.03	ribosomal protein S19e (S16a)
MMP0163	4	1.06	0.20	putative arsenical pump-driving ATPase
MMP0174	6	1.28	0.07	HD phosphohydrolase family member
MMP0176	9	1.36	0.07	CDC48 cell division cycle protein family member
MMP0179	8	1.34	0.03	phosphoribosylformylglycinamidine synthase II
MMP0185	2	1.23	0.00	5'-methylthioadenosine phosphorylase
MMP0187	2	1.13	0.03	thiamine biosynthesis protein, putative
MMP0194	2	0.83	0.14	conserved hypothetical protein
MMP0196	5	0.76	0.11	ABC-type iron (III) transport system, periplasmic binding protein
MMP0197	4	0.77	0.08	ABC-type iron (III) transport system, permease component
MMP0199	2	0.97	0.19	conserved hypothetical archaeal protein
MMP0212	9	0.83	0.11	glycyl-tRNA synthetase
MMP0218	2	1.43	0.03	conserved hypothetical protein
MMP0227	4	1.16	0.06	anaerobic ribonucleoside-triphosphate reductase
MMP0228	3	0.73	0.11	N^2N^2-dimethylguanosine tRNA methyltransferase
MMP0233	2	0.99	0.04	conserved hypothetical archaeal protein
MMP0251	5	1.01	0.08	proteasome, subunit alpha
MMP0253	3	0.96	0.13	acetyl-CoA synthetase (ADP-forming), alpha and beta subunits
MMP0258	165	0.95	0.02	ribosomal protein L12a
MMP0259	4	0.53	0.46	ribosomal protein L10e
MMP0260	10	0.95	0.07	ribosomal protein L1p
MMP0261	2	0.85	0.04	DNA-directed RNA polymerase, subunit L
MMP0263	3	0.76	0.10	tyrosyl-tRNA synthetase
MMP0276	2	1.57	0.06	conserved hypothetical protein
MMP0291	2	0.98	0.16	hydrogenase expression/formation protein related
MMP0297	3	1.00	0.07	translation initiation factor aIF-2, subunit beta
MMP0298	13	0.84	0.08	ribosomal protein L15e
MMP0312	2	0.86	0.16	conserved hypothetical archaeal protein
MMP0317	18	0.96	0.05	conserved hypothetical protein
MMP0319	2	1.15	0.05	precorrin-2 C-20 methyltransferase
MMP0325	3	1.16	0.06	glyceraldehyde 3-phosphate dehydrogenase
MMP0340	15	0.98	0.04	pyruvate carboxylase, subunit B
MMP0341	4	1.26	0.07	pyruvate carboxylase, subunit A
MMP0345	2	1.11	0.06	conserved hypothetical protein
MMP0346	2	0.83	0.17	2-hydroxyglutaryl-CoA dehydratase (component D) related protein

MMP0369	5	1.08	0.12	conserved hypothetical protein
MMP0372	35	0.98	0.05	F_{420}- dependent methylenetetrahydromethanopterin dehydrogenase
MMP0377	15	1.05	0.03	isoleucyl-tRNA synthetase related
MMP0383	146	0.92	0.01	S-layer protein
MMP0386	28	1.14	0.01	archaeal histone A
MMP0391	8	1.04	0.06	aspartate aminotransferase
MMP0393	2	0.99	0.01	phosphoesterase-like protein
MMP0396	2	1.01	0.02	enolase
MMP0397	3	1.21	0.04	alanyl-tRNA synthetase
MMP0413	2	0.84	0.05	conserved hypothetical protein
MMP0414	6	1.51	0.03	threonyl-tRNA synthetase
MMP0415	2	0.87	0.02	tyrosine protein kinase
MMP0423	8	0.83	0.08	hypothetical protein
MMP0427	4	1.09	0.10	replication factor C, small subunit
MMP0437	13	0.92	0.06	putative *A. fulgidus* predicted coding region AF2307
MMP0457	12	0.80	0.10	probable ATP-dependent RNA helicase
MMP0462	7	1.03	0.04	possible predicted protein
MMP0463	2	1.16	0.05	hypothetic protein
MMP0495	2	0.79	0.14	conserved hypothetical protein
MMP0509	2	1.36	0.15	formylmethanofuran dehydrogenase, subunit A
MMP0511	2	0.83	0.04	molybdenum-containing formylmethanofuran dehydrogenase, subunit C
MMP0527	7	1.04	0.03	conserved hypothetical archaeal protein
MMP0532	4	0.85	0.11	conserved hypothetical protein
MMP0540	4	1.16	0.10	phosphoribosylaminoimidazole-succinocarboxamide synthase
MMP0545	2	1.17	0.14	molybdenum cofactor biosynthesis protein: MoeA N-terminal region, domain I and II: MoeA C-terminal, domainIV
MMP0572	27	0.83	0.08	peptidylprolyl isomerase, FKBP-type
MMP0576	2	0.86	0.05	dihydrodipicolinate synthase
MMP0584	5	0.93	0.11	valyl-tRNA synthetase
MMP0589	5	0.97	0.04	conserved hypothetical protein
MMP0591	3	0.97	0.11	conserved hypothetical archaeal protein
MMP0593	7	0.96	0.06	Walker type ATPase
MMP0594	2	1.53	0.11	conserved hypothetical archaeal protein
MMP0595	2	1.07	0.05	conserved hypothetical protein
MMP0598	6	1.07	0.10	archaeal phosphoglycerate mutase-related
MMP0605	2	1.08	0.02	conserved hypothetical protein
MMP0620	7	1.36	0.11	methyl coenzyme M reductase, component A2
MMP0629	3	1.20	0.22	conserved hypothetical archaeal protein
MMP0641	9	0.93	0.05	ribosomal protein L7Ae: ribosomal protein L7Ae/L30e/S12e/Gadd45 family

MMP0649	2	1.04	0.03	carbamoyl transferase
MMP0650	8	1.13	0.05	acetohydroxyacid synthase, large subunit
MMP0651	2	1.30	0.10	acetohydroxyacid synthase, small subunit
MMP0654	8	0.95	0.06	ketol-acid reductoisomerase
MMP0657	2	0.81	0.06	conserved hypothetical protein
MMP0658	3	1.23	0.07	*moaA*/ *nifB*/ *pqqE* family
MMP0663	5	1.08	0.04	sulfate transporter: sulfate transporter/ antisigma-factor antagonist STAS
MMP0667	8	0.90	0.09	ribosomal protein S2
MMP0669	14	0.85	0.04	ribosomal protein S3Ae
MMP0678	14	0.98	0.08	predicted transcriptional regulator; helix-turn-helix motif
MMP0680	6	0.88	0.09	uracil phosphoribosyltransferase
MMP0683	4	0.92	0.19	conserved hypothetical protein
MMP0684	3	2.05	0.06	heat shock protein Hsp20
MMP0688	6	0.87	0.13	phenylalanyl-tRNA synthetase, subunit alpha
MMP0692	2	1.28	0.04	conserved hypothetical protein
MMP0696	5	1.26	0.11	prolyl-tRNA synthetase, *proS*
MMP0697	2	0.88	0.26	leucyl-tRNA synthetase
MMP0712	2	0.96	0.19	similar to amino acid ABC transporter substrate-binding protein
MMP0713	6	1.06	0.06	indolepyruvate oxidoreductase, subunit alpha 2
MMP0720	3	0.70	0.09	prismane
MMP0728	5	0.97	0.06	excinuclease ABC, subunit C
MMP0731	2	1.03	0.07	protein of unknown function DUF6
MMP0756	3	0.90	0.24	conserved hypothetical protein
MMP0772	2	1.14	0.06	hypothetical protein
MMP0780	7	0.97	0.08	conserved hypothetical protein
MMP0783	2	0.74	0.20	conserved hypothetical protein
MMP0792	2	1.01	0.03	membrane protein
MMP0812	2	0.85	0.10	conserved hypothetical protein
MMP0814	2	0.87	0.07	hypothetical protein
MMP0831	7	0.93	0.10	uroporphyrinogen decarboxylase, *uroD*
MMP0832	2	1.09	0.06	conserved hypothetical protein
MMP0853	15	0.95	0.06	nitrogenase iron protein (nitrogenase component II)
MMP0859	5	0.92	0.17	iron-molybdenum cofactor biosynthesis protein, subunit N
MMP0872	4	5.84	0.04	porphobilinogen deaminase
MMP0879	2	1.05	0.08	seryl-tRNA synthetase
MMP0880	2	1.20	0.20	2-oxosuberate synthase, last step
MMP0885	3	1.10	0.08	TPR repeat:ATP/GTP-binding site motif A (P-loop)
MMP0890	3	0.91	0.08	superfamily II helicase
MMP0893	2	1.05	0.12	CTP synthase
MMP0894	8	0.88	0.10	GMP synthase (glutamine-hydrolyzing)
MMP0895	2	1.02	0.00	TPR repeat

MMP0915	3	1.03	0.04	nucleoside triphosphate: 5'-deoxyadenosylcobinamide phosphate nucleotidyltransferase
MMP0916	6	1.22	0.05	conserved hypothetical protein
MMP0925	19	0.94	0.06	chemotaxis protein, *cheW*
MMP0931	2	0.73	0.06	probable chemotaxis-related protein
MMP0944	2	0.60	0.02	hypothetical protein
MMP0946	2	1.40	0.02	Asp-tRNA(Asn)/ Glu-tRNA(Gln) amidotransferase, subunit B
MMP0948	9	0.78	0.09	conserved hypothetical protein
MMP0953	5	1.22	0.04	precorrin-3B C17-methyltransferase
MMP0956	7	0.66	0.18	DNA topoisomerase I
MMP0961	2	1.10	0.10	conserved hypothetical protein
MMP0971	6	1.52	0.06	adenylosuccinate lyase
MMP0988	5	1.15	0.12	RNA methyltransferase related protein
MMP1011	5	1.07	0.09	glutamyl-tRNA synthetase
MMP1013	8	1.05	0.06	carbamoyl-phosphate synthase large chain
MMP1015	5	0.95	0.04	transcription factor CBF/NF-Y/archaeal histone: histone-fold/TFIID-TAF/NF-Y domain
MMP1018	8	0.80	0.06	(R)-citramalate synthase
MMP1021	5	0.95	0.12	conserved hypothetical protein
MMP1024	4	0.94	0.02	MCM family related protein
MMP1026	16	0.99	0.12	arginyl-tRNA synthetase
MMP1028	2	1.38	0.03	unnamed protein product
MMP1031	12	1.15	0.05	adenylate kinase
MMP1032	5	1.04	0.06	replication protein A
MMP1037	2	0.93	0.05	protein of unknown function DUF163
MMP1039	2	0.92	0.01	A_1A_0 ATPase, subunit I
MMP1044	55	0.99	0.03	A_1A_0 ATPase, subunit A
MMP1045	43	0.96	0.03	A_1A_0 ATPase, subunit B
MMP1047	7	0.86	0.16	conserved hypothetical protein
MMP1053	3	0.90	0.09	heterodisulfide reductase, subunit B2
MMP1054	6	0.89	0.11	heterodisulfide reductase, subunit C2
MMP1057	3	1.06	0.09	hypothetical protein
MMP1060	4	1.01	0.07	cysteinyl-tRNA synthetase
MMP1070	2	1.11	0.07	conserved hypothetical archaeal protein
MMP1085	12	1.05	0.04	conserved hypothetical protein
MMP1086	3	0.79	0.13	conserved hypothetical protein
MMP1090	2	1.16	0.10	UDP-glucose 4-epimerase related
MMP1094	9	1.05	0.05	phosphoenolpyruvate synthase
MMP1100	3	1.00	0.06	putative transricptional regulator
MMP1116	4	1.07	0.06	endoglucanase
MMP1129	5	0.89	0.03	peptidyl-prolyl cis-trans isomerase, cyclophilin type
MMP1131	2	0.79	0.06	peptide chain release factor aRF, subunit 1

MMP1133	4	1.25	0.06	L-sulfolactate dehydrogenase/(S)-hydroxyglutaric acid dehydrogenase
MMP1136	4	1.08	0.05	rubrerythrin
MMP1141	4	1.08	0.04	Lhr-like RNA helicase
MMP1142	3	0.98	0.08	metallo-phosphoesterase: serine/threonine-specific protein phosphatase
MMP1146	2	1.05	0.03	amidophosphoribosyltransferase
MMP1148	2	1.21	0.15	small nuclear ribonucleoprotein (Sm protein)
MMP1153	8	1.16	0.04	energy conserving hydrogenase B, large subunit
MMP1157	2	1.79	0.09	desulfoferrodoxin, ferrous iron-binding site
MMP1169	4	1.11	0.09	conserved hypothetical protein
MMP1186	4	0.93	0.06	eukaryotic thiol (cysteine) protease, active site:ATP/GTP-binding site motif A (P-loop):Sigma-54 factor interaction domain
MMP1188	6	0.86	0.05	conserved hypothetical archaeal protein
MMP1190	3	0.98	0.18	peptidylprolyl isomerase, FKBP-type
MMP1191	14	1.08	0.04	N^5,N^{10}-methenyltetrahydromethanopterin cyclohydrolase
MMP1199	9	1.02	0.06	phosphate transport system regulatory protein-related
MMP1203	3	1.00	0.10	cobalamin (vitamin B12) biosynthesis CbiD protein
MMP1206	23	1.00	0.03	glutamine synthetase
MMP1208	7	0.80	0.30	translation initiation factor aIF-2, subunit gamma
MMP1211	6	0.96	0.09	putative hydroxymethyl glutaryl-coenzyme A synthase
MMP1216	2	1.34	0.09	histidinol-phosphate aminotransferase
MMP1218	2	0.95	0.08	conserved hypothetical protein
MMP1219	5	1.18	0.08	putative dinG ATP-dependent helicase
MMP1238	7	0.80	0.06	TonB-dependent receptor protein: biotin synthase
MMP1245	10	1.10	0.04	tungsten containing formylmethanofuran dehydrogenase, subunit F
MMP1247	9	0.97	0.04	tungsten containing formylmethanofuran dehydrogenase, subunit D
MMP1248	13	1.03	0.06	tungsten containing formylmethanofuran dehydrogenase, subunit A
MMP1249	2	0.88	0.20	tungsten containing formylmethanofuran dehydrogenase, subunit C
MMP1255	3	0.93	0.07	phenylalanyl-tRNA synthetase, subunit beta
MMP1257	4	0.87	0.12	conserved hypothetical protein
MMP1265	6	0.92	0.11	glutamyl-tRNA(Gln) amidotransferase, subunit E
MMP1266	2	1.40	0.02	glutamyl-tRNA(Gln) amidotransferase, subunit D
MMP1271	4	0.98	0.10	2-oxoisovalerate oxidoreductase, subunit alpha
MMP1272	5	1.05	0.15	2-oxoisovalerate oxidoreductase, subunit beta
MMP1274	17	0.92	0.06	acetyl-CoA synthetase, AMP-forming-related
MMP1290	4	1.04	0.11	conserved hypothetical protein
MMP1292	4	1.09	0.09	glucan 1,4-alpha-glucosidase (glucoamylase)
MMP1296	3	1.18	0.10	ADP-dependent phosphofructokinase

MMP1297	7	0.92	0.13	formate dehydrogenase, subunit beta
MMP1298	25	0.99	0.05	formate dehydrogenase, subunit alpha
MMP1299	36	1.07	0.03	carbonic anhydrase
MMP1301	2	1.03	0.08	formate transporter
MMP1303	2	0.44	0.78	sensory transduction histidine kinase
MMP1305	2	0.68	0.01	conserved hypothetical protein
MMP1306	7	0.99	0.08	conserved hypothetical protein
MMP1308	12	0.84	0.05	transaldolase
MMP1310	3	1.07	0.15	IMP cyclohydrolase
MMP1314	3	1.07	0.13	phosphoesterase, RecJ-like:RNA binding S1:OB-fold nucleic acid binding domain related protein
MMP1318	2	1.42	0.08	lysyl-tRNA synthetase
MMP1320	10	0.76	0.13	ribosomal protein S4p (S9e)
MMP1321	4	1.09	0.15	ribosomal protein S11
MMP1325	23	0.89	0.04	ribosomal protein S9p
MMP1330	3	0.82	0.10	hydrogenase expression/formation protein, *hupF/hypC*
MMP1337	2	0.87	0.03	hydrogenase maturation protease related
MMP1341	7	1.16	0.09	DNA repair exonuclease of the SbcD/Mre11-family
MMP1347	15	1.32	0.02	archaeal histone B
MMP1352	8	0.94	0.06	NAD-binding site:TonB-dependent receptorprotein: thiamine biosynthesis Thi4 protein
MMP1354	4	0.79	0.18	thiamine biosynthesis protein:THUMP domain
MMP1360	5	0.80	0.18	RNA polymerase H/23 kD subunit
MMP1361	8	0.96	0.04	DNA-directed RNA polymerase subunit B
MMP1362	2	1.08	0.12	glycoside hydrolase, family 1:DNA-directed RNA polymerase, beta subunit: ATP/GTP-binding site motif A (P-loop)
MMP1363	6	0.74	0.15	RNA polymerase, subunit alpha
MMP1364	5	0.74	0.10	RNA polymerase, subunit A/beta/A
MMP1368	20	0.91	0.05	ribosomal protein S7p
MMP1369	32	0.97	0.04	translation elongation factor EF-2
MMP1370	95	1.08	0.02	translation elongation factor EF-1, subunit alpha
MMP1373	9	0.96	0.11	conserved hypothetical archaeal protein
MMP1379	2	1.01	0.03	thymidylate synthase
MMP1382	19	1.07	0.05	coenzyme F_{420}-reducing hydrogenase, subunit alpha
MMP1383	5	0.96	0.16	coenzyme F_{420}-reducing hydrogenase, subunit delta
MMP1397	5	1.00	0.12	structural maintenance of chromosome protein
MMP1401	14	0.87	0.04	translation elongation factor aEF-1 beta
MMP1403	2	0.95	0.00	ribosomal protein L22p
MMP1404	8	0.99	0.06	ribosomal protein S3p
MMP1409	10	1.00	0.05	ribosomal protein L14p
MMP1411	27	0.89	0.04	ribosomal protein S4e
MMP1412	5	0.93	0.04	ribosomal protein L5p
MMP1414	8	0.88	0.06	ribosomal protein S8p

MMP1415	7	0.89	0.08	ribosomal protein L6p
MMP1416	4	0.81	0.15	ribosomal protein L32e
MMP1419	3	0.82	0.16	ribosomal protein S5p
MMP1420	9	0.83	0.15	ribosomal protein L30p
MMP1432	2	0.98	0.03	adenylosuccinate synthase
MMP1433	18	0.90	0.06	ribosomal protein L11
MMP1436	5	0.83	0.23	cell division protein FtsZ
MMP1437	11	0.86	0.04	DNA topoisomerase VI A
MMP1474	7	1.03	0.06	isoleucyl-tRNA synthetase
MMP1489	5	1.17	0.08	inositol monophosphate related protein
MMP1500	7	1.17	0.12	cell division protein FtsZ2
MMP1504	2	1.32	0.05	pyruvate oxidoreductase (synthase), subunit beta
MMP1505	15	1.14	0.06	pyruvate oxidoreductase (synthase), subunit alpha
MMP1507	4	1.24	0.08	pyruvate oxidoreductase (synthase), subunit gamma
MMP1515	8	1.08	0.06	chaperonin GroEL (thermosome, Hsp60 family)
MMP1527	3	1.26	0.09	aminotransferase (subgroup I)
MMP1543	7	0.95	0.06	ribosomal protein L3p
MMP1544	7	0.82	0.09	ribosomal protein L4p
MMP1546	6	0.86	0.10	ribosomal protein L2p
MMP1551	2	0.69	0.41	signal recognition particle protein SRP54
MMP1555	46	1.06	0.03	methyl-coenzyme M reductase I, subunit beta
MMP1558	24	1.05	0.02	methyl-coenzyme M reductase I, subunit gamma
MMP1559	149	0.97	0.05	methyl-coenzyme M reductase I, subunit alpha
MMP1566	4	0.77	0.15	N^5-methyltetrahydromethanopterin: methyltransferase, subunit G, *mtrG*
MMP1567	39	0.83	0.06	N^5-methyltetrahydromethanopterin:methyltransferase, subunit H
MMP1570	2	0.97	0.11	TatD-related protein
MMP1577	3	1.12	0.08	histone acetyltransferase
MMP1579	20	0.81	0.08	probable ribosomal protein S15p/S13e
MMP1581	2	0.93	0.14	putative DNA helicase
MMP1582	5	0.92	0.07	pyruvoyl-dependent arginine decarboxylase, PvlArgDC, alpha and beta subunits
MMP1589	4	1.02	0.04	carbamoyl-phosphate synthase small chain
MMP1595	7	0.88	0.09	ATP/GTP-binding site motif A (P-loop):PUA domain: queuine/other tRNA-ribosyltransferase: uncharacterized domain 2
MMP1611	9	0.92	0.10	conserved hypothetical protein
MMP1614	2	1.58	0.19	histidyl-tRNA synthetase
MMP1616	10	1.20	0.04	aspartyl-tRNA synthetase
MMP1624	2	1.06	0.04	polyferredoxin
MMP1630	2	0.99	0.02	ATP/GTP-binding site motif A (P-loop):ABC transporter:AAA ATPase

MMP1632	2	0.75	0.03	solute-binding protein/glutamate receptor: bacterial extracellular solute-binding protein, family 3
MMP1637	10	1.41	0.04	conserved hypothetical archaeal protein
MMP1640	8	0.98	0.08	archaeal S-adenosylmethionine synthetase (MAT)
MMP1643	4	1.05	0.10	conserved hypothetical protein
MMP1647	10	0.96	0.09	proteasome-activating nucleotidase (PAN)
MMP1659	4	0.99	0.21	aspartate carbamoyltransferase, catalytic subunit
MMP1663	4	0.84	0.14	conserved hypothetical protein
MMP1665	4	1.25	0.05	hypothetical protein
MMP1666	2	0.42	0.23	flagellin B1 percursor
MMP1667	3	0.36	0.38	flagellin B2
MMP1670	5	0.68	0.15	flagella accessory protein D
MMP1671	3	0.59	0.29	flagella accessory protein E
MMP1674	3	0.93	0.08	flagella accessory protein H
MMP1691	17	1.15	0.05	tungsten containing formylmethanofuran dehydrogenase, subunit B
MMP1694	5	1.24	0.08	F_{420}-non-reducing hydrogenase, subunit alpha
MMP1695	3	1.22	0.07	F_{420}-non-reducing hydrogenase subunit
MMP1697	18	1.05	0.04	heterodisulfide reductase, subunit A
MMP1700	5	0.93	0.07	Na^+/solute symporter
MMP1714	8	1.17	0.08	conserved hypothetical protein
MMP1716	3	1.23	0.09	H_2-forming methylenetetrahydromethanopterin dehydrogenase related protein
MMP1720	3	1.02	0.13	conserved hypothetical archaeal protein

[a] Numbers of peptide pairs measured for the ORF.

[b] Mean of the S590/S2 ratio of protein levels.

[c] Standard error of the mean or the standard deviation/$\sqrt{N}$.

Table S2-2. DNA loci associated with Mma10b *in vivo* as identified by ChIP analysis.

Position in chromosome		N[a]	ORF	Annotation
Start	End			
2838	2976	0		Large Subunit Ribosomal RNA
3324	3503	0		Small Subunit Ribosomal RNA
103909	104089	0	MMP0094	Archaeal zinc-finger domain protein
117566	117705	0	MMP0109	ABC transporter permease protein
122413	122542	2	MMP0113	DNA topoisomerase I
162574	163406	2	MMP0152	Transporter, Divalent Anion:Sodium Symporter family
170204	170353	0	MMP0160	Coenzyme F390 Synthetase/Phenylacetate-coenzyme A ligase
195446	195573	2	MMP0187	Thiamine biosynthesis protein *thiC*
248536	248693	2	MMP0243	Protoporphyrinogen oxidase
313480	313651	2	MMP0317	Fructose-1,6-bisphosphatase
314940	315413	2	MMP0318	Dihydroxy-acid dehydratase
381989	382108	2	MMP0383	S-layer protein
382499	382571	0	MMP0383	S-layer protein
497987	498104	2	MMP0494	ATP-dependent helicase
527465	527782	2	MMP0521	Transporter
530053	530316	2	MMP0524	hypothetical protein
530091	530508	2	MMP0524	Hypothetical protein
606258	606475	2	MMP0610	archaeosine tRNA-ribosyltransferase
607131	607484	2	MMP0611	Metal-dependent hydrolase
667222	667356	2	MMP0679	Na^+/H^+ antiporter
683026	683293	0	MMP0694	Metallo-beta-lactamase protein
700789	700971	2	MMP0709	hypothetical protein
708871	708980	2	MMP0715	Coenzyme F390 Synthetase/Phenylacetate-coenzyme A ligase
808020	808160	0	MMP0814	Hypothetical protein
1022435	1022653	2	MMP1030	Hypothetical membrane spanning protein
1038072	1038248	2	MMP1044	V-type ATP synthase alpha
1083985	1084186	0	MMP1091	UTP--glucose-1-phosphate uridylyltransferase
1098186	1098448	0	MMP1108	Magnesium and cobalt transport protein *corA*
1107611	1107737	2	MMP1118	Zinc finger protein
1110085	1110396	2	MMP1120	Two component system histidine kinase
1180280	1180673	1	MMP1193	Hypothetical protein
			MMP1194	Hypothetical protein
1204060	1204208	2	MMP1216	Threonine-phosphate decarboxylase

1233285	1233604	1	MMP1249	Tungsten-containing formylmethanofuran dehydrogenase, subunit C
1242113	1242339	2	MMP1259	NADH dehydrogenase
1307469	1307986	2	MMP1322	DNA-directed RNA polymerase subunit D
			MMP1323	LSU ribosomal protein L18E
1309228	1309345	0	MMP1326	DNA-directed RNA polymerase subunit N
1341696	1341955	2	MMP1362	DNA-directed RNA polymerase subunit B'
1345100	1345294	2	MMP1363	DNA-directed RNA polymerase subunit A'
1414376	1415144	2	MMP1443	GTP-binding protein
1416392	1416514	0	MMP1445	GMP synthase
1445011	1445161	2	MMP1485	Molybdenum cofactor biosynthesis protein B
1611534	1611725	0	MMP1668	Flagellin B2 precursor
1612078	1612366	1	MMP1669	Flagella related protein FlaC
1617482	1617726	2	MMP1676	Flagella related protein FlaJ
1649672	1649973	2	MMP1712	Transcriptional regulators, LysR family

[a] Number of DNA binding motifs as predicted by the Motif Locator program with a score cutoff of 9.0 (http://www.cmbl.uga.edu/software/motloc.html).